INAUGURAL-DISSERTATION

zur

Erlangung der Doktorwürde

der

Naturwissenschaftlich-Mathematischen Gesamtfakultät

der

RUPRECHT-KARLS-UNIVERSITÄT

HEIDELBERG

vorgelegt von

Dipl.–Math. Tony Huschto

aus Bad Muskau in Sachsen

Tag der mündlichen Prüfung

....

Numerical Methods for

Random Parameter Optimal Control

and the

Optimal Control of Stochastic Differential Equations

Betreuer

PROFESSOR DR. SEBASTIAN SAGER
PROFESSOR DR. MARK PODOLSKIJ

Tony Huschto
Dipl.–Math.

Interdisziplinäres Zentrum für Wissenschaftliches Rechnen
Ruprecht-Karls-Universität Heidelberg
Im Neuenheimer Feld 368
69120 Heidelberg
Germany

tony.huschto@iwr.uni–heidelberg.de

Für CLAUDIA und HUGO

Zusammenfassung

Die vorgelegte Arbeit befasst sich mit der Untersuchung und Entwicklung numerischer Methoden zur Lösung von Optimalsteuerungsproblemen, die durch stochastische Phänomene unterschiedlichster Art beeinflusst werden. Im ersten Teil werden dabei Problemstellungen bearbeitet, die durch zufällig verteilte Parameter charakterisiert sind, während im anschließenden zweiten Teil zeitabhängige stochastische Prozesse die Grundlage der Dynamik des zu untersuchenden Systems bilden. Das Ziel dieser Untersuchungen ist dabei jeweils, das ursprüngliche Ausgangsproblem in eines zu transformieren, welches mittels *existierender (direkter) Methoden der deterministischen optimalen Steuerung* gelöst werden kann – hier ist dies BOCKs direkte Mehrzielmethode.

Im Rahmen dieser Transformation werden im ersten Abschnitt Ansätze der *stochastischen Programmierung* sowie der *robusten* und *wahrscheinlichkeitstheoretischen Optimierung* benutzt. Für ein spezifisches Anwendungsbeispiel aus der mathematischen Wirtschaftsforschung, welches die Preisermittlung von Geltungskonsumgütern in Rezessionen untersucht, werden unter Berücksichtigung dieser Verfahren – insbesondere eines *Entscheidungsbaum-Ansatzes* sowie *Approximationen robuster Worst-Case-Szenarien* und finanzmathematischer Werkzeuge wie *Value at Risk* und *Conditional Value at Risk* – neue numerische Lösungsmethoden entwickelt und analysiert. Besonderes Augenmerk liegt dabei auf den notwendigen Reformulierungen der resultierenden Optimalsteuerungsprobleme, speziell für Value at Risk und Conditional Value at Risk, sowie der Diskussion und Interpretation der ermittelten Ergebnisse in Abhängigkeit von der unsicheren Rezessionsdauer, der unsicheren Rezessionsstärke und Steuerungsverzögerungen. Die gewonnenen neuen ökonomischen Erkenntnisse können dabei als wichtiger Schritt auf dem Weg zu einem besseren Verständnis realer Preisfindungsstrategien aufgefasst werden.

Im zweiten Teil der Arbeit wird, basierend auf der WIENER *Chaosentwicklung* eines stochastischen Prozesses und dem MALLIAVIN-*Kalkül*, ein System von gekoppelten gewöhnlichen Differentialgleichungen entwickelt, welches die die Dynamik des Prozesses beschreibende stochastische Differentialgleichung vollständig charakterisiert. Da dieses System im Allgemeinen unendlich viele Gleichungen enthält, wird zur Gewährleistung der numerischen Anwendbarkeit anschließend eine rigorose *Fehlerschätzung* in Abhängigkeit der Ordnung der Chaosentwicklung bewiesen. Um das generelle Vorgehen dieser Entwicklung auf *stochastische Optimalsteuerungsprobleme* übertragen zu können, wird weiterhin ein Ansatz gezeigt, der die Charakteristik der auftretenden *Feedback-Steuerung* bewahrt. Dies macht es möglich, eine *neue direkte Methode zur Lösung stochastischer Optimalsteuerungsprobleme auf endlichem Zeithorizont* herzuleiten. Die Anwendbarkeit und die Güte des entwickelten Verfahrens werden durch die numerische Bearbeitung mehrerer Problemstellungen aufgezeigt. Zum Abschluss wird das ökonomische Beispiel aus dem ersten Teil erneut aufgegriffen und unter dem Gesichtspunkt einer zeitabhängigen Rezessionsstärke, d.h. eines stochastischen Prozesses, untersucht. Insbesondere wird durch die Anwendungsbeispiele deutlich, dass die existierenden numerischen Verfahren für deterministische Optimalsteuerungsprobleme auf Aufgabenstellungen mit stochasti-

schen Differentialgleichungen ausgeweitet werden können.

Abstract

This thesis considers the investigation and development of numerical methods for optimal control problems that are influenced by stochastic phenomena of various type. The first part treats tasks characterized by random parameters, while in the subsequent second part time-dependent stochastic processes are the basis of the dynamics describing the analyzed systems. In each case the investigations aim to transform the original problem into one that can be tackled by *existing (direct) methods of deterministic optimal control*—here we prefer BOCK's direct multiple shooting approach.

In the context of this transformation, in the first part approaches from *stochastic programming* as well as *robust* and *probabilistic* optimization are used. Regarding a specific application from mathematical economics, which considers pricing conspicuous consumption products in periods of recession, new numerical procedures are developed and analyzed with due regard to those techniques—in particular, a *scenario tree approach*, *approximations of robust worst-case settings*, and financial tools as the *Value at Risk* and *Conditional Value at Risk*. Furthermore, necessary reformulations of the resulting optimal control problems, in particular for Value at Risk and Conditional Value at Risk, as well as the discussion and interpretation of results determined depending on an uncertain recession duration, an uncertain recession strength, and control delays are in focus. The gained economic insight can be seen as an important step in the direction of a better understanding of real-world pricing strategies.

In the second part of the thesis, based on the WIENER *chaos expansion* of a stochastic process and on MALLIAVIN *calculus*, a system of coupled ordinary differential equations is developed that completely characterizes the stochastic differential equation describing the dynamics of the process. As in general this system includes infinitely many equations, a rigorous *error estimation* depending on the order of the chaos decomposition is proven in order to guarantee the numerical applicability. To transfer the generic procedure of the chaos expansion to *stochastic optimal control problems*, a method to preserve the feedback character of the occurring control process is shown. This allows the derivation of a *novel direct method to solve finite-horizon stochastic optimal control problems*. The appropriability and accuracy of this methodology are demonstrated by treating several problem instances numerically. Finally, the economic application of the first part is revisited under the viewpoint of dealing with a time-dependent recession strength, i.e., a stochastic process. In particular, those applications illustrate that the existing methods of deterministic optimal control can be extended to problems including stochastic differential equations.

x

Danksagung

Mein aufrichtiger und tief empfundener Dank gilt meinen Lehrern und Mentoren *Professor Dr. Sebastian Sager* und *Professor Dr. Mark Podoloskij*. Nur durch ihre immerwährende Unterstützung, ihr umfangreiches Wissen (gepaart mit der Fähigkeit, mir einen kleinen Teil davon zu vermitteln) und ihr Vertrauen konnte diese Arbeit entstehen. Besonders ihre offene und freundschaftliche Art und Hilfsbereitschaft lassen mich auf fünf spannende und freudige Jahre zurückblicken.

Des Weiteren möchte ich *Professor Dr. Sabine Pickenhain* danken. Ohne sie wäre ich niemals in den Genuss eines Auslandsstudiums in Schweden – mit all seinen glücklichen Folgen – gekommen oder hätte nur im Entferntesten daran gedacht, mich mit stochastischen Differentialgleichungen zu befassen.

Zum Entstehen dieser Arbeit an der *Naturwissenschaftlich-Mathematischen Gesamtfakultät* der *Ruprecht-Karls-Universität Heidelberg* haben auch die Mitglieder der Arbeitsgruppe *Mathematical and Computational Optimization* bzw. ihrer Nachfolgegruppe *Mathematical Algorithmic Optimization* beigetragen. Unsere Diskussionen und Gedankenaustausche habe ich sehr genossen, die tollen Anregungen und Ideen waren nicht nur einmal der Stoß in die richtige Richtung. Es ist schön, Bestandteil dieser Gruppe zu sein!

Eine weitere Gruppe, die nicht unerwähnt bleiben darf, umfasst *Professor Dr. emer. Gustav Feichtinger*, *Professor Dr. Richard Hartl*, *Professor Dr. Peter Kort* und ihre jeweiligen Arbeitsgruppen. Unsere gemeinsame Projektarbeit und die damit verbundenen Reisen nach Wien haben mir sehr viel Freude bereitet und indirekt den Einstieg in die Methoden und Herangehensweisen des Wissenschaftlichen Rechnens erleichtert.

Für die finanzielle und akademische Unterstützung und Weiterbildung möchte ich mich außerdem bei der *Heidelberger Graduiertenschule der mathematischen und computergestützten Methoden für die Wissenschaften*, dem *Interdisziplinären Zentrum für Wissenschaftliches Rechnen* der Ruprecht-Karls-Universität Heidelberg und der *Otto-von-Guericke-Universität Magdeburg* bedanken.

Meinen Eltern *Christine* und *Fred* bin ich zutiefst dankbar für ihre bedingungslose Liebe und Hilfe. Sie sind der Grundstein, weshalb ich überhaupt an diesem Punkt bin. Zudem möchte ich auch meiner Schwester *Theresa* und meiner *Schwiegerschwester Christina* danken; oftmals hat es sehr geholfen, mich einfach reden zu lassen.

Ganz besonderer und nicht annähernd in Worte zu fassender Dank gilt meiner Frau *Claudia*. Ihre grenzenlose Liebe und Geduld half mir nicht nur in den verzweifelten Tagen, sie bereichert mich jeden Tag!

Speyer und Heidelberg, im August 2014 *Tony Huschto*

"'Cause we don't stutter when we sing
Our melodies grow little wings"
DAVE HAUSE—*The Shine*

Contents

0 Introduction

Preface

Making decisions is one of nature's vital keys. And ever since an action or stance has been selected from alternative possibilities, the task of decision-making has been studied.

Quite naturally it is performed in such a way that the choices resulting from weighting the advantages and disadvantages with the help of rational arguments or irrational preferences are in some sense optimal. A mathematical translation leads us to *optimization* problems, where our goal is to find decisions that minimize or maximize a certain performance criterion and that are often influenced by additional side conditions. One subdiscipline of optimization—generally referred to as *optimal control*—considers dynamic systems that are driven by differential equations. These dynamics mathematically describe how the system changes over time, depending on the current state of the system and possible external control mechanisms.

The modeling, simulation, and optimization of Optimal Control Problems (OCPs) has attracted growing attention in recent decades, with versatile applications in biology, chemistry, engineering, mechanics, transport, logistics, and economics. The enormous advances made through that research allow for a treatment of more and more complex systems.

In practice, however, the specification of the dynamic behavior is not only affected by the state and control, but as well by additional extrinsic influences. In some instances, e.g., the modeling of groundwater flows or transport processes in porous media, the strict deterministic law of the differential equation is disturbed by time-independent parameters characterizing material properties. Often, they can only be provided with a specific uncertainty. In other problems, e.g., systems determined by fluctuation and dissipation, or financial problems including stock prices, there might not even by an underlying deterministic basic rule. Then additional noise has to be taken into account as a source of the uncertainty. To differentiate systems that are influenced by uncertain components from those determined by time-dependent noisy behavior, we speak of *Random Differential Equations (RDEs)* and *Stochastic Differential Equations (SDEs)*, respectively.

This thesis aims for a better understanding of decision-making when uncertainty is present. We regard OCPs determined by either RDEs and SDEs and study how far and under which preliminaries it is possible to use the sophisticated numerical ideas and methodologies of optimal control when investigating stochastic phenomena.

For solving deterministic OCPs numerically, the *direct "first discretize, then optimize" approaches* have become the preferred method in practical applications. Among them, the *collocation* [20, 39, 40] and *multiple shooting* ideas [46, 162, 201] are the most prominent ones. They discretize the infinite-dimensional control space and transform the original problem into a *Nonlinear Program (NLP)*, which can afterwards be solved by specially tailored Sequential Quadratic Programming (SQP) [162] or interior point methods [41].

When random influences enter the considered problems, in *uncertainty quantification* one gen-

erally differentiates the source of uncertainty into *aleatoric* and *epistemic* [180]. While aleatoric uncertainty describes truly random effects through stochastic quantities and processes, epistemic uncertainty focuses on structural model uncertainties, model parameters, realization and discretization errors. Research areas of uncertainty quantification in mathematical optimization include *model predictive control* [137, 140], *optimum experimental design* [86, 145], *model discrimination* [14, 112, 227], *dual control* [88, 89], and *robustification* techniques. Particularly these latter ideas, e.g., by linearization [74, 136] and sigmapoint approaches [207], multiple set-point [209] or confidence ellipsoid optimization [114], have attracted much attention. These robust methods reach beyond the classical *worst-case analysis* and characterize probabilistic guarantees in terms of a *budget of uncertainty* [38]. Obtaining similar results from a quite different viewpoint, *probabilistic optimization* techniques [211] including expectation and variance-based approaches or typically financial instruments like Value at Risk (VaR) or Conditional Value at Risk (CVaR) became very popular.

While the ideas mentioned up to now mostly apply to OCPs with RDEs, purely Stochastic Optimal Control Problems (SOCPs) driven by SDEs require fundamentally different solution methodologies. In economics and finance, particularly in portfolio management problems [92], they are the usual modeling framework and have been analyzed extensively during the past decades. Basically, problems belonging to the class of finite-horizon SOCPs can be solved through the corresponding HAMILTON-JACOBI-BELLMAN *(HJB)* equation [141, 146, 195], by applying the *Stochastic Maximum Principle (SMP)* [30, 43, 154], or using *direct approaches*. However, these ideas differ essentially from the deterministic all-at-once approaches. They comprise mainly discretizing MARKOV *chain* methods [148, 156, 157] or *quantization* techniques [173, 174, 197, 198], which always require solving a resulting BELLMAN equation.

In recent years, the concept of *Polynomial Chaos (PC)* became more and more popular. Going back to early considerations of WIENER [246], the (generalized) PC of a random variable is an abstract FOURIER decomposition of the random variable in terms of orthogonal polynomials depending on basis random variables spanning the underlying stochastic space. WIENER's original idea is based on GAUSSian random variables using HERMITE polynomials. In [56] this concept has been generalized for (nearly) arbitrary distributions. Since then, *stochastic* GALERKIN *methods* were developed and refined [66, 100, 159, 181, 193, 237, 244].

The traditional PC approaches are mainly used in the context of RDEs, but both in the context of ordinary and partial differential ones. When regarding time-dependent stochastic processes, progress has been made in the field of specific Stochastic Partial Differential Equations (SPDEs). By using WIENER's chaos expansion and MALLIAVIN calculus [177, 178, 192, 194] these equations were simulated by transforming the original SPDE into a system of Partial Differential Equations (PDEs) [113, 164, 169, 170, 172, 182, 245].

However, in the context of SOCPs, the application of WIENER chaos based ideas has not been studied to our knowledge.

Aims and Contributions of the Thesis

The aim of this thesis is to support understanding of how to find optimal decisions for OCPs that are influenced by uncertain effects. In the first part this is done by considering time-independent uncertainty in the parameters, in the second part we regard problems that are determined by time-dependent stochastic processes. The insights that are obtained in this work

are explained in the following.

In Part I, particularly Chapters 2 and 3, we give an overview of different ideas of robust and probabilistic optimization, compare them to each other and to the general concept of stochastic optimization. In particular, we elaborately analyze the specific economic problem of pricing conspicuous consumption products in periods of recession. This problem includes parameter uncertainty in both the duration and the strength of the recession, as well as a delayed impact of pricing decision on the system's dynamics. Hence, we first develop a structure-exploiting numerical approach that discretizes the uncertainty in the recession length by two tailored settings of a scenario tree and tackles the delay by a slack control. Thus, we obtain a mathematical model that can be compared to the approach of stochastic optimization. When the recession strength enters our problem as an additional source of uncertainty, we extensively investigate the effects of the robust and probabilistic optimization perspectives. Especially for the probabilistic methods of VaR and CVaR, we describe and analyze the needed adaptations for implementing these approaches in the optimal control context. Throughout Chapter 3 we provide economic insight in the (partially unexpected) effects of adding the uncertainty and delay effects to the conspicuous consumption model. Furthermore, for the first time we discuss the strengths and weaknesses of four applied robust and probabilistic optimization approaches from both the computational and the specific economic point of view. Therefore, our analysis in Part I can be seen as a step in the direction of understanding real-world pricing strategies better, particularly under the aspect of robustification techniques.

In Part II we focus on OCPs where the state process is driven by a SDE. Based on MALLIAVIN calculus we construct an infinite-dimensional propagator system of coupled Ordinary Differential Equations (ODEs) that completely describe the original SDE in Chapter 6. After explaining the different truncation steps that are necessary to use this propagator numerically, we prove an error estimator for the truncated chaos expansion of a stochastic process driven by a SDE. This is done first for the geometric BROWNian motion process, because we are able to solve the propagator system for this process analytically. Afterwards we provide a more general error analysis that is founded on multiple MALLIAVIN derivatives of the underlying stochastic process. By treating controlled SDEs within this WIENER chaos framework and developing new ideas to preserve the feedback character of the control process appearing within a SOCP, in Chapter 7 we reformulate the original SOCP as a deterministic one. Thus, we deduce a novel generic methodology for solving finite-horizon continuous SOCPs with the help of state-of-the-art methods for deterministic optimal control. The numerical examples we investigate in the first sections of Chapter 8 validate this new mathematical framework with huge computational advantages compared to standard ideas in stochastic optimal control. In the second part we return to the conspicuous consumption problem of Chapter 3, regarding the recession strength as a time-dependent stochastic process. Reformulating the customized problem leads to a propagator Differential-Algebraic Equation (DAE) system, which can still be efficiently tackled with deterministic optimal control methods. Therefore, this novel methodology pioneers the extension of sophisticated methods for deterministic control to the broad context of random processes and SDEs.

Contributions to Publications

During the work on this thesis, we contributed to one conference publication and three journal articles. In the following, we describe the contents of these papers and the contributions of the author of this thesis.

[118] T. Huschto, G. Feichtinger, P. M. Kort, R. F. Hartl, S. Sager, and A. Seidl. Numerical Solution of a Conspicuous Consumption Model with Constant Control Delay. *Automatica*, 47:1868–1877, 2011.

In this work we analyze the economic OCP of pricing conspicuous consumption products in periods of recession. Based on [61, 63], we formulate and investigate this problem as a multi-stage OCP that takes uncertainty of the recession length and an additional delay effect of the pricing strategy into account. The new parts of this paper are the structure-exploiting, result-driven numerical scenario tree approach to solve this non-standard problem as well as the consideration of the delay effect.

The work evolved from a collaboration of mathematicians and economists from Vienna, Heidelberg, and Tilburg. While SEBASTIAN SAGER and TONY HUSCHTO focused on the mathematical aspects of the project, PETER KORT and RICHARD HARTL provided various of the economic interpretations of the obtained results. SAGER initiated the work on scenario trees to discretize the uncertainty. HUSCHTO's main contributions were the reformulated approach and the analytical results presented in the article. As the first author, he as well wrote the publication. He implemented the problems in joined work with SAGER. The remaining authors contributed in discussions and reviews of the paper before submission.

[117] T. Huschto and S. Sager. Pricing Conspicuous Consumption Products in Recession Periods with Uncertain Strength. *EURO Journal on Decision Processes*, 2, 2014. (to appear)

This article extends the work of [118] by considering the strength of the recession as an additional source of uncertainty. To that end, we compare different approaches of robust optimization and optimization under uncertainty in the context of optimally pricing conspicuous consumption products. For the first time, we discuss the strengths and weaknesses of all applied methods under the viewpoints of computational complexity and their economic implications. As first and corresponding author, TONY HUSCHTO mainly wrote the article, developed the necessary adaptations to apply the VaR and CVaR approach to the conspicuous consumption setting, and implemented the models. SEBASTIAN SAGER contributed in the discussions and structured and reviewed the article before submission.

[115] T. Huschto and S. Sager. Stochastic Optimal Control in the Perspective of the Wiener Chaos. In *Proceedings of the 12th European Control Conference*, pages 3059–3064, 2013.

This conference proceedings paper is a summary of the WIENER chaos expansion method for numerically solving SDEs and SOCPs. We describe the mathematical ideas of the WIENER chaos and MALLIAVIN calculus briefly and apply them to deduce the propagator of a SDE. We adapt this concept to SOCPs, generating the novel approach for solving such problems. We illustrate the method by regarding the standard linear-quadratic stochastic regulator and compare the numerical results of the chaos approach with the analytical solution of the problem.

TONY HUSCHTO constructed the propagator using MALLIAVIN calculus and developed the mathematical ideas for solving SOCPs with the help of this approach. He implemented and an-

alyzed the numerical problem and wrote the publication. SEBASTIAN SAGER contributed in numerical discussions and the review process of the paper before submission.

[116] T. Huschto and S. Sager. Solving Stochastic Optimal Control Problems by a Wiener Chaos Approach. *Vietnam Journal of Mathematics*, 42:83–113, 2014.

This journal article extends [115] by adding more mathematical depth to the provided ideas, concepts, developments, and numerical implementations. We additionally investigate the non-linear regulator problem and compare our novel methodology with an existing direct method for stochastic control.

As first and corresponding author, TONY HUSCHTO developed and investigated the mathematical concepts and implementations that finally lead to this publication. In the course of this, he profited from the fruitful discussions with both MARK PODOLSKIJ and SEBASTIAN SAGER. Before submission, the latter contributed as well to the review process of the paper.

Thesis Overview

The thesis consists of two major parts and altogether eight chapters. The first part treats deterministic OCPs influenced by random parameters. The second part focuses on SOCPs. The chapters are structured as follows.

In Chapter 1 we introduce the classes of *OCPs* for dynamic processes described by *deterministic ODE* or *DAE* systems that are the resulting products of all ideas presented in this thesis. We survey the three major solution methodologies for these classes, namely *indirect approaches* based on PONTRYAGIN's Maximum Principle (PMP), the *dynamic programming* and *HJB principles*, and *direct approaches*. The latter idea is our method of choice for all numerical experiments on OCPs and is introduced in detail in this chapter as well.

Chapter 2 regards OCPs that are influenced by parameter disturbances. We consider two distinct ideas for introducing the parameter uncertainty. The set-based approach of *robust optimization* is compared to the stochastic viewpoint of *probabilistic optimization*. For both classes we exemplarily describe methods to efficiently reformulate the original problems into numerically solvable ones and address the important question of how to measure or budget the risk that is included. This leads us to the connections between the robust and probabilistic viewpoints and the differentiation to stochastic optimization.

In Chapter 3 we analyze the special economic problem of pricing *conspicuous consumption products in periods of recession*. We introduce the underlying mathematical model that already includes a source of uncertainty as the duration of the recession is not known beforehand. Afterwards, we focus on the numerical implementation of the problem, discretizing the recession end by a general scenario tree approach and different arrangements of the tree, and a reformulation of the time delay that is apparent within the problem. Then we enhance the model by assuming the strength of the recession to be uncertain and apply the methods of Chapter 2 to the general scenario tree setting. We discuss the strengths and weaknesses of all used ideas both from a computational and economical point of view. A major part of this chapter is a discussion of the economic implications of the time delay and of the incorporation of an uncertain recession strength in detail.

Chapter 4 introduces the general *stochastic background* needed in the further course of the thesis. We describe stochastic processes upon a probability space and specifically focus on the

Brownian motion process, its properties, and a first expansion of it. Moreover, we introduce stochastic integrals in comparison with their deterministic counterparts and present implications on differential equations.

In Chapter 5 we address the Wiener *chaos expansion* of a stochastic process. We start by considering one-dimensional Hermite polynomials and extend them stepwise to a basis of the probability space in which the investigated processes live. This is done by defining multi-dimensional Gaussian random vectors using a basis of the Hilbert space L^2. The first form of chaos expansion results. In the second part of the chapter we give an overview of Malliavin *calculus* providing a stochastic counterpart of differential calculus that is essential in the subsequent chapters. In particular, we introduce the Malliavin derivative and an integration by parts formula. With the help of this methodology, we additionally present the original form of Wiener chaos expansion, which is based upon multiple Wiener integrals instead of Hermite polynomials.

In Chapter 6 we investigate how to solve SDEs numerically with the help of the Wiener chaos expansion. Beforehand, we give a short impression on stochastic numerical integration schemes originating from their deterministic equivalents. Then we adapt the Wiener chaos expansion to SDEs with the help of Malliavin calculus. This results in the *propagator* ODE system completely describing the original SDE. In order to use this infinite-dimensional system numerically, we present truncation methods. Finally, we develop an *error analysis* for the chaos expansion of the stochastic process determined by a SDE, depending on the two dimensions of truncation. Thereby, we exemplary investigate the geometric Brownian motion before we prove a more general error estimate.

Chapter 7 we analyze *finite-horizon continuous OCPs* that are determined by *SDEs* instead of ODEs. We compare such problems to deterministic OCPs and, based on the differences, present standard methodologies to solve SOCPs. These include again *indirect methods* based on the SMP, the *HJB* approach, and *direct methods*. Thereafter, we apply the ideas of Chapters 5 and 6 to SOCPs. By deploying an expansion of the stochastic control process we obtain a reformulation of the SOCP as a completely deterministic OCP that can be solved by sophisticated methods of deterministic optimal control.

In the final Chapter 8 we investigate the performance of the novel approach to solve finite-horizon continuous SOCPs. We start by considering the linear-quadratic stochastic regulator problem and an extended nonlinear version of this problem to analyze the effects of different truncation types and order on optimal controls, objective function values, and expectations and variances of the resulting stochastic processes. Furthermore, we discuss the computational complexity of the approach and the strengths and weaknesses of the proposed methodology, also in comparison to standard approaches. We conclude with returning to the conspicuous consumption problem of Chapter 3. We treat the recession strength as a stochastic process and obtain a propagator system of DAEs.

Setup for Computational Experiments

The computational results presented throughout this thesis have been obtained on a 64-bit *Ubuntu*® *Linux™ 12.10* system running on a machine with an *Intel*® *Core™ i7 920* CPU with 2.67 GHz and 18 GB main memory. Of the CPU's four physical cores only one single core has been used.

To obtain the computational results and visualize them for this thesis, the following software packages have been used:

- MATLAB® *v.7.6.0 (R2008a)* to generate the multi-indices used within the WIENER chaos approach, to solve the propagator systems of the geometric BROWNian motion example, to generate the MUSCOD-II application source and data files, and to create the plot data files, particularly from the MUSCOD-II output,
- MUSCOD-II *v.6.0* to discretize and solve all deterministic OCPs,
- SOCSol4L to compute the reference solutions of the nonlinear stochastic regulator problem in MATLAB®,
- *gnuplot v.4.6* to visualize all computational results.

Part I

Random Parameter Optimal Control

1 The Direct Multiple Shooting Approach for Optimal Control Problems

In this introductory chapter we start by considering the class of continuous Optimal Control Problems (OCPs). These problems are the outcome of many reformulations proposed in this thesis. We analyze different approaches to solve variants of the problems numerically and discuss particularly the direct multiple shooting method, which is our method of choice for the numerical applications presented in Chapters 3 and 8. The chapter is based on the very detailed introduction to numerical methods for optimal control that can be found in [137].

1.1 Problem Formulation

Definition 1.1 (Continuous Optimal Control Problem)

A continuous OCP is a constrained infinite-dimensional optimization problem of the form

$$\min_{\boldsymbol{u}(\cdot)} \quad J(\boldsymbol{x}(\cdot), vecz(\cdot), \boldsymbol{u}(\cdot); \boldsymbol{p}) \tag{1.1a}$$

$$s.t. \quad \dot{\boldsymbol{x}}(t) = \boldsymbol{f}(t, \boldsymbol{x}(t), \boldsymbol{z}(t), \boldsymbol{u}(t); \boldsymbol{p}) \quad \forall t \in \mathcal{T}, \tag{1.1b}$$

$$0 = \boldsymbol{g}(t, \boldsymbol{x}(t), \boldsymbol{z}(t), \boldsymbol{u}(t); \boldsymbol{p}) \quad \forall t \in \mathcal{T}, \tag{1.1c}$$

$$\boldsymbol{0} \leqslant \boldsymbol{c}(t, \boldsymbol{x}(t), \boldsymbol{z}(t), \boldsymbol{u}(t); \boldsymbol{p}) \quad \forall t \in \mathcal{T}, \tag{1.1d}$$

$$\boldsymbol{0} \leqq \boldsymbol{r}(\{\boldsymbol{x}(t_i), \boldsymbol{z}(t_i)\}), \quad \{t_i\} \subset \mathcal{T}. \tag{1.1e}$$

Therein the dynamic process $\boldsymbol{x} : \mathcal{T} \to \mathbb{R}^{n_x}$ on the time horizon $\mathcal{T} \stackrel{\text{def}}{=} [t_0, t_f] \subset \mathbb{R}$ and the algebraic state $\boldsymbol{z} : \mathcal{T} \to \mathbb{R}^{n_z}$ are described by a system of Differential-Algebraic Equations (DAEs) (1.1b)–(1.1c) with Ordinary Differential Equation (ODE) right hand side function $\boldsymbol{f} : \mathcal{T} \times \mathbb{R}^{n_x} \times \mathbb{R}^{n_z} \times \mathbb{R}^{n_u} \to \mathbb{R}^{n_x}$ and algebraic equation $\boldsymbol{g} : \mathcal{T} \times \mathbb{R}^{n_x} \times \mathbb{R}^{n_z} \times \mathbb{R}^{n_u} \to \mathbb{R}^{n_z}$. It is affected by a control $\boldsymbol{u} : \mathcal{T} \to \mathbb{R}^{n_u}$ to minimize a performance index $J : \mathcal{X} \times \mathcal{Z} \times \mathcal{U} \to \mathbb{R}$ and to satisfy path constraints $\boldsymbol{c} : \mathcal{T} \times \mathbb{R}^{n_x} \times \mathbb{R}^{n_z} \times \mathbb{R}^{n_u} \to \mathbb{R}^{n_c}$ and linearly separable point constraints $\boldsymbol{r} : (\mathbb{R}^{n_x})^{m+1} \times (\mathbb{R}^{n_z})^{m+1} \to \mathbb{R}^{n_r}$ on a finite number $m + 1$ of grid points $\{t_i\} \subset \mathcal{T}$, $0 \leqslant i \leqslant m$. Moreover, the behavior of the system is affected by model parameters $\boldsymbol{p} \in \mathcal{R} \subset \mathbb{R}^{n_p}$. $\triangle$

The variable $\boldsymbol{x}(t)$ describes the system state of the dynamic process at any time instant $t \in \mathcal{T}$. We define $\mathcal{X} \stackrel{\text{def}}{=} \{\boldsymbol{x} : \mathcal{T} \to \mathbb{R}^{n_x}\}$ to be the set of all dynamic state trajectories. The variable $\boldsymbol{z}(t)$ describes the algebraic state at any time instant $t \in \mathcal{T}$ and we define $\mathcal{Z} \stackrel{\text{def}}{=} \{\boldsymbol{z} : \mathcal{T} \to \mathbb{R}^{n_z}\}$ to be the set of all algebraic state trajectories. The processes $\boldsymbol{x}(\cdot)$ and $\boldsymbol{z}(\cdot)$ can be affected by a control input $\boldsymbol{u}(t)$ at any time $t \in \mathcal{T}$. We assume the function $\boldsymbol{u} : \mathcal{T} \to \mathbb{R}^{n_u}$ to be measurable and define $\mathcal{U} \stackrel{\text{def}}{=} \{\boldsymbol{u} : \mathcal{T} \to \mathbb{R}^{n_u} \mid \boldsymbol{u} \text{ measurable}\}$ to be the set of all such control functions. Furthermore, the system state is affected by the appearance of model parameters $\boldsymbol{p} \in \mathcal{R} \subset \mathbb{R}^{n_p}$ in the system's dynamics (1.1b), path constraints (1.1d), and objective function (1.1a). In this chapter, the model parameters $\boldsymbol{p}$ are fixed.

To ensure existence and uniqueness of the DAE system's solution, we assume $f : \mathcal{T} \times \mathbb{R}^{n_x} \times \mathbb{R}^{n_u} \to \mathbb{R}^{n_x}$ to be piecewise LIPSCHITZ continuous. Furthermore, we assume the derivative of the algebraic equation g with respect to the algebraic states z to be invertible. Then by the *Implicit Function Theorem* we get a function $z(t), x(t), u(t); p)$ which solves (1.1c). We speak of an *(differential) index one DAE*, because in that case we derive an explicit ODE system by differentiating one time. Hence, we obtain existence and uniqueness of solutions as in the ODE case. The constraint function $c : \mathcal{T} \times \mathbb{R}^{n_x} \times \mathbb{R}^{n_z} \times \mathbb{R}^{n_u} \to \mathbb{R}^{n_c}$ restricts the set of admissible state and control trajectories $x(\cdot)$, $z(\cdot)$, and $u(\cdot)$. It may contain mixed path and control constraints, restrict the set of initial values $x(t_0)$, and contain boundary conditions for the trajectories. Finally, the point constraint function $r : (\mathbb{R}^{n_x})^{m+1} \times (\mathbb{R}^{n_z})^{m+1} \to \mathbb{R}^{n_r}$ imposes point-wise constraints on the states in a finite number of grid points $\{t_i\} \subset \mathcal{T}$, $0 \leqslant i \leqslant m$ that may be coupled in time. Possible uses are the specification of boundary conditions such as initial and terminal states. They need to be linearly separable to ensure decoupling in the subsequently resulting KARUSH-KUHN-TUCKER (KKT) matrix. The presented OCP of Definition 1.1 clearly is an infinite-dimensional optimization problem, the unknowns to be determined being the control trajectory $u(\cdot)$ and the resulting dynamic and algebraic state trajectores $x(\cdot)$ and $z(\cdot)$ of the process.

Problem (1.1) can be specialized to include a large number of additional characteristics. Definition 1.2 constitutes a first important extension.

Definition 1.2 (Multi-Stage OCP)

A multi-stage optimal control problem is a constrained infinite-dimensional optimization problem of the form

$$\min_{u_i(\cdot)} \quad \sum_{i=0}^{M-1} J_i(x_i(\cdot), z_i(\cdot), u_i(\cdot); p) \tag{1.2a}$$

$$\text{s.t.} \quad \dot{x}_i(t) = f_i(t, x_i(t), z_i(t), u_i(t); p) \quad \forall t \in \mathcal{T}_i, \quad 0 \leqslant i \leqslant M-1, \tag{1.2b}$$

$$0 = g_i(t, x_i(t), z_i(t), u_i(t); p) \quad \forall t \in \mathcal{T}_i, \quad 0 \leqslant i \leqslant M-1, \tag{1.2c}$$

$$x_{i+1}(t_{i+1}) = f_i^{\text{tr}}(x_i(t_{i+1}), z_i(t_{i+1})), \quad 0 \leqslant i \leqslant M-1, \tag{1.2d}$$

$$0 \leqslant c_i(t, x_i(t), z_i(t), u_i(t); p), \quad \forall t \in \mathcal{T}_i, \quad 0 \leqslant i \leqslant M-1, \tag{1.2e}$$

$$0 \leqq r_i(\{x_j(t_k), z_j(t_k)\}), \quad \{t_k\} \subset \mathcal{T}, 0 \leqslant i, j \leqslant M-1. \tag{1.2f}$$

Here the time horizon $\mathcal{T} = [t_0, t_f] \subset \mathbb{R}$ is divided into M stage intervals $\mathcal{T}_i \stackrel{\text{def}}{=} [t_i, t_{i+1}] \subset \mathbb{R}$, $0 \leqslant i \leqslant M-1$, with $t_0 < t_1 < \cdots < t_M = t_f$. On each model stage the dynamic process $x_i : \mathcal{T}_i \to \mathbb{R}^{n_{x_i}}$ and the algebraic process $z_i : \mathcal{T} \to \mathbb{R}^{n_{z_i}}$ are determined by a system of DAEs with ODE right hand side function $f_i : \mathcal{T}_i \times \mathbb{R}^{n_{x_i}} \times \mathbb{R}^{n_{z_i}} \times \mathbb{R}^{n_{u_i}} \to \mathbb{R}^{n_{x_i}}$ and algebraic right hande side function $g_i : \mathcal{T}_i \times \mathbb{R}^{n_{x_i}} \times \mathbb{R}^{n_{z_i}} \times \mathbb{R}^{n_{u_i}} \to \mathbb{R}^{n_{z_i}}$ and affected by a control $u_i : \mathcal{T}_i \to \mathbb{R}^{n_{u_i}}$ to minimize an objective $J_i : \mathcal{X}_i \times \mathcal{Z}_i \times \mathcal{U}_i \to \mathbb{R}$ and to satisfy path constraints $c_i : \mathcal{T}_i \times \mathbb{R}^{n_{x_i}} \times \mathbb{R}^{n_{z_i}} \times \mathbb{R}^{n_{u_i}} \to \mathbb{R}^{n_{c_i}}$ and linearly separable point constraints $r_i : (\mathbb{R}^{n_{x_0}} \times \cdots \times \mathbb{R}^{n_{x_{M-1}}})^{m+1} \times (\mathbb{R}^{n_{z_0}} \times \cdots \times \mathbb{R}^{n_{z_{M-1}}})^{m+1} \to \mathbb{R}^{n_{r_i}}$ on a finite number of grid points $\{t_k\} \subset \mathcal{T}$, $0 \leqslant k \leqslant m$. The M model stages of the optimization problem (1.2) are coupled via explicit transitions $f_i^{\text{tr}} : \mathbb{R}^{n_{x_i}} \times \mathbb{R}^{n_{z_i}} \to \mathbb{R}^{n_{x_{i+1}}}$ and the point constraints $r_i(\cdot)$. Again, the system's behavior is affected by fixed model parameters $p \in \mathcal{R} \subset \mathbb{R}^{n_p}$. △

Objective Functions

The performance index $J(\boldsymbol{x}(\cdot), \boldsymbol{z}(\cdot), \boldsymbol{u}(\cdot); \boldsymbol{p})$ of the OCP (1.1) evaluated on the time horizon $\mathcal{T}$ usually is a general objective function that consists of an integral contribution, the LAGRANGE type objective with integrand $L(t, \boldsymbol{x}(t), \boldsymbol{z}(t), \boldsymbol{u}(t); \boldsymbol{p})$, and an end-point contribution, the MAYER type objective $M(t_{\mathrm{f}}, \boldsymbol{x}(t_{\mathrm{f}}), \boldsymbol{z}(t_{\mathrm{f}}); \boldsymbol{p})$. Hence,

$$J(\boldsymbol{x}(\cdot), \boldsymbol{z}(\cdot), \boldsymbol{u}(\cdot); \boldsymbol{p}) = \int_{t_0}^{t_{\mathrm{f}}} L(t, \boldsymbol{x}(t), \boldsymbol{z}(t), \boldsymbol{u}(t); \boldsymbol{p}) \, \mathrm{d}t + M(t_{t_{\mathrm{f}}}, \boldsymbol{x}(t_{\mathrm{f}}), \boldsymbol{z}(t_{\mathrm{f}}); \boldsymbol{p}). \qquad (1.3)$$

Analogously, the performance indices $J_i(\cdot)$ of (1.2) are defined on each model stage horizon $\mathcal{T}_i$ for $0 \leqslant i \leqslant M-1$. For certain instances, as in Chapter 7, it is beneficial to consider only objective functions of either the LAGRANGE or MAYER type. In that case the necessary transformation can be calculated straightforwardly.

Constraint Types

In the context of the constraint functions $\boldsymbol{c}(\cdot)$ and $\boldsymbol{r}(\cdot)$ we have to distinguish several types depending on their incorporated structure. Decoupled constraints do not connect state or control trajectories at different instants in time. They can act on the entire time horizon $\mathcal{T}$ or stage horizon $\mathcal{T}_i$, $0 \leqslant i \leqslant M-1$,

$$0 \leqslant \boldsymbol{c}(t, \boldsymbol{x}(t), \boldsymbol{z}(t), \boldsymbol{u}(t); \boldsymbol{p}) \quad \forall t \in \mathcal{T} \qquad (1.4)$$

or only on certain grid points

$$0 \leqslant \boldsymbol{r}(\{\boldsymbol{x}(t_i), \boldsymbol{z}(t_i)\}) \quad \{t_i\} \subset \mathcal{T}, 0 \leqslant i \leqslant m. \qquad (1.5)$$

They inherit a separability property which is important in the context of efficient numerical algorithms, compare [137].
Coupled constraints connect the state process in finitely many grid points $t_i \in \mathcal{T}$, $0 \leqslant i \leqslant m.$,

$$0 \leqslant \boldsymbol{r}(\{\boldsymbol{x}(t_i), \boldsymbol{z}(t_i)\}) \quad \{t_i\} \subset \mathcal{T}. \qquad (1.6)$$

Common coupled constraints are boundary or periodicity constraints that act only on the initial and terminal point of the time horizon, t_0 and t_{f}. In multi-stage OCPs coupled point constraints $\boldsymbol{r}(\cdot)$ are often necessary to define transitions between state trajectories of different stages or to initialize additional state process components [118].

Variable Time Horizons

Often OCPs are stated on a fixed time horizon $\mathcal{T} = [t_0, t_{\mathrm{f}}] \subset \mathbb{R}$. But free initial or terminal times lead to variable horizon lengths. Especially in multi-stage OCPs of the form (1.2) this is a common property as switches between different model stages need not be fixed. Thus, a time transformation $t(\cdot)$ is needed to restate the OCP on a normalized control horizon $\tau \in [0,1] \subset \mathbb{R}$. We define

$$t(\tau) \stackrel{\text{def}}{=} t_0 + h\tau, \quad h = t_{\mathrm{f}} - t_0, \qquad (1.7)$$

for the OCP (1.1) and

$$t(\tau, h_i) \stackrel{\text{def}}{=} t_0 + \sum_{l=0}^{i-1} h_l + h_i \tau, \quad h_i = t_{i+1} - t_i, \, 0 \leqslant i \leqslant M - 1, \tag{1.8}$$

for a multi-stage OCP (1.2).

1.2 Solution Methods for Optimal Control Problems

Methods for finding solutions to optimal control problems of type (1.1) are generally based on very disparate ideas. Built upon BELLMAN's *Principle of Optimality* is the *dynamic programming* algorithm. Additionally, we mention *indirect approaches* emerging from PONTRYAGIN's *Maximum Principle (PMP)* and often referred to as "first optimize, then discretize" methods. In contrast to these, we give a detailed view on *direct* or "first discretize, then optimize" ideas as *collocation* and *shooting* methods. Combining the benefits of both direct approaches for optimal control, our preferred choice is the *direct multiple shooting* method. All numerical applications in this thesis focus on that framework.

For simplicity, in this section we assume that the OCP (1.1) does not include algebraic states $\mathbf{z}$.

1.2.1 Dynamic Programming

The basis of the *dynamic programming* technique arises directly from the principle of optimality stated by BELLMAN [25].

> "An optimal policy has the property that whatever the initial state and initial decision are, the remaining decisions must constitute an optimal policy with regard to the state resulting from the first decision."

Theorem 1.1 (Principle of Optimality; [25])
Let $(\mathbf{x}^\star(\cdot), \mathbf{u}^\star(\cdot))$ be the optimal solution of an OCP on the interval $\mathcal{T} = [t_0, t_f] \subset \mathbb{R}$ and let $\bar{t} \in \mathcal{T}$ be an intermediate point in that interval. Then $(\mathbf{x}^\star(\cdot), \mathbf{u}^\star(\cdot))$ is an optimal solution on $[\bar{t}, t_f] \subseteq \mathcal{T}$ for the initial value $\bar{\mathbf{x}} = \mathbf{x}^\star(\bar{t})$.   △

Thus, BELLMAN's principle says that if we have an optimal solution on the entire time horizon $\mathcal{T} = [t_0, t_f]$, then any subarc of that solution restricted on the interval $[\bar{t}, t_f]$ with $t_0 \leqslant \bar{t} \leqslant t_f$ is optimal as well, compare Figure 1.1. In general, the reverse direction does not hold. A concatenation of optimal solutions on a partition of the horizon $\mathcal{T}$ is not necessarily optimal on the entire $\mathcal{T}$. [33, 34, 76] give an extensive overview of BELLMAN's principle of optimality, the dynamic programming algorithm, and its applications in optimal control.

As we will return to the idea of dynamic programming in the context of stochastic optimal control in Chapter 7, we briefly review its fundaments.

Definition 1.3 (Continuous Cost-to-go Function)
On the time interval $[\bar{t}, t_f] \subset \mathcal{T} \subset \mathbb{R}$ the cost-to-go *function $V(\cdot)$ for problem (1.1) is defined as*

$$V(\bar{t}, \bar{\mathbf{x}}) \stackrel{\text{def}}{=} \min_{\substack{\mathbf{u}(\cdot) \\ \mathbf{x}(\bar{t}) = \bar{\mathbf{x}}}} \left\{ \int_{\bar{t}}^{t_f} L(t, \mathbf{x}(t), \mathbf{u}(t); \mathbf{p}) \, \mathrm{d}t + M(t_f, \mathbf{x}(t_f); \mathbf{p}) \right\} \tag{1.9}$$
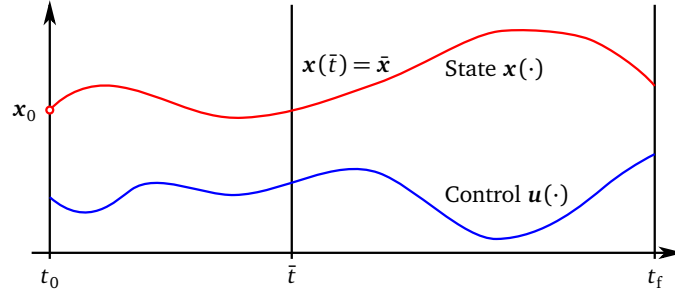
Figure 1.1: Illustration of BELLMAN's principle of optimality for an optimal solution $(x^\star(\cdot), u^\star(\cdot))$.

for feasible $x(\cdot)$ and $u(\cdot)$, where $x(\cdot)$ is defined through (1.1b). △

We consider a time grid on the horizon $\mathcal{T}$,

$$t_0 < t_1 < \ldots < t_N = t_f. \tag{1.10}$$

Constructed on this grid we obtain a recursive formulation of the cost-to-go function $V(\cdot)$.

Theorem 1.2 (Recursive Cost-to-go Function; [33])

At the time instant t_j, $0 \leqslant j \leqslant N-1$, the optimal cost-to-go function $V(\cdot)$ for problem (1.1) *can be expressed recursively as*

$$V(t_j, x_j) \overset{\text{def}}{=} V(t_{j+1}, x_{j+1}) + \min_{\substack{u(\cdot) \\ x(t_j) = x_j}} \int_{t_j}^{t_{j+1}} L(t, x(t), u(t); p) \, dt \tag{1.11}$$

with

$$x_{j+1} = x_j + \int_{t_j}^{t_{j+1}} f(t, x(t), u(t); p) \, dt \tag{1.12}$$

and feasible $u(\cdot)$. For $j = N$, i.e., $t_N = t_f$, it holds $V(t_N, x_N) \overset{\text{def}}{=} M(t_N, x_N; p)$. △

Following Theorem 1.2, we generate the dynamic programming recursion that is easily applicable to numerical computations. Therefore, we discretize the state space $\mathcal{X}$ and start from the terminal time point $t_f = t_N$ with $V(t_N, x_N) = M(t_N, x_N; p)$. By the help of the recursive cost-to-go function (1.11) we compute the optimal objective value, the value of the optimal state trajectory $x^\star(\cdot)$, and the control trajectory $u^\star(\cdot)$ for each grid point t_j in a backward iteration from $j = N-1$ to $j = 0$. Hence we need to calculate a solution to the short horizon problems (1.11) for all feasible values x_j and to tabulate the values of $V(\cdot)$ with corresponding u_j and x_j.

Equation (1.11) often appears in its continuous form. We will return to this HAMILTON-JACOBI-BELLMAN *(HJB) equation* in the stochastic context again.

Theorem 1.3 (HAMILTON-JACOBI-BELLMAN Equation; [33])

Let the optimal cost-to-go function $V(\cdot)$ of an OCP of the form (1.1) *be sufficiently smooth and*

the terminal time point t_f *fixed. Then the* HJB equation

$$-\frac{\partial V}{\partial t}(t, \boldsymbol{x}) = \min_{\boldsymbol{u}(\cdot)} \left\{ L(t, \boldsymbol{x}, \boldsymbol{u}; \boldsymbol{p}) + \frac{\partial V}{\partial \boldsymbol{x}}(t, \boldsymbol{x}) f(t, \boldsymbol{x}, \boldsymbol{u}; \boldsymbol{p}) \right\} \tag{1.13}$$
$$V(t_f, \boldsymbol{x}) = M(t_f, \boldsymbol{x}(t_f); \boldsymbol{p})$$

holds for all $t \in \mathcal{T}$ *and* $\boldsymbol{x}$ *given through* (1.1b). $\triangle$

The advantage of dynamic programming is that it searches the entire state space—at least on the chosen discrete grid—, yielding a global solution to the given optimal control problem on that grid. The inclusion of constraints is straightforward as they merely restrict the state space. Furthermore, the dynamic programming methodology provides a precomputable look-up table for the optimal control values for all feasible states. This makes it highly suitable in the context of closed-loop control, where the optimizer is interested in feedback laws, i.e., optimal control trajectories $\boldsymbol{u}^\star(\cdot)$ depending on the state $\boldsymbol{x}(\cdot)$. Nevertheless, the described requirements of discretizing the state and control space lead to the so-called "curse of dimensionality". Even for quite small problem instances the discretizations attain high dimensions and, followingly, computation times.

1.2.2 Indirect Methods Based on the PMP

Indirect methods emerge from applying the PMP to the OCP (1.1) and optimizing in an infinite-dimensional function space. Its basic idea lies in introducing *adjoint variables* that measure how much the objective function deviates depending on changes in the state trajectory $\boldsymbol{x}(\cdot)$ or the constraint functions $\boldsymbol{c}(\cdot)$, $\boldsymbol{r}(\cdot)$. Then the PMP states necessary conditions of optimality depending on the state, the control, the constraints, and the adjoint variables [120, 202]. For certain special examples these conditions can be solved analytically, however, often they are used to transform the original OCP into a Boundary Value Problem (BVP) that can be tackled numerically by *shooting* or *collocation* methods, cf. [53, 196]. Nevertheless, setting up the appropriate BVP already includes the determination of the optimal control $\boldsymbol{u}^\star(\cdot)$ and its possibly existing switching structure.

In general, indirect methods are very useful to obtain structural information on the process and the optimal solution, e.g., in economic applications by interpreting the adjoint variables as taxes and analyzing their behavior in time. As the optimization problem is solved in an infinite dimensional function space, the optimal control profiles are exact and no approximation is needed, in contrast to the direct methods presented below. In the resulting BVP all degrees of freedom for choosing the optimal control $\boldsymbol{u}^\star(\cdot)$ vanish, whereas indirect methods appear worthwhile for problems with a large number of controls. Furthermore, by the optimization in function space feedback laws $\boldsymbol{u}^\star(\boldsymbol{x}(\cdot))$ may be computed directly.

However, obtaining solutions to general OCPs is intricate in most cases. Several special cases have to be treated separately, particularly if general path and control constraints are incorporated. Then the structure of the optimal solution is not known a priori as state dependent switches may occur. The necessary conditions of optimality have to be derived analytically for every problem instance, i.e., for varying initial data, parameters, or additional constraints. Hence, indirect methods are a suitable choice for analyzing the general solution structure of an OCP, especially in selected infinite horizon settings, but are not preferred for calculating

fast numerical solutions to optimal control problems.

1.2.3 Direct Methods

In contrast to the indirect methods for optimal control that discretize the necessary optimality conditions and solve the resulting BVP, *direct methods* transform the original infinite dimensional OCP into one in finitely many degrees of freedom with finitely many constraints. In that fashion, they are often referred to as "first discretize, then optimize" methods. One can apply sophisticated and powerful ideas from nonlinear programming to finally solve the problem, i.e., the appearing KKT conditions, to optimality. Hence, direct methods are well suited for practical large-scale problems as they do not suffer from the curse of dimensionality or extensive analytical spadework.

One characteristic of these approaches is to discretize the controls $u(\cdot)$ on a finite time grid of the considered horizon $\mathcal{T}$. From an application point of view this is highly motivated as often the space $\mathcal{U}$ of feasible decisions is restricted in such a way, e.g., that boilers for chemical reactions provide only constant heating levels over prescribed time intervals, or that prices in economic problems can be set only in certain intervals.

Let a finite time grid of N intervals be given as

$$t_0 < t_1 < \ldots < t_N = t_\mathrm{f}. \tag{1.14}$$

We discretize the controls $u(\cdot)$ on this grid via

$$u(t) = \varphi_i(t, q_i) \quad \forall t \in [t_i, t_{i+1}], \, 0 \leqslant i \leqslant N-1, \tag{1.15}$$

with $q_i \in \mathbb{R}^{n_{q_i}}$ and a function $\varphi_i : [t_i, t_{i+1}] \times \mathbb{R}^{n_{q_i}} \to \mathbb{R}^{n_u}$ with compact support. The most common examples for these functions are

- piecewise constant, i.e., $u(t) = q_i \; \forall t \in [t_i, t_{i+1}]$,
- piecewise linear, i.e., $u(t) = q_{i,1} + q_{i,2}(t - t_i) \; \forall t \in [t_i, t_{i+1}]$,
- piecewise cubic, trigonometric, or cyclometric.

Certainly one may select different discretization types $\varphi_\cdot(\cdot)$ for the control trajectory components $u_j(\cdot)$, $1 \leqslant j \leqslant \mathbb{R}^{n_u}$.

Direct Single Shooting

In *direct single shooting*, going back to [111] and [219], we regard the differential state $x(\cdot)$ as dependent variable of the control $u(\cdot)$ based on the discretization (1.15). We use numerical integration techniques to obtain the state as a function $x(t; x_0, q)$ of finitely many controls $q = (q_0, \ldots, q_{N-1}) \in \mathbb{R}^{n_q}$, $n_q = n_{q_0} + \ldots + n_{q_{N-1}}$, and the initial value x_0, by solving the corresponding Initial Value Problem (IVP). After this control discretization the OCP (1.1) becomes

$$\min_{q} \quad \sum_{i=0}^{N-1} \int_{t_i}^{t_{i+1}} L(t, x(t), \varphi_i(t, q_i); p) + M(t_\mathrm{f}, x(t_\mathrm{f}); p) \tag{1.16a}$$

$$\text{s.t.} \quad \dot{x}(t) = f(t, x(t), \varphi_i(t, q_i); p) \quad \forall t \in [t_i, t_{i+1}], \, 0 \leqslant i \leqslant N-1, \tag{1.16b}$$

$$0 \leqslant c(t, x(t), \varphi_i(t, q_i); p) \quad \forall t \in [t_i, t_{i+1}], \, 0 \leqslant i \leqslant N-1, \tag{1.16c}$$

$$0 \leqq r(\{x(t_j)\}), \qquad \{t_j\} \subset \mathcal{T}. \tag{1.16d}$$

Problem (1.16) can be summarized as a Nonlinear Program (NLP) in the unknowns $(\boldsymbol{x}_0, \boldsymbol{q}) \in \mathbb{R}^{n^x + n^q}$ and finally be solved by appropriate NLP methods like Sequential Quadratic Programming (SQP) techniques [94, 191, 247].
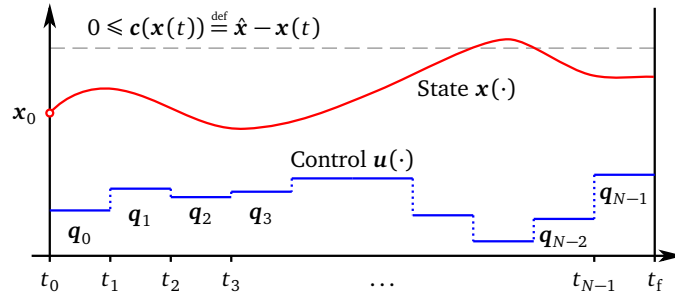
Figure 1.2: Illustration of the direct single shooting approach applied to an optimal control problem.

As the constraints $\boldsymbol{c}(\cdot)$ and $\boldsymbol{r}(\cdot)$ are often discretized to hold only on the finite grid (1.14), instead of the time intervals $[t_i, t_{i+1}]$, solutions might be obtained that are feasible for the single shooting problem (1.16) but not the original OCP (1.1) (compare Figure 1.2 as well). Hence, a relaxation of the constraints, including them in the objective function via penalty terms, or refining the time grid might become important. Besides this property of direct single shooting, there are a number of additional drawbacks of the method. As the resulting NLP depends only on the initial value $\boldsymbol{x}_0$ of the state and the control variables $\boldsymbol{q}$, it is essential to use initial guesses that are already close to the optimal solution. For certain chosen initializations the solution to the induced IVP need not exist as the process might evolve into singularities over time. Aside from that, error propagation of the integration procedure may thwart the numerical computation of the solution. Initial guesses within such a small convergence region are certainly hard to detect in practice. Moreover, even if prior insight in the behavior of the process exists, it cannot be used in the direct single shooting framework. From the NLP perspective the nonlinearities probably included in the ODE system of (1.1) are often challenging and small changes in the initial data may cause large changes in the solution or severe constraint violations. Nevertheless, direct single shooting is popular in practice due to its plain idea and implementation, with the resulting NLP inheriting a comparatively small number of unknowns.

Direct Collocation

The basic idea of *collocation* methods is to *not* regard the state $\boldsymbol{x}(\cdot)$ as a dependent variable, but to solve simulation and optimization tasks at the same time. Therefore, collocation is often named a simultaneous—or all-at-once—approach. In the context of BVPs it has been introduced in [214, 240], generalizations to OCPs go back to [20, 40, 239].
Again we define a (fine) grid

$$t_0 < t_1 < \ldots < t_N = t_{\mathrm{f}}$$

and denote $h_i = t_{i+1} - t_i$, $0 \leqslant i \leqslant N - 1$. Then on each such interval $[t_i, t_{i+1}]$ we consider an additional partition into K subintervals, i.e., $0 = \tau_0 < \tau_1 < \ldots < \tau_K = 1$, resulting in $t = t_i + \tau h_i$ with $\tau \in [0, 1]$ and $t \in [t_i, t_{i+1}]$. The state $\boldsymbol{x}(\cdot)$ is interpolated on $[t_i, t_{i+1}]$ with polynomials of degree K, e.g., LAGRANGE polynomials, yielding a discretization using K new

optimization variables of dimension n^x per interval $[t_i, t_{i+1}]$, $0 \leqslant i \leqslant N - 1$. The controls may be discretized in a different way, however, often this is performed on the same time grid by one of the control discretizations (1.15) defined above. Note that the state trajectory $x(\cdot)$ needs to be continuous, which is ensured by introducing continuity conditions, i.e., adding nonlinear equality constraints at the time instants t_i, $1 \leqslant i \leqslant N$. General path and point constraints are treated by enforcing their discretized counterparts on the collocation grid points.

Hence, the collocation approach results in a large but sparse NLP that again can be solved by powerful methods like tailored SQP or sparse interior point methods [42, 242].

Compared to direct single shooting, in direct collocation a priori information of the system's behavior can be included in the resulting NLP by appropriate initialization of the state trajectory variables. Further on, the spreading of perturbations in computing the state trajectory can be reduced by allowing small violations of the introduced matching conditions in the course of the NLP solution. The convergence region of direct collocation is thus highly enlarged.

A difficulty in collocation approaches is the use of *adaptive* solvers for the included ODE system. For treating highly nonlinear or stiff systems this may be of particular importance in order to obtain satisfying solutions. In collocation this can only be overcome by large numbers K of subintervals.

1.3 BOCK's Direct Multiple Shooting Method for Optimal Control

Like for the single shooting approach, the basis of *multiple shooting* can be found in solution methods for BVPs, compare [45, 53, 196]. In the context of OCPs the direct multiple shooting idea goes back to work of HANS GEORG BOCK [46, 201]. It is a hybrid method of the aforementioned approaches in the sense that it combines the advantages of collocation and direct single shooting. I.e., discretizing the state trajectory allows the incorporation of a priori knowledge of the process via state initialization, while still solving underlying IVPs and, therefore, being able to rely on efficient adaptive solvers [5, 6, 22, 80, 200]. Furthermore, with direct multiple shooting stability of the solution is heavily improved and the influences of nonlinearities are compensated [8]. All numerical computations of OCPs within this thesis are performed using the direct multiple shooting software MUSCOD-II. A detailed description of it can be found in [160].

Let us consider the OCPs (1.1) or (1.2), assuming all appearing functions to be twice continuously differentiable with respect to the unknowns of the problem. Again we discretize the controls $u(\cdot)$ on a (coarse) time grid to obtain a computationally tractable representation of our original problem. Therefore, let

$$t_0 < t_1 < \ldots < t_N = t_f$$

be a (not necessarily equidistant) partition of $\mathcal{T} = [t_0, t_f]$ as in (1.14), that we will denote as the *shooting grid* $\{t_i\}$ from now on. To keep notations simple, in the following we assume this grid to coincide with the grid induced by the point constraints $r(\cdot)$ as introduced in (1.1e). Of course, all methodological ideas presented now can be derestricted to hold for differing shooting and constraint grids. On each interval $[t_i, t_{i+1}]$, $0 \leqslant i \leqslant N - 1$, we use a control

discretization (1.15), i.e.,

$$\boldsymbol{u}_i(t) = \boldsymbol{\varphi}_i(t, \boldsymbol{q}_i),$$

with base functions $\boldsymbol{\varphi}_i \colon [t_i, t_{i+1}] \times \mathbb{R}^{n_{q_i}} \to \mathbb{R}$ that need not be equal for each component of the control trajectory. We require local support of the base functions to ensure separability of the discretized problem. For certain discretization types, e.g., piecewise linear control base functions, one may claim continuity of the control trajectory even after discretization. Therefore one has to add continuity conditions on $\boldsymbol{u}(\cdot)$ in all points of the shooting grid $\{t_i\}$. Obviously, the choice of control discretization type $\varphi.(\cdot)$ directly influences the quality of the approximated solution to the original OCP. More information on that can be found in, e.g., [138].

Additional to the control discretization that is equivalent to the direct single shooting approach in Section 1.2.3, we use a parameterization of the dynamic and algebraic state trajectories $\boldsymbol{x}(\cdot)$ and $\boldsymbol{z}(\cdot)$ on the shooting grid $\{t_i\}$. To that end, we introduce auxiliary initial values $\boldsymbol{s}_i^x \in \mathbb{R}^{n_x}$, $\boldsymbol{s}_i^z \in \mathbb{R}^{n_z}$, $0 \leqslant i \leqslant N-1$, with $\boldsymbol{s}_0^x = \boldsymbol{x}_0$, $\boldsymbol{s}_0^z = \boldsymbol{z}_0$ to obtain N separated IVPs on the time intervals $[t_i, t_{i+1}] \subset \mathcal{T}$, i.e.,

$$\dot{\boldsymbol{x}}_i(t) = \boldsymbol{f}(t, \boldsymbol{x}_i(t), \boldsymbol{z}_i(t), \boldsymbol{\varphi}_i(t, \boldsymbol{q}_i); \boldsymbol{p}) \quad \forall t \in [t_i, t_{i+1}], \quad 0 \leqslant i \leqslant N-1, \tag{1.17a}$$

$$0 = \boldsymbol{g}(t, \boldsymbol{x}_i(t), \boldsymbol{z}_i(t), \boldsymbol{\varphi}_i(t, \boldsymbol{q}_i); \boldsymbol{p}) \quad \forall t \in [t_i, t_{i+1}], \quad 0 \leqslant i \leqslant N-1, \tag{1.17b}$$

$$\boldsymbol{x}_i(t) = \boldsymbol{s}_i^x, \tag{1.17c}$$

$$\boldsymbol{z}_i(t) = \boldsymbol{s}_i^z. \tag{1.17d}$$

As in direct single shooting, this allows to apply sophisticated integrators to obtain the solutions on each time interval, see [5, 6, 23]. We have to assure consistency of the algebraic equations

$$0 = \boldsymbol{g}(t, \boldsymbol{x}_i(t), \boldsymbol{z}_i(t), \boldsymbol{\varphi}_i(t, \boldsymbol{q}_i); \boldsymbol{p}) \quad \forall t \in [t_i, t_{i+1}], \quad 0 \leqslant i \leqslant N-1. \tag{1.18}$$

Additionally, we have to insert *matching conditions* as in collocation to ensure continuity of transitions between adjacent intervals, i.e., of the state trajectories $\boldsymbol{x}(\cdot)$ over the entire horizon $\mathcal{T}$,

$$\boldsymbol{0} = \boldsymbol{x}_i(t_{i+1}; t_i, \boldsymbol{s}_i^x, \boldsymbol{s}_i^z, \boldsymbol{q}_i) - \boldsymbol{s}_{i+1}^x, \quad 0 \leqslant i \leqslant N-1. \tag{1.19}$$

Therein, the term $\boldsymbol{x}_i(t_{i+1}; t_i, \boldsymbol{s}_i^x, \boldsymbol{s}_i^z, \boldsymbol{q}_i)$ denotes the terminal value of the integrated trajectory, i.e., the solution of the IVP (1.17), in the interval $[t_i, t_{i+1}]$ when the initial values $\boldsymbol{s}_i^x$, $\boldsymbol{s}_i^z$ and control values $\boldsymbol{q}_i$ are chosen.

The resulting vector of unknowns of the multiple shooting approach for the OCP (1.1) is given by

$$\boldsymbol{w} \stackrel{\text{def}}{=} \left(\boldsymbol{s}_0^x, \boldsymbol{s}_0^z, \boldsymbol{q}_0, \ldots, \boldsymbol{s}_{N-1}^x, \boldsymbol{s}_{N-1}^z, \boldsymbol{q}_{N-1}, \boldsymbol{s}_N^x, \boldsymbol{s}_N^z \right) \in \mathbb{R}^{(N+1)n_x + (N+1)n_z + n_q} \tag{1.20}$$

The number of unknowns in $\boldsymbol{w}$ can be reduced to the number of unknowns in the single shooting approach by applying *condensing* techniques. An extensive introduction to that topic can be found in [137, 160].

In the multi-stage case of OCP (1.2) with free transition times t_j between adjacent stages an additional time transformation as in (1.8) is necessary for constructing the final NLP. This
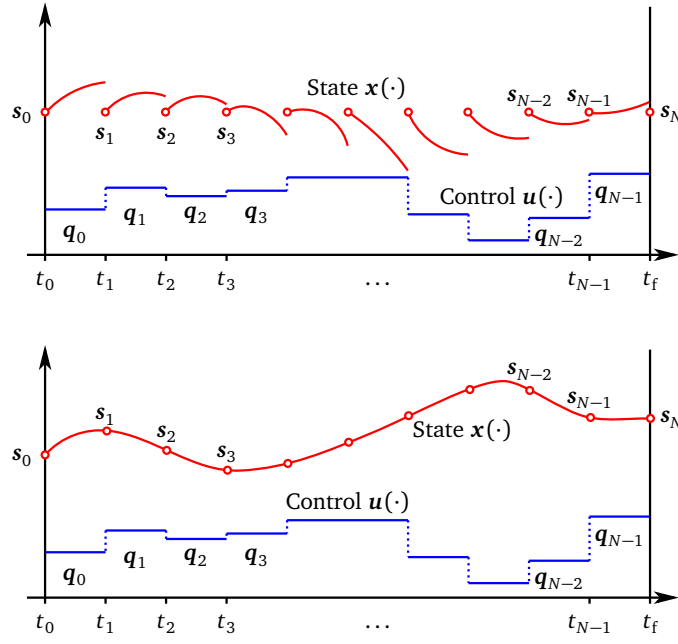
Figure 1.3: Illustration of the direct multiple shooting approach for OCPs. The *top* figure shows the initial situation of the method. An initialization of the shooting nodes is chosen and the matching conditions of the IVPs are possibly violated. The *bottom* figure then shows a converged solution of the resulting NLP with satisfied matching conditions.

requires the reformulation of the DAE description of the state on model stage j, $0 \leqslant j \leqslant M-1$, following

$$\frac{\mathrm{d}\boldsymbol{x}_j}{\mathrm{d}\tau}(\tau) \overset{\text{def}}{=} h_j \boldsymbol{f}_j(t(\tau, h_j), \boldsymbol{x}_j(\tau), \boldsymbol{z}_j(\tau), \varphi_j(\tau, \boldsymbol{q}_j); \boldsymbol{p}), \tag{1.21a}$$

$$0 = \boldsymbol{g}_j(t(\tau, h_j), \boldsymbol{x}_j(\tau), \boldsymbol{z}_j(\tau), \varphi_j(\tau, \boldsymbol{q}_j); \boldsymbol{p}). \tag{1.21b}$$

The multiple shooting idea then is applicable to every model stage j using N_j shooting nodes, resulting in a vector of unknowns per stage that is given by

$$\boldsymbol{w}_j \overset{\text{def}}{=} \left(\boldsymbol{s}_{j,0}^x, \boldsymbol{s}_{j,0}^z, \boldsymbol{q}_{j,0}, \ldots, \boldsymbol{s}_{j,N_j-1}^x, \boldsymbol{s}_{j,N_j-1}^z, \boldsymbol{q}_{j,N_j-1}, \boldsymbol{s}_{j,N_j}^x, \boldsymbol{s}_{j,N_j}^z, h_j\right), \tag{1.22}$$

eventually yielding

$$\boldsymbol{w} \overset{\text{def}}{=} \left(\boldsymbol{w}_j\right)_{0 \leqslant j \leqslant M-1}. \tag{1.23}$$

In both cases (1.1) and (1.2) the objective function is separable, making it computable separately on each corresponding interval and model stage. The path constraint function $\boldsymbol{c}(\cdot)$ is discretized to hold only on the multiple shooting grid $\{t_i\}$, i.e.,

$$\boldsymbol{0} \leqslant \boldsymbol{c}_i(t_i, \boldsymbol{s}_i^x, \boldsymbol{s}_i^z, \varphi_i(t_i, \boldsymbol{q}_i); \boldsymbol{p}), \quad 0 \leqslant i \leqslant N, \tag{1.24}$$

where $N = \sum_j N_j$ denotes the total number of shooting nodes for discretizing the time horizon $\mathcal{T}$. This discretization generally enlarges the feasible set of solutions to the discretized OCP in comparison with the original continuous one. It certainly affects the optimal solution

in a way such that there may occur constraint violations between grid points. In most application instances those violations are negligible. If they have a severe influence on the solution or if feasibility is necessary on the entire time horizon $\mathcal{T}$, they might be overcome by choosing adapted, finer multiple shooting grids or using semi-infinite programming techniques for tracking constraint violations [203, 204].

The resulting NLP of the direct multiple shooting method after applying the presented ideas reads

$$\min_{s^x, s^z, q} \quad \sum_{i=0}^{N} E_i(t_i, s_i^x, s_i^z, q_i; p) \tag{1.25a}$$

$$\text{s.t.} \quad 0 = x_i(t_{i+1}; t_i, s_i^x, s_i^z, q_i) - s_{i+1}^x, \quad 0 \leqslant i \leqslant N-1, \tag{1.25b}$$

$$0 = g_i(t_i, s_i^x, s_i^z, q_i; p), \quad 0 \leqslant i \leqslant N-1, \tag{1.25c}$$

$$0 \leqslant c_i(t_i, s_i^x, s_i^z, \varphi_i(t_i, q_i); p), \quad 0 \leqslant i \leqslant N, \tag{1.25d}$$

$$0 \leqq r_i(t_i, s_i^x, s_i^z, \varphi_i(t_i, q_i)), \quad 0 \leqslant i \leqslant N, \tag{1.25e}$$

where $E_i(\cdot)$ summarizes the separately computed objective function of each interval.

This NLP incorporates more variables than the direct single shooting NLP, but the special structure of this program can be exploited efficiently. This is especially due to the separability of the objective function and the constraints $c(\cdot)$ and $r(\cdot)$ with respect to the unknowns (s_i, q_i), which follows from the control discretization (1.15). Only the matching conditions (1.19) couple unknowns on adjacent shooting nodes.

Eventually, constrained NLP or specially tailored SQP techniques [162] are employed to solve (1.25), including an efficient exploitation of structures in the NLP and the efficient treatment of algebraic terms through relaxations [161]. Therein, the principle of *Internal Numerical Differentiation (IND)* is used to derive the sensitivities of the ODE or DAE solution [5, 6] and a *condensing* algorithm [46, 162] to obtain small dense Quadratic Programs (QPs) that are solved within each SQP iteration to progress towards the NLP solution. For further details we refer to, e.g., [5, 73, 84, 137, 160, 161, 162, 230]. Here, we would only like to mention one advantage of the direct multiple shooting approach that will be beneficial for the computations of Chapter 3. Because control functions, constraints, and multiple shooting variables are—preferably—discretized on a common grid, the HESSian of the LAGRANGian $\mathcal{L}(\cdot)$ is block-structured for linearly coupled point constraints (1.1e)/(1.2f). When $i \neq j$

$$\frac{\nabla^2 \mathcal{L}(w_1, \ldots, w_N)}{\partial w_i \partial w_j} = 0$$

holds for the variable vectors w_j, $j = 0, \ldots, M-1$. This allows applying BROYDEN-FLETCHER-GOLDFARB-SHANNO (BFGS) updates to every single multiple shooting block [46]. These *high-rank updates* typically lead to a fast accumulation of higher order information and, thus, to fast convergence [191].

Alternative methods to the condensing approach include the use of structure-exploiting linear algebra, complementary condensing [139], or nonsmooth NEWTON techniques [96]

1.4 Summary

In this introductory chapter we defined the classes of OCPs that are crucial for the remaining work in thesis. The underlying dynamic processes of the problems are modeled by ODE systems. In particular, we addressed multi-stage OCPs that we will return to in the following chapter.

We surveyed numerical approaches for solving this class of problems. Our method of choice for the remainder of the thesis is the direct multiple shooting method, a state-of-the-art simultaneous approach for solving optimization and simulation tasks at the same time. Direct multiple shooting combines the advantages of direct single shooting and collocation, creating highly structured NLPs, allowing the use of sophisticated adaptive solvers for the included IVPs, and thus yielding excellent convergence properties.

2 Optimal Control Problems with Uncertain Parameters

We start our work on Optimal Control Problems (OCPs) that are determined by uncertain influences by investigating problems where the disturbances are modeled by parameters that we do not have complete information about. We survey two distinct ideas on how to introduce the uncertainty through those parameters and address the question on how we can measure the risk that is involved by them. Exemplarily, we consider and discuss several approaches to tackle OCPs including uncertain parameters, depending on the preferences of the optimizer and the origin and implications of the problem to be solved.

This introduction is mainly based on [38, 211]. In a condensed form, focussing on the approaches and their discussion, it appears in [117].

2.1 Robust Optimization

In optimization we often have to deal with situations, where the problem is affected by external disturbances or uncertainties in the parameters. In most cases the corresponding solutions are very sensitive to even small perturbations in these influences, which may cause different or even critical results when applying controls of the undisturbed problem in reality. Therefore, appropriate controls have to be determined to guarantee a certain kind of robustness against the uncertainties.

Starting with the traditional robust control theory [77, 254], which concentrates mainly on stability and tractability assertions, there grew two basic approaches to incorporating parameter uncertainty into optimization problems, which appear quite disparate at first sight. While in *robust optimization* the uncertainty model is basically deterministic and *set-based,* the second perspective builds upon a *probabilistic* description of the uncertainty. We will take a closer look on this second idea in the subsequent Section 2.2.

The fundaments of robust optimization lie in the development of *decision theory* and *worst-case analysis*. In the context we are considering here, pioneering work has been done by AHARON BEN-TAL and ARKADI NEMIROVSKI [26, 27] and LAURENT EL GHAOUI [81, 82]. As the decision-makers look for solutions that are feasible for *any* realization of uncertainty in a given set, important topics of robust optimization are tractability of the problems, conservativeness of the obtained solutions, and predictions on probabilistic guarantees determined a priori depending on the size and structure of the considered uncertainty set. In [38] this is referred to as the *budget of uncertainty,* addressing the compromise the decision-maker has to make between robustness or probabilistic protection and performance.

Let us start by considering the OCP

$$\min_{\boldsymbol{x}(\cdot), \boldsymbol{u}(\cdot)} \quad J(\boldsymbol{x}(\cdot), \boldsymbol{u}(\cdot); \boldsymbol{p}) \tag{2.1a}$$

$$\text{s.t.} \quad \dot{\boldsymbol{x}}(t) = \boldsymbol{f}(\boldsymbol{x}(t), \boldsymbol{u}(t); \boldsymbol{p}), \qquad t \in \mathcal{T}, \, \boldsymbol{p} \in \mathcal{R}, \tag{2.1b}$$

$$0 \geqslant \boldsymbol{c}(\boldsymbol{x}(t), \boldsymbol{u}(t); \boldsymbol{p}), \qquad t \in \mathcal{T}, \, \boldsymbol{p} \in \mathcal{R}, \tag{2.1c}$$

$$\boldsymbol{x}(t_0) = x_0 \tag{2.1d}$$

with the state process $\boldsymbol{x} : \mathcal{T} \to \mathbb{R}^{n_x}$ defined on the time horizon $\mathcal{T} = [t_0, t_\mathrm{f}]$, control $\boldsymbol{u} : \mathcal{T} \to \mathbb{R}^{n_u}$, and model parameters $\boldsymbol{p} \in \mathcal{R} \subset \mathbb{R}^{n_p}$. The smooth real valued functions $J, \boldsymbol{f}, \boldsymbol{c}$ characterize the objective (2.1a), state dynamics defined by the Ordinary Differential Equation (ODE) (2.1b) and path constraints (2.1c), respectively.

In optimization under uncertainty the interest focuses particularly on the constraints $\boldsymbol{c}(\cdot)$, depending on the parameters $\boldsymbol{p}$. In the robust optimization approach those parameters are considered to originate from an *uncertainty set* $\mathcal{R}$. Based on that classification, one searches to find a solution that is independent of the de facto occurring data, i.e., feasible for all realizations of $\boldsymbol{p} \in \mathcal{R}$. Thus, the sets of all state and control trajectories (cf. Definition 1.1) depend on the parameter $\boldsymbol{p}$ and we denote $\mathcal{X}(\mathcal{R}) \stackrel{\text{def}}{=} \{\boldsymbol{x} : \mathcal{T} \to \mathbb{R}^{n_x} \mid \boldsymbol{p} \in \mathcal{R}\}$, $\mathcal{X}(\mathcal{R}) \stackrel{\text{def}}{=} \{\boldsymbol{x} : \mathcal{T} \to \mathbb{R}^{n_x} \mid \boldsymbol{p} \in \mathcal{R}\}$.

In traditional worst-case analysis, the set $\mathcal{R}$ is the overall domain the parameters $\boldsymbol{p}$ can be located in, but in modern robust optimization $\mathcal{R}$ is regarded much more differentiatedly. It is used to express the decision-makers preferences. The bigger it is, the lower the objective will be as we can relate the size of $\mathcal{R}$ to the number of constraints $\boldsymbol{c}(\cdot)$ that have to be satisfied. I.e., if we consider a continuous uncertainty set, we obtain an infinite number of constraints $\boldsymbol{c}(\cdot)$ that need to be satisfied. In the same way, the bigger the uncertainty set is, the smaller we can expect the probability of failure to be. Hence, robust optimization has to deal with the question of how to choose $\mathcal{R}$ in order to stipulate the extent of safety compared to the expected return, while keeping the problem tractable at the same time.

As indicated in Equation (2.1a), the objective function $J(\cdot)$ can comprise a dependency on the uncertain parameter $\boldsymbol{p}$ as well. In some problem instances it is beneficial to transfer the uncertainty included in the objective to an additional constraint by introducing an auxiliary state variable, cf. [211]. Then the resulting objective is left unaffected by uncertain parameters. However, here we leave the cost function $J(\cdot)$ unchanged. Constraints, that are unaffected by uncertainty are integrated in the framework of (2.1c) by assuming that the corresponding part of the compounded entire uncertainty set $\mathcal{R}$ is only a singleton.

If we consider the OCP (2.1) depending on $\boldsymbol{p}$ within an abstract uncertainty set $\mathcal{R}$, it is not at all clear when we can efficiently solve this problem. In general, the robust counterpart to an arbitrary convex optimization problem is often intractable [26, 38]. For linear problems a lot of progress has been made, cf. [27, 28, 36, 37], but already robust quadratic optimization leads to semi-definite problems. [38] gives many examples, ideas, and references on research about these problems and how to at least efficiently approximate solutions to them.

[38] proposes several important types of uncertainty sets $\mathcal{R}$, each one including a specific possibility to control its size and, therefore, the adaptivity to the decision-maker's preferences. The most prominent example, which will as well be the center of attention when we come to incorporating the ideas of robust optimization to the OCP (2.1), is the *quadratic* or *ellipsoidal*

uncertainty set

$$\mathcal{R}^{\mathrm{Q}}(\varpi) = \left\{ \boldsymbol{p} \,\middle|\, (\boldsymbol{p} - \bar{\boldsymbol{p}})^T \Sigma^{-1} (\boldsymbol{p} - \bar{\boldsymbol{p}}) \leqslant \varpi^2 \right\}, \tag{2.2}$$

which has been initiated in linear problems in [27, 81, 82]. Therein, we consider all parameters $\boldsymbol{p}$ that are located within an ellipsoid around the mean vector $\bar{\boldsymbol{p}}$. This ellipsoid is characterized by the confidence parameter ϖ and tilted by the covariance Σ of the parameters. By choosing this type of uncertainty set, the main focus lies on the first two moments of the uncertainty and no additional information about the specific underlying distribution is needed. By controlling ϖ (or the covariance, if this is due to, e.g., educated guesses) the already designated budget of uncertainty receives a more tangible meaning.

Apart from the ellipsoidal uncertainty set, [36] introduces *cardinality constrained uncertainty sets*, where each component of the parameter has to lie in an interval around its nominal value. Then the decision-maker has the possibility to control the total weight of deviation from this nominal value within the corresponding intervals. By that means, the number of parameters that are allowed to deviate imply the budget of desired uncertainty. Additionally, by that approach one is able to consider worst cases for a selected subset of parameter components. Certainly, this idea makes the arising robustified problem much more conservative in comparison to the other mentioned methods, but as a side effect it causes it to become insensitive against model uncertainties as well. In general, analyzing cardinality constrained uncertainty sets leads to nonconvex problems. But particularly in linear robust optimization it allows for a tractable reformulation by taking the natural convex relaxation and a dual formulation of the inner maximization problem (i.e., the one corresponding to the constraints) [36].

The *norm uncertainty set* provided in [37] describes the uncertainty by using general norms, like ℓ_1-, ℓ_2,- or ℓ_∞-norms. This procedure has the advantage of obtaining a convex optimization problem if the constraints have to be satisfied with respect to the appropriate dual norms.

Robust Control

Let us return to the ellipsoidal uncertainty set $\mathcal{R}^{\mathrm{Q}}(\varpi)$. The constraint $\boldsymbol{c}(\boldsymbol{x}(\cdot), \boldsymbol{u}(\cdot); \boldsymbol{p}) \leqslant 0$ in the OCP (2.1) is substituted by

$$0 \geqslant \max_{\|\boldsymbol{p} - \bar{\boldsymbol{p}}\|_{2, \Sigma^{-1}} \leqslant \varpi} \boldsymbol{c}(\boldsymbol{x}(t), \boldsymbol{u}(t); \boldsymbol{p}), \quad t \in \mathcal{T}, \tag{2.3}$$

depending on the nominal (or mean return) vector $\bar{\boldsymbol{p}}$, the covariance matrix Σ, and the desired confidence level ϖ. This formulation clearly includes the traditional worst-case analysis, where the goal is to eliminate all possible risk. However, even if the considered uncertainty set is restricted by ϖ, the resulting problem will be a semi-infinite for continuous $\mathcal{R}^{\mathrm{Q}}(\varpi)$. This necessitates approximations of (2.3) to make the resulting optimization problem numerically solvable.

Linearization

A first idea to approximate the robust problem with constraint (2.3) was proposed in [74, 175, 185]. If the constraint function is monotone within the parameter set and can be approximated

by a suitable TAYLOR expansion, it follows that up to first order we have

$$\max_{\|p-\bar{p}\|_{2,\Sigma^{-1}} \leqslant \varpi} c(x(\cdot),u(\cdot);p) \approx c(x(\cdot),u(\cdot);\bar{p}) + \varpi \left\| \frac{\mathrm{d}}{\mathrm{d}p} c(x(\cdot),u(\cdot);\bar{p}) \right\|_{2,\Sigma} \qquad (2.4)$$

with the notations as used before. Thus, we can reformulate the given OCP by replacing the constraint (2.3) by the linearization (2.4).

The remaining question is how to deal with the uncertainty within the objective function $J(\cdot)$. The most common variants are inserting the nominal value $\bar{p}$, i.e.,

$$\tilde{J}(x(\cdot),u(\cdot);p) = J(x(\cdot),u(\cdot);\bar{p}),$$

relying on an expectation

$$\tilde{J}(x(\cdot),u(\cdot);p) = \mathbb{E}[J(x(\cdot),u(\cdot);p)],$$

or using the measure already applied to the constraint. The latter idea results in optimizing over a (possibly different) uncertainty set depending on the characteristics of the random parameter p to a confidence level ϖ_0.

Then we can finally reformulate the original OCP (2.1) as

$$
\begin{aligned}
\min_{x(\cdot),u(\cdot)} \quad & \tilde{J}(x,u;p) \\
\text{s.t.} \quad & \dot{x}(t) = f(x(t),u(t);\bar{p}), && t \in \mathcal{T}, \\
& 0 \geqslant c(x(t),u(t);\bar{p}) + \varpi \left\| \frac{\mathrm{d}}{\mathrm{d}p} c(x(\cdot),u(\cdot);\bar{p}) \right\|_{2,\Sigma}, && t \in \mathcal{T}, \\
& x(t_0) = x_0,
\end{aligned}
\qquad (2.5)
$$

depending on the choice of objective function $\tilde{J}(\cdot)$.

The Sigmapoint Approach

An alternative approach to solve robust OCPs was proposed in [207]. It is based on the *Unscented Transformation* technique [108, 128] for propagating distributed information through given nonlinear models. This idea allows to combine a moderate computational effort of the linearized worst-case formulation with the higher accuracy of, e.g. a high-order TAYLOR approximation of the constraint (2.3). The fundamental idea of the unscented transformation is to choose modified constraints $\tilde{c}(x(\cdot),u(\cdot);p)$ such that satisfying these new constraints results in satisfying the original constraints $c(x(\cdot),u(\cdot);p)$ for all parameters p within the critical subspace for a given probability level ζ, i.e.,

$$\tilde{c}(x(\cdot),u(\cdot);p) \leqslant 0 \quad \Rightarrow \quad \mathbb{P}[c(x(\cdot),u(\cdot);p) \leqslant 0] \geqslant \zeta.$$

Possible choices of the modified constraints are the principal axis endpoints of the constraint distribution. But in order to identify these endpoints, the mapping of the parameter distribution onto the constraints has to be known, which is often difficult. A remedy to this is using so-called *sigmapoints* with corresponding weights and propagate these through the underlying

model. If the weighted sigmapoints approximate the distribution of the parameters $\boldsymbol{p}$, one can approximate the distribution of the constraints by that means, cf. [128]. As [129] showed, this allows to match the first two moments of the constraint distribution exactly.

One choice for choosing the modified constraints $\tilde{\boldsymbol{c}}(\cdot)$ (using parameters that are normally distributed) is

$$\tilde{\boldsymbol{c}}(\boldsymbol{x}(\cdot), \boldsymbol{u}(\cdot); \boldsymbol{p}_i) = \boldsymbol{c}(\boldsymbol{x}(\cdot, \boldsymbol{u}(\cdot); \bar{\boldsymbol{p}}) + \varpi \|\boldsymbol{c}(\boldsymbol{x}(\cdot), \boldsymbol{u}(\cdot); \bar{\boldsymbol{p}}) - \boldsymbol{c}(\boldsymbol{x}(\cdot), \boldsymbol{u}(\cdot); \boldsymbol{p}_i)\|_2, \qquad i = 0, \dots, 2n_p, \tag{2.6a}$$

with the sigmapoints

$$\boldsymbol{p}_0 = \bar{\boldsymbol{p}}, \tag{2.6b}$$
$$\boldsymbol{p}_i = \bar{\boldsymbol{p}} + \sqrt{\Sigma_i}, \quad i = 1, \dots, n_p, \tag{2.6c}$$
$$\boldsymbol{p}_{n_p+i} = \bar{\boldsymbol{p}} - \sqrt{\Sigma_i}, \quad i = 1, \dots, n_p,, \tag{2.6d}$$

cf. [207]. Therein, $\bar{\boldsymbol{p}}$ is the nominal parameter of dimension n_p, Σ_i is the i-th row or column of the covariance matrix Σ, and ϖ again some predefined confidence level.

For not normally distributed parameters the resulting approximation of the constraint distribution may be erroneous, which can cause bad approximations of the robust solutions. Still, industrial applications [207] have shown that using modified constraints

$$\tilde{\boldsymbol{c}}(\boldsymbol{x}(\cdot), \boldsymbol{u}(\cdot); \boldsymbol{p}_i) = \boldsymbol{c}(\boldsymbol{x}(\cdot), \boldsymbol{u}(\cdot); \boldsymbol{p}_i) \tag{2.7}$$

instead of (2.6a), with the sigmapoints defined as in (2.6b)–(2.6d), leads to reasonable approximations, even if the parameters are not normally distributed.

Thus, the resulting robust OCP becomes

$$\begin{aligned}
\min_{\boldsymbol{x}(\cdot), \boldsymbol{u}(\cdot)} \quad & \tilde{J}(\boldsymbol{x}, \boldsymbol{u}; \boldsymbol{p}) \\
\text{s.t.} \quad & \dot{\boldsymbol{x}}(t) = \boldsymbol{f}(\boldsymbol{x}(t), \boldsymbol{u}(t); \boldsymbol{p}_i), \qquad t \in \mathcal{T}, \quad i = 0, \dots, n_p, \\
& 0 \geqslant \tilde{\boldsymbol{c}}(\boldsymbol{x}(t), \boldsymbol{u}(t); \boldsymbol{p}_i), \qquad t \in \mathcal{T}, \quad i = 0, \dots, n_p, \\
& \boldsymbol{x}(t_0) = \boldsymbol{x}_0,
\end{aligned} \tag{2.8}$$

where the objective function $\tilde{J}(\cdot)$ is given as in the previous paragraph, including possible formulations based on the introduced sigmapoints.

2.2 Coherence and Probabilistic Optimization

The second basic approach to optimization under uncertainty is premised on the assumption that the decision-maker has certain knowledge about the probabilistic behavior of the uncertain parameter $\boldsymbol{p} \in \mathcal{R}$. Instead of restricting this parameter set to fit specific perceptions and desiring to obtain feasibility of the solution for all parameters $\boldsymbol{p}$ within the (possibly restricted and size-controlled) uncertainty set, here we consider the entire set $\mathcal{R}$, but adjust the expectations on feasibility in a probability-based manner. Nevertheless, the decision-maker still has to take his decision before all information is available. From that point of view, and by taking

a look at the OCP (2.1) again, the forthcoming ideas can be complemented by considering the constraints (2.1c) in terms of safeguards or, in other words, in terms of surrogates for potential loss.

Reconsidering (2.1c), i.e., the constraints

$$c(x(t), u(t); p) \leqslant 0$$

for all $p \in \mathcal{R}$ with $\mathcal{R} \subset \mathbb{R}^{n_p}$, then choosing a control $u(\cdot)$ determines a function $x(\cdot; p)$ depending on p [211]. Now the idea of incorporating the concept of risk is based on the assumption that $\mathcal{R}$ has the structure of a *probability space*; its elements p are *random variables*, cf. Appendix A.

This description opens up the possibility to differentiate the likelihood of future states x depending on the likelihood of $p \in \mathcal{R}$. In that way, the constraints $c(\cdot)$ become random variables as well.

However, by replacing the original constraint (2.1c) by a random variable constraint, one has to reconsider the way these constraints are treated within the problem: Equality constraints are nearly impossible to meet at all and inequality constraints need an additional examination on whether and when they are actually satisfied. If no such measure is used, the resulting formulation coincides with the worst-case situation we have mentioned already in the previous section.

In order to establish such a measure, the fundamental idea is to condense the random variable constraint that we obtain by choosing a control $u(\cdot)$ back into a number [211]. Approaches that are traditionally used for that purpose include *guessing the future*, i.e., fixing an estimate of the unknown quantity, the *worst-case analysis*, relying on *expectations values* or *standard deviation units*, or using *chance constraints* with specified confidence levels ζ, i.e., replacing the original constraint by

$$\mathbb{P}[c(x, u; p \leqslant 0] \geqslant \zeta.$$

Quantification of Risk

The quantification of risk addresses two disparate ideas, depending on people's appraisal of uncertainty and its possible consequences. [211] refers to the *measures of deviation* as those treating the amount of risk in a random variable by its actual degree of uncertainty, i.e., its deviation from being constant. In contrast the *measures of the risk of loss* quantify the appearing risk in terms of a surrogate for the overall costs that may occur. This second idea—often named the *measures of risk* for short—is the most commonly used one in the probability-based part of optimization under uncertainty.

The quantification of risk into a single number that can be efficiently used in the optimization context, is done by the introduction of an additional functional R to be applied to the components of the constraints vector (but not necessarily the same one for each component). But then the next important question arises: What properties have to be fulfilled to make such a functional a good quantifier of risk? PHILIPPE ARTZNER and his co-workers provided an answer to these considerations from a finance point of view by characterizing the *coherent* measures of risk, cf. [12]. They introduced an axiomatic framework to decide, whether a risk measure can be "used to effectively regulate or manage risk" [12]. It has proven that this notion is useful in

a much wider context, whereas the original idea has been extended and refined by R. TYRELL ROCKAFELLAR, leading to the following definition, cf. [211] and the references therein.

Definition 2.1 (Coherent Measure of Risk)

A functional $R: L^2 \to (-\infty, \infty]$ is called a coherent measure of risk in the extended sense *if it satisfies*

  (i) $R(C) = C$ *for constants C,*

  (ii) $R((1 - \lambda)X + \lambda Y) \leqslant (1 - \lambda)R(X) + \lambda R(Y)$ *for all $X, Y \in L^2$ and $\lambda \in [0, 1]$,*

 (iii) $R(X) \leqslant R(Y)$ *for $X \leqslant Y$,*

 (iv) $R(X) \leqslant 0$ *when $R(X^k) \leqslant 0$ for a sequence of random variables $(X_k)_{k \in \mathbb{N}}$ converging to the random variable X with respect to the norm $\|X\|_2 = \sqrt{\mathbb{E}[X^2]}$, i.e., if $\|X_k - X\|_2 \to 0$ as $k \to \infty$.*

It is called a coherent measure of risk in the basic sense *if it additionally satisfies*

  (v) $R(\lambda X) = \lambda R(X)$ *for any $\lambda > 0$ and all $X \in L^2$.*

Within Definition 2.1, the space L^2 denotes the linear space of random variables X with finite second moment, i.e., $\mathbb{E}[X^2] < \infty$, cf. [211].

Remark 2.1

A key property of the concept of coherence emphasized in [12] is the *subadditivity*

$$R(X + Y) \leqslant R(X) + R(Y).$$

It follows from the *convexity* (ii) and the *positive homogeneity* (v) properties of Definition 2.1. In particular in financial applications this is crucial. If X and Y are loss variables for two portfolios, then the total risk of loss should not be increased by combining these portfolios into one. Often this is also called *diversification*.

Another important aspect that is closely related to coherence is the *acceptability* of the included risk. Given a coherent risk measure R, we refer to the risk of a loss variable X as being acceptable if $R(X) \leqslant 0$, otherwise it might be unacceptable if, e.g., the measure underestimates the consequences of failure. By that means, there is a form of compromise established as the concept allows constraint violations. The important notion is the extent of that violation. From [211, Theorem 1] we find that if R is a coherent measure of risk, replacing $\boldsymbol{c}(\cdot) \leqslant 0$ by $R(\boldsymbol{c}(\cdot)) \leqslant 0$ maintains convexity, certainty of constraints, and the insensitivity to scaling. Further on, we note that $R(\boldsymbol{c}(\cdot)) \leqslant 0$ is equivalent to requiring the risk of $\boldsymbol{c}(\cdot)$ being acceptable. Therefore, we ensure that the incorporation of the measure R for replacing the original constraint preserves the properties of the underlying problem.

From the technical perspective of Definition 2.1, guessing the future, the worst-case analysis, and relying on expectations are coherent measures of risk in the basic sense, whereas the use of standard deviation units or chance constraints does not give a coherent measure. In both cases, the convexity property (ii) cannot be guaranteed, i.e., the diversification principle is not satisfied in general.

Nevertheless, before introducing the most famous coherent measure of risk—the *Conditional Value at Risk (CVaR)*—let us take a closer look on chance constraints.

Chance Constraints or Value at Risk

One of the most popular approaches for safeguarding in financial mathematics, e.g., in portfolio optimization, is the use of chance constraints. We require the constraints $c(\cdot) \leqslant 0$ to be satisfied only with a given probability ζ. Such a formulation is identical to the *Value at Risk (VaR)* [12, 127].

Definition 2.2 (Value At Risk/Quantile)

For a random variable X with cumulative distribution function $F_X \colon \mathbb{R} \to [0,1]$ (cf. Definition A.6) and a given probability level $\zeta \in [0,1]$ the Value at Risk *of X is the mapping* $\mathrm{VaR} \colon [0,1] \to \mathbb{R}$ *given by*

$$\mathrm{VaR}_\zeta(X) \stackrel{\text{def}}{=} q_\zeta(X) = \inf_{x \in \mathbb{R}} \{ F_X(x) \geqslant \zeta \}. \tag{2.9}$$

Therein, $q_\zeta(X)$ denotes the ζ-quantile of X, which is by definition equal to the VaR. △

Hence, if we pass to a chance constraint for the original constraint $c(\cdot) \leqslant 0$, the following relation holds true, cf. [211].

$$\mathbb{P}\left[c(x, u; p) \leqslant 0\right] \geqslant \zeta \quad \Longleftrightarrow \quad q_\zeta(c(x, u; p)) \leqslant 0 \quad \Longleftrightarrow \quad \mathrm{VaR}_\zeta(c(x, u; p)) \leqslant 0. \tag{2.10}$$

Incorporating this into our original OCP (2.1), we obtain the safeguarding problem with VaR constraint

$$\min_{x(\cdot), u(\cdot)} \tilde{J}(x, u; p) \tag{2.11a}$$

$$\text{s.t.} \qquad \dot{x}(t) = f(x(t), u(t); p), \qquad\qquad t \in \mathcal{T}, \tag{2.11b}$$

$$0 \geqslant \mathrm{VaR}_\zeta(c(x(t), u(t); p)), \qquad t \in \mathcal{T}, \tag{2.11c}$$

$$x(t_0) = x_0, \tag{2.11d}$$

where ζ denotes again the desired probability level. Certainly, one can use the VaR formulation (with a different probability level ζ') for the objective function as well rather than using the nominal value or an expectation value.

The OCP (2.11) is a *bilevel optimization problem*. The implementation of the VaR constraint (2.11c) requires knowing the distribution of the constraint c depending on the variable p, which in most instances is not readily available. Furthermore, both the dynamic equation (2.11b) and the constraint have to be evaluated for all possible realization of the parameter p as they become random variables as well. If p is discretely distributed, this may include only a finite number of events $p_1, \ldots, p_n$ with appropriate probability $\mathbb{P}_1, \ldots, \mathbb{P}_n$, for continuously distributed random parameters there are generally infinitely many realizations.

For constraints depending on only one uncertain parameter we obtain the following reformulation, cf. [117], that we will use in the following Chapter 3.

Theorem 2.1

If the constraint function $c(\cdot)$ is a continuous function of the one-dimensional random variable p and monotone in p, then

$$\mathrm{VaR}_\zeta(c(\cdot; p)) \leqslant 0 \geqslant \zeta \quad \Longleftrightarrow \quad c(\cdot; \mathrm{VaR}_\zeta(p)) \leqslant 0. \tag{2.12}$$

△

Proof We define $p^{\min} \stackrel{\text{def}}{=} \arg\min\{p \mid c(\cdot; p) = 0\}$ and calculate by using the relation (2.10)

$$
\begin{aligned}
\mathbb{P}[c(\cdot; p) \leqslant 0] \geqslant \zeta \quad &\Longleftrightarrow \quad \mathbb{P}[p \leqslant p^{\min}] \geqslant \zeta \\
&\Longleftrightarrow \quad \text{VaR}_\zeta(p) \leqslant p^{\min} \\
&\Longleftrightarrow \quad c(\cdot; \text{VaR}_\zeta(p)) \leqslant 0.
\end{aligned}
$$

$\square$

By applying Theorem 2.1 to reformulate the VaR constraint (2.11c) the complexity of problem (2.11) can be reduced. If the distribution of the random parameter p is known one can directly determine its VaR given a specified probability level ζ.

For multi-dimensional parameters $\boldsymbol{p}$ Theorem 2.1 can only be used if the components of $\boldsymbol{p}$ are independent and treated as individual VaR constraints.

Conditional Value at Risk

The VaR is not a coherent measure of risk, because of the violation of the diversification principle. As an alternative, the Conditional Value at Risk (CVaR) has been introduced in [1, 2, 212, 213]. Given a random variable X with respect to a probability level ζ, the CVaR is described as the expectation of X in conditional distribution of its upper ζ-tail. This tail summarizes all outcomes of X in the upper part of the range of X, its probability is then $1 - \zeta$. In general this tail would be the interval $[q_\zeta(X), \infty)$, but only if there does not appear a jump at $q_\zeta(X)$. The CVaR, setting it apart from the traditional VaR, regards not only the occurrence of negative outcomes (or losses), but also their extent (or amount). Thus, the CVaR is a more cautious risk measure than the VaR.

Definition 2.3 (Conditional Value At Risk (ACERBI))
The Conditional Value at Risk *of a random variable X to the probability level ζ is given as*

$$
\text{CVaR}_\zeta(X) = \frac{1}{1-\zeta} \int_\zeta^1 \text{VaR}_z(X) \, \mathrm{d}z. \tag{2.13}
$$

$\triangle$

Definition 2.3, originating from [1], confirms the above statement directly. As a more application-oriented version, in [212, 213] the following equivalent version is established.

Lemma 2.1 ([212, 213])
For a random variable X and probability level ζ we obtain the CVaR by the minimization formula

$$
\text{CVaR}_\zeta(X) = \min_{\vartheta \in \mathbb{R}} \left\{ \vartheta + \frac{1}{1-\zeta} \mathbb{E}[\max\{0, X - \vartheta\}] \right\}. \tag{2.14}
$$

$\triangle$

This term leads to an important connection to the VaR again (apart from the one given by (2.13)), i.e., [211]

$$
\text{VaR}_\zeta(X) = \text{left endpoint of } \arg\min_{\vartheta \in \mathbb{R}} \left\{ \vartheta + \frac{1}{1-\zeta} \mathbb{E}[\max\{0, X - \vartheta\}] \right\}. \tag{2.15}
$$

Example 2.1 gives an impression of the connection between the VaR and the CVaR of a random variable X to some specified probability level ζ by calculating and visualizing the terms.

Example 2.1

Consider the exponentially distributed random variable $X \sim \text{Exp}(\lambda)$ with rate parameter λ. X is supported on $[0, \infty)$ and has the cumulative distribution function (cdf)

$$F_X(x) = \begin{cases} 1 - e^{-\lambda x}, & x \geqslant 0 \\ 0, & x < 0. \end{cases}$$

The quantile function $q_\zeta(X) \colon [0,1] \to [0, \infty)$ of X to a given probability level ζ is calculated with the help of the inverse function of F_X, yielding

$$q_\zeta(X) = -\frac{\ln(1-\zeta)}{\lambda}, \qquad 1 \leqslant \zeta < 1,$$

with the limit for $\zeta \to 1$ being ∞. Thus, if we fix $\lambda = 1$ and consider the probability level $\zeta = 0.9$, we obtain

$$\text{VaR}_{\zeta=0.9}(X) = q_\zeta(X) = -\ln(0.1) \approx 2.303.$$

By (2.13) we get

$$\begin{aligned} \text{CVaR}_{\zeta=0.9}(X) &= \frac{1}{1-\zeta} \int_\zeta^1 -\ln(1-z)\,\mathrm{d}z \\ &= \frac{1}{1-\zeta} \left[z - (z-1)\ln(1-z) \right]_\zeta^1 \\ &= 10 \cdot (\zeta-1)(\ln(1-\zeta)-1) \approx 3.303. \end{aligned}$$

Figure 2.1 visualizes the connection.
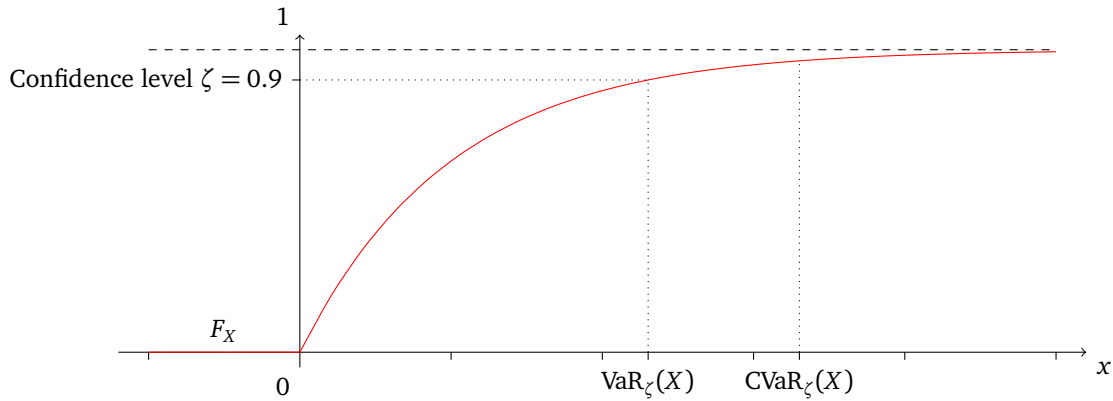
Figure 2.1: Visualization of the VaR and CVaR of an exponentially distributed random variable X and given probability level ζ.

For practical applications, another property of CVaR has shown to be important, cf. [211].

Theorem 2.2 ([211])

The CVaR of a random variable $X \in L^2$ depends continuously on the probability level $\zeta \in (0,1)$

and has the limits

$$\lim_{\zeta \to 0} \mathrm{CVaR}_\zeta(X) = \mathbb{E}[X] \quad \text{and} \quad \lim_{\zeta \to 1} \mathrm{CVaR}_\zeta(X) = \sup X. \tag{2.16}$$

$\triangle$

Remark 2.2

Note that for $\zeta \to 1$ the $\mathrm{VaR}_\zeta(X)$ tends to $\sup X$ as well, but it does *not* tend to $\mathbb{E}[X]$ for $\zeta \to 0$. To check this, we consider the quantiles of the normally distributed random variable $X \sim \mathcal{N}(\mu, \sigma)$. It holds $\lim_{\zeta \to 0} q_\zeta(X) = -\infty$.

Safeguarding a robust OCP with CVaR constraints can be formalized analogous to the approach before. We obtain the new problem

$$\min_{x(\cdot), u(\cdot)} \tilde{J}(x, u; p) \tag{2.17a}$$

$$\text{s.t.} \qquad \dot{x}(t) = f(x(t), u(t); p), \qquad\qquad t \in \mathcal{T}, \tag{2.17b}$$

$$0 \geqslant \mathrm{CVaR}_\zeta(c(x(t), u(t); p)), \qquad t \in \mathcal{T}, \tag{2.17c}$$

$$x(t_0) = x_0. \tag{2.17d}$$

With the minimization rule (2.14) the constraint (2.17c) can be readily implemented into the original problem, without extra care of the VaR. The distribution of the constraint function $c(\cdot)$ depending on the parameter p, however, is still important for calculating the inner expectation in the minimization rule. Additionally, the evaluation of that inner expectation is generally difficult for continuously distributed random variables or discretely distributed random variables with infinitely many events.

The constraint $\mathrm{CVaR}_\zeta(c(x, u; p)) \leqslant 0$ has to be fulfilled within the whole time interval $\mathcal{T}$. Thus, the control parameter ϑ of (2.14) has to be derived for every $t \in \mathcal{T}$ and we obtain an additional control function $\vartheta(\cdot)$ in that context.

Basically, the transition to a multi-dimensional parameter p can be done straightforwardly. If the components of the random variable p are independent, each can be treated by a separate CVaR constraint. In the case of a joint distribution, the focus lies on the evaluation of the inner expectation. In each of the mentioned instances, the additional control function $\boldsymbol{\vartheta} \colon \mathcal{T} \to \mathbb{R}^{n_p}$ increases the complexity of the problem considerably.

Finally, due to Theorem 2.2 the analysis of expectation-based and worst-case approaches can be performed in the context of CVaR as well. [11] investigated the performance of the CVaR approach with a confidence level ζ close to one in comparison with the worst-case measure in the context of portfolio optimization. By numerical analysis it is shown therein, that for certain problem instances it can be beneficial to use a CVaR approximation even if one wishes to optimize the worst-case behavior.

2.3 Connecting Robust, Probabilistic, and Stochastic Optimization

Using a measures of risk to describe uncertain constraints in optimization under uncertainty gives us an immediate impression of how reliable the computed solutions are through the underlying probabilistic description. The use of an uncertainty set in robust optimization does

not provide such a probabilistic safeguard. Nevertheless, one of the key questions in robust optimization is how the choice and adjustment of a specific uncertainty set $\mathcal{R}$ and the corresponding robust feasibility work on the probability of feasibility [38]. I.e., if $u(\cdot)$ is a solution to (2.1) and $x(\cdot)$ the appropriate state trajectory, what is the smallest probability ζ such that

$$x \in \mathcal{X}(\mathcal{R}),\, u \in \mathcal{U}(\mathcal{R}) \quad \Rightarrow \quad \mathbb{P}[c(x, u; p) > 0] \leqslant \zeta$$

under some assumptions on the distribution that the uncertain parameter p could underly? The first such connection between an uncertainty set and the probability of a robust feasible solution has been developed in [28] for the ellipsoidal set. In a related fashion, [36, 37] provided probabilistic guarantees for special cardinality constrained uncertainty sets in linear problems. [186] went even further by inferring risk measures from uncertainty sets.

Starting from the opposite viewpoint, i.e., using (possibly very limited) distributional information about the parameter p to choose an elaborate uncertainty set, has attracted attention as well. In [188] chance constraints have been considered in traditional robust optimization through convex approximations, [55, 85] incorporated them by using sampling techniques. [35] focused on coherent risk management tools and the implications they have on the structure of an uncertainty set in robust linear optimization problems. One example, that is given in [38], considers the CVaR. If the random variable (or, constraint) depending on the uncertain parameter p is supposed to satisfy the CVaR condition given through (2.14) for a probability level ζ, and p follows a discrete distribution with support $\{p_1, \ldots, p_n\}$ and corresponding probabilities $\{\mathbb{P}_1, \ldots, \mathbb{P}_n\}$, then the uncertainty set

$$\mathcal{R}^{\mathrm{CVaR}}(\zeta) = \mathrm{conv}\left(\left\{\frac{1}{\zeta}\sum_{i \in \mathcal{J}} p_i \mathbb{P}_i + \left(1 - \frac{1}{\zeta}\sum_{i \in \mathcal{J}} \mathbb{P}_i\right) p_j \,\middle|\, \mathcal{J} \subseteq \{1, \ldots, n\},\right.\right.$$
$$\left.\left. j \in \{1, \ldots, n\} \setminus \mathcal{J}, \sum_{i \in \mathcal{J}} \mathbb{P}_i \leqslant \zeta\right\}\right)$$

belongs to that random variable, cf. [38].

Both of the mentioned methodologies tackle optimization or control problems in the single-stage case. I.e., the decision-maker has to set his choice before any of the uncertainty is realized. In contrast to this *static* approach [38], in the *dynamic* decision-making context this restriction is relaxed. One allows decisions to be made successively to some extent in order to use the additional information that enters into the problem when the realization of an uncertain parameter takes place. Starting again with the work in traditional robust control, robust *adaptable* optimization has developed. One form of it is the well-known *open-loop feedback* control. The static solution over all stages is computed and the first-stage decision is implemented. Afterwards, the complete procedure is repeated for the next stage. In two-stage *stochastic optimization* [205, 216, 224] the feasibility constraints of the single-stage optimization problem are relaxed and shifted to the objective. This is done by assuming that after the first-stage decisions are implemented and the realization of the uncertainty takes place, the decision-maker has the opportunity to ensure that the constraints are satisfied by counteracting bad consequences or taking advantage of good outcomes. By that, the introduction of recourse decision-making identifies an option of *hedging*. However, for this method to work, again a probabilistic description of the uncertainty is needed. This approach can be extended

to a multi-stage environment straightforwardly. Additional to stochastic programming, the *dynamic programming* idea can as well be extended to robust dynamic programming and robust MARKOV decision process setting, cf. [33, 34, 206].

2.4 Summary

In this chapter we surveyed optimization problems that are affected by uncertainties in the parameters. We gave an introduction to the two most prominent general strategies to regard such problems—a probabilistic and a set-based view.

For the class of robust OCPs in the sense of BERTSIMAS [38], we described the linearization and sigmapoint methods to efficiently reformulate the original problems into numerically solvable ones, regarding the implied budget of uncertainty. From the contrary viewpoint of the probabilistic approach, including the concept of coherence introduced by ARTZNER and ROCKAFELLAR [12, 211], we analyzed the VaR and the CVaR ideas originating from the economic sciences. In order to simplify the original VaR constraint leading to a bilevel optimization problem (2.11), we developed a reformulation of that constraint, which allows transferring the calculation of the VaR from the random constraint to only the random parameter. Additionally, we adapted the original definition of the CVaR to apply them in the optimal control context.

Finally, we regarded the connection between the robust and the probabilistic viewpoint. From their specific perspectives, both ideas give the decision-maker an impression on the risk of failure that remains and needs to be accepted after solving the problem. Additionally, we compared them to stochastic optimization.

We will apply different methods from both approaches to an economic OCP in the following chapter, where we also discuss the strengths and weaknesses of the considered approaches from the economic and computational perspective.

3 Numerical Application: Conspicuous Consumption Products in Periods of Recession

On the following pages we apply the results of the previous chapter to the economic problem of pricing conspicuous consumption products in periods of recession. We introduce the underlying model and establish a strategy to solve this problem numerically with the help of the direct multiple shooting approach. Already at this stage, uncertainty in form of the duration of the recession enters. Afterwards, we consider the strength of the crisis as an additional source of uncertainty and apply the presented methods of robustification and risk measuring to the problem.

This chapter is based on [117, 118].

3.1 The Underlying Economic Model

Our general interest in this application chapter lies in finding optimal pricing strategies for conspicuous consumption products in periods of recession. In particular, we focus on critical economic situations like the credit crunch recession that started in 2007. Besides a reduction in demand, which is quite usual for a recession, in the credit crunch recession capital markets cease to function. Hence, firms cannot borrow or issue new shares to finance their operations. They need to self-finance their investments [79]:

> "... the only option is to ride out the recession. But companies can do this only if they have enough liquidity ..."

The characteristic of conspicuous goods is that demand does not only depend on price, but in addition it depends on the good's reputation, which increases in price. The product's reputation as being expensive allows people to signal their wealth to observers, which in turn increases the reputation of the consumer [187]:

> "Why are people so keen on wearing brand-labeled clothes and owning other luxury-branded products to pay a premium for them?
> The answer appears to be to gain social status."

Examples of conspicuous goods are luxury hotels [236], expensive cars, or fashionable clothes. The topic of how to price conspicuous goods is treated in, e.g., [9, 10, 61, 63, 147].

In that course, the firm' manager has to face the following tradeoff: To keep the future demand of his product at a high level, he wants to charge a high price for the conspicuous good. However, during the recession demand as such is low and high prices deplete it even more.

This, in turn, may cause negative cash levels that are tantamount to bankruptcy in situations, where the firm has no possibility to obtain additional money from the capital markets.

The model we will analyze in the following extends the original one presented in [61, 63] by introducing a delayed effect of the charged price on the reputation of the product. Starting with the work of [130], the inclusion of time delays is a very popular and effective advancement in economic—and especially capital accumulation—problems, cf. [13, 19, 49, 83]. In our setting it means that a current price decrease has no immediate effect on the good's reputation which has been built up during the past. Only after a phase of accustoming price changes really start to influence the consumers behavior and, therefore, the good's reputation.

3.1.1 Model Formulation

We consider an economic setting with a *recession period* followed by a *normal economic period*. For the rest of this chapter, the value τ will denote the endpoint of the crisis, compare Figure 3.1.
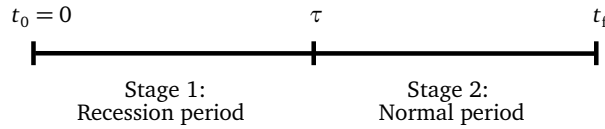
Figure 3.1: Stages $[t_0, \tau]$ and $[\tau, t_f]$ of the recession model.

The dynamics of our model includes two states. The *brand image* $A(\cdot)$ of the firm evolves in both periods proportional to the price $P(\cdot)$, i.e., according to the differential equation

$$\dot{A}(t) = \kappa(\gamma P(t - \sigma) - A(t)). \tag{3.1}$$

In the dynamics of the reputation $A(\cdot)$, the constant control delay $\sigma \geq 0$ retards the connection between changing the price $P(\cdot)$ and its consequence on the development of $A(\cdot)$. Equation (3.1) covers that, as usual with conspicuous goods, the exclusiveness of the brand goes up with the price, which works positively on demand. Compared to the literature, the delay is a new feature, which captures the fact that consumers first have to get used to a new situation before they adjust their purchase decisions. In particular, if a good is known to be exclusive, a sudden price reduction at first instance does not change this perception. However, after a while consumers "forget" the old situation, implying that they start recognizing that the good is less exclusive, and reputation starts to decrease. Note that if the recession ends at time τ, we still have the direct influence of the price set during the final time interval of length σ of the recession. For a fixed price $\bar{P}$ equation (3.1) yields a steady state of $\bar{A} = \gamma \bar{P}$.

The *available cash* $B(\cdot)$ becomes crucial when the capital markets cease to function and firms have to budget with their reserves as they cannot borrow money or issue new shares. It depends on the gains $P(\cdot) D(\cdot)$, fixed costs C, and the short-time interest δ, leading to

$$\dot{B}(t) = P(t)D(A(t), P(t)) - C + \delta B(t). \tag{3.2}$$

Therein the demand $D(\cdot)$ is driven by the brand image and the pricing strategy $P(\cdot)$, which will be the control of our problem. It is essentially influenced by the economic stage, i.e., in

the normal period (N) we have

$$D_{\mathrm{N}}(A(t), P(t)) = m - \frac{P(t)}{A(t)^{\beta}}, \tag{3.3a}$$

whereas in the recession phase (R) the demand is reduced to

$$D_{\mathrm{R}}(A(t), P(t)) = D_{\mathrm{N}}(A(t), P(t)) - \varsigma. \tag{3.3b}$$

The positive constant ς measures the *strength of the crisis*, the adjustment parameter $0 < \beta < 1$ is given, and m corresponds to the *potential market size*.

The objective of the company is to maximize the expected value of profit over the finite or infinite time horizon $\mathcal{T} = [0, t_{\mathrm{f}}]$ of interest. The profit is composed of two parts: the gains $J_{\mathrm{N}}(\cdot)$ of the normal economic period $(\tau, t_{\mathrm{f}}]$ and an impulse dividend of the cash reserve at the end of the recession phase, i.e., $B(\tau)$, resulting in the stage objective $J_{\mathrm{R}}(\cdot)$. This dividend is included as the capital market is assumed to become functional again in the normal economic period and firms can freely borrow and lend cash then. Thus, the firm does not need a positive $B(\cdot)$ on $(\tau, t_{\mathrm{f}}]$. For a fixed τ and given discount rate r and fixed costs C, the objective function $J_{\mathrm{res}}(\cdot)$ of this two-stage Optimal Control Problem (OCP) is calculated as

$$\begin{aligned}
J_{\mathrm{res}}(A(\cdot), B(\cdot), P(\cdot); \tau) &\stackrel{\mathrm{def}}{=} J_{\mathrm{R}}(A(\cdot), B(\cdot), P(\cdot); \tau, r) + J_{\mathrm{N}}(A(\cdot), B(\cdot), P(\cdot); \tau, r, C) \\
&= \mathrm{e}^{-r\tau} B(\tau) + \int_{\tau}^{t_{\mathrm{f}}} \mathrm{e}^{-rt} \left(P(t) D_{\mathrm{N}}(A(t), P(t)) - C \right) \mathrm{d}t,
\end{aligned} \tag{3.4}$$

being the sum of the two stage components.

However, typically the recession length τ separating the two stages is not known beforehand to decision-makers. An individual firm also has no influence on when the recession ends. Therefore, we assume that the length of the recession period τ is an exponentially distributed random variable. Then the goal is to maximize the expectation value of the Net Present Value (NPV) at time τ, i.e., the objective function (3.4) is weighted by the exponential probability density function with rate parameter λ,

$$J(A(\cdot), B(\cdot), P(\cdot); \tau) \stackrel{\mathrm{def}}{=} \mathbb{E}\left[\mathrm{NPV}(\tau)\right] = \int_{0}^{t_{\mathrm{f}}} \lambda \mathrm{e}^{-\lambda\tau} J_{\mathrm{res}}(A(\cdot), B(\cdot), P(\cdot); \tau) \mathrm{d}\tau. \tag{3.5}$$

This yields the OCP

$$\max_{P(\cdot)} J(A(\cdot), B(\cdot), P(\cdot); \tau) \tag{3.6a}$$

$$\text{s.t.} \quad \dot{A}(t) = \kappa(\gamma P(t - \sigma) - A(t)), \qquad t \in \mathcal{T}, \tag{3.6b}$$

$$\dot{B}(t) = P(t) D_{\mathrm{R}}(A(t), P(t)) - C + \delta B(t), \qquad t \in [0, \tau], \tag{3.6c}$$

$$A(0) = A_0, \quad B(0) = B_0, \tag{3.6d}$$

$$P(t) = \eta(t), \qquad t \in [-\sigma, 0], \tag{3.6e}$$

$$0 \leqslant D_{\mathrm{R/N}}(A(t), P(t)), \qquad t \in \mathcal{T}, \tag{3.6f}$$

$$P(t) \geqslant 0, \qquad t \in \mathcal{T}, \tag{3.6g}$$

$$B(t) \geqslant 0, \qquad t \in [0, \tau], \tag{3.6h}$$

with $D_{R/N}(A(t), P(t))$ given as in (3.3) and $B(t)$ negligible in the normal period $(\tau, t_f]$. This problem is a non-standard OCP in the sense that uncertainty and control delays are present, making analytical investigations difficult. In [62] it is shown that an important class of models with delays can be transformed into equivalent problems without delays. However, the present model does not fit in this family. This is because the control $P(\cdot)$ appears with a delay in one state equation and without in the other one. Hence, it is not possible to eliminate the delay using a time transformation. Therefore, we propose a different approach in the next section, leading us back to a form of stochastic optimization.

3.1.2 Numerical Implementation

We propose to use reformulations to transfer the OCP (3.6) with objective function (3.5) into a more standard form that can be efficiently solved. In Chapter 1 we presented such a standard multi-stage formulation, cf. (1.2), and gave an introduction to our preferred method to solve such a problem, i.e., BOCK's direct multiple shooting method. Thus, in the following paragraphs we present a discretization of the uncertainty and a reformulation of the time delays.

Discretization of the Probability Density Function

Our starting point for approximating the considered OCP is to discretize the exponential distribution of the random variable τ by defining a time grid

$$0 = \tau_0 < \tau_1 < \ldots < \tau_n < t_f. \tag{3.7}$$

In what follows, switches from the recession period to the normal stage will only be possible at these times τ_i, $i = 1, \ldots, n$. The recession ends at τ_i with a specified probability $\mathbb{P}_i$. We use an equidistant discretization of the grid (3.7), resulting in a geometric distribution

$$\mathbb{P}_i = \int_{\tau_{i-1}}^{\tau_i} \lambda\, e^{-\lambda t}\, dt = e^{-\lambda \tau_{i-1}} - e^{-\lambda \tau_i}, \qquad i = 1, \ldots, n-1, \tag{3.8a}$$

$$\mathbb{P}_n = 1 - \sum_{j=1}^{n-1} \mathbb{P}_j. \tag{3.8b}$$

The discretized distribution can be used to reformulate the maximization of the expected value as a multi-stage OCP of type (1.2), by using a *scenario tree*. As a result of this, the emerging problem can be viewed as a problem of stochastic optimization, cf. Chapter 2.3. However, this formulation is not unique. One possibility is to use a *staircase-like* approach, increasing the number of variables as the number of possible recession ends τ_i increases. This approach is illustrated schematically in Figure 3.2 and results in $M = n + 1$ model stages, where n is the number of discretizations of the probability density function as in (3.7). The dimensions $n_{x_i} = 2 + i$ of differential states and $n_{u_i} = 1 + i$ of control functions, $i = 0, \ldots, M - 1$, are different on the model stages. The transition functions (1.2d) are defined by

$$A_{i,j}(\tau_i) = A_{i-1,j}(\tau_i), \quad 1 \leqslant j \leqslant i, \tag{3.9a}$$

$$A_{i,i+1}(\tau_i) = A_{i-1,1}(\tau_i), \tag{3.9b}$$

$$B_{i,1}(\tau_i) = B_{i-1,1}(\tau_i), \tag{3.9c}$$

$t_0 = 0$ Stage 0	τ_1 Stage 1	τ_2 Stage 2	τ_3	τ_{n-1} Stage $n-1$	τ_n Stage n t_f
R $\quad P_1(t)$ $\quad A_{0,1}(t)$ $\quad B_{0,1}(t)$	R $\quad P_1(t)$ $\quad A_{1,1}(t)$ $\quad B_{1,1}(t)$	R $\quad P_1(t)$ $\quad A_{2,1}(t)$ $\quad B_{2,1}(t)$	$\cdots$	R $\quad P_1(t)$ $\quad A_{n-1,1}(t)$ $\quad B_{n-1,1}(t)$	N $\quad P_{n+1}(t)$ $\quad A_{n,n+1}(t)$ $\quad S_n$
	N $\quad P_2(t)$ $\quad A_{1,2}(t)$ $\quad S_1$	N $\quad P_2(t)$ $\quad A_{2,2}(t)$ $\quad S_1$		N $\quad P_2(t)$ $\quad A_{n-1,2}(t)$ $\quad S_1$	N $\quad P_2(t)$ $\quad A_{n,2}(t)$ $\quad S_1$
		N $\quad P_3(t)$ $\quad A_{2,3}(t)$ $\quad S_2$	$\cdots$	N $\quad P_3(t)$ $\quad A_{n-1,3}(t)$ $\quad S_2$	N $\quad P_3(t)$ $\quad A_{n,3}(t)$ $\quad S_2$
				$\vdots$	$\vdots$
				N $\quad P_n(t)$ $\quad A_{n-1,n}(t)$ $\quad S_{n-1}$	N $\quad P_n(t)$ $\quad A_{n,n}(t)$ $\quad S_{n-1}$

Figure 3.2: Control and state variables in the multi-stage formulation of the OCP (3.6) with a period indicator R for a recession and N for a normal economic stage. The additional tags S_1–S_n denote the possible normal stage scenarios, i.e., S_1 characterizes the scenario of the recession ending at τ_1.
This reformulation was obtained by assuming that the recession ends at time instant τ_i with probability $\mathbb{P}_i$, $i = 1, \ldots, n$, reducing the probability of the recession enduring and resulting in the depicted scenario tree. In each stage, the overall probability of all scenarios equals one.

t_0 τ_1 τ_2 τ_3 τ_{n-1} τ_n t_f	τ_1 t_f	τ_2 t_f	τ_{n-1} t_f
R $\mid$ R $\mid$ R $\mid$ $\cdots$ $\mid$ R $\mid$ N $\quad S_n$	N $\quad S_1$	N $\quad S_2$	$\cdots$ N $\quad S_{n-1}$

Stage 0 · Stage 1 · Stage 2 · Stage $n-1$ · Stage n · Stage $n+1$ · Stage $n+2$ · Stage $2n-1$

Figure 3.3: Rearranged scheme for the discretization of the random end time τ of the recession. Again, the symbols denote a recession (R), a normal stage (N), and the appropriate normal stage scenario (S_1–S_n). The time instants t_1 to t_{n-1} indicate necessary transitions of the OCP, cf. Equation (3.10).

for all model stages $i = 1, \ldots, n-1$, and

$$A_{n,n+1}(\tau_n) = A_{n-1,1}(\tau_n). \tag{3.9d}$$

At each time instant τ_i one has to distinguish between transitions (3.9a), (3.9c) of the brand image A and the cash B for the ongoing recession and the initialization (3.9b), (3.9d) of the additional differential states $A_{i,i+1}$ that are necessary for the normal period beginning at τ_i, compare Figure 3.2.

The probability of a normal stage scenario S_i starting at time instant τ_i remains constant until the terminal time t_f of the problem. Hence, at τ_i the probability of an enduring recession is reduced by $\mathbb{P}_i$ and, accordingly, tends to zero for $n \to \infty$. Additionally, we note that in each model stage the summarized probability of the recession and all normal stage scenarios equals to one.

The second possibility is to use linearly coupled point constraints of type (1.2f) instead of transitions to initialize the new variables. All possible scenarios at τ_i are concatenated, resulting

in $M = 2n$ model stages. This *flat* arrangement of stages is shown in Figure 3.3.

In contrast to the first formulation, the model stage dimensions $n_{x_i} = 2$ for $i = 0, \ldots, n-1$ and $n_{x_i} = 1$ for $i = n, \ldots, M-1$ of differential states and $n_{u_i} = 1$ for $i = 0, \ldots, M-1$ of controls are (almost) constant. The coupled point constraints (1.2f) are given by

$$A_{i,1}(t_{i-n}) = A_{i-n-1,1}(\tau_{i-n}), \quad n+1 \leqslant i \leqslant 2n-1. \tag{3.10}$$

The first n stages are recession periods with continuous transitions of all states. They differ in the objective function. The transition from the last recession stage n to the subsequent normal period that starts at time $t = \tau_n$ is continuous, too. However, the model stage lengths of this approach vary. While all n recession stages have the constant duration $h = \tau_i - \tau_{i-1}$, the n normal period stages have a length of $t_f - \tau_i$, $i = 1, \ldots, n$.

Then we obtain for the staircase-like approach to discretize the probability density function, indexed by $k = 1$, the objective function

$$\Phi_i^1(A_{i,\cdot}(t), B_{i-1,1}(\tau_i), P(t); \tau_i, \boldsymbol{P}_i)$$
$$= \mathbb{P}_i\, e^{-r\tau_i} B_{i-1,1}(\tau_i) + \sum_{j=1}^{i} \mathbb{P}_j \int_{\tau_i}^{\tau_{i+1}} e^{-rt} \left(P(t) D_N(A_{i,j+1}(t), P(t)) - C \right) dt \tag{3.11a}$$

for $i = 1, \ldots, n$, the transition functions (compare (1.2d) and (3.9))

$$A_{i,j}(\tau_i) = f_{i,j}^{1,\mathrm{tr}A}(A_{i-1,j}(\tau_i)) = \begin{cases} A_{i-1,j}(\tau_i), & 1 \leqslant i \leqslant n-1, \ 1 \leqslant j \leqslant i, \\ A_{i-1,1}(\tau_i), & 1 \leqslant i \leqslant n, \ j = i+1, \end{cases} \tag{3.11b}$$

$$B_{i,1}(\tau_i) = f_i^{1,\mathrm{tr}B}(B_{i-1,1}(\tau_i)) = B_{i-1,1}(\tau_i), \quad 1 \leqslant i \leqslant n-1, \tag{3.11c}$$

and the coupled point constraint functions

$$r_i^{1,\mathrm{eq}} \equiv 0, \tag{3.11d}$$

where $\boldsymbol{P}_i = (\mathbb{P}_1, \mathbb{P}_2, \ldots, \mathbb{P}_i)$.

The concatenated approach, indexed by $k = 2$, is defined by the functions

$$\Phi_i^2(A_{n+i,1}(t), B_{i-1,1}(\tau_i), P(t); \tau_i, \boldsymbol{P}_i)$$
$$= \mathbb{P}_i\, e^{-r\tau_i} B_{i-1,1}(\tau_i) + \mathbb{P}_i \int_{\tau_i}^{t_f} e^{-rt} \left(P(t) D_N(A_{n+i,1}(t), P(t)) - C \right) dt, \tag{3.12a}$$

for $i = 1, \ldots, n$,

$$A_{i,1}(\tau_i) = f_{i,1}^{2,\mathrm{tr}A}(A_{i-1,1}(\tau_i)) = A_{i-1,1}(\tau_i), \quad 1 \leqslant i \leqslant n, \tag{3.12b}$$

$$B_{i,1}(\tau_i) = f_i^{2,\mathrm{tr}B}(B_{i-1,1}(\tau_i)) \qquad\qquad = B_{i-1,1}(\tau_i), \quad 1 \leqslant i \leqslant n-1, \tag{3.12c}$$

$$r_i^{2,\mathrm{eq}}(A_{i,1}(t_{i-n}), A_{i-n-1,1}(\tau_{i-n}))$$
$$= A_{i,1}(t_{i-n}) - A_{i-n-1,1}(\tau_{i-n}), \quad n+1 \leqslant i \leqslant M-1. \tag{3.12d}$$

Reformulation of the Time Delay

In the context of optimization the methodological background for the treatment of the time delay in (3.6) are *functional differential equations*. In [143] they are tackled by a modified version of PONTRYAGIN's Maximum Principle (PMP), whereas [67] uses a combination of the *methods of steps* and a tailored shooting method to numerically solve economic problems including delayed time arguments in both the state and control variables. A very general approach for solving Initial Value Problems (IVPs) in *delay differential equations* can be found in [163].

[51] gives two possibilities to reformulate an OCP with delayed equation of motion as in (3.6) into an instantaneous problem: In the first idea the time horizon t_f is splitted into m parts of length σ. Then, the system's dynamics is formulated separately on each of the resulting intervals. By interpreting them as independent and introducing new state and control variables, we can formulate a system of m differential equations on the time horizon $[0, \sigma]$. This, in turn, can be used to reformulate the original OCP. Furthermore, one has to introduce coupled boundary conditions to ensure the continuity of the state variable. The approach may give additional insight from an analytical point of view, cf. [51]. However, it requires the determination of $m-1$ control paths in the interval $[0, \sigma]$. For small values of the delay σ this results in a large number of state and control functions.

Therefore, we prefer a second reformulation. We introduce a second control function $u_2(t) = P(t)$ that denotes the unretarded control at time t, whereas $u_1(t) = P(t-\sigma)$ characterizes the delayed one. They are coupled via equalities $u_1(t) = u_2(t-\sigma)$ for $t \geqslant \sigma$ and $u_1(t) = \eta(t-\sigma)$ for $0 \leqslant t \leqslant \sigma$.

Taking either the staircase (3.11) or flat (3.12) discretization of uncertainty presented in the previous paragraph, $k = 1, 2$, we obtain the discretized OCP

$$\max_{u_1(\cdot), u_2(\cdot)} \sum_{i=1}^{n} \Phi_i^k(\tau_i, A_{(k-1)n+i, \cdot}(t), B_{i-1,1}(\tau_i), u_2(t), \boldsymbol{P}_i) \tag{3.13a}$$

$$\text{s.t.} \quad \dot{A}_{i,j}(t) = \kappa(\gamma u_1(t) - A_{i,j}(t)), \qquad t \in \mathcal{T}, \tag{3.13b}$$
$$0 \leqslant i \leqslant M-1, \ j \in \mathcal{J}^k,$$

$$\dot{B}_{i,1}(t) = u_2(t) D_R(A_{i,1}(t), u_2(t)) - C + \delta B_{i,1}(t), \quad t \in [0, \tau_i], \tag{3.13c}$$
$$0 \leqslant i \leqslant n-1,$$

$$u_1(t) = \eta(t-\sigma), \qquad t \in [0, \sigma], \tag{3.13d}$$

$$u_1(t) = u_2(t-\sigma), \qquad t \in [\sigma, t_f], \tag{3.13e}$$

$$A_{0,1}(0) = A_0, \quad B_{0,1}(0) = B_0, \tag{3.13f}$$

$$0 \leqslant D_{R/N}(A_{i,j}(t), u_2(t)), \qquad t \in \mathcal{T}, \tag{3.13g}$$

$$u_1(t) \geqslant 0, \quad u_2(t) \geqslant 0, \qquad t \in \mathcal{T}, \tag{3.13h}$$

$$B_{i,1}(t) \geqslant 0, \qquad t \in [0, \tau_i], \tag{3.13i}$$
$$1 \leqslant i \leqslant n-1,$$

$$A_{i,j}(\tau_i) = f_{i,j}^{k, \mathrm{tr}A}(A_{i-1,j}(\tau_i)), \qquad 1 \leqslant i \leqslant n, \ j \in \mathcal{J}^k, \tag{3.13j}$$

$$B_{i,1}(\tau_i) = f_i^{k, \mathrm{tr}B}(B_{i-1,1}(\tau_i)), \qquad 1 \leqslant i \leqslant n-1, \tag{3.13k}$$

$$0 = r_i^{k, \mathrm{eq}}(A_{i,1}(t_{i-n}), A_{i-n-1,1}(\tau_{i-n})), \qquad n+1 \leqslant i \leqslant M-1, \tag{3.13l}$$

where $\mathcal{J}^1 \overset{\text{def}}{=} \{j \mid 1 \leqslant j \leqslant i+1\}$ and $\mathcal{J}^2 \overset{\text{def}}{=} \{j \mid j = 1\}$.

This problem still contains a delayed term, but it is not apparent in the system's dynamics anymore. It has moved to a constraint (3.13e) on the controls. This can be efficiently dealt with with Bock's multiple shooting method we introduced in Section 1.3 for the special case of a constant delay. Note as well, that by treating the uncertainty in the duration of the recession by a scenario tree approach, the resulting problem (3.13) is closely related to a stochastic programming problem. We will discuss its consequences in the following sections.

3.2 Results of the Control Delay Case

3.2.1 Parametrical Setting

As suggested in [61, 63], we use the following set of parameters in our numerical treatment:

$$
\begin{aligned}
&\kappa = 2.0, \quad \gamma = 5.0, \qquad C = 7.5, \quad \delta = 0.05, \\
&m = 3.0, \quad \beta = 0.5, \qquad r = 0.1, \quad \lambda = 0.5, \\
&\varsigma_1 = 0.7, \quad \varsigma_2 = 0.836, \quad \varsigma_3 = 1.25.
\end{aligned}
\tag{3.14a}
$$

The choice for the parameters r, δ, and λ is based on the assumption that we measure time in years and that the historically expected duration of the recession is two years. We set β assuming that an increase in reputation will influence less and less customers. The more fashionable the product is, the more specialized is its market niche. See [63] for a motivation of the remaining parameters.

A key result of [63] was that the authors were able to distinguish three different types of recessions corresponding to the *severity of the demand reduction* and the resulting optimal strategy. Following their results, the values of the parameter ς indicate a *mild* ($\varsigma_1 = 0.7$), *intermediate* ($\varsigma_2 = 0.836$), and *severe* ($\varsigma_3 = 1.25$) economic crisis.

Due to the discretization of τ we need to further specify the last possible endpoint of the recession,

$$
\tau_n = 20.
\tag{3.14b}
$$

This implies that in our setting the probability of the recession persisting longer than that is low, i.e., $\mathbb{P}[\tau > 20] = 4.54 \cdot 10^{-5}$. For the control delay we choose

$$
\sigma = 0.25.
\tag{3.14c}
$$

To accomplish this, two equidistant discretization step lengths are applied, first with $n_1 = 20$, i.e., $h = \tau_i - \tau_{i-1} = 1.0$, and $n_2 = 40$, i.e., $h = 0.5$. Each of them is combined with four shooting nodes per one time unit, i.e., per one year. Then condition (3.13e) can be implemented via interior point constraints applied on the shooting nodes.

For convenience, the overall final time t_f is chosen to be

$$
t_f = 21 \text{ (years)},
\tag{3.14d}
$$

so that we definitely have a small normal period of one year in all possible stages, cf. Figures 3.2 and 3.3.

In the subsequent sections we provide some computational results. They are obtained with the following combinations of number of discretization points n (cf. (3.7)), recession parameter ς, initial values (A_0, B_0), and initial price paths η (constant on the time interval $[-\sigma, 0]$) for the delayed model, cf. Table 3.1.

Before we investigate the economic consequences that the combination of an uncertain recession length and the presence of a time delay have on decision-making for conspicuous consumption product, let us briefly mention the computational performance of the proposed reformulations.

3.2.2 Computational Performance

As discussed in Section 3.1.2, different mathematically equivalent reformulations of the OCP (3.6) exist. However, they are by no means equivalent from a computational point of view.

Table 3.2 compares the computational performance of the two different approaches to discretize the uncertainty. With the staircase formulation (3.11) (cf. Figure 3.2) the overall time horizon is quite small. However, the number of state variables is increased compared to the concatenated arrangement of the second reformulation (3.12), leading to more steps of the error-controlled, adaptive integrator. More significant, however, is the impact of more blocks in the HESSian of the LAGRANGian. They are used for high-rank updates, compare Section 1.3. This leads to a drastic increase in local convergence and hence to a decrease of the number of Sequential Quadratic Programming (SQP) iterations [162] and overall computation time, as can be seen in Table 3.2 for the undelayed case $\sigma = 0$. These results carry over to the case with time lag $\sigma > 0$. Therefore, in the following we will concentrate on the formulation (3.12) visualized in Figure 3.3. This includes Tables 3.3 and 3.4 as well.

As already observed in [51], the first approach to handle time lags σ (cf. Section 3.1.2) is computationally inferior to the second one, although it might be interesting from an analytical point of view. E.g., for Scenarios 4–12 the number of 1800 additional state and 1799 control functions needs to be included. Therefore, we will use the second formulation in the following for our calculations. Table 3.3 gives an overview of the moderate increase in the dimension of the resulting Nonlinear Program (NLP).

Table 3.4 gives an indication of the computational expense for including delays. The main part of the computational time is needed for the *condensing* algorithm, see [46, 161], which is almost identical for both cases, as the state dimension is independent of σ. The main extra cost is solving the Quadratic Programs (QPs), as the runtime depends crucially on the number of control variables. Therefore, asymptotically for $\sigma > 0$ getting smaller and smaller, the QP runtime will become more and more dominant.

3.2.3 Analytical Results

We deduce analytical results that help us to obtain a better insight into the qualitative changes related to the introduction of the time lag σ. We investigate the steady state in the normal period of our model (3.6) and compare it with the result of the undelayed case, i.e., $\sigma = 0$. The integral term of the objective function $J(\cdot)$ in (3.4) corresponds to the normal economic period, where the capital markets are working again and we are not using the cash state $B(\cdot)$

Table 3.1: Different scenarios used for computational performance tests and visualizations. Note that some of these scenarios are used in both a delayed ($\sigma = 0.25$) and undelayed problem ($\sigma = 0$), others in only one of them. In undelayed settings η is obsolete and denoted by "—".

Scenario	n	ς	A_0	B_0	η
1	20	0.7	10.0	5.0	—
2	20	0.836	20.0	5.0	—
3	20	1.25	100.0	100.0	—
4	40	0.7	10.0	5.0	7.406785
5	40	0.7	0.1	5.0	4.296460
6	40	0.7	10.0	2.0	7.088001
7	40	0.7	$\bar{A}_d^N$	5.0	$\bar{P}_d^N$
8	40	0.7	$\bar{A}_d^N$	1.0	$\bar{P}_d^N$
9	40	0.7	$\bar{A}_d^N$	0.1	$\bar{P}_d^N$
10	40	0.836	0.1	10.0	3.917962
11	40	0.836	0.1	10.0	3.5
12	40	0.836	0.1	10.0	3.0
13	40	0.836	0.1	10.0	2.5
14	40	0.836	20.0	5.0	8.153575
15	40	0.836	0.1	8.0	3.917948
16	40	0.836	25.0	3.5	8.671824
17	40	0.836	$\bar{A}_d^N$	1.0	$\bar{P}_d^N$
18	40	0.836	0.1	7.05	—
19	40	0.836	63.0	0.05	—
20	40	0.836	0.1	9.8	3.5
21	40	0.836	73.5	0.1	12.517549
22	40	1.25	100.0	100.0	10.751307
23	40	1.25	0.1	100.0	2.924618
24	40	1.25	40.0	80.0	7.855208
25	40	1.25	80.0	50.0	9.922934
26	40	1.25	0.1	60	2.924617
27	40	1.25	$\bar{A}_d^N$	50.0	$\bar{P}_d^N$
28	40	1.25	$\bar{A}_d^N$	70.0	—
29	40	1.25	0.1	76.0	—
30	40	1.25	$\bar{A}_d^N$	71.5	$\bar{P}_d^N$
31	40	1.25	0.1	79.5	2.924580

Table 3.2: Comparison of the computational performance of the different schemes for discretizing the duration of the recession τ, cf. (3.11), (3.12), and Figures 3.2, 3.3, respectively. The results correspond to the undelayed case, i.e., $\sigma = 0$.
The faster convergence of (3.12) (recognizable in SQP iterations and runtime) is due to the high-rank updates mentioned in Section 1.3. The scenarios are listed in Table 3.1.

Scenario item	Staircase scheme (3.11)		Linear scheme (3.12)	
	# of SQP	time (in s)	# of SQP	time (in s)
1	846	5259	51	1341
2	829	1312	35	835
3	858	1411	102	2969
4	1254	67131	102	21443
14	1716	93773	48	9615
22	915	47285	102	24163

Table 3.3: Comparison of the size of the resulting NLP for the delayed and the undelayed recession model. Note that these details refer to the concatenated reformulation of the scenario tree, i.e., (3.12). Furthermore, n is again the number of discretization points of the recession length.

	Undelayed model		Delayed model	
	$n = 20$	$n = 40$	$n = 20$	$n = 40$
discr. points	940	1840	940	1840
variables	3797	7437	4738	9278
eq. constraints	2855	5595	3797	7437
ineq. constraints	7594	14874	9476	18556

Table 3.4: Number of iterations and CPU runtime for undelayed and delayed scenarios, cf. Table 3.1. Again, the information refers to the linear formulation of the recession length discretization. The computational effort is moderately higher, when delays are taken into account.

Scenario	Undelayed model		Delayed Model	
	# of SQP	time (in s)	# of SQP	time (in s)
6	71	14103	60	20238
7	102	24515	98	28422
16	70	12896	102	28787
17	69	14796	82	24466
24	81	18114	81	22166
27	101	24456	101	29404

anymore. Let $\bar{A}^N_{d/nd}$ and $\bar{P}^N_{d/nd}$ denote the normal period's steady state brand image and price in the delayed (d) and the undelayed (nd) case, respectively.

Lemma 3.1

The normal period steady state brand image and price of the recession problem (3.6) *are given by*

$$\bar{A}^N_d = \left(\frac{\gamma m (r+\kappa)\,e^{r\sigma}}{2(r+\kappa)\,e^{r\sigma} - \beta\kappa} \right)^{\frac{1}{1-\beta}}, \qquad \bar{P}^N_d = \frac{\bar{A}^N_d}{\gamma}. \tag{3.15}$$

depending on the size of the time delay σ.   △

Proof By using the PMP [101, 120] we calculate

$$\bar{A}^N_{nd} = \left(\frac{\gamma m (r+\kappa)}{2(r+\kappa) - \beta\kappa} \right)^{\frac{1}{1-\beta}}, \qquad \bar{P}^N_{nd} = \frac{\bar{A}^N_{nd}}{\gamma}. \tag{3.16}$$

In the model's delayed version the maximum principle is far more complex, cf. [83]. However, in the normal period the stationary state of the corresponding one-dimensional problem can be derived using the results in [248]. We substitute

$$F(t) \stackrel{\text{def}}{=} F(A(t), P(t)) = P(t)\left(m - \frac{P(t)}{A(t)^\beta} \right) - C$$

and obtain the HAMILTONian

$$\mathcal{H} = e^{-rt}F(t) + \mu(t+\sigma)\cdot\kappa\gamma P(t) - \mu(t)\cdot\kappa A(t)$$

with the co-state variable $\mu(t)$. This induces the system

$$\dot{A}(t) = \kappa(\gamma P(t-\sigma) - A(t))$$
$$\dot{P}(t) = \frac{1}{\frac{\partial^2}{\partial P^2}F(t)}\left((r+\kappa)\frac{\partial}{\partial P}F(t) + \kappa\gamma\, e^{-r\sigma}\frac{\partial}{\partial A}F(t+\sigma) - \frac{\partial^2}{\partial P \partial A}F(t)\dot{A}(t) \right)$$

that directly gives us the stationary price $\bar{P}^N_d$. Further on, it yields

$$\frac{(r+\kappa)\,e^{r\sigma}}{\kappa\gamma} = -\frac{\frac{\partial}{\partial A}F(t+\sigma)}{\frac{\partial}{\partial P}F(t)}$$

and, therefore, the equality

$$(r+\kappa)\,e^{r\sigma} = -\frac{\beta\kappa(\bar{A}^N_d)^{1-\beta}}{\gamma m - 2(\bar{A}^N_d)^{1-\beta}}$$

that determines the stationary state of the brand image and the price

$$\bar{A}^N_d = \left(\frac{\gamma m (r+\kappa)\,e^{r\sigma}}{2(r+\kappa)\,e^{r\sigma} - \beta\kappa} \right)^{\frac{1}{1-\beta}}, \qquad \bar{P}^N_d = \frac{\bar{A}^N_d}{\gamma}. \qquad \square$$
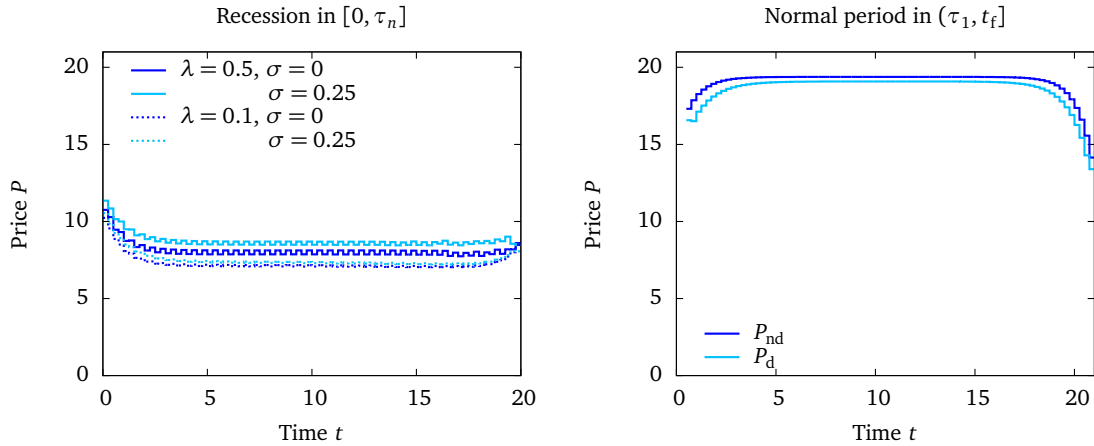
Figure 3.4: Exemplary optimal price paths of the recession problem (3.6).
The *left* plot depicts a recession period lasting until τ_n (using Scenario 22). During the recession phase $P_{\mathrm{d}} > P_{\mathrm{nd}}$ holds, but the difference in between depends on the size of the rate parameter λ.
The *right* plot visualizes a normal economic stage, also for Scenario 22. By way of better illustration this graphic shows price paths of a normal period beginning already at time τ_1. Note that neither λ nor the strength ς of the recession have any influence on these paths.

This latter result obviously includes the special case (3.16). The used parameters (3.14) determine the values

$$\bar{A}_{\mathrm{nd}}^{\mathrm{N}} = 96.899414, \qquad\qquad \bar{P}_{\mathrm{nd}}^{\mathrm{N}} = 19.379883, \qquad\qquad (3.17\text{a})$$
$$\bar{A}_{\mathrm{d}}^{\mathrm{N}} = 95.421259, \qquad\qquad \bar{P}_{\mathrm{d}}^{\mathrm{N}} = 19.084252. \qquad\qquad (3.17\text{b})$$

They coincide with the numerical results we obtained. One can see the impact of the delay very clearly. The benefit of keeping the price up is obtained later in the delayed world, while the benefit of reducing it (with instantaneous profit) is still obtained immediately.

In the recession period the verification and calculation of steady states cannot be done this straightforwardly. Further on, the so-called *weak* SKIBA *curves* play an important role. They are also known as *threshold* or *weak DNSS curves* , cf. [71, 222, 223, 228]; see also [101]. Weak SKIBA characterizes the threshold property of this curve separating different long-term solutions. Which strategy has to be applied is history-dependent and, thus, particularly depends on the initial state values. While the authors of [61] were able to derive several results of the non-delayed case analytically, for the delayed model this is much more difficult.

3.2.4 Numerical Results

In our approach to discretize the original recession problem (3.6) we assume a finite and discrete grid of possible switching times τ_i, $i = 1, \ldots, n$. We think that this transformation to the finite-time case is well justified, as the influence of the errors caused by the discretization are small. The intervals between the switching instants τ_i are short and the probability (3.8b) for switching the stage at the last possible time τ_n is only marginally higher than it would be in the infinite case.

In [61] possible pricing strategies in recession periods are explained depending on the value of ς. Additionally, the impact of these pricing policies on the development of the reputation
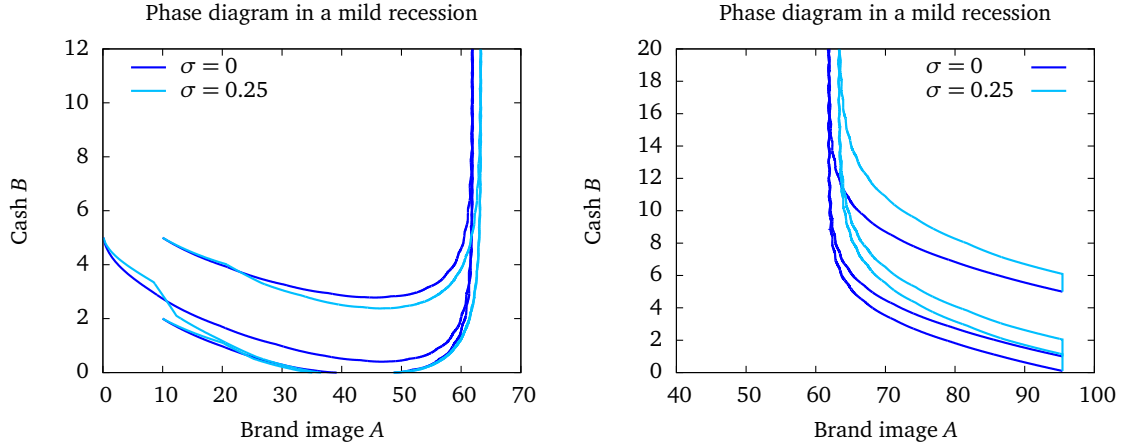
Figure 3.5: Evolution of optimal trajectories over time in a phase diagram with brand image $A(\cdot)$ and capital $B(\cdot)$. They start in the initial value (A_0, B_0) according to Table 3.1 and evolve until $(A(\tau_n), B(\tau_n))$. Optimal solutions of a delayed ($\sigma = 0.25$) and the undelayed ($\sigma = 0$) model are shown for a *mild* recession, i.e., $\varsigma_1 = 0.7$.

Further on, the two figures differ in the assumptions on the economic phase *prior* to the considered recession. The *left* plot is based on the assumption that for $t \in [-\sigma, 0]$ the recession has already been present (Scenarios 4–6 (from top to bottom)), the *right* plot depicts the result if for $t \in [-\sigma, 0]$ a steady state normal economic period existed, i.e., $A_0 = \bar{A}_d^N$, $\eta = \bar{P}_d^N$ (Scenarios 7–9).

Due to the introduction of the delay the recession's steady state of the brand image $\bar{A}_d^R$ (and correspondingly $\bar{P}_d^R$) is greater than in the undelayed case.

$A(\cdot)$ and the cash $B(\cdot)$ is characterized. In the delayed world the behavior of the firm is qualitatively similar. In a *severe crisis*, i.e., $\varsigma_3 = 1.25$, the brand image and/or cash required to avoid bankruptcy are particularly large. The milder the crisis is, the less reputation/cash is needed. In all cases the cash state diverges to infinity if the firm survives with certainty.

The main result of our analysis of problem (3.6) is the relation

$$
\begin{aligned}
P_d(t) &> P_{nd}(t), \quad 0 \leqslant t \leqslant \tau, \\
P_d(t) &< P_{nd}(t), \quad \tau \leqslant t \leqslant t_f,
\end{aligned}
\tag{3.18}
$$

which can be seen in Figure 3.4.

The optimal solution of the normal period follows the results of Section 3.2.3. Due to the delay σ there is a less direct effect of the price P_d on the dynamics of the brand image A. This reduces the incentive to set a high price, as a lower price raises revenues, which consequently raises the value of the objective function immediately.

In the recession period, however, the opposite relation holds. A direct consequence of this is visible in Figures 3.5 and 3.6: The vertical line indicating the divergence of the cash state B in an infinite horizon setting is shifted to a value $\bar{A}_d^R$ of reputation that is higher than the respective value $\bar{A}_{nd}^R$ in the non-delayed case.

While the negative effect of smaller revenues with higher prices (independent of the economic period) is the same for both the delayed and the undelayed case, there are also two positive aspects of increasing the price P_d.

The first effect is that the brand image A will increase as well during the recession, implying that the bankruptcy probability reduces. This effect is stronger the less the delay σ is. Hence, this first impact is the strongest in the non-delayed case.
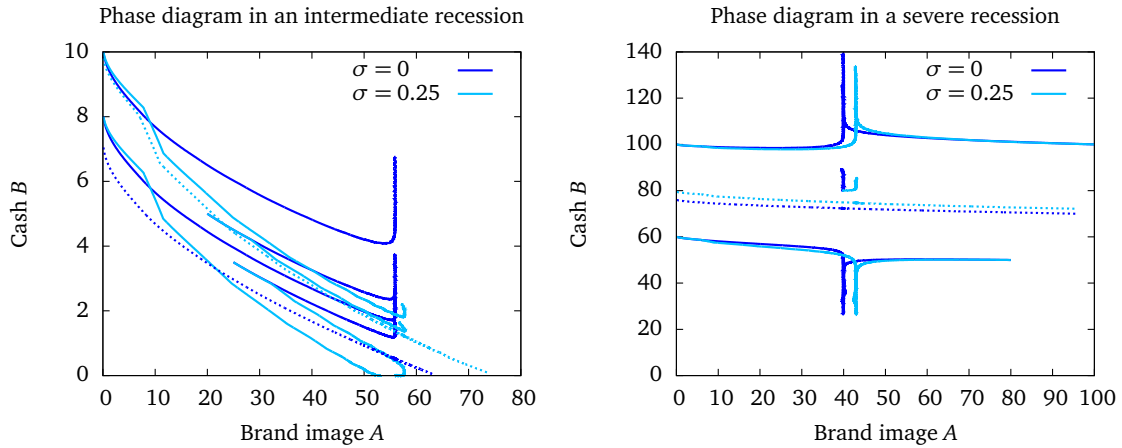
Figure 3.6: Phase diagram as in the *left* plot of Figure 3.5 for an intermediate and severe recession.
The *left* plot depicts Scenarios 10, 14–16, the *right* one Scenarios 22–26.
In analogy to weak SKIBA curves, the dotted lines based on Scenarios 18–21 (*left*) and 28–31 (*right*) indicate the initial values which separate the state space into the ones (above) that do not lead to bankruptcy and the ones (below) that do. After the introduction of the time lag σ the bankruptcy region becomes larger. This results in an upwards-adjustment of the weak SKIBA curve in the delayed case.

Given that the recession will be terminated somewhere during the next time interval of duration σ, the second effect of increasing P_{d} is that the reputation goes up after the recession, implying that the revenue of the normal period rises. This effect occurs with the probability $\mathbb{P}[\tau \in [t, t+\sigma]]$ that the recession will be over during the next interval of length σ, hence, it is stronger the larger the delay is. But it is completely absent in the undelayed case.

According to the first effect, which is comparable to the impact in the normal period, it will hold that $P_{\mathrm{d}} < P_{\mathrm{nd}}$ then. The second effect will imply the opposite relation during the recession stage. Note that this second impact only occurs with $\mathbb{P}[\tau \in [t, t+\sigma]]$, i.e., it depends on the size of σ and the probability density function.

In our case (with $\sigma = 0.25$) the second effect dominates, meaning that the mentioned probability is large enough. For the first effect to dominate we have to decrease this probability by either reducing the time lag or end of recession probability parameter λ. The results of the latter possibility can be seen in the *right* plot of Figure 3.4.

In a more vivid way we can interpret this second effect by assuming that the crisis ends at time $\hat{\tau}$. In the undelayed case the firm can start building up their reputation $A(\cdot)$ immediately after the realization of $\hat{\tau}$ by charging higher prices—supposing that it has survived recession. The effect on $A(\cdot)$ comes directly. If $\sigma > 0$ the impact of rising prices after $\hat{\tau}$ only starts to have a positive outcome from time $\hat{\tau} + \sigma$ onwards. In the initial phase of the then apparent normal period $[\hat{\tau}, \hat{\tau} + \sigma]$ the demand is directly influenced by the price set in the last interval of the recession. Hence, increasing prices in $[\hat{\tau} - \sigma, \hat{\tau}]$ leads to a higher reputation σ time units later. I.e., the demand is also higher in the period $[\hat{\tau}, \hat{\tau} + \sigma]$, which generates higher revenues during the first phase of the normal period. As the firm does not know beforehand when the recession will be over, there is always a positive probability that the current time t is located in the period $[\hat{\tau} - \sigma, \hat{\tau}]$. Keeping this in mind, the firm has an additional incentive to keep prices up in recession periods when a delay is apparent, avoiding to damage the reputation too much. Otherwise their product will still perceived to be comparatively cheap for some time period after the recession is over.

Phase diagram in an intermediate recession
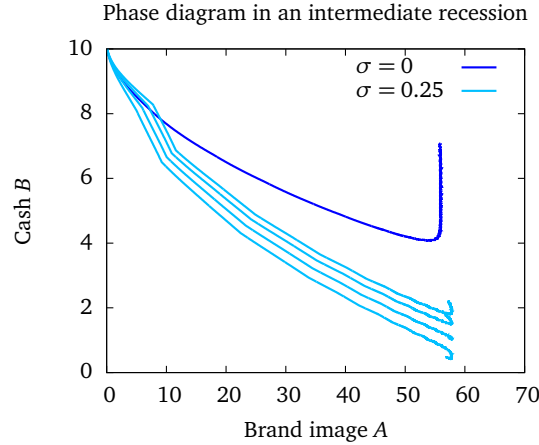
Figure 3.7: Phase diagram as in the *left* plot of Figure 3.5 for Scenarios 10–13 (grey lines from top to bottom). It is obvious that the initial control path η has a considerable influence on the firm's future situation.

Another important result can be observed in Figure 3.6. As observed already in [63], in cases of an intermediate or severe recession there is a weak SKIBA curve separating the regions of possible bankruptcy and certain survival. If $\sigma > 0$ this curve is adjusted upwards to some extent. With the incorporation of the delay in our model it is less easy for the firm to survive the crisis because the effect of changing the price $P(\cdot)$ on the brand image is less direct. This explains why the bankruptcy region becomes larger.

At the end of this Section we want to remark that the condition (3.13d) causes two main scenarios we have to distinguish in the delayed model. The economic stage that is apparent in the time prior to the planning period $[0, t_{\mathrm{f}}]$ can either be a normal or a recession stage. We consider two slightly simplified cases.

In the first one we assume a steady state corresponding to the normal economic period in the interval $[-\sigma, 0]$, i.e., we have already one "switching" occurrence at the beginning of the horizon. We initialize the retarded control with $\eta = \bar{P}_{\mathrm{d}}^{\mathrm{N}}$ and the brand image with $A_0 = \bar{A}_{\mathrm{d}}^{\mathrm{N}}$. Then the system evolves as shown in the *right* plot of Figure 3.5. The non-smooth behavior of the trajectories there is quite natural. At $t = 0$ the recession begins and the demand is reduced immediately due to the influence of ς. Hence, prices will drop and the firm's cash decreases. However, the brand image in the time interval $[0, \sigma]$ develops according to the high steady state price $\bar{P}_{\mathrm{d}}^{\mathrm{N}}$, i.e., it remains at its level. Only thereafter the condition (3.13e) becomes active and the reputation reacts to the lower prices.

The second case is more complicated. If we suppose a persisting recession stage, it is very hard to find a satisfying initialization η for the retarded price in the interval $[0, \sigma]$. In our calculations we started with the optimal price obtained in the first interval of the non-delayed model. This causes the kink in the initial part of the trajectories in Figures 3.5 and 3.6. Experiments of varying the value of η changed the amplitude of this deformation slightly, see Figure 3.7. In this special scenario the different initializations also had a qualitative influence on the bankruptcy probability of the firm. If the combination of brand image and cash moves below the weak SKIBA curve, the firm has to face bankruptcy in the long run. This happens for small initial prices, whereas high ones lead to certain survival.

3.3 Protection Against an Uncertain Recession Strength

Up to now only the duration of the crisis has been considered as a random variable, its strength was assumed to be known. However, in real world economics firms cannot grasp the strength of the recession beforehand, often they have to deal with this special situation while it is already apparent. To make a step towards gaining more insight into those real world effects, in the following we regard the recession strength ς as a random variable as well. Decision-makers do not know the actual magnitude of the crisis before they really have to face it. Hence, they have to apply pricing strategies that are in some sense *robust* against the real strength to avoid bankruptcy of the firm or to ascertain that the risk of possible failures is *acceptable*.

Consequently, the bankruptcy constraint $B(t; \varsigma) \geqslant 0$ (cf. Equation (3.6h)) becomes uncertain now and can be addressed by the approaches introduced in the previous Chapter 2. In this sense we also have to adapt the objective function (3.5) to the new situation.

A reasonable choice from an economic point of view is to reduce prices at the beginning of the crisis such that the company can cope with an average-heavy recession indicated by a certain $\hat{\varsigma}$, i.e., using the objective function (cf. (3.4))

$$J_{\text{res}}^1(A(\cdot), B(\cdot), P(\cdot); \tau, \hat{\varsigma}) = \mathrm{e}^{-r\tau} B(\tau, \hat{\varsigma}) + \int_\tau^{t_\mathrm{f}} \mathrm{e}^{-rt} \left(P(t) D_\mathrm{N}(A(t), P(t)) - C \right) \mathrm{d}t. \quad (3.19\mathrm{a})$$

Then prices can be reduced further if the crisis turns out to be more severe than expected first. The big disadvantage of that objective is that if the actual ς is smaller than anticipated, the firm cannot increase profit by setting higher prices as those are not optimal for the selected objective function (3.19a). Hence, to include the possibility of setting the highest possible price, the objective should be based on the situation where we have no recession, i.e.,

$$J_{\text{res}}^2(A(\cdot), B(\cdot), P(\cdot); \tau, \varsigma = 0) = \mathrm{e}^{-r\tau} B(\tau, 0) + \int_\tau^{t_\mathrm{f}} \mathrm{e}^{-rt} \left(P(t) D_\mathrm{N}(A(t), P(t)) - C \right) \mathrm{d}t. \quad (3.19\mathrm{b})$$

With that choice the reduction of prices during a recession of strength ς is only depending on the uncertain constraint $B(t; \varsigma) \geqslant 0$ being active.

In order to treat the end time τ of the recession as a exponentially distributed random variable again, the final objective function is the expectation of the NPV at τ, yielding

$$J^i(A(\cdot), B(\cdot), P(\cdot); \tau, \varsigma) \stackrel{\text{def}}{=} \int_0^{t_\mathrm{f}} \lambda \, \mathrm{e}^{-\lambda\tau} \, J_{\text{res}}^i(A(\cdot), B(\cdot), P(\cdot); \tau, \varsigma) \, \mathrm{d}\tau \qquad (3.20)$$

for $i = 1, 2$.

For the following considerations we regard only non-delayed problems. A positive time lag $\sigma > 0$ has no additional influence on the decision-making task.

3.3.1 The Resulting Control Problems

Linearization

The linearization approach (and the sigmapoint idea) introduced in the previous Chapter depend on distributed parameters, preferably normally distributed ones. Let ς be a Gaussian ran-

dom variable truncated to the interval $0 \leqslant \varsigma \leqslant m$ with mean value $\bar{\varsigma}$ and variance Σ. The truncation becomes necessary to guarantee that the constraint for the demand to be positive can be satisfied for all realizations of ς. However, for our choices of mean-variance-combinations (cf. Section 3.3.3) the differences to a standard normal distribution are neglectable.

The original bankruptcy constraint $B(t) \geqslant 0$ is replaced as in (2.5) to obtain

$$0 \leqslant B(t; \bar{\varsigma}) + \varpi \left\| \frac{\mathrm{d}}{\mathrm{d}\varsigma} B(t; \bar{\varsigma}) \right\|_{2,\Sigma}. \tag{3.21}$$

Thus, the constraint depends on the choices of the desired probability level ϖ and the variance Σ. Still, if the variance of the random parameter is not given but object of our investigation, we can fix the probability level to, say, $\varpi = 1$ and consider only different values of Σ indicating a combination of both notions.

The resulting problem reads

$$\begin{aligned}
\max_{P(\cdot)} \quad & J^i(A(\cdot), B(\cdot), P(\cdot); \tau, \varsigma) \\
\text{s.t.} \quad & \dot{A}(t) = \kappa(\gamma P(t) - A(t)), && t \in \mathcal{T}, \\
& \dot{B}(t) = P(t) D_{\mathrm{R}}(A(t), P(t)) - C + \delta B(t), && t \in [0, \tau], \\
& A(0) = A_0, \quad B(0) = B_0, && \\
& 0 \leqslant D_{\mathrm{R/N}}(A(t), P(t)), && t \in \mathcal{T}, \\
& P(t) \geqslant 0, && t \in \mathcal{T}, \\
& 0 \leqslant B(t; \bar{\varsigma}) + \varpi \left\| \frac{\mathrm{d}}{\mathrm{d}\varsigma} B(t; \bar{\varsigma}) \right\|_{2,\Sigma}, && t \in [0, \tau],
\end{aligned} \tag{3.22}$$

with $D_{\mathrm{R/N}}(\cdot)$ as in (3.3) and $J^i(\cdot)$, $i = 1, 2$, denoting the objective function as proposed in (3.19a) and (3.19b), respectively.

Sigmapoint Approach

For ς having a truncated normal distribution on the interval $0 \leqslant \varsigma \leqslant m$ with mean $\bar{\varsigma}$ and variance Σ, we use the sigmapoints

$$\varsigma_0 = \bar{\varsigma} \tag{3.23a}$$
$$\varsigma_1 = \bar{\varsigma} + \sqrt{\Sigma} \tag{3.23b}$$
$$\varsigma_2 = \bar{\varsigma} - \sqrt{\Sigma} \tag{3.23c}$$

and the modified constraint

$$B(t; \varsigma_j) \geqslant 0, \quad j = 0, 1, 2. \tag{3.24}$$

The emerging robust OCP becomes

$$
\max_{P(\cdot)} \quad J^i(A(\cdot), B(\cdot), P(\cdot); \tau, \varsigma)
$$

$$
\begin{aligned}
\text{s.t.} \quad & \dot{A}(t) = \kappa(\gamma P(t) - A(t)), & t \in \mathcal{T}, \\
& \dot{B}(t) = P(t)D_{\mathrm{R}}(A(t), P(t)) - C + \delta B(t), & t \in [0, \tau], \\
& A(0) = A_0, \quad B(0) = B_0, & \\
& 0 \leqslant D_{\mathrm{R/N}}(A(t), P(t)), & t \in \mathcal{T}, \\
& P(t) \geqslant 0, & t \in \mathcal{T}, \\
& 0 \leqslant B(t; \varsigma_j), & t \in [0, \tau], \quad j = 0, 1, 2,
\end{aligned}
\tag{3.25}
$$

with the notations as introduced before. The type of constraint function requires the implementation of the cash state dynamics for every sigmapoint ς_i, $i = 0, 1, 2$.

Value at Risk

We consider the chance constraint $\mathbb{P}[B(t; \varsigma) \geqslant 0] \geqslant \zeta$ for a given probability level ζ. As mentioned in Section 2.2, technically we have to include the distribution of the constraint $B(\cdot) \geqslant 0$ depending on the uncertain recession strength ς to calculate the appropriate probabilities. To overcome this difficulty, in the conspicuous consumption problem we can make use of Theorem 2.1.

Corollary 3.1
With the assumptions of the original recession model given by (3.6) *and* (3.5) *we deduce for a random parameter $\varsigma \in \mathcal{L}^2$ that*

$$
\mathbb{P}[B(t; \varsigma) \geqslant 0] \geqslant \zeta \quad \Longleftrightarrow \quad B(t; \mathrm{VaR}_\zeta(\varsigma)) \geqslant 0.
\tag{3.26}
$$

$\triangle$

Proof The dynamics of the cash state $B(\cdot)$ are given by

$$
\dot{B}(t; \varsigma) = P(t)D_{\mathrm{R}}(A(t), P(t)) - C + \delta B(t; \varsigma).
$$

As

$$
B(t; \varsigma) = B(0; \varsigma) + \int_0^t \dot{B}(s; \varsigma)\, \mathrm{d}s,
$$

we obtain the variational differential equation

$$
B_\varsigma(t; \varsigma) = B_\varsigma(0; \varsigma) + \int_0^t \left[P_\varsigma(s)D_{\mathrm{R}}(A(s), P(s)) + P(s)\frac{\partial}{\partial \varsigma}D_{\mathrm{R}}(A(s), P(s)) \right.
$$
$$
\left. + \delta B_\varsigma(s; \varsigma) \right] \mathrm{d}s.
\tag{3.27}
$$

From the results of [63, 118] we assume both the price $P(\cdot)$ and the demand in the recession period $D_{\mathrm{R}}(A(\cdot), P(\cdot))$ to be monotonically decreasing in ς. Hence, as the initial cash state $B(0; \varsigma)$

is independent of the recession strength, $\delta > 0$, and the price $P(\cdot)$ and demand $D_R(\cdot)$ are non-negative for all t, we conclude

$$B_\varsigma(t; \varsigma) \leq 0 \quad \forall t \text{ and } \forall \varsigma. \tag{3.28}$$

Then we can apply Theorem 2.1 (for $c(B) = -B$) to deduce the result. $\qquad\square$

Hence, we obtain the OCP

$$
\begin{aligned}
&\max_{P(\cdot)} \quad J^i(A(\cdot), B(\cdot), P(\cdot); \tau, \varsigma) \\
&\text{s.t.} \quad \dot{A}(t) = \kappa(\gamma P(t) - A(t)), && t \in \mathcal{T}, \\
&\qquad \dot{B}(t) = P(t)D_R(A(t), P(t)) - C + \delta B(t), && t \in [0, \tau], \\
&\qquad A(0) = A_0, \quad B(0) = B_0, \\
&\qquad\quad 0 \leq D_{R/N}(A(t), P(t)), && t \in \mathcal{T}, \\
&\qquad P(t) \geq 0, && t \in \mathcal{T}, \\
&\qquad\quad 0 \leq B(t; \mathrm{VaR}_\zeta(\varsigma)), && t \in [0, \tau],
\end{aligned}
\tag{3.29}
$$

for some given probability level $0 \leq \zeta \leq 1$ and the notations from before.

The evaluation of the reformulated Value at Risk (VaR) constraint $0 \leq B(t; \mathrm{VaR}_\zeta(\varsigma))$ still requires knowledge of the distribution of ς. With that information at hand, the implementation of the constraint necessitates one additional state variable $B(t; \mathrm{VaR}_\zeta(\varsigma))$ (apart from the one needed for the evaluation of the objective function).

Conditional Value at Risk

Analogous to the procedure in Section 2.2 we incorporate the Conditional Value at Risk (CVaR) constraint into our conspicuous consumption model. For fixed t the probabilistic constraint becomes (remembering $-B(t; \varsigma) \leq 0$)

$$0 \geq \mathrm{CVaR}_\zeta(-B(t; \varsigma)) = \min_{\vartheta \in \mathbb{R}} \left\{ \vartheta + \frac{1}{1-\zeta} \mathbb{E}\left[\max\{0, -B(t; \varsigma) - \vartheta\}\right] \right\}. \tag{3.30}$$

But as this constraint has to hold for all time instants $t \in [0, \tau]$, i.e., during the overall possible recession period, the control parameter ϑ in the minimization rule (3.30) actually becomes a control function $\vartheta(t)$. Thus, the resulting robust OCP reads

$$
\begin{aligned}
&\max_{P(\cdot), \vartheta(\cdot)} \quad J^i(A(\cdot), B(\cdot), P(\cdot); \tau, \varsigma) \\
&\text{s.t.} \quad \dot{A}(t) = \kappa(\gamma P(t) - A(t)), && t \in \mathcal{T}, \\
&\qquad \dot{B}(t) = P(t)D_R(A(t), P(t)) - C + \delta B(t), && t \in [0, \tau], \\
&\qquad A(0) = A_0, \quad B(0) = B_0, \\
&\qquad\quad 0 \leq D_{R/N}(A(t), P(t)), && t \in \mathcal{T}, \\
&\qquad P(t) \geq 0, && t \in \mathcal{T}, \\
&\qquad\quad 0 \geq \vartheta(t) + \frac{1}{1-\zeta} \mathbb{E}\left[\max\{0, -B(t; \varsigma) - \vartheta(t)\}\right], && t \in [0, \tau],
\end{aligned}
\tag{3.31}
$$

where the additional control function $\vartheta(\cdot)$ is necessary only during the recession and becomes redundant in a normal phase.

However, the evaluation of the CVaR constraint (3.30) requires calculating the inner expectation value. This in turn is derived with respect to the distribution of $B(\cdot; \varsigma)$ depending on the random recession strength. For a continuous distribution of ς, an appropriate approximation to a discrete random variable—as we have used to treat the exponentially distributed random recession end τ in Section 3.1.2—might be necessary. Then the calculation of the inner expectation simplifies to a sum over cash states depending on the n_ς possible outcomes of ς multiplied with the corresponding probabilities. Certainly, this demands the implementation of n_ς auxiliary cash states.

3.3.2 Strengths and Weaknesses of the Approaches

Theoretical Aspects

As we have already mentioned in Section 2.2, the traditional approaches in optimization under uncertainty, i.e., guessing the future, worst-case analysis, and relying on expectations, are coherent measures of risk in the basic sense, cf. Definition 2.1 and [12, 211]. Nevertheless, they inherit many disadvantages. Worst-case approaches take into account every possible outcome of the uncertain parameters, no matter how unlikely it may be. While this characteristic of the worst-case approaches becomes crucial in applications like safeguarding chemical processes or to avoid irreversible reactions in runaway processes [150], in economic situations it is often too conservative. In many such circumstances decision-makers accept a certain amount of risk of failure in order to achieve greater gains.

Both the linearization and sigmapoint methods, compare Sections 2.1 and 3.3.1, allow the investigation of desired confidence levels ϖ as proposed in [38] if the variance Σ is known. Otherwise combinations of ϖ and σ have to be considered. From an economic point of view, the sigmapoint approach has advantages over the linearization method as it allows deeper economic insight in the behavior of the solution. This is induced by the auxiliary cash state variables that are needed to treat the constraints for all sigmapoints. In contrast to the worst-case approaches the expectation-based ideas provide acceptable risks even if desirable outcomes merely compensate the undesirable ones. Hence, they are often too optimistic to be applied in questions of economics.

To overcome the general difficulties of worst-case and expectation based ideas, especially in the field of finance, the VaR attracted much attention. Unfortunately, despite its broad usage, it is generally not a coherent measure of risk [12, 211]. Thus, in the special case of portfolio optimization, the VaR does not satisfy the diversification principle [12]. Moreover, it tends towards optimistic estimations of uncertain situations as it does not provide a grasp on the seriousness of constraint violations [211]. These properties are a severe disadvantage in risk management or in an economic situation where the firm has the possibility to borrow money at the market and the corresponding interest rates increase with the amount of needed cash. In our considered conspicuous consumption model with malfunctioning capital markets, however, the extent of violating a constraint, namely the bankruptcy constraint $B(\cdot) \geqslant 0$, is less important, as the firm has to face bankruptcy in any case where $B(\cdot)$ becomes negative. Thus, the negative connotation of the VaR is unjustified in our special economic case.

As mentioned before, the CVaR provides a more cautious approach to safeguarding than the

incorporation of pure chance constraints by the VaR, because it rates constraint violations caused by decisions. Additionally, it has been proven under various assumptions that the CVaR describes a coherent measure of risk [2, 213], which constitutes it to be a reliable quantifier of risk. However, in our special economic situation the classification of constraint violations by using the CVaR is a subordinate issue, which can cause the resulting pricing strategies to be very risk-averse or even too conservative.

Numerical Effort

Besides the theoretical and economical aspects of using the presented robustification techniques, there are as well broad differences from the numerical point of view.

The general formulation of an ellipsoidal robust constraint (2.3) leads to a semi-infinite OCP that is very hard to solve numerically. Therefore, an approximation of (2.3) by either the linearization or the sigmapoint approach is necessary. The resulting problems (3.22) and (3.25) can be efficiently solved by existing methods like, e.g., Bock's direct multiple shooting approach, cf. Section 1.3. For highly nonlinear problems that linearization idea can cause approximation errors, whereas the robustness of solutions obtained by it cannot be guaranteed. As a remedy higher order approximation schemes may become useful, compare the method proposed in [109]. Another possibility [74, 75] is to replace the inner minimization term by its sufficient optimality condition. All of the listed ideas result in a far more difficult problem as additional equations have to be considered. Consequently, the computational effort increases considerably. Within the sigmapoint approach, however, the computational complexity is extended by additional path constraints that require the implementation of cash state variables depending on the propagated sigmapoints (3.23).

In general the VaR is difficult to work with numerically, e.g., if loss distributions feature "fat tails" or jumps, cf. [213]. In our context and reasoned by the considerations above, particularly Theorem 2.1 and Corollary 3.1, we only need the distribution of ς to calculate its VaR for a given confidence level ζ. Thus, the incorporation of the VaR constraint in the conspicuous consumption model can be done very efficiently as only one additional cash state variable and one additional path constraint are needed.

By contrast, implementing the CVaR is far more complex. The minimization rule (3.30) induces that besides the additional control variable $\vartheta(\cdot)$ the calculation of the expectation within the formula is needed. For a discrete distribution of the random recession strength ς—which might be obtained by some appropriate approximation of a continuous distribution—, this can be achieved by introducing n_ς auxiliary cash state variables depending on the values the random variable attains with a corresponding probability. Thus, the computational effort increases with the number n_ς of those auxiliary cash state variables.

To illustrate the differences in the costs of solving the multi-stage OCPs resulting from the different robustification methods, Table 3.5 presents the overall dimensions of the NLPs obtained by transforming those problems with the direct multiple shooting approach. Note that we limited our investigations here to the—numerically superior—rearranged formulation of the scenario tree to discretize the uncertain recession length, depicted in Figure 3.3.

Within Table 3.5 we can see that the smallest resulting problem we obtain when using the VaR approach. As more additional state variables and/or constraints are needed for both robust approaches, those problems are slightly larger, whereas the CVaR is the largest one. This is mainly

Table 3.5: Dimensions of the NLPs problems resulting from the conspicuous consumption problem (3.6) with the presented robustification/probabilistic techniques (linearization and sigmapoint approach, VaR and CVaR and choosing between the objective functions (3.19a) determined by $\varsigma = \bar{\xi}$ and (3.19b) determined by $\varsigma = 0$.
The smallest problem we obtain for the VaR approach, the largest one for the CVaR. This is caused by the necessity of auxiliary cash state variables and, mainly, an additional control function.

	Linearization (3.22)	Sigmapoint (3.25)	VaR (3.29)	CVaR (3.31)
Objective function $J^1(\cdot)$ (3.19a)				
# discr. points	1840	1840	1840	1840
# variables	12957	11195	9316	18632
# eq. constr.	11112	9351	7473	14946
# ineq. constr.	27754	27910	18752	37384
Objective function $J^2(\cdot)$ (3.19b)				
# discr. points	1840	1840	1840	1840
# variables	16676	13074	9316	20511
# eq. constr.	14829	11229	7473	16824
# ineq. constr.	35192	31668	18752	41142

caused by the second control function that is required to implement the constraint. These variations are reflected in the Central Processing Unit (CPU) time behavior as well, compare Table 3.6. While the differences in the number of state functions of the linearization/sigmapoint/VaR approach do not influence the average runtime (per SQP iteration) and its distribution among the parts of the solving procedure much, the additional control function of the CVaR approach does. The runtime of that robustification method is noticably higher, as the effort to solve the QPs becoming more prominent.

3.3.3 Numerical Results of the Uncertain Strength Case

The following numerical results are again based on the parameters defined in (3.14) and the assumption that the recession lasts at most 20 years, whereas the overall considered time horizon is $t_{\mathrm{f}} = 21$ years. Additionally, we choose the initial reputation and cash to be

$$
\begin{aligned}
A_0^1 &= 20.0, & B_0^1 &= 10.0, \\
A_0^2 &= 40.0, & B_0^2 &= 50.0,
\end{aligned}
\tag{3.32}
$$

which both correspond to economic starting points, where the firm can cope with an intermediate (A_0^1, B_0^1) or severe (A_0^2, B_0^2) recession for a certain time period, but which does not hold enough capital reserves to survive a continuing recession [63, 118]. Finally, the random variable ς for the linearization and the sigmapoint approaches is characterized by its mean value

Table 3.6: Exemplary computation times in h:min:s for solving the NLP problems of Table 3.5. Note that solving the problem with CVaR constraint is most expensive, due to the additional control function. The remaining approaches need comparable computation times.

	Linearization (3.22)		Sigmapoint (3.25)		VaR (3.29)		CVaR (3.31)	
			Objective function $J^1(\cdot)$ (3.19a)					
IND	1:19	(1.0%)	24	(0.3%)	11	(0.2%)	1:00	(0.3%)
state int.	15	(0.2%)	5	(0.1%)	3	(0.0%)	8	(0.0%)
condensing	1:59:04	(87.3%)	2:06:42	(84.6%)	1:34:02	(86.9%)	4:24:36	(67.9%)
solving QP	15:46	(11.5%)	22:27	(15.0%)	1359	(12.9%)	2:03:56	(31.8%)
rest	3	(0.0%)	2	(0.0%)	2	(0.0%)	4	(0.0%)
	2:16:27	(39 SQP)	2:29:40	(43 SQP)	1:48:17	(34 SQP)	6:29:44	(62 SQP)
			Objective function $J^2(\cdot)$ (3.19b)					
IND	2:26	(1.5%)	26	(0.4%)	13	(0.1%)	52	(0.3%)
state int.	21	(0.2%)	5	(0.1%)	4	(0.1%)	6	(0.0%)
condensing	2:17:26	(86.6%)	:1:44:53	(86.2%)	2:20:47	(86.5%)	3:29:15	(70.0%)
solving QP	18:21	(11.6%)	16:12	(13.3%)	21:41	(13.3%)	1:28:49	(29.7%)
rest	4	(0.1%)	2	(0.0%)	2	(0.0%)	4	(0.0%)
	2:38:38	(41 SQP)	2:01:38	(35 SQP)	2:42:47	(42 SQP)	4:59:06	(42 SQP)

$$\bar{\varsigma} = 0.836 \tag{3.33}$$

and varying values of variance Σ. For analyzing the VaR and CVaR, we assume that we know a certain distribution of the random variable, e.g., by historical data. Thus, we define ς of these approaches through

$$
\begin{aligned}
\mathbb{P}[\varsigma = 0.5] &= 0.1 \\
\mathbb{P}[\varsigma = 0.7] &= 0.3 \\
\mathbb{P}[\varsigma = 0.836] &= 0.4 \\
\mathbb{P}[\varsigma = 0.9] &= 0.15 \\
\mathbb{P}[\varsigma = 1.25] &= 0.05.
\end{aligned}
\tag{3.34}
$$

Linearization and Sigmapoint Approaches

Both methods to approximate the robust formulation (2.3) depend only on the variance Σ if we fix the confidence level $\varpi = 1$, i.e., considering a combination of these two notions as we assume the exact variance of the random recession strength to be unknown. Figures 3.8 and 3.9 depict the optimal price paths in the recession period $[0, \tau]$ of problems (3.22) and (3.25), respectively, when the objective function is $J^1(A(\cdot), B(\cdot), P(\cdot); \tau, \varsigma)$ and initial values A_0^1, B_0^1 are used.
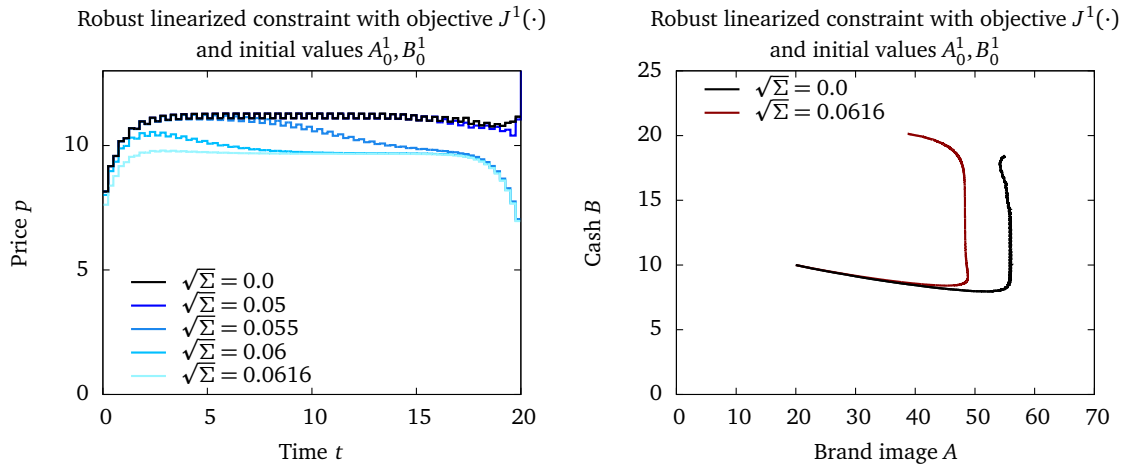
Figure 3.8: Robust price paths of the recession phase (*left* plot) and exemplary phase diagram (*right* plot) for problem (3.22) with objective function $J^1(\cdot)$ obtained by using the linearization approach (3.21). The price paths depend on the variance Σ of the uncertain recession strength if we fix the confidence level $\varpi = 1$. Then higher variances require decision-makers to decrease prices appropriately.
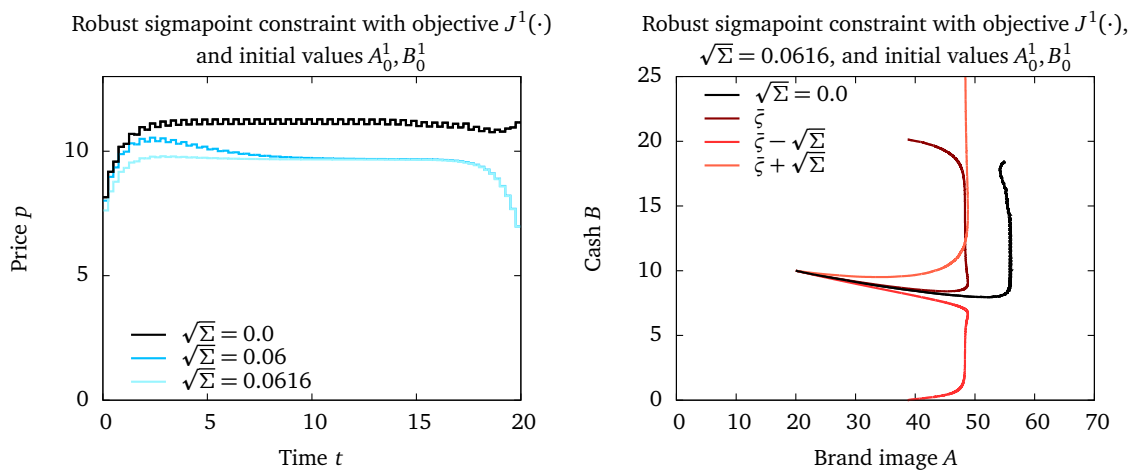

Figure 3.9: Robust price paths of the recession phase (*left*) and exemplary phase diagram (*right*) for problem (3.25) with objective function $J^1(\cdot)$ obtained by using the sigmapoint approach. The phase diagram depicts the connection of brand image state and the cash states depending on the sigmapoints ς_i, $i = 0, 1, 2$.

We notice that both approaches yield equal optimal pricing strategies and objective values (compare Table 3.7). For very low variances the prices during the recession phase do not have to be reduced, as the objective function already includes some caution towards the realization of ς and the initial cash B_0 is enough to keep the cash state positive during the complete recession even if the worst possible outcome of ς based on Σ takes place. For higher variances the decision-maker has to decrease prices in order to survive the recession.

Only for the combination of objective function $J^2(\cdot)$ and initial values (A_0^1, B_0^1) we notice gaps between the optimal objective function values. This is caused by the differences in the resulting constraints in interaction with the objective. E.g., let us consider the results for $\Sigma = 0.0/\zeta = 0.0$. Both robust approaches deal with the constraint $B(t; \bar{\varsigma} = 0.836) \geqslant 0$ (which can be seen best by looking at the constraints of the sigmapoint approach), whereas the VaR constraint becomes $B(t; \mathrm{VaR}_0(\varsigma) = 0.5) \geqslant 0$. The CVaR constraint tends to $\mathbb{E}[B(t; \varsigma] \geqslant 0$, cf. Theorem 2.2.

Additionally, Table 3.7 shows how much of the overall gains is lost, if decision-makers have to reduce prices according to an uncertain recession strength with mean $\bar{\varsigma}$ and variance Σ. Note that the actual profit is obtained during the normal economic stage, but is strongly depending on the reputation level the firm can keep during the crisis.

In the phase diagrams of Figures 3.8 and 3.9 the implications of decreasing prices can be seen: consistent with its dynamics, the firm's brand image is damaged as well. The great economic advantage of the sigmapoint approach here is that due to the additional cash state variables needed to implement the modified constraints (3.24) based on the sigmapoints (3.23) (especially for $\varsigma_2 = \bar{\varsigma} + \sqrt{\Sigma}$), we can see the actual reason of reducing prices. It is caused by the decision-maker's optimal strategy to balance prices in a way that the firm operates into a *zero cash-situation* at time $t = 20$ (years) when the economic crisis will finally be over (due to our assumption of $\tau_n = 20$). Naturally, in an ever-lasting recession the firm finally has to face bankruptcy, if its initial reputation and cash stock are not sufficiently high.

However, the decision-maker's optimal strategy is based on another important principle. Prices have to be kept as high as possible as long as possible in order to preserve the reputation of the product, as this will guarantee the firms success once the crisis is over. Therefore, in the beginning of the recession the optimal strategy is charging the optimal, i.e., highest possible price for the chosen objective function assuming there is no chance of a stronger crisis. Only when the recession persists longer, prices eventually have to be reduced according to the worst possible realization of ς determined by the variance Σ and the firm's incentive to keep cash until τ_n. By this strategy the brand image remains at a high level in the first period of the recession when it is very probable that τ is reached soon. In that situation the gains of the normal economic stage are higher as if the decision-maker set a constant price during the longest possible duration τ_n of the recession. The same behavior can often be observed at the very end of the longest possible recession—rather than fixing the price at some constant level $\tilde{P}$, it is more profitable reducing prices considerably at the last possible instance when this measure is successful and concurrently being able to set a (slightly) higher price $P > \tilde{P}$ in the period before. The general effect can be noticed in Figures 3.8 and 3.9 but more obviously in Figure 3.10, which shows the optimal price paths of problem (3.22) with the objective function $J^2(A(\cdot), B(\cdot), P(\cdot); \tau, \varsigma)$ and both sets of initial values. Clearly, it is more apparent for smaller variances. In general, this adaptive shape is closely related to optimal strategies from stochastic optimization. Here, it is certainly induced by our scenario tree approach to discretize

Table 3.7: Optimal objective values J^* for the robust/probabilistic conspicuous consumption problems (3.22), (3.25), (3.29), and (3.31). It is shown how much is lost if we regard the different approaches with varying values of variance Σ (for the robust approaches (3.22) and (3.25)) or ζ-level (for the probabilistic problems (3.29) and (3.31)) in comparison with the nominal solution (i.e., $\Sigma = 0$ or $\zeta = 0$). Note that the major part of this objective value is obtained during the normal economic phase depending on the performance during the recession.

We can see that both methods of robust approximation give equal results. Further on, the relation between the ζ-levels in the VaR and CVaR approaches and the confidence levels in the linearization and sigmapoint ideas (included indirectly in the variances) is observable, as well as the differences in the cautiousness of VaR and CVaR. Note that the gaps in the nominal objective values (regarding $\Sigma = 0.0/\zeta = 0.0$, particularly for objective function $J^2(\cdot)$ and initial values (A_0^1, B_0^1)) are caused by differences in the resulting constraints.

| Linearization (3.22)		Sigmapoint (3.25)		VaR (3.29)		CVaR (3.31)	
$\sqrt{\Sigma}$	J^*	$\sqrt{\Sigma}$	J^*	ζ	J^*	ζ	J^*
Objective function $J^1(\cdot)$ (3.19a) and (A_0^1, B_0^1)							
0.0	88.5342	0.0	88.5342	0.0	88.5344	0.0	88.5344
0.06	88.5055	0.06	88.5055	0.9	88.5344	0.4	88.5343
0.0616	88.4009	0.0616	88.4009	0.92	88.5343	0.45	88.5338
				0.93	88.5338		
				0.94	88.5099		
Objective function $J^2(\cdot)$ (3.19b) and (A_0^1, B_0^1)							
0.0	106.8768	0.0	106.8768	0.0	107.6456	0.0	107.2890
0.02	106.3943	0.02	106.3943	0.4	107.6321	0.3	106.2436
0.04	105.3583	0.04	105.3583	0.8	106.8768	0.4	104.3689
0.06	102.4368	0.06	102.4368	0.9	105.1500	0.45	103.6880
0.0616	101.4003	0.0616	101.4003	0.94	102.5151		
Objective function $J^2(\cdot)$ (3.19b) and (A_0^2, B_0^2)							
0.0	146.5020	0.0	146.5020	0.0	146.5021	0.0	146.5019
0.06	146.5006	0.06	146.5006	0.4	146.5021	0.8	146.4537
0.2	146.4839	0.2	146.4839	0.9	146.5015	0.9	145.7950
0.3	145.5607	0.3	145.5607	0.96	146.4734	0.92	145.7755
0.4	143.0664	0.4	143.0664	0.99	144.7815	0.95	142.4378
0.414	142.4379	0.414	142.4379	1.0	142.4379		
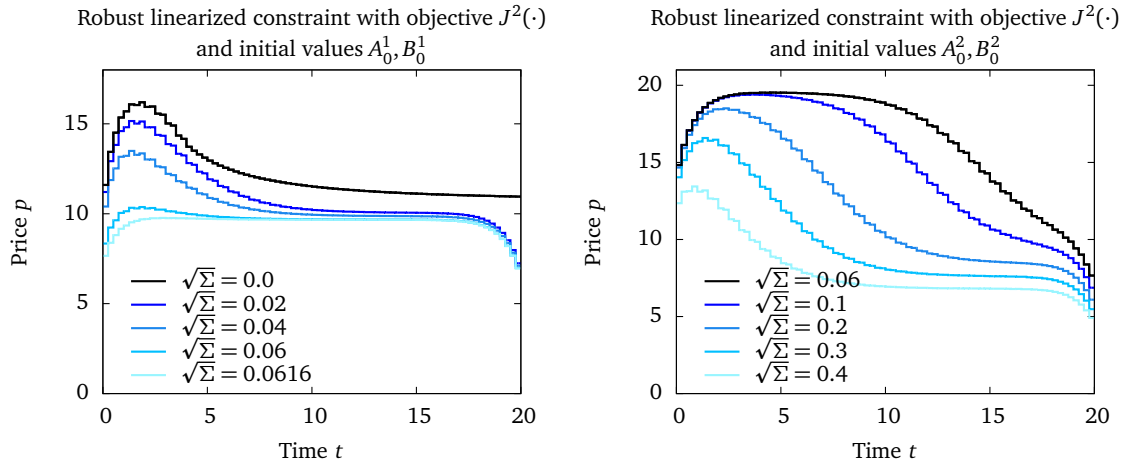
Figure 3.10: Robust price paths of the recession phase as in Figure 3.8, but for the objective function $J^2(\cdot)$ and initial values A_0^1, B_0^1 (*left* plot) and A_0^2, B_0^2 (*right*). With higher initial values the firm can cope with more serious situations.

the terminal time τ of the recession.

Moreover, in Figure 3.10 the connection between the variance and the reduction of prices is observable more directly as if the objective of the firm depends on the no-recession situation. Additionally, the right plot shows optimal prices if the firm starts with a higher initial reputation and capital stock. Then it can even cope with situations where the variance of the random recession strength is assumed to be relatively large, including the (worst possible) realization of a severe recession characterized by $\varsigma = 1.25$. This results because for the set of large initial values (A_0^2, B_0^2) prices can be decreased further than for the set of small initial values. For the latter set, we cannot calculate solutions corresponding to large variances of ς or even the worst case, as this solution is infeasible.

Value at Risk

In order to calculate the VaR of the random recession strength we use the definition (3.34) of ς. Therefore, the mean of the random variable defined by that distribution varies a little from the value $\bar{\varsigma}$ we have used in the last paragraph. Nevertheless, for reasons of comparison, we still implement the first alternative of the objective function $J^1(\cdot)$ with $\bar{\varsigma}$. The actual quantiles of the recession strength corresponding to a given probability level ζ can be obtained by linear interpolation of the distribution given in (3.34).

Figures 3.11–3.13 depict solutions of Problem (3.29). As already noticed in the previous paragraph for the robust approaches, when considering the objective function $J^1(\cdot)$ including a pre-assumption of an intermediate recession strength, prices have to be reduced only for relatively large probability levels ζ. Therefore, economic challenges favor the second choice of objective function $J^2(\cdot)$ based on a no-recession scenario. Then the connection between the desired confidence level ζ and the price reductions becomes more apparent.

From comparing the optimal objective values of the VaR and the robust linearization and sigmapoint approaches in Table 3.7, we see a certain correspondence between the probability levels ζ of VaR and the confidence level/variance-combination within the robust formulations, even as they are based on very different assumptions on the random variable ς. In contrast to the linearization and sigmapoint idea, the nominal solution of the VaR approach with objec-
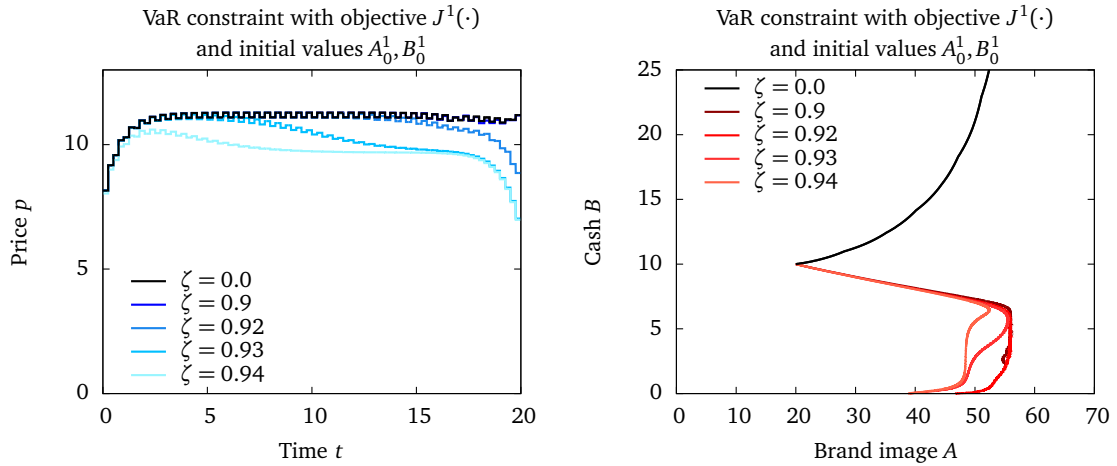
Figure 3.11: Robust price paths of the recession phase (*left*) and exemplary phase diagram (*right*) for problem (3.29) with objective function $J^1(\cdot)$ obtained by using the probability constraint as in Corollary 3.1. In the phase diagram the brand image is plotted against the cash state variable $B(t; \text{VaR}_\zeta(\varsigma))$ corresponding to the desired confidence level ζ.
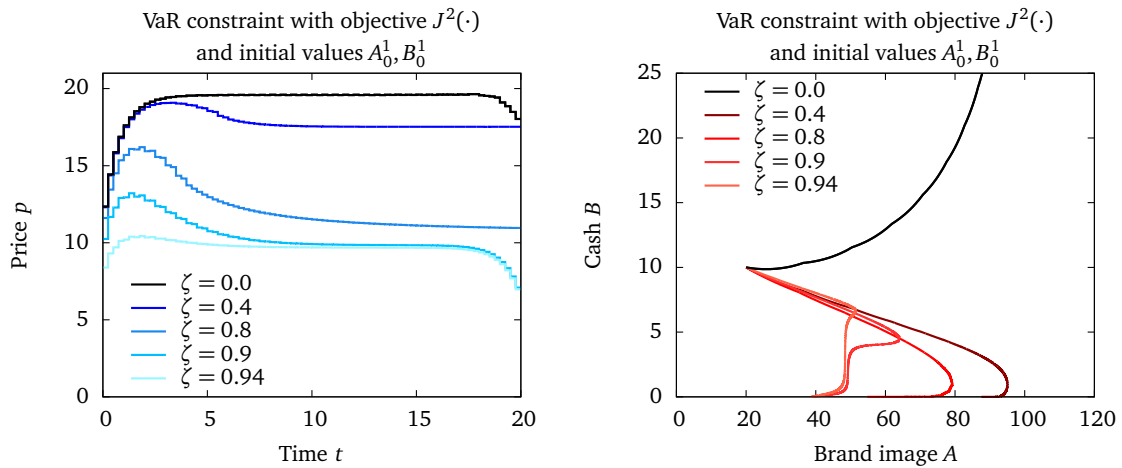
Figure 3.12: Robust price paths of the recession phase and phase diagram as in Figure 3.11, but for the objective function $J^2(\cdot)$ and initial values A_0^1, B_0^1.

tive function $J^2(\cdot)$ is obtained by the constraint $\mathbb{P}[B(t; \varsigma) \geqslant 0] \geqslant 0$, i.e., by a constraint that considers a no recession-scenario. Thus, the corresponding objective value is higher than for the robust formulations.

Like in the sigmapoint approach, the additional state variable $B(t, \text{VaR}_\zeta(\varsigma))$ that is needed to implement the chance constraint allows for more economic insight, as we can see how the firm's cash evolves into zero when the crisis lasts for the worst possible duration τ_n. Furthermore, in the phase diagrams of Figures 3.12 and 3.13—observe particularly the trajectories corresponding to the probability level $\zeta = 0.4$—we can see how the initial conditions impinge on a long persisting recession: while it is not possible for the firm to survive a very long ($\tau > 20 = \tau_n$) recession with initial conditions $(A_0, B_0) = (20.0, 10.0)$ for the corresponding recession strength as $B(\cdot)$ evolves towards zero, this is the case if the initial conditions are $(A_0, B_0) = (40.0, 50.0)$, where $B(\cdot)$ evolves to infinity.

In general we can observe that applying the VaR as robustification measure leads to very reasonable pricing strategies depending on the probability levels ζ and, therefore, the VaR of the uncertain recession strength ς based on its definition (3.34). Due to the fact that a rating
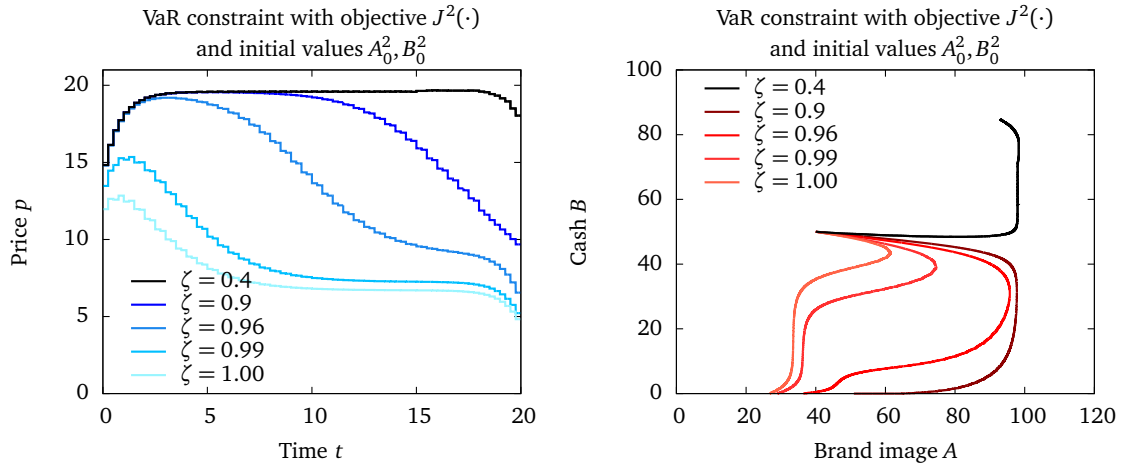
Figure 3.13: Robust price paths of the recession phase and phase diagram as in Figure 3.11, but for the objective function $J^2(\cdot)$ and initial values A_0^2, B_0^2.

of violations of the constraint $\text{VaR}_\zeta(B(t;\varsigma)) \geqslant 0$ plays a subordinate role in the conspicuous consumption model, the results do not suffer from the VaR not being a coherent measure of risk.

Conditional Value at Risk

Again, we use ς as defined in (3.34), but include $\bar{\varsigma}$ in the first objective function $J^1(\cdot)$ again. Furthermore, the expectation operator within the CVaR constraint (3.30) turns into a summation due to the discrete definition of ς. Therefor, we have to implement five auxiliary cash state variables depending on the possible outcomes of the recession strength.

The solutions of Problem (3.31) for both variants of the objective function and both sets of initial values can be seen in Figures 3.14 and 3.15. The price paths behave qualitatively equal as in the aforementioned approaches, apart from the fact that prices obtained with a CVaR constraint are more cautious than prices obtained with, e.g., a VaR constraint (compare the objective values and corresponding ζ-levels in Table 3.7 as well). It means, that for a given confidence level ζ the corresponding prices $P_{\text{CVaR}}(\cdot)$ obtained with a CVaR constraint are lower than the prices $P_{\text{VaR}}(\cdot)$ obtained with one of the other approaches, e.g., the VaR. Compare, for instance, the left plots in Figures 3.13 and 3.15.

Moreover, from Table 3.7 we notice that the nominal value of the CVaR approach is based on the CVaR constraint corresponding to the expectation value $\mathbb{E}[B(t;\varsigma)]$, compare Theorem 2.2. This is again different from the robust methods and the VaR, where the nominal solution is based on a constraint with $\bar{\varsigma}$ and $\varsigma = 0$, respectively, compare Remark 2.2. The cautiousness of this method is reflected in the optimal objective values of corresponding ζ-levels as well.

With linearized robustification, sigmapoints, and the VaR we obtain a cash state $B(\cdot)$ that corresponds directly to the robustified constraint. Hence, we can analyze the behavior of the constraint in a phase diagram of reputation A and cash B. With the CVaR approach this is not the case, as the constraint is realized via the minimization rule (2.14). Therefore, in both Figures 3.14 and 3.15 we depict cash state trajectories during the recession phase $[0, \tau_n]$ for a specific realization of the random variable ς, i.e., $\varsigma = 0.9$ which occurs with a probability of 15 percent. One notices, e.g., from Figure 3.14, that the cash state $B(t, \varsigma = 0.9)$ corresponding to a recession with that particular strength can drop below zero, but still the desired confi-
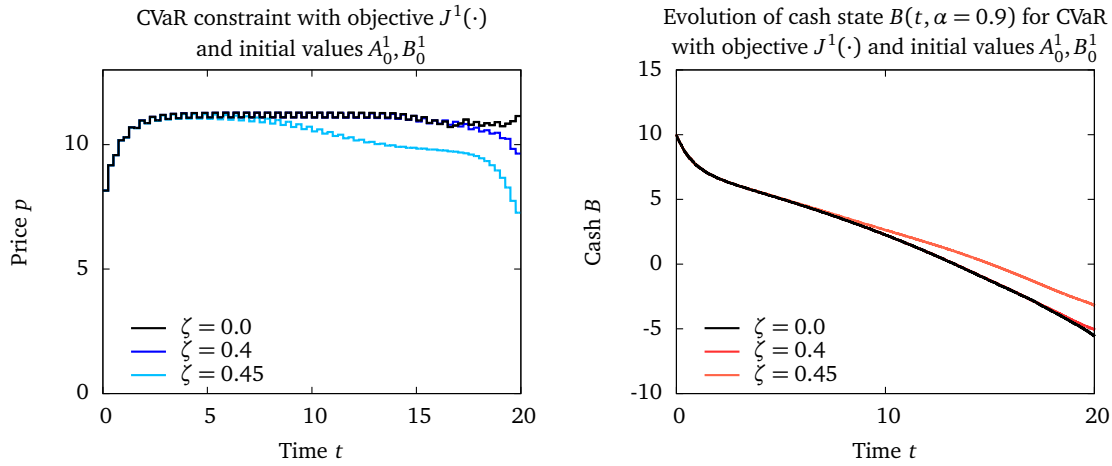
Figure 3.14: Robust price paths of the recession phase (*left* plot) and exemplary cash state trajectory $B(\cdot)$ during this phase (*right* plot) for problem (3.31) with objective function $J^1(\cdot)$. The cash trajectory is depicted for an intermediate recession of strength $\varsigma = 0.9$.
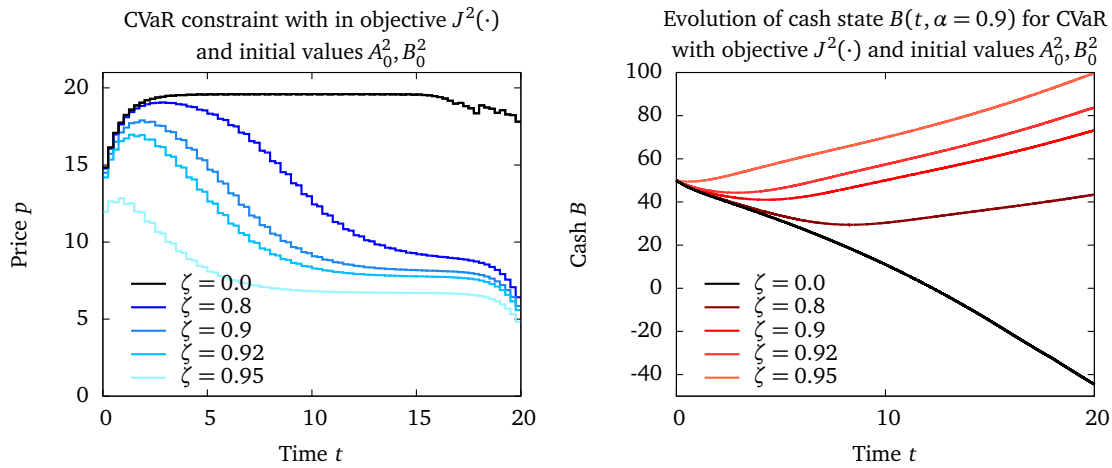

Figure 3.15: Robust price paths of the recession phase and phase diagram as in Figure 3.14, but for the objective function $J^2(\cdot)$ and initial values A_0^2, B_0^2.

dence level (of, e.g., $\zeta = 0.45$) is reached. If the confidence level is increased, then in order to fulfill this level prices have to be adjusted in a way such that eventually the cash state for $\varsigma = 0.9$ remains positive for all possible durations of the recession and only the cash states corresponding to the severe recession may become negative.

Furthermore, caused by the classification of constraint violations in the CVaR approach due to the minimization formula (2.14), the approach tends to be a bit too conservative in the context of the conspicuous consumption problem. Hence, the CVaR is a very risk-averse version of safeguarding.

3.4 Summary

In this chapter we analyzed the pricing of conspicuous consumption products in economic crisis periods. In order to gain a better insight in the development of strategies applicable in real-world economics, we investigated different sources of uncertainty entering the deterministic model—an uncertain recession duration and strength—and their implications to economic

decision-making. Further on, we discussed the computational and economic implications as well as strengths and weaknesses of the applied methods.

We started by tackling the uncertain recession duration by a specific scenario tree approach leading to a problem related to stochastic optimization. As an additional step towards real-world behavior, we considered a control delay influencing the pricing strategies and incorporated it into the OCP by introducing a slack control variable.

Economically, the introduction of the delay leads to enlarged bankruptcy regions. Depending on the size of the delay and the probability distribution of the recession end, it is optimal to set higher prices in the recession phase of the delayed case compared to the undelayed world, and vice versa in the normal economic stage.

The treatment of the uncertain recession strength happened through selected approaches known from optimization under uncertainty in combination with the general setting of the scenario tree. Thus, the adjustment of prices in the recession stage is based on the desired confidence level and optimally conducted adaptively depending on the uncertain duration of the crisis period.

Representing the approach of set-based robust optimization, we applied the linearization and sigmapoint ideas to reformulate the corresponding robust constraint. Both approaches yielded similarly computationally complex problems; however, the enhanced economic insight of the sigmapoint approach turned out to be very beneficial.

Further on, we considered the probability-based ideas of VaR and CVaR offering the decision-makers a more direct way to balance their strategies between risking negative outcomes and maximizing profit. While the VaR approach can be implemented with a slightly lower complexity compared to the robust reformulations, the CVaR is computationally very expensive due to the additional control function. In connection with coherent measures of risk, the VaR is often estimated negatively because of its lack of coherence, while the CVaR holds this property. In the conspicuous consumption problem, however, the CVaR approach results in slightly too conservative safeguarding policies as its classification of negative outcomes is not significant here. The VaR, in contrast, leads to reliable strategies.

Nevertheless, all considered methods can produce infeasible results if the initial values are too low for the desired confidence levels to be fulfilled.

In general, our numerical approach of applying structure-exploiting direct numerical methods has proven to be an adequate means to solve the appearing non-standard OCPs and to collect detailed insight into solution structures of complex economic systems. In that sense, it provides a valuable aid to support economic decision-making tasks and analytical studies.

However, in respect of a real-world behavior of the proposed model and the deduced pricing strategies, we need to consider a time-dependent recession strength. By this enhancement all appearing processes become stochastic, whereas the mathematical concepts we have used up to now cannot be used (directly) anymore. In the second part of this thesis, we investigate Stochastic Optimal Control Problems (SOCPs) and present a novel idea to treat them in such a way that we can solve them by the sophisticated methods of deterministic optimal control.

Part II

Stochastic Optimal Control

4 Stochastic Processes

In this chapter we introduce the stochastic framework of the subsequently presented ideas of this thesis. Thereby, we focus on the BROWNian motion or WIENER process, which will be the driving force of all appearing stochastic processes, and discuss the implications of incorporating these processes within integrals and differential equations.

4.1 Stochastic Processes

Definition 4.1 (Stochastic Process)
A stochastic process $X = \{X_t \mid t \in \mathcal{T}\} = \{X_t\}_{t \in \mathcal{T}}$ is a collection of random variables on a probability space $(\Omega, \mathcal{F}, \mathbb{P})$. △

Hence, the stochastic process can be represented as a function $X \colon \mathcal{T} \times \Omega \to \mathbb{R}^{n_X}$ with the common notation $X(t, \omega) = X_t(\omega)$. $X_t(\cdot)$ is a $\mathcal{F}$-measurable random variable for fixed $t \in \mathcal{T}$. For fixed sample $\omega \in \Omega$ the function $X_{\cdot}(\omega)$ is called a *sample path*, *trajectory*, or *realization* of the process X. If $\mathcal{T}$ is a countable set, the process X is merely an indexed sequence of random variables.

In the remainder of this thesis we always interpret the index $t \in \mathcal{T}$ as the time. Further on, we consider $\mathcal{T} \subseteq \mathbb{R}$, in most cases it will be the interval $\mathcal{T} = [0, t_\mathrm{f}]$.

Definition 4.2 (Filtration, Adapted Process)
On a given probability space $(\Omega, \mathcal{F}, \mathbb{P})$, a non-decreasing family $\{\mathcal{F}_t\}_{t \in \mathcal{T}}$ of σ-algebras of $\mathcal{F}$ with $\mathcal{F}_t \subseteq \mathcal{F}_s \subseteq \mathcal{F}$ for all $0 \leqslant t < s < \infty$ is called filtration *of $\mathcal{F}$.*
A stochastic process $\{X_t\}_{t \in \mathcal{T}}$ is called adapted *or* non-anticipative *to the filtration $\{\mathcal{F}_t\}_{t \in \mathcal{T}}$ if $X_t(\cdot)$ is $\mathcal{F}_t$-measurable for all $t \in \mathcal{T}$.* △

The BROWNian Motion

With these definitions at hand, we introduce the most prominent stochastic process appearing in this work.

Definition 4.3 (BROWNian Motion, WIENER Process)
The standard, one-dimensional BROWNian motion *or* WIENER process *$\{B_t, \mathcal{F}_t\}_{t \in \mathcal{T}}$ is an adapted stochastic process defined on the probability space $(\Omega, \mathcal{F}, \mathbb{P})$ with the following properties:*
  (i) $B_0 = 0$ *with probability 1,*
 (ii) *$\{B_t\}_{t \in \mathcal{T}}$ is a process with* independent increments, *i.e., for all $0 \leqslant t_0 < t_1 < \ldots < t_n$ the increments $B_{t_1} - B_{t_0}, \ldots, B_{t_n} - B_{t_{n-1}}$ are independent,*
(iii) *$\{B_t\}_{t \in \mathcal{T}}$ has* stationary increments, *i.e., for all $t, s, v \geqslant 0$ it holds $B_t - B_s \sim B_{t+v} - B_{s+v}$,*
 (iv) *B_t has a* GAUSSian distribution, *i.e., $B_t \sim \mathcal{N}(0, t)$ for all $t \geqslant 0$.*

△

Remark 4.1

Note that the filtration $\{\mathcal{F}_t\}_{t\in\mathcal{T}}$ is an essential part of Definition 4.3. However, cf. [132], if a process $\{B_t\}_{t\in\mathcal{T}}$ is given without it, and the properties (ii)–(iv) hold, then $\{B_t, \mathcal{F}_t^B\}_{t\in\mathcal{T}}$ is a BROWNian motion. Therein, $\{\mathcal{F}_t^B\}_{t\in\mathcal{T}}$ is the filtration generated by the BROWNian motion itself.

Corollary 4.1 ([195])

For the standard BROWN*ian motion* $\{B_t\}_{t\in\mathcal{T}}$ *we obtain*

(i) $B_t - B_s \sim \mathcal{N}(0, t - s)$,

(ii) $\mathrm{Cov}[B_t, B_s] = \min\{t, s\}$. $\triangle$

From its relationship to the GAUSSian distribution, the BROWNian motion inherits many additional properties. It is a GAUS*sian process* as well, meaning that for all time instants $t_1, \ldots, t_n$, $n \in \mathbb{N}$, the random vectors $(B_{t_1}, \ldots, B_{t_n})^T$ have a joint normal distribution. It is $\frac{1}{2}$-*self similar*, i.e., for $\tau > 0$ and $t \in \mathcal{T}$ we obtain $B_{\tau t} \sim \mathcal{N}(0, \tau t) \sim \sqrt{\tau} B_t$, which is sometimes mentioned as *scaling property* of $\{B_t\}_{t\in\mathcal{T}}$.

Furthermore, $\{B_t\}_{t\in\mathcal{T}}$ is a *martingale* with respect to $\{\mathcal{F}_t\}_{t\in\mathcal{T}}$. Thus, the conditional expectation $\mathbb{E}[B_t \mid \mathcal{F}_s] = B_s$ for all $0 \leqslant s \leqslant t$. That is, given a BROWNian motion up to time s, the expectation of B_t for $t \geq s$ conditional on the information we accumulated up to time instant s is the process at that time s.

The trajectories of the BROWNian motion are continuous with probability 1 and *nowhere differentiable*, cf. [132]. Particularly in the context of stochastic integration in Section 4.2 this becomes significant, together with the variation of the process $\{B_t\}_{t\in\mathcal{T}}$. Therefore, let Π_n be a partition of $\mathcal{T} = [t_0, t_{\mathrm{f}}]$, i.e., $\Pi_n \stackrel{\text{def}}{=} \{t_0 < t_1 < \ldots < t_n = t_{\mathrm{f}}\}$, and the mesh of this partition be

$$\|\Pi_n\| = \max_{1\leqslant i\leqslant n}(t_i - t_{i-1}).$$

Then the *true $k-$th variation* of a (one-dimensional) process $\{X_t\}_{t\in\mathcal{T}}$ is defined as

$$\vartheta_k(X) \stackrel{\text{def}}{=} \sup_{\Pi_n} \sum_{i=1}^{n} \left|X_{t_i} - X_{t_{i-1}}\right|^k. \tag{4.1}$$

For the BROWNian motion it can be shown [235] that

$$\vartheta_k(B) < \infty \quad \Longleftrightarrow \quad k > 2. \tag{4.2}$$

If we restrict our considerations to sequences of partitions Π_n with $\|\Pi_n\|_2 \to 0$ for $n \to \infty$, we find, cf. [132], that

$$\sum_{i=1}^{n} \left|B_{t_i} - B_{t_{i-1}}\right|^2 \to t_{\mathrm{f}} \quad \text{in } L^2, \tag{4.3}$$

that is

$$\lim_{n\to\infty} \mathbb{E}\left[\left(\sum_{i=1}^{n}\left|B_{t_i} - B_{t_{i-1}}\right|^2 - t_{\mathrm{f}}\right)^2\right] = 0. \tag{4.4}$$

Hence, the BROWNian motion is said to be of *quadratic variation* on the interval $\mathcal{T}$. However, almost all of its paths are of *unbounded (first) variation* on every time interval. If Π_n denotes again a sequence of partitions of $\mathcal{T}$ with $\|\Pi_n\| \to 0$ for $n \to \infty$, then [132]

$$\sum_{i=1}^{\infty} \left| B_{t_i} - B_{t_{i-1}} \right| \to \infty \quad \text{with probability 1.} \tag{4.5}$$

The KARHUNEN-LOÈVE Expansion

The KARHUNEN-LOÈVE *Expansion (KLE)* [133, 168] characterizes a stochastic process $\{X_t\}_{t \in \mathcal{T}}$ by representing it through an infinite sum of linear combinations of orthogonal functions. Therefore, it can be compared to a function's FOURIER series representation.

If the considered process $\{X_t\}_{t \in \mathcal{T}}$ is defined over the horizon $\mathcal{T} = [t_0, t_f]$, any orthonormal basis of the HILBERT space $\mathfrak{H} = L^2([t_0, t_f])$ can be used to determine an expansion of the process, cf. [56] or Chapter 5. The KLE in particular is based on the *best* possible basis, meaning that it minimizes the mean-square error of the resulting expansion, which can be shown directly with the help of MERCER's theorem [210].

Theorem 4.1 (KARHUNEN-LOÈVE Theorem; [133, 168])
Let $\{X_t\}_{t \in \mathcal{T}}$ be a square-integrable random process (i.e., a process with finite second moment for all $t \in \mathcal{T}$) over the probability space $(\Omega, \mathcal{F}, \mathbb{P})$ and defined for times t from the closed and bounded interval $\mathcal{T} = [t_0, t_f]$. Moreover, let its expectation be given by $\mathbb{E}[X_t] = \mu(t)$ with mean value function $\mu \colon \mathbb{R} \to \mathbb{R}$ and its covariance by $\mathrm{Cov}[X_s, X_t] = K(s, t)$ with symmetric, continuous, and non-negative kernel function $K \colon \mathbb{R} \times \mathbb{R} \to \mathbb{R}$.
Then the KLE of X_t is given as

$$X_t(\omega) = \mu(t) + \sum_{i=1}^{\infty} \sqrt{\lambda_i} \varphi_i(t) \xi_i(\omega), \tag{4.6}$$

where $\{\lambda_i\}_{i \geqslant 1}$ are the decreasingly ordered non-zero eigenvalues of the operator $\mathcal{A}_K \colon L^2([t_0, t_f]) \to L^2([t_0, t_f])$ defined by

$$A_K(\psi(t)) \stackrel{\text{def}}{=} \int_{t_0}^{t_f} K(s, t) \psi(s) \, \mathrm{d}s,$$

and $\{\varphi_i(\cdot)\}_{i \geqslant 1}$ the corresponding eigenfunctions. The ξ_i, $i \geqslant 1$, are uncorrelated random variables with zero mean and unit variance.
Moreover, the KLE minimizes the total mean-square error of any approximation of X_t determined in terms of an orthonormal basis of $L^2([t_0, t_f])$ and truncated at order $N \in \mathbb{N}$. △

If the original process $\{X_t\}_{t \in \mathcal{T}}$ is a GAUSSIAN process, the random variables ξ_i, $i \geqslant 1$, of the KLE (4.6) have a joint GAUSSIAN distribution and are independent.
The KLE of the BROWNian motion $\{B_t\}_{t \in [0,1]}$ with $\mathbb{E}[B_t] = 0$ and $\mathrm{Cov}[B_s, B_t] = \min\{s, t\}$ is determined through the eigenvalues and eigenfunctions

$$\lambda_i = \frac{1}{\left(i - \frac{1}{2}\right)^2 \pi^2}, \qquad \varphi_i(t) = \sqrt{2} \sin\left(\left(i - \frac{1}{2}\right) \pi t\right), \qquad i \geqslant 1, \tag{4.7}$$
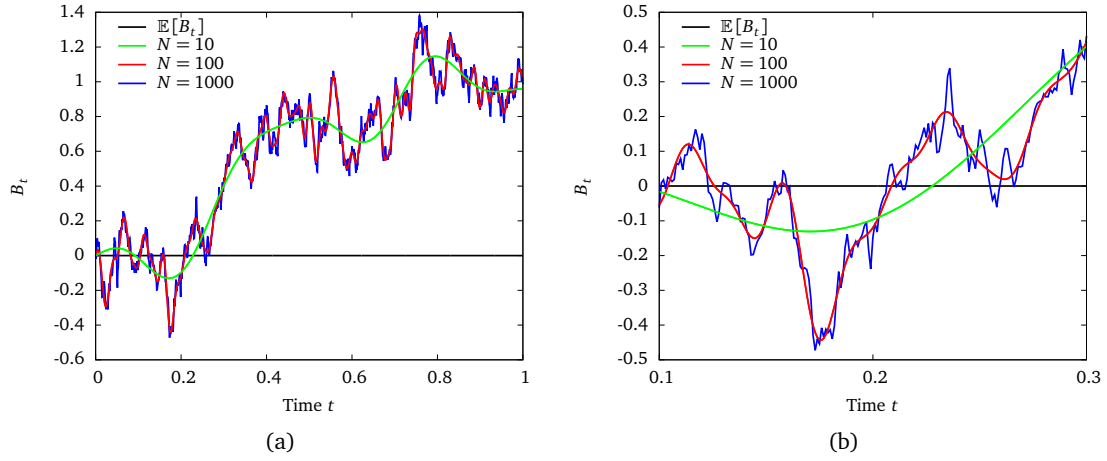
Figure 4.1: Example paths for the truncated KLE of a BROWNian motion B_t together with its expectation function. The *left* figure (a) shows sample paths for varying truncation orders N on the time horizon $t \in [0, 1]$, the *right* one (b) a zoomed part of that plot.

of the covariance kernel, yielding the expansion

$$B_t = \sum_{i=1}^{\infty} \frac{\sqrt{2} \sin\left(\left(i - \frac{1}{2}\right) \pi t\right)}{\left(i - \frac{1}{2}\right) \pi} \xi_i \qquad (4.8)$$

with independent GAUSSian random variables $\xi_i \sim \mathcal{N}(0, 1)$ for all $i \geq 1$. This representation is only valid for $t \in [0, 1]$, on larger intervals the increments of the expansion are not independent. This issue can be resolved by a time-scaling argument, cf. [172] or Chapter 5.2. Note that (4.8) is still nowhere differentiable as the series is not absolutely convergent. Figure 4.1 depicts sample paths of the BROWNian motion's KLE for different truncation orders N.

As the random variables ξ_i, $i \geq 1$, of expansion (4.8) are independent, its convergence rate is determined by

$$\mathbb{E}\left[\left|B_t - B_t^N\right|^2\right] = \sum_{i=N+1}^{\infty} \frac{2 \sin\left(\left(i - \frac{1}{2}\right) \pi t\right)^2}{\left(i - \frac{1}{2}\right)^2 \pi^2} \leq \sum_{i=N+1}^{\infty} \frac{2}{\left(i - \frac{1}{2}\right)^2 \pi^2} \leq \sum_{i=N}^{\infty} \frac{2}{i^2 \pi^2} \leq \frac{1}{\pi N} \quad (4.9)$$

with B_t^N denoting the BROWNian motion's series expansion truncated at the Nth summand, i.e.,

$$B_t^N = \sum_{i=1}^{N} \sqrt{\lambda_i} \varphi_i(t) \xi_i.$$

We complete this section by proving a result that we will make use of later on.

Lemma 4.1

For $t \in [0, 1]$ the sum formula

$$\sum_{i=1}^{\infty} \frac{2 \sin\left(\left(i - \frac{1}{2}\right) \pi t\right)^2}{\left(i - \frac{1}{2}\right)^2 \pi^2} = t \qquad (4.10)$$

holds. △

Proof From the Brownian motion's KLE and the fact that all ξ_i, $i \in \mathbb{N}$, are independent, standard Gaussian random variables, we have

$$\mathbb{E}\left[B_t^{\,2}\right] = \sum_{i=1}^{\infty} \frac{2\sin\left(\left(i-\frac{1}{2}\right)\pi t\right)^2}{\left(i-\frac{1}{2}\right)^2 \pi^2},$$

on the other hand, its variance necessitates $\mathbb{E}\left[B_t^{\,2}\right] = t$. □

4.2 The Itō Stochastic Integral

As we have seen so far, the Brownian motion is a nowhere differentiable stochastic process of unbounded variation on any interval $\mathcal{T} = [t_0, t_f]$. Still, in order to study the evolution of systems depending on that process in the context of differential equations, rigorous calculus has to be set up. Therein, stochastic integrals play the crucial role, whereas differentials only obtain a meaning when they appear in such an integral.

In general, stochastic integrals can be constructed based on any continuous, square-integrable martingale M_t equipped with a filtration $\mathcal{F}_t$ [132, 152]. In this work we focus only on the special case of the Brownian motion as it has been done first by Kiyoshi Itō [122].

Due to the unbounded variation of the Brownian motion an integral of the form

$$I_t(X) = \int_{t_0}^{t} X_s(\omega)\,\mathrm{d}B_s(\omega)$$

for a given stochastic process $\{X_t\}_{t\in\mathcal{T}}$ cannot be defined pathwise (depending on a fixed $\omega \in \Omega$). Furthermore, the integral $I_t(B)$ does not exist as a Riemann-Stieltjes integral.

To define $I_t(\cdot)$ in an appropriate manner, let a Brownian motion $\{B_t\}_{t\in\mathcal{T}}$ be given together with its natural filtration $\{\mathcal{F}_t\}_{t\in\mathcal{T}}$ (that is the smallest σ-algebra generated by the Brownian motion up to time t and the null sets of $\mathcal{F}$). The integrand process $\{X_t\}_{t\in\mathcal{T}}$ be an $\mathcal{F}_t$-adapted, measurable, real-valued random process which is bounded uniformly in t and ω.

Definition 4.4 (Simple Stochastic Process)
A random process $\{S_t\}_{t\in\mathcal{T}}$ over a probability space $(\Omega, \mathcal{F}, \mathbb{P})$ is called a simple *process if a sequence $t_0 < t_1 < \ldots < t_{n+1} = t_f$ and a sequence of random variables $(\xi_i(\omega))_{0\leqslant i\leqslant n}$ with $\sup_i |\xi_i(\omega)| \leqslant C \in \mathbb{R}$ for all $\omega \in \Omega$ exist, such that ξ_i is $\mathcal{F}_{t_i}$-measurable and S_t can be written as*

$$S_t(\omega) = \sum_{i=0}^{n-1} \xi_i(\omega)\mathbb{1}_{[t_i,t_{i+1})}(t) + \xi_n(\omega)\mathbb{1}_{[t_n,t_{n+1}]}(t), \quad t \in [t_0, t_f], \omega \in \Omega. \tag{4.11}$$

△

Hence, the sample paths of a simple process $\{S_t\}_{t\in\mathcal{T}}$ are piecewise constant and we obtain

Definition 4.5 (Itō Stochastic Integral for a Simple Process)
Given a simple process $\{S_t\}_{t\in\mathcal{T}}$ as in Definition 4.4, its Itō *stochastic integral is defined as*

$$I_t(S) = \int_{t_0}^{t} S_s\,\mathrm{d}B_s \stackrel{\text{def}}{=} \sum_{i=0}^{j} S_{s_i}\left(B_{s_{i+1}} - B_{s_i}\right) = \sum_{i=0}^{j} \xi_i \Delta_i B, \tag{4.12}$$

where $0 \leqslant j \leqslant n$ is the unique integer for which $t \in [t_j, t_{j+1})$ resp. $t \in [t_n, t_{n+1}]$, and where ξ_i and $\Delta_i B$ are independent for all i. △

Eventually, the following theorem can be proven, yielding the ITŌ integral.

Theorem 4.2 ([132, 141, 194])
Let $\{X_t\}_{t \in \mathcal{T}}$ over $(\Omega, \mathcal{F}, \mathbb{P})$ be an $\mathcal{F}_t$-adapted, square-integrable stochastic process (with $\mathcal{F}_t$ being the natural filtration of the BROWNian motion again). Then there is a sequence $\left(X_t^{(m)}\right)_{m \in \mathbb{N}}$ of simple processes for which

$$\int_{t_0}^{t_{\mathrm{f}}} \mathbb{E}\left[\left|X_t - X_t^{(m)}\right|^2\right] \mathrm{d}t \to 0 \tag{4.13}$$

holds for $m \to \infty$. △

Hence, the class of simple, adapted processes is dense in the space $L_{\mathrm{A}}^2(\mathcal{T} \times \Omega)$ of $\mathcal{F}_t$-adapted, square-integrable random processes.

Followingly, as for any process $X \in L_{\mathrm{A}}^2(\mathcal{T} \times \Omega)$, $\varepsilon > 0$, $K > 0$, we obtain

$$\mathbb{P}\left[\left|\int_{t_0}^{t_{\mathrm{f}}} X_t \, \mathrm{d}B_t\right| > \varepsilon\right] \leqslant \mathbb{P}\left[\int_{t_0}^{t_{\mathrm{f}}} X_t^2 \, \mathrm{d}t > K\right] + \frac{K}{\varepsilon^2},$$

cf. [194], we can extend the ITŌ integral (4.12) to all $X_t \in L_{\mathrm{A}}^2(\mathcal{T} \times \Omega)$. Its existence is proven with the help of DOOB's maximal inequality for martingales [208] and the BOREL-CANTELLI Lemma [48, 57]. That is, if

$$I_t^{(m)}(X) \stackrel{\mathrm{def}}{=} \int_{t_0}^{t} X_s^{(m)} \, \mathrm{d}B_s,$$

the limit of the so-defined sequence of stochastic integrals satisfies

$$\mathbb{E}\left[\left|I_t(X) - I_t^{(m)}(X)\right|^2\right] \xrightarrow{m \to \infty} 0. \tag{4.14}$$

Definition 4.6 (General ITŌ Integral)
The random process $\{I_t(X)\}_{t \in \mathcal{T}}$ that is defined uniquely with probability 1 through (4.14) is called the ITŌ integral of the process $\{X_t\}_{t \in \mathcal{T}} \in L_{\mathrm{A}}^2(\mathcal{T} \times \Omega)$. We write

$$I_t(X) \stackrel{\mathrm{def}}{=} \int_{t_0}^{t} X_s \, \mathrm{d}B_s, \quad t \in \mathcal{T}. \tag{4.15}$$

△

Remark 4.2
While defining the ITŌ integral for simple processes as (compare (4.12))

$$\sum_{i=0}^{j} S_{s_i} \left(B_{s_{i+1}} - B_{s_i}\right),$$

we have chosen the left end point of the interval $[s_i, s_{i+1})$ to evaluate the process $F_\cdot$. However, in contrast to usual RIEMANN-STIELTJES integrals, the choice of that evaluation point is not

arbitrary in the context of stochastic integrals. It has an important effect on the result of the summation.

Using the left end point s_i defines the ITŌ integral, which is the most famous variant and the preferred choice in financial mathematics due to its property of being non-anticipative.

Choosing instead the midpoint $\frac{1}{2}(s_i + s_{i+1})$ results in a stochastic integral that is *anticipative* and often used in the physical sciences in connection with LANGEVIN equations [158]. It is called the STRATONOVICH *stochastic integral* [231], formally denoted by

$$\int_{t_0}^{t_f} X_t \circ \mathrm{d}B_t. \tag{4.16}$$

A comparison of both types can be found, e.g., in [141, 195].

The ITŌ integral has the following important properties:

(i) For every $t \in \mathcal{T}$ $I_t(X)$ is a random variable with

$$\mathbb{E}\left[\int_{t_0}^{t} X_s \, \mathrm{d}B_s\right] = 0, \tag{4.17}$$

$$\mathbb{E}\left[\left(\int_{t_0}^{t} X_s \, \mathrm{d}B_s\right)^2\right] = \int_{t_0}^{t} \mathbb{E}\left[X_s{}^2\right] \mathrm{d}s. \tag{4.18}$$

(ii) The ITŌ integral is a linear operator.

(iii) It is a $\mathcal{F}_t$-martingale, i.e., for all $s \leqslant t$

$$\mathbb{E}\left[\int_{t_0}^{t} X_u \, \mathrm{d}B_u \,\middle|\, \mathcal{F}_s\right] = \int_{t_0}^{s} X_u \, \mathrm{d}B_u. \tag{4.19}$$

4.3 ITŌ's Formula

The ITŌ formula is the stochastic counterpart to the *change of variable* formula or *chain rule* in deterministic differential calculus. It is the essential tool in working with Stochastic Differential Equations (SDEs). Yet, as the stochastic integral (4.15) inherits the martingale property (4.19) of the BROWNian motion, the known procedures of classical differential calculus cannot be applied.

Definition 4.7 (One-dimensional ITŌ Process)
A one-dimensional ITŌ process on the probability space $(\Omega, \mathcal{F}, \mathbb{P})$ is a stochastic process $\{X_t\}_{t\in\mathcal{T}}$ defined over $\mathcal{T} = [t_0, t_f]$ of the form

$$X_t(\omega) = X_{t_0}(\omega) + \int_{t_0}^{t} b(s, \omega) \, \mathrm{d}s + \int_{t_0}^{t} \sigma(s, \omega) \, \mathrm{d}B_s. \tag{4.20}$$

The first integral in (4.20) *is a standard RIEMANN or LEBESGUE integral for $\omega \in \Omega$ with the integrand function $b \colon \mathcal{T} \times \Omega \to \mathbb{R}$ being jointly LEBESGUE and $\mathcal{F}$-measurable, $\mathcal{F}_t$-measurable for*

all $t \in \mathcal{T}$, and

$$\mathbb{P}\left[\int_{t_0}^{t} |b(s, \omega)| \, \mathrm{d}s < \infty \quad \forall t \in \mathcal{T}\right] = 1.$$

The second integral in (4.20) is the introduced ITŌ *integral with $\sigma : \mathcal{T} \times \Omega \to \mathbb{R}$ being jointly* LEBESGUE *and $\mathcal{F}$-measurable and $\mathcal{F}_t$-measurable for all $t \in \mathcal{T}$ as well, and*

$$\mathbb{P}\left[\int_{t_0}^{t} \sigma(s, \omega)^2 \, \mathrm{d}s < \infty \quad \forall t \in \mathcal{T}\right] = 1.$$

<div align="right">△</div>

Often (4.20) is written symbolically in differential form

$$\mathrm{d}X_t(\omega) = b(t, \omega) \, \mathrm{d}t + \sigma(t, \omega) \, \mathrm{d}B_t(\omega), \tag{4.21}$$

keeping in mind that in stochastic calculus every differential is only defined by its corresponding integral.

Now we can state

Theorem 4.3 (One-dimensional ITŌ Formula; [132, 141])
Let $\{X_t\}_{t \in \mathcal{T}}$ be a one-dimensional ITŌ *process given through (4.21). Furthermore, let $f : \mathcal{T} \times \mathbb{R} \to \mathbb{R}$ be a twice continuously differentiable function. Then $Y_t = f(t, X_t)$ determines an* ITŌ *process as well, and* ITŌ's *formula in dimension one holds with probability 1, i.e.,*

$$\mathrm{d}Y_t = \left(\frac{\partial f}{\partial t}(t, X_t) + b(t)\frac{\partial f}{\partial x}(t, X_t) + \frac{1}{2}\sigma(t)^2 \frac{\partial^2 f}{\partial x^2}(t, X_t)\right)\mathrm{d}t + \sigma(t)\frac{\partial f}{\partial x}(t, X_t)\,\mathrm{d}B_t, \tag{4.22}$$

where we have suppressed the dependency on the chance parameter $\omega \in \Omega$ to ease notation. △

In the case of a n_B-dimensional BROWNian motion $\boldsymbol{B} = \left(B^1, \ldots, B^{n_B}\right)^T$ we state the *multi-dimensional* ITŌ *formula* for a n_X-dimensional stochastic process $\boldsymbol{X} = \left(X^1, \ldots, X^{n_X}\right)^T$ given through

$$\mathrm{d}X_t^i = b^i(t)\,\mathrm{d}t + \sum_{j=1}^{n_B} \sigma^{ij}(t)\,\mathrm{d}B_t^j, \quad 1 \leqslant i \leqslant n_X, \tag{4.23}$$

with each $b^i(\cdot)$, $\sigma^{ij}(\cdot)$, $1 \leqslant i \leqslant n_X$, $1 \leqslant j \leqslant n_B$, satisfying the assumptions of Definition 4.7.

Theorem 4.4 (Multi-dimensional ITŌ Formula; [132, 141])
Let $\{\boldsymbol{X}_t\}_{t \in \mathcal{T}}$ be a n_X-dimensional ITŌ *process and $f : \mathcal{T} \times \mathbb{R}^{n_X} \to \mathbb{R}^{n_Y}$ be twice continuously differentiable. Then $\boldsymbol{Y}_t = f(t, \boldsymbol{X}_t)$ determines a n_Y-dimensional* ITŌ *process with each component Y_t^k, $1 \leqslant k \leqslant n_Y$, satisfying the* ITŌ *formula*

$$\mathrm{d}Y_t^k = \frac{\partial f^k}{\partial t}(t, X_t)\,\mathrm{d}t + \sum_{i=1}^{n_X} \frac{\partial f^k}{\partial x^i}(t, X_t)\,\mathrm{d}X_t^i + \frac{1}{2}\sum_{i=1}^{n_X}\sum_{j=1}^{n_X} \frac{\partial^2 f^k}{\partial x^i \partial x^j}\,\mathrm{d}X_t^i\,\mathrm{d}X_t^j. \tag{4.24}$$

<div align="right">△</div>

4.4 Stochastic Differential Equations

Considering differential equations with *random effects* leads to two very different types of equations. As we have seen in Chapter 2, the first class appears when Ordinary Differential Equations (ODEs) are analyzed for random coefficients, parameters, or random initial conditions. These equations are often named *Random Differential Equations (RDEs)* [141] and can be solved pathwise, with the solution process having differentiable sample paths.

The second class is determined by irregular stochastic processes, e.g., GAUSSian white noise. They are called *Stochastic Differential Equations (SDEs)*. Their solutions inherit the BROWNian motion's property of holding non-differentiable trajectories. The focus of the following chapters will be on that second class of equations.

Let bounded measurable functions $\boldsymbol{b} \colon \mathcal{T} \times \mathbb{R}^{n_X} \to \mathbb{R}^{n_X}$ and $\boldsymbol{\sigma} \colon \mathcal{T} \times \mathbb{R}^{n_X} \to \mathbb{R}^{n_X \times n_B}$ be given and consider the SDE

$$
\boldsymbol{X}_t = \boldsymbol{X}_{t_0} + \int_{t_0}^{t} \boldsymbol{b}(s, \boldsymbol{X}_s) \, \mathrm{d}s + \int_{t_0}^{t} \boldsymbol{\sigma}(s, \boldsymbol{X}_s) \, \mathrm{d}\boldsymbol{B}_s,
\tag{4.25}
$$

or, written again in (symbolic) differential form

$$
\mathrm{d}\boldsymbol{X}_t = \boldsymbol{b}(t, \boldsymbol{X}_t) \, \mathrm{d}t + \boldsymbol{\sigma}(t, \boldsymbol{X}) \, \mathrm{d}\boldsymbol{B}_t.
\tag{4.26}
$$

Therein, $\boldsymbol{b}(\cdot)$ is called the *drift* and $\boldsymbol{S}(\cdot) = \boldsymbol{\sigma}(\cdot)\boldsymbol{\sigma}(\cdot)^T$ the *diffusion* term of (4.25) or (4.26), resp. Then we can define different notions of a solution to a SDE, cf. [157].

Definition 4.8 (Solution to a SDE)
Let $\{\boldsymbol{B}_t\}_{t \in \mathcal{T}}$ be a given BROWNian motion and the initial value $\boldsymbol{X}_{t_0}$ a given $\mathcal{F}_{t_0}$-measurable random vector. Then by a solution to the SDE (4.25) we mean a continuous $\mathcal{F}_t$-adapted process $\{\boldsymbol{X}_t\}_{t \in \mathcal{T}}$ satisfying (4.25) with probability 1. △

Definition 4.9 (Strong and Weak Existence)
If, given a probability space $(\Omega, \mathcal{F}, \mathbb{P})$, a filtration $\{\mathcal{F}_t\}_{t \in \mathcal{T}}$, a BROWNian motion $\{\boldsymbol{B}_t\}_{t \in \mathcal{T}}$, and a $\mathcal{F}_{t_0}$-measurable initial condition $\boldsymbol{X}_{t_0}$, a $\mathcal{F}_t$-adapted process $\{\boldsymbol{X}_t\}_{t \in \mathcal{T}}$ exists which satisfies (4.25) for all $t \in \mathcal{T}$, we speak of strong existence.

If, given any probability measure ν, there exist a probability space $(\Omega, \mathcal{F}, \mathbb{P})$, a filtration $\{\mathcal{F}_t\}_{t \in \mathcal{T}}$, a BROWNian motion $\{\boldsymbol{B}_t\}_{t \in \mathcal{T}}$, and a $\mathcal{F}_t$-adapted process $\{\boldsymbol{X}_t\}_{t \in \mathcal{T}}$ satisfying (4.25) for all $t \in \mathcal{T}$, as well as $\mathbb{P}\big[\boldsymbol{X}_{t_0} \in \mathcal{F}_{t_0}\big] = \nu(\mathcal{F}_{t_0})$, then we speak of weak existence. △

Definition 4.10 (Strong and Weak Uniqueness)
For a given probability space $(\Omega, \mathcal{F}, \mathbb{P})$, a filtration $\{\mathcal{F}_t\}_{t \in \mathcal{T}}$, and a BROWNian motion $\{\boldsymbol{B}_t\}_{t \in \mathcal{T}}$, suppose $\{\boldsymbol{X}_t^1\}_{t \in \mathcal{T}}$ and $\{\boldsymbol{X}_t^2\}_{t \in \mathcal{T}}$ are strong solutions to (4.25). Then strong uniqueness holds if

$$
\mathbb{P}\big[\boldsymbol{X}_{t_0}^1 = \boldsymbol{X}_{t_0}^2\big] = 1 \quad \Longrightarrow \quad \mathbb{P}\big[\boldsymbol{X}_t^1 = \boldsymbol{X}_t^2 \quad \forall t \in \mathcal{T}\big] = 1.
$$

Given weak sense solutions $\big\{(\Omega^i, \mathcal{F}^i, \mathbb{P}^i), \{\mathcal{F}_t^i\}_{t \in \mathcal{T}}, \{\boldsymbol{B}_t^i\}_{t \in \mathcal{T}}, \{\boldsymbol{X}_t^i\}_{t \in \mathcal{T}}\}$, $i = 1, 2$, to the SDE (4.25), weak uniqueness holds if equality of the distributions induced on $\mathbb{R}^{n_X}$ by $\boldsymbol{X}_{t_0}^i$ under $\mathbb{P}^i$, $i = 1, 2$, implies the equality of the distributions on $C(\mathcal{T} \times \mathbb{R}^{n_X})$ by $\boldsymbol{X}_t^i$ under $\mathbb{P}^i$, $i = 1, 2$. △

Similar to investigations in ODE theory [105], the natural way to show existence and uniqueness results for SDEs is to assume local LIPSCHITZ conditions in the space variable of the in-

tegrand functions $b(\cdot)$ and $\sigma(\cdot)$ and certain conditions of boundedness. Then the PICARD-LINDELÖF iterations converge to a solution that is unique [123, 132].

Theorem 4.5 (Strong Uniqueness for (4.25); [132])
Suppose the coefficients $b(\cdot)$ and $\sigma(\cdot)$ of the SDE (4.25) are locally LIPSCHITZ continuous, i.e., for all $n \in \mathbb{N}$ there exists a constant $K_n > 0$ such that for all $t \in \mathcal{T}$, $\|x\|_2 \leqslant n$, $\|y\|_2 \leqslant n$ it holds

$$\|b(t,x) - b(t,y)\|_2 + \|\sigma(t,x) - \sigma(t,y)\|_2 \leqslant K_n \|x - y\|_2.$$

Then strong uniqueness holds for (4.25). △

Remark 4.3
In the previous and the following Theorems we use the notation $\|\cdot\|_2$ to denote the (EUCLIDean) norm of a $(n \times m)$-matrix, i.e.,

$$\|\Sigma\|_2^2 = \sum_{i=1}^{n} \sum_{j=1}^{m} \Sigma_{ij}{}^2.$$

Remark 4.4
Following the lines of ODEs, the local LIPSCHITZ condition is not sufficient to guarantee global existence of a solution. Therefor, additional assumption are necessary to prevent *explosions* at times $t \in \mathcal{T}$.

Theorem 4.6 (Existence and Uniqueness Theorem for SDEs; [132, 195])
Let $\mathcal{T} = [t_0, t_\mathrm{f}]$ be a given time horizon and $b: \mathcal{T} \times \mathbb{R}^{n_X} \to \mathbb{R}^{n_X}$, $\sigma: \mathcal{T} \times \mathbb{R}^{n_X} \to \mathbb{R}^{n_X \times n_B}$ be measurable functions satisfying the global LIPSCHITZ and linear growth conditions

$$\|b(t,x) - b(t,y)\|_2 + \|\sigma(t,x) - \sigma(t,y)\|_2 \leqslant K\|x - y\|_2, \tag{4.27}$$

$$\|b(t,x)\|_2^2 + \|\sigma(t,x)\|_2^2 \leqslant K^2(1 + \|x\|_2^2), \tag{4.28}$$

for all $x, y \in \mathbb{R}^{n_X}$, $t \in \mathcal{T}$, and constant $K > 0$. Moreover, let ξ be a random variable independent of the BROWNian motion $\{B_t\}_{t \in \mathcal{T}}$ and such that

$$\mathbb{E}\left[\|\xi\|_2^2\right] < \infty.$$

Then the SDE

$$\mathrm{d}X_t = b(t, X_t)\,\mathrm{d}t + \sigma(t, X_t)\,\mathrm{d}B_t, \quad X_{t_0} = \xi, \quad t \in \mathcal{T}, \tag{4.29}$$

has a t-continuous strong solution $X_t(\omega)$ that is unique in the strong sense and adapted to the filtration $\mathcal{F}_t^{\xi}$ generated by ξ and B_s, $s \leqslant t$. It is square-integrable, i.e., for every $t_\mathrm{f} > 0$ there exists a constant C depending only on K and t_f such that

$$\mathbb{E}\left[\|X_t\|_2^2\right] \leqslant C\left(1 + \mathbb{E}\left[\|\xi\|_2^2\right]\right) \mathrm{e}^{Ct} < \infty \quad t \in \mathcal{T}. \tag{4.30}$$

△

In the case of a one-dimensional SDE the LIPSCHITZ conditions of the coefficient can be weakened.

Theorem 4.7 ([251])

Let a one-dimensional SDE over $\mathcal{T}$ be given through

$$\mathrm{d}X_t = b(t, X_t)\,\mathrm{d}t + \sigma(t, X_t)\,\mathrm{d}B_t \tag{4.31}$$

with coefficients $b(\cdot)$ and $\sigma(\cdot)$ satisfying

$$|b(t, x) - b(t, y)| \leqslant k(|x - y|), \tag{4.32}$$

$$|\sigma(t, x) - \sigma(t, y)| \leqslant h(|x - y|), \tag{4.33}$$

for all $t \in \mathcal{T}$, $x, y \in \mathbb{R}$, and where $k \colon \mathbb{R}^+ \to \mathbb{R}^+$ is a strictly increasing and concave function with $k(0) = 0$ and $\int_0^\varepsilon k(u)^{-1}\,\mathrm{d}u = \infty \; \forall \varepsilon > 0$, and $h \colon \mathbb{R}^+ \to \mathbb{R}^+$ is a strictly increasing function with $h(0) = 0$ and $\int_0^\varepsilon h(u)^{-2}\,\mathrm{d}u = \infty \; \forall \varepsilon > 0$. Then strong uniqueness holds for (4.31). △

More detailed investigations of existence and uniqueness theorems for SDEs, varying the assumptions on the drift and diffusion coefficient functions can be found in, e.g., [65, 132]. One natural consideration to solve SDEs seems to utilize the KLE (4.8) of the BROWNian motion. As for every $t \in [0, 1]$ and $\xi_i \sim \mathcal{N}(0, 1)$, $1 \leqslant i \leqslant N$,

$$B_t^N = \sum_{i=1}^N \frac{\sqrt{2}\sin\left(\left(i - \frac{1}{2}\right)\pi t\right)}{\left(i - \frac{1}{2}\right)\pi}\xi_i$$

converges in L^2 to B_t for $N \to \infty$, one might assume that the solution X_t^N of the ODE

$$\mathrm{d}X_t^N = b(t, X_t^N)\,\mathrm{d}t + \sigma(t, X_t^N)\,\mathrm{d}B_t, \quad X_{t_0}^N = x_0,$$

converges to the solution X_t of the original ITŌ SDE

$$\mathrm{d}X_t = b(t, X_t)\,\mathrm{d}t + \sigma(t, X_t)\,\mathrm{d}B_t, \quad X_{t_0} = x_0$$

as well. However, this is in general not the case, emphasizing the cautiousness that is necessary in dealing with SDEs. In [249] and, in a related fashion in [233], it is shown that the sequence $\left(X_t^N\right)_{n \in \mathbb{N}}$ in fact converges in the mean to the solution of the STRATONOVICH type SDE

$$\mathrm{d}X_t = b(t, X_t)\,\mathrm{d}t + \sigma(t, X_t) \circ \mathrm{d}B_t \tag{4.34}$$

$$= \left(b(t, X_t) + \frac{1}{2}\sigma(t, X_t)\frac{\partial}{\partial t}\sigma(t, X_t)\right)\mathrm{d}t + \sigma(t, X_t)\,\mathrm{d}B_t,$$

where the second equation is the ITŌ type counterpart of (4.34), derived by the STRATONOVICH transformation formula [231]. A comparable result is presented in [176] for approximating only the BROWNian motion process by an appropriate polygon.

4.5 Summary

In this introductory chapter we presented the stochastic basis of the subsequent ideas of this thesis. The dynamic processes of our considerations become stochastic processes defined upon some probability space and descendent from the standard BROWNian motion process.

We have seen that ordinary definitions of integrals, known from common differential calculus, fail to hold and that this is overcome by considering stochastic integrals instead. Thus, the dynamics of our stochastic state processes have to be described by stochastic instead of ordinary differential equations, by including ITō integrals.

5 WIENER Chaos Expansion and MALLIAVIN Calculus

In this chapter we survey the WIENER chaos expansion of a stochastic process. We introduce it with the help of HERMITE polynomials first and develop its connection to multiple stochastic integrals thereafter. To that end we give an overview on MALLIAVIN calculus, as it provides the powerful principles for applying the WIENER chaos expansion to stochastic differential equations in the following chapter.

5.1 HERMITE Polynomials

Definition 5.1 (HERMITE Polynomials)
The n-th normalized HERMITE polynomial $H_n(x)$, $x \in \mathbb{R}$, is defined through

$$H_0(x) = 1, \tag{5.1a}$$

$$H_n(x) = \frac{(-1)^n}{\sqrt{n!}} \exp\left(\frac{x^2}{2}\right) \frac{\mathrm{d}^n}{\mathrm{d}x^n}\left(\exp\left(-\frac{x^2}{2}\right)\right), \quad n \geqslant 1. \tag{5.1b}$$

$\triangle$

From Definition 5.1 one can directly deduce the following result, which is stated in [234] for standard (non-normalized) HERMITE polynomials.

Lemma 5.1 ([234])
The normalized HERMITE polynomials $H_n(\cdot)$, $n \in \mathbb{N}_0$, have the following properties:

$$\frac{\mathrm{d}}{\mathrm{d}x} H_n(x) = \sqrt{n} H_{n-1}(x), \tag{5.2}$$

$$\sqrt{n+1} H_{n+1}(x) = x H_n(x) - \sqrt{n} H_{n-1}(x). \tag{5.3}$$

$\triangle$

Proof (adapted from [234]) The generating function of the HERMITE polynomials is given via [221]

$$\varphi_H(t,x) \stackrel{\text{def}}{=} \exp\left(\frac{x^2}{2} - \frac{1}{2}(x-t)^2\right) \tag{5.4}$$

$$= \exp\left(\frac{x^2}{2}\right) \sum_{i=0}^{\infty} \frac{\mathrm{d}^i}{\mathrm{d}t^i}\left(\exp\left(-\frac{1}{2}(x-t)^2\right)\right)\Big|_{t=0} \cdot \frac{t^i}{i!}$$

$$= \sum_{i=0}^{\infty} \frac{t^i}{\sqrt{i!}} H_i(x).$$

As this series converges uniformly, (5.2) follows from $\frac{\partial \varphi_H}{\partial x} = t f$, i.e.,

$$\sum_{i=1}^{\infty} \frac{t^i}{\sqrt{i!}} \frac{\mathrm{d}}{\mathrm{d}x} H_i(x) \overset{!}{=} \sum_{i=0}^{\infty} \frac{t^{i+1}}{\sqrt{i!}} H_i(x) = \sum_{i=1}^{\infty} \frac{t^i}{\sqrt{(i-1)!}} H_{i-1}(x)$$

and (5.3) from $\frac{\partial \varphi_H}{\partial t} = (x - t) f$, i.e.,

$$\sum_{i=1}^{\infty} \sqrt{i} \frac{t^{i-1}}{\sqrt{(i-1)!}} H_i(x) = \sum_{i=0}^{\infty} \sqrt{i+1} \frac{t^i}{\sqrt{i!}} H_{i+1}(x)$$

$$\overset{!}{=} \sum_{i=0}^{\infty} \frac{t^i}{\sqrt{i!}} x H_i(x) - \sum_{i=0}^{\infty} \frac{t^{i+1}}{\sqrt{i!}} H_i(x)$$

$$= \sum_{i=0}^{\infty} \frac{t^i}{\sqrt{i!}} x H_i(x) - \sum_{i=0}^{\infty} \frac{t^i}{\sqrt{i!}} \frac{\mathrm{d}}{\mathrm{d}x} H_i(x)$$

and using (5.2). □

Definition 5.2 (GAUSSian measure)
The GAUSSian measure μ is defined as

$$\mu(\mathrm{d}x) = \varrho(x)\,\mathrm{d}x, \qquad \varrho(x) = \frac{1}{\sqrt{2\pi}} \exp\left(-\frac{x^2}{2}\right), \tag{5.5}$$

where $\mathrm{d}x$ is corresponding to the LEBESGUE measure as usual. Then $L^2(\mathbb{R}, \mu)$ is the space of square-integrable functions with GAUSSian measure, i.e.,

$$L^2(\mathbb{R}, \mu) = \left\{ f : \mathbb{R} \to \mathbb{R} \,\middle|\, \int_{\mathbb{R}} f(x)^2 \, \mu(\mathrm{d}x) < \infty \right\}. \tag{5.6}$$

The inner product of this space is defined as

$$\langle f, g \rangle_{L^2(\mathbb{R}, \mu)} = \int_{\mathbb{R}} f(x) g(x) \, \mu(\mathrm{d}x) \tag{5.7}$$

for all $f, g \in L^2(\mathbb{R}, \mu)$. △

With these definitions at hand, we prove the starting point of all further developments.

Lemma 5.2 ([234])
The HERMITE polynomials $\{H_n(\cdot) \mid n \in \mathbb{N}_0\}$ form a complete orthonormal basis of the HILBERT space $L^2(\mathbb{R}, \mu)$. △

Remark 5.1
As $H_0 \equiv 1$, for a standard GAUSSian random variable $\xi \sim \mathbb{N}(0, 1)$, i.e., $\xi \in \mathbb{R}$, we deduce

$$\mathbb{E}[H_n(\xi)] = \langle H_n(\xi), H_0(\xi) \rangle_{L^2(\mathbb{R}, \mu)} = 0 \quad \forall n \geqslant 1.$$

Hence, the (normalized) HERMITE polynomial $H_n(\cdot)$, $n \geqslant 1$ of a standard GAUSSian random variable is again a random variable with zero mean and unit variance.

Proof (of Lemma 5.2, adapted from [234]) To show the orthonormality of the HERMITE polynomials $H_n(\cdot)$, $n \in \mathbb{N}_0$, we use the definition of the GAUSSIAN measure (5.5) to deduce

$$\langle H_n(x), H_m(x)\rangle_{L^2(\mathbb{R},\mu)} = \int_{-\infty}^{\infty} \frac{1}{\sqrt{2\pi}} \frac{(-1)^n}{\sqrt{n!}} \frac{\mathrm{d}^n}{\mathrm{d}x^n}\left(\exp\left(-\frac{x^2}{2}\right)\right) H_m(x)\,\mathrm{d}x.$$

Without loss of generality we assume $n > m$ first, the opposite relation gives an analogous result. Integration by parts and property (5.2) of the HERMITE polynomials yield

$$\langle H_n(x), H_m(x)\rangle_{L^2(\mathbb{R},\mu)} = \int_{-\infty}^{\infty} \frac{1}{\sqrt{2\pi}} \frac{(-1)^{n-1}}{\sqrt{n!}} \frac{\mathrm{d}^{n-1}}{\mathrm{d}x^{n-1}}\left(\exp\left(-\frac{x^2}{2}\right)\right) \sqrt{m}H_{m-1}(x)\,\mathrm{d}x,$$

and, therefore, applying integration by parts $n-1$ additional times, gives

$$\langle H_n(x), H_m(x)\rangle_{L^2(\mathbb{R},\mu)} = 0 \quad \forall n \neq m.$$

For $n = m$ we obtain

$$\begin{aligned}
\langle H_n(x), H_n(x)\rangle_{L^2(\mathbb{R},\mu)} &= \int_{-\infty}^{\infty} \frac{1}{\sqrt{2\pi}} \frac{(-1)^{n-1}}{\sqrt{(n-1)!}} \frac{\mathrm{d}^{n-1}}{\mathrm{d}x^{n-1}}\left(\exp\left(-\frac{x^2}{2}\right)\right) H_{n-1}(x)\,\mathrm{d}x, \\
&= \int_{-\infty}^{\infty} \frac{1}{\sqrt{2\pi}} \exp\left(-\frac{x^2}{2}\right)\,\mathrm{d}x \\
&= 1.
\end{aligned}$$

Completeness of the system we show by concluding that a function $p \in L^2(\mathbb{R},\mu)$ has to be identical to zero if $\langle H_n(x), p(x)\rangle_{L^2(\mathbb{R},\mu)} = 0$ for all $n \in \mathbb{N}_0$. Therefor, we consider again the generating function $\varphi_H(t,x)$ of the HERMITE polynomials and, determined by it,

$$\Theta(t) = \langle \varphi_H(t,x), p(x)\rangle_{L^2(\mathbb{R},\mu)} = \int_{-\infty}^{\infty} \varphi_H(t,x)p(x)\varrho(x)\,\mathrm{d}x.$$

Then

$$\begin{aligned}
\left.\frac{\mathrm{d}^n}{\mathrm{d}t^n}\Theta(t)\right|_{t=0} &= \int_{-\infty}^{\infty} \left.\frac{\partial^n}{\partial t^n}\varphi_H(t,x)\right|_{t=0} \cdot p(x)\varrho(x)\,\mathrm{d}x \\
&= \int_{-\infty}^{\infty} \sum_{i=n}^{\infty} \prod_{j=0}^{n-1} \sqrt{i-j} \left.\frac{t^{i-n}}{\sqrt{(i-n)!}} H_i(x)\right|_{t=0} \cdot p(x)\varrho(x)\,\mathrm{d}x \\
&= \int_{-\infty}^{\infty} \sqrt{n!}H_n(x)p(x)\varrho(x)\,\mathrm{d}x = 0 \quad \forall n \in \mathbb{N}_0
\end{aligned}$$

by assumption, where we used the convention $0^0 = 1$. Hence, $\Theta(t)$ has to be identical to zero, giving

$$\Theta(t) = \exp\left(-\frac{t^2}{2}\right)\sum_{i=0}^{\infty} \frac{t^i}{i!} \int_{-\infty}^{\infty} x^i p(x)\varrho(x)\,\mathrm{d}x = 0.$$

We conclude that $\langle x^i, p(x)\rangle_{L^2(\mathbb{R},\mu)} = 0$ for all $i \in \mathbb{N}_0$ and, therefore, $p \equiv 0$ in $L^2(\mathbb{R},\mu)$, as the

monomials generate a dense subspace of $L^2(\mathbb{R}, \mu)$, cf. [192]. □

A product of two HERMITE polynomials is again a polynomial, which can be expressed as a linear combination of HERMITE polynomials, due to the next important formula, compare [59, 190] and, in particular, [172]. Extensions of it to more than two HERMITE polynomial factors can be found in, e.g., [59, 90].

Lemma 5.3 ([172])
For any $n, m > 0$ it holds

$$H_n(x)H_m(x) = \sum_{p \leqslant \min\{n,m\}} \bar{C}(n, m, p)H_{n+m-2p}(x) \tag{5.8}$$

with

$$\bar{C}(n, m, p) = \sqrt{\binom{n}{p}\binom{m}{p}\binom{n+m-2p}{n-p}}. \tag{5.9}$$

△

Proof ([172]) The definition of the generating function $\varphi_H(\cdot)$ of the HERMITE polynomials $H_n(\cdot)$ directly yields

$$\varphi_H(t, x)\varphi_H(s, x) = \sum_{n=0}^{\infty}\sum_{m=0}^{\infty} \frac{H_n(x)H_m(x)}{\sqrt{n!m!}} t^n s^m. \tag{5.10}$$

On the other hand, it gives as well

$$\varphi_H(t, x)\varphi_H(s, x) = \exp\left(\frac{x^2}{2} - \frac{1}{2}(x-t)^2 + \frac{x^2}{2} - \frac{1}{2}(x-s)^2\right)$$

$$= \exp(st)\exp\left(\frac{x^2}{2} - \frac{1}{2}(x-(s+t))^2\right)$$

$$= \sum_{p=0}^{\infty} \frac{(st)^p}{p!} \sum_{i=0}^{\infty} \frac{H_i(x)}{\sqrt{i!}}(s+t)^i$$

$$= \sum_{p=0}^{\infty}\sum_{i=0}^{\infty} \frac{H_i(x)}{p!} \sum_{j=0}^{i} \binom{i}{j}\frac{1}{\sqrt{i!}} t^{p+j}s^{p+i-j}.$$

Now let $n = p + j$ and $m = p + i - j$. Because $j \leqslant i$, we can reason from $p = n - i \geqslant 0$ and $i - j = m - p \geqslant 0$ that $p \leqslant \min\{n, m\}$. This in return gives (as $i = m - p + j = n + m - 2p$)

$$\varphi_H(t, x)\varphi_H(s, x) = \sum_{n=0}^{\infty}\sum_{m=0}^{\infty}\sum_{p \leqslant \min\{n,m\}} \frac{\sqrt{(n+m-2p)!}H_{n+m-2p}(x)}{p!(n-p)!(m-p)!} t^n s^m. \tag{5.11}$$

Comparing (5.10) and (5.11) finally yields

$$H_n(x)H_m(x) = \sum_{p \leqslant \min\{n,m\}} \sqrt{\frac{n!}{p!(n-p)!}\frac{m!}{p!(m-p)!}\frac{(n+m-2p)!}{(n-p)!(m-p)!}}H_{n+m-2p}(x). \quad □$$

To finish this section, we extend Lemma 5.2.

Theorem 5.1 ([194])

Let $\xi, \zeta \sim \mathcal{N}(0,1)$ be jointly GAUSSian distributed. Then for all $n, m \geqslant 0$ we obtain

$$\mathbb{E}[H_n(\xi)H_m(\zeta)] = (\mathbb{E}[\xi\zeta])^n \delta_{n,m}. \tag{5.12}$$

$\triangle$

Proof (following [192]) The generating function $\varphi_H(\cdot)$ and the characteristic function of joint GAUSSian random variables gives for all $s, t \in \mathbb{R}$ and $\xi, \zeta \sim \mathcal{N}(0,1)$

$$\mathbb{E}[\varphi_H(s,\xi)\varphi_H(t,\zeta)] = \mathbb{E}\left[\exp\left(s\xi - \frac{s^2}{2}\right)\exp\left(t\zeta - \frac{t^2}{2}\right)\right] = \exp(st\mathbb{E}[\xi\zeta]).$$

Now taking the $(n+m)$-th partial derivative at $s = t = 0$ yields

$$\frac{\partial^{n+m}}{\partial s^n \partial t^m}\mathbb{E}[\varphi_H(s,\xi)\varphi_H(t,\zeta)]\bigg|_{\substack{s=0\\t=0}} = \mathbb{E}\left[\frac{\partial^n}{\partial s^n}\varphi_H(s,\xi)\bigg|_{s=0}\frac{\partial^n}{\partial t^n}\varphi_H(t,\zeta)\bigg|_{t=0}\right]$$

$$= \mathbb{E}\left[\sqrt{n!}H_n(\xi)\sqrt{m!}H_m(\zeta)\right]$$

and

$$\frac{\partial^{n+m}}{\partial s^n \partial t^m}\exp(st\mathbb{E}[\xi\zeta])\bigg|_{\substack{s=0\\t=0}} = \frac{\partial^n}{\partial s^n}\left(\exp(st\mathbb{E}[\xi\zeta])(s\mathbb{E}[\xi\zeta])^m\right)\bigg|_{\substack{s=0\\t=0}}$$

$$= \begin{cases} 0, & n \neq m, \\ n!\,(\mathbb{E}[\xi\zeta])^n, & n = m. \end{cases}$$

$\square$

5.2 WIENER **Chaos Expansion**

In Section 4.1 we have already investigated the KARHUNEN-LOÈVE Expansion (KLE) of a stochastic process $\{X_t\}_{t \in \mathcal{T}}$. Now we will focus on a generalized setting leading to the WIENER *chaos expansion*.

To start, let $f \in L^2(\mathbb{R}, \mu)$ be a function of a GAUSSian random variable $\xi \in \mathcal{N}(0,1)$. Then $\mathbb{E}[f(\xi)^2] < \infty$. Thus, the random variable $f(\xi)$ has the FOURIER-HERMITE expansion

$$f(\xi) = \sum_{n=0}^{\infty} f_n H_n(\xi), \tag{5.13}$$

since the HERMITE polynomials form an orthonormal basis of $L^2(\mathbb{R}, \mu)$. The coefficients $\{f_n\}_{n \geqslant 0}$ are defined in a FOURIER-like manner via

$$f_n = \mathbb{E}[f(\xi)H_n(\xi)]. \tag{5.14}$$

This expansion is the simplest form of the one proven by NORBERT WIENER [246]. It has been generalized by ROBERT CAMERON and WILLIAM MARTIN [56] to hold for arbitrarily distributed random variables ξ.

Equation (5.14) directly gives

$$f_0 = \mathbb{E}[f(\xi)]$$

and through the orthonormality of the HERMITE polynomials we get

$$\mathbb{V}[f(\xi)] = \mathbb{E}[f(\xi)^2] - \mathbb{E}[f(\xi)]^2 = \mathbb{E}\left[\sum_{n=0}^{\infty}\sum_{m=0}^{\infty} f_n f_m H_n(\xi) H_m(\xi)\right] - f_0{}^2$$
$$= \sum_{n=1}^{\infty} f_n{}^2.$$

Let the truncated series (5.13) be denoted as

$$f^N(\xi) = \sum_{n=0}^{N} f_n H_n(\xi). \tag{5.15}$$

It converges fast if $f(\cdot)$ is a very smooth function. The decreasing rate is given through the following result:

Lemma 5.4 ([172])
Assume $f : \mathbb{R} \to \mathbb{R}$ is a function being k times continuously differentiable. Then the FOURIER-HERMITE coefficients f_n of expansion (5.13) decay as

$$f_n = \begin{cases} \frac{(-1)^n}{\sqrt{n!}}\mathbb{E}[f^{(n)}(\xi)], & n \leqslant k, \\ \frac{(-1)^k}{\sqrt{n\cdot\ldots\cdot(n-k+1)}}\mathbb{E}[f^{(k)}(\xi)], & n > k, \end{cases} \tag{5.16}$$

where the expectation is again with respect to the GAUSSian measure. If f is infinitely often continuously differentiable, f_n decays exponentially

$$f_n = \mathcal{O}(e^{-cn})$$

with constant $c > 0$. △

Convergence results of the expansion (5.13) can be found, e.g., in [50]. Based on Lemma 5.4 one can show that the truncated expansion (5.15) converges in the mean.

An extension to the multi-dimensional case is straightforward. If $\xi = (\xi_1, \ldots, \xi_{n_X})$ is a standard GAUSSian random vector with independent components ξ_i, $1 \leqslant i \leqslant n_X$, $\boldsymbol{\alpha} = (\alpha_1, \ldots, \alpha_{n_X})$ a finite index with non-negative subindices α_i, $1 \leqslant i \leqslant n_X$, and μ^{n_X} is the n_X-multiple GAUSSian measure, then $\{H_{\boldsymbol{\alpha}}\}_{\boldsymbol{\alpha}\geqslant 0}$ is an orthonormal basis of $L^2(\mathbb{R}^{n_X}, \mu^{n_X})$ with each $H_{\boldsymbol{\alpha}}(\cdot)$ defined through

$$H_{\boldsymbol{\alpha}}(\xi) = \prod_{i=1}^{n_X} H_{\alpha_i}(\xi_i). \tag{5.17}$$

If $g : \mathbb{R}^{n_X} \to \mathbb{R}$, $g(\xi)$ is a function of the random vector ξ with $\mathbb{E}[g(\xi)] < \infty$, then there exists

a FOURIER-HERMITE expansion of $g(\xi)$ with

$$g(\xi) = \sum_\alpha g_\alpha H_\alpha(\xi), \qquad g_\alpha = \mathbb{E}\big[g(\xi)H_\alpha(\xi)\big]. \tag{5.18}$$

The expansions developed up to now are the starting point of the so-called *Polynomial Chaos (PC)* approaches. Especially in recent years this field has attracted growing attention with applications ranging from mechanical stress considerations [16] to robust shape optimization [220, 226]. Introductions to PC and detailed discussions on its strengths and weaknesses can be found in, e.g., [15, 16, 70, 100, 134, 250].

It also provides an alternative methodology to tackle Optimal Control Problems (OCPs) influenced by random parameters as we have discussed them in Chapters 2 and 3. However, especially in the context of the economic recession model the resulting control problems grow rapidly in the number of variables and, therefore, additional structure exploitations and numerical procedures are indispensable to apply PC ideas to this particular problem.

But let us look upon such an expansion from a different angle. Consider the real, separable HILBERT space $\mathfrak{H}$. Then we define:

Definition 5.3 (Isonormal GAUSSIAN Process)
A stochastic process $W = \{W(h) \mid h \in \mathfrak{H}\}$ defined on a probability space $(\Omega, \mathcal{F}, \mathbb{P})$ and over a HILBERT space $\mathfrak{H}$ is an isonormal GAUSSIAN process *if W is a centered GAUSSIAN family of random variables such that $\mathbb{E}[W(h)W(g)] = \langle h, g\rangle_\mathfrak{H}$ for $h, g \in \mathfrak{H}$.* △

Example 5.1
A very simple example is to suppose $\mathfrak{H} = \mathbb{R}$ and let $\xi \sim \mathcal{N}(0,1)$ be a standard GAUSSIAN random variable. Then $\{W(a) = a\xi \mid a \in \mathbb{R}\}$ is an isonormal GAUSSIAN process over $\mathbb{R}$.

Example 5.2
Let $\mathfrak{H} = L^2(\mathcal{T})$ with $\mathcal{T} = [0, t_\mathrm{f}]$ and t_f being either finite or infinite. Then for each $h \in L^2(\mathcal{T})$ we define

$$W(h) = \int_\mathcal{T} h(t)\, \mathrm{d}B_t$$

via the ITŌ integral and obtain an isonormal GAUSSIAN process. This is often also called WIENER *integral of h over $\mathcal{T}$.*

From now on we assume that the underlying HILBERT space $\mathfrak{H}$ is set to be $L^2(\mathcal{T})$. Furthermore, $\mathcal{F}$ is supposed to be generated by the isonormal GAUSSIAN process W.

Definition 5.4 (n-th WIENER Chaos)
For each $n \in \mathbb{N}_0$ we denote by $\mathcal{H}_n$ the closed linear subspace of $L^2(\Omega, \mathcal{F}, \mathbb{P})$ generated by the random variables $\{H_n(W(h)) \mid h \in L^2(\mathcal{T}), \|h\|_{L^2(\mathcal{T})} = \sqrt{\langle h, h\rangle_{L^2(\mathcal{T})}} = 1\}$. This space $\mathcal{H}_n$ is called the n-th WIENER chaos. △

From that definition we obtain that $\mathcal{H}_0$ is the set of constants, $\mathcal{H}_1$ coincides with the set of random variables $\{W(h) \mid h \in L^2(\mathcal{T})\}$, and for $n \neq m$ the spaces $\mathcal{H}_n$ and $\mathcal{H}_m$ are orthogonal for the scalar product of $L^2(\Omega, \mathcal{F}, \mathbb{P})$.

As the sum $\mathcal{H}_0 \oplus \mathcal{H}_1 \oplus \ldots$ is direct in $L^2(\Omega, \mathcal{F}, \mathbb{P})$, we obtain an equivalent statement to the WIENER-ITŌ chaos expansion of [246] and [56].

Theorem 5.2 ([113, 194])
The space $L^2(\Omega, \mathcal{F}, \mathbb{P})$ can be decomposed into the infinite orthogonal sum of subspaces $\mathcal{H}_n$, i.e.,

$$L^2(\Omega, \mathcal{F}, \mathbb{P}) = \bigoplus_{n=0}^{\infty} \mathcal{H}_n. \tag{5.19}$$

△

As a direct consequence we get:

Corollary 5.1 ([192])
For every random variable $X \in L^2(\Omega, \mathcal{F}, \mathbb{P})$ we obtain a unique expansion

$$X = \sum_{n=0}^{\infty} X_n \tag{5.20}$$

with $X_n \in \mathcal{H}_n$. This series converges in $L^2(\Omega, \mathcal{F}, \mathbb{P})$.

△

Suppose now $\{m_i(\cdot)\}_{i \in \mathbb{N}}$ is a basis of our HILBERT space $L^2(\mathcal{T})$. Further on, $\mathcal{I}$ be the set of all multi-indices $\boldsymbol{\alpha} = (\alpha_1, \alpha_2, \ldots)$ defined via

$$\mathcal{I} \stackrel{\text{def}}{=} \{\boldsymbol{\alpha} = (\alpha_i)_{i \in \mathbb{N}} \mid \alpha_i \in \mathbb{N}_0 \ \forall i \in \mathbb{N}\} \tag{5.21}$$

such that all components, except a finite number of them, are equal to zero. Let $|\boldsymbol{\alpha}| = \sum_{i=1}^{\infty} \alpha_i$ be the *order* of the multi-index $\boldsymbol{\alpha}$. Then for any $\boldsymbol{\alpha} \in \mathcal{I}$ we define

$$\Psi^{\boldsymbol{\alpha}} \stackrel{\text{def}}{=} \prod_{i=1}^{\infty} H_{\alpha_i}(W(m_i)) \tag{5.22}$$

and obtain that the family of random variables $\{\Psi^{\boldsymbol{\alpha}} \mid \boldsymbol{\alpha} \in \mathcal{I}\}$ is an orthonormal system, i.e.,

$$
\begin{aligned}
\mathbb{E}\left[\Psi^{\boldsymbol{\alpha}}\Psi^{\boldsymbol{\beta}}\right] &= \mathbb{E}\left[\prod_{i=1}^{\infty} H_{\alpha_i}(W(m_i))H_{\beta_i}(W(m_i))\right] \\
&= \prod_{i=1}^{\infty} \mathbb{E}\left[H_{\alpha_i}(W(m_i))H_{\beta_i}(W(m_i))\right] \\
&= \prod_{i=1}^{\infty} \delta_{\alpha_i, \beta_i} = \delta_{\boldsymbol{\alpha}, \boldsymbol{\beta}}.
\end{aligned}
$$

This yields the following statement:

Theorem 5.3 ([194])
For any $n \in \mathbb{N}$ the random variables $\{\Psi^{\boldsymbol{\alpha}} \mid \boldsymbol{\alpha} \in \mathcal{I}, |\boldsymbol{\alpha}| = n\}$ form a complete orthonormal system in $\mathcal{H}_n$. Hence, $\{\Psi^{\boldsymbol{\alpha}} \mid \boldsymbol{\alpha} \in \mathcal{I}\}$ is a complete orthonormal system in $L^2(\Omega, \mathcal{F}, \mathbb{P})$.

△

Based on these constructions we obtain a WIENER chaos expansion of random processes $\{X_t\}_{t \in \mathcal{T}}$ that are determined by the BROWNian motion $\{B_t\}_{t \in \mathcal{T}}$ and, thus, itself GAUSSian processes. In particular, we directly get a FOURIER-HERMITE expansion of the BROWNian motion itself again. With the basis $\{m_i(\cdot)\}_{i \in \mathbb{N}}$ of $L^2(\mathcal{T})$ (with $\mathcal{T} = [0, t_{\text{f}}]$) we denote the independent, standard

GAUSSian random variables

$$\eta_i = W(m_i) = \int_0^{t_f} m_i(t)\,\mathrm{d}B_t. \tag{5.23}$$

and reason the following result.

Theorem 5.4 ([172])

The standard BROWNian *motion* $\{B_t\}_{t\in\mathcal{T}}$ *has for all* $t \in \mathcal{T}$ *the* FOURIER-HERMITE *expansion*

$$B_t = \sum_{i=1}^{\infty} \eta_i \int_0^t m_i(s)\,\mathrm{d}s \tag{5.24}$$

with independent $\eta_i \sim \mathcal{N}(0,1)$ *for all* $i \in \mathbb{N}$. △

Proof ([172]) Let $\mathbb{1}_{[0,t]}(\cdot)$ again be the characteristic function of the interval $[0,t]$. $\mathbb{1}_{[0,t]}(\cdot) \in L^2(\mathcal{T})$ and it has the expansion

$$\mathbb{1}_{[0,t]}(s) = \sum_{i=1}^{\infty} \langle \mathbb{1}_{[0,t]}(\cdot), m_i(\cdot)\rangle_{L^2(\mathcal{T})} m_i(s) = \sum_{i=1}^{\infty} m_i(s) \int_0^t m_i(u)\,\mathrm{d}u,$$

yielding

$$B_t = \int_0^t \mathrm{d}B_s = \int_0^{t_f} \mathbb{1}_{[0,t]}(s)\,\mathrm{d}B_s = \int_0^{t_f} \sum_{i=1}^{\infty} m_i(s) \int_0^t m_i(u)\,\mathrm{d}u\,\mathrm{d}B_s$$

$$= \sum_{i=1}^{\infty} \int_0^t m_i(u)\,\mathrm{d}u \int_0^{t_f} m_i(s)\,\mathrm{d}B_s = \sum_{i=1}^{\infty} \eta_i \int_0^t m_i(u)\,\mathrm{d}u. \qquad \square$$

The expansion (5.24) converges in the mean-square sense. Furthermore, in comparison with Definition 5.4 and (5.20) we note that it consists only of elements of the chaos space $\mathcal{H}_1$. E.g., consider the basis $\{m_i(\cdot)\}_{i\in\mathbb{N}}$ of the HILBERT space $L^2([0,1])$ given through the cosine functions

$$m_i(t) = \sqrt{2}\cos\left(\left(i - \frac{1}{2}\right)\pi t\right), \qquad t \in [0,1], i \in \mathbb{N}. \tag{5.25}$$

Then (5.24) coincides with the KLE (4.8) of the BROWNian motion with convergence rate $\frac{1}{\pi N}$, where N denotes the order of truncation.

To obtain a first basis family of the HILBERT space $L^2([0,t_f])$, we can generalize (5.25) by

$$m_i(t) = \sqrt{\frac{2}{t_f}}\cos\left(\left(i - \frac{1}{2}\right)\frac{\pi t}{t_f}\right), \qquad t \in [0,t_f], i \in \mathbb{N}. \tag{5.26}$$

A second choice are the shifted cosine functions

$$m_1(t) = \frac{1}{\sqrt{t_f}}, \qquad m_j(t) = \sqrt{\frac{2}{t_f}}\cos\left((j-1)\frac{\pi t}{t_f}\right), j \geqslant 2, \qquad t \in [0,t_f]. \tag{5.27}$$

Because [252] shows that the particular choice of the complete, orthonormal basis of the underlying L^2-space is unimportant in the construction of the BROWNian motion, another pos-

sibility are the HAAR wavelets [104, 132] in $L^2([0,1])$ given through

$$m_1^{(0)}(t) = 1, \qquad t \in [0,1], \tag{5.28a}$$

and

$$m_k^{(n)}(t) = \begin{cases} 2^{\frac{n-1}{2}}, & \frac{k-1}{2^n} \leqslant t < \frac{k}{2^n}, \\ -2^{\frac{n-1}{2}}, & \frac{k}{2^n} \leqslant t < \frac{k+1}{2^n}, \\ 0, & \text{otherwise}, \end{cases} \tag{5.28b}$$

for all $n \geqslant 1$ and $k \in I(n)$, where $I(n)$ is the set of odd integers between 0 and 2^n. Then the BROWNian motion process $\{B_t\}_{t \in [0,1]}$ can be expanded [132, 167] as

$$B_t = \sum_{i=0}^{\infty} \sum_{j \in I(i)} \eta_j^{(i)} \int_0^t m_j^{(i)}(s)\, \mathrm{d}s, \qquad t \in [0,1], \tag{5.29}$$

with independent $\eta_j^{(i)} \sim \mathcal{N}(0,1)$ for all i, j. Often, the appearing integrals $M_j^{(i)}(\cdot) \overset{\text{def}}{=} \int_0^{\cdot} m_j^{(i)}(s)\, \mathrm{d}s$ are referred to as SCHAUDER functions.

As a generalization of Equation (5.13) and following from Theorem 5.2 and Corollary 5.1 we obtain the next result.

Theorem 5.5 ([56])

Assume that for any $t \in \mathcal{T}$ the random variable X_t is a functional of the BROWNian motion and $X \in L^2(\Omega, \mathcal{F}, \mathbb{P})$. Then X_t has the FOURIER-HERMITE expansion

$$X_t = \sum_{\boldsymbol{\alpha} \in \mathcal{I}} x_{\boldsymbol{\alpha}}(t)\Psi^{\boldsymbol{\alpha}}(\boldsymbol{\eta}) \tag{5.30}$$

with $\Psi^{\boldsymbol{\alpha}}(\boldsymbol{\eta})$ defined via (5.22) and (5.23). △

Remark 5.2

As for the simple expansion (5.13), we derive the moments of the process $\{X_t\}_{t \in \mathcal{T}}$ directly as

$$\mathbb{E}[X_t] = x_0(t), \qquad \mathbb{V}[X_t] = \sum_{\substack{\boldsymbol{\alpha} \in \mathcal{I} \\ \boldsymbol{\alpha} \neq 0}} x_{\boldsymbol{\alpha}}^2(t). \tag{5.31}$$

Analogously, all higher moments can be expressed only by means of the coefficients $x_{\boldsymbol{\alpha}}(\cdot)$ as well.

For computational reasons throughout the rest of this work, we add the following useful results, cf. [172]. As a generalization of Lemma 5.3 we have:

Lemma 5.5 ([172])

The product of two basis polynomials $\Psi^{\cdot}$ is given as

$$\Psi^{\boldsymbol{\alpha}}(\boldsymbol{\eta})\Psi^{\boldsymbol{\beta}}(\boldsymbol{\eta}) = \sum_{\boldsymbol{\gamma} \leqslant \min\{\boldsymbol{\alpha}, \boldsymbol{\beta}\}} \bar{C}(\boldsymbol{\alpha}, \boldsymbol{\beta}, \boldsymbol{\gamma})\Psi^{\boldsymbol{\alpha}+\boldsymbol{\beta}-2\boldsymbol{\gamma}}(\boldsymbol{\eta}) \tag{5.32}$$

with $\bar{C}(\cdot)$ determined as in (5.9). △

Therein, all multi-index operations are defined component-wise, i.e., $\min\{\boldsymbol{\alpha}, \boldsymbol{\beta}\} = (\min\{\alpha_i, \beta_i\})_{i \in \mathbb{N}}$, $\boldsymbol{\alpha}! = \prod_{i=1}^{\infty} \alpha_i!$, $\boldsymbol{\alpha} + \boldsymbol{\beta} = (\alpha_i + \beta_i)_{i \in \mathbb{N}}$, and $\boldsymbol{\alpha} \leqslant \boldsymbol{\beta}$ holds if $\alpha_i \leqslant \beta_i$ for all $i \in \mathbb{N}$.

Theorem 5.6 ([172])

Given the two chaos expansions

$$X_t = \sum_{\boldsymbol{\alpha} \in \mathcal{I}} x_{\boldsymbol{\alpha}}(t) \Psi^{\boldsymbol{\alpha}}(\boldsymbol{\eta}), \qquad Y_t = \sum_{\boldsymbol{\beta} \in \mathcal{I}} y_{\boldsymbol{\beta}}(t) \Psi^{\boldsymbol{\beta}}(\boldsymbol{\eta}),$$

and $\mathbb{E}\left[|X_t Y_t|^2\right] < \infty$, the product $X_t Y_t$ has the chaos expansion

$$X_t Y_t = \sum_{\boldsymbol{\alpha} \in \mathcal{I}} \sum_{\boldsymbol{\gamma} \in \mathcal{I}} \sum_{0 \leqslant \boldsymbol{\beta} \leqslant \boldsymbol{\alpha}} C(\boldsymbol{\alpha}, \boldsymbol{\beta}, \boldsymbol{\gamma}) x_{\boldsymbol{\alpha} - \boldsymbol{\beta} + \boldsymbol{\gamma}}(t) y_{\boldsymbol{\beta} + \boldsymbol{\gamma}}(t) \Psi^{\boldsymbol{\alpha}}(\boldsymbol{\eta}). \tag{5.33}$$

with the constant

$$C(\boldsymbol{\alpha}, \boldsymbol{\beta}, \boldsymbol{\gamma}) = \sqrt{\binom{\boldsymbol{\alpha}}{\boldsymbol{\beta}}\binom{\boldsymbol{\beta} + \boldsymbol{\gamma}}{\boldsymbol{\gamma}}\binom{\boldsymbol{\alpha} - \boldsymbol{\beta} + \boldsymbol{\gamma}}{\boldsymbol{\gamma}}}. \tag{5.34}$$

$\triangle$

Remark 5.3

The following proof originates from [172]. We quote it as an introduction to the discussing Remark 5.4, which considers possible difficulties with Equation (5.33).

Proof ([172]) From Lemma 5.5 we get

$$X_t Y_t = \sum_{\boldsymbol{\alpha} \in \mathcal{I}} \sum_{\boldsymbol{\beta} \in \mathcal{I}} x_{\boldsymbol{\alpha}}(t) y_{\boldsymbol{\beta}}(t) \sum_{\boldsymbol{\gamma} \leqslant \min\{\boldsymbol{\alpha}, \boldsymbol{\beta}\}} \bar{C}(\boldsymbol{\alpha}, \boldsymbol{\beta}, \boldsymbol{\gamma}) \Psi^{\boldsymbol{\alpha} + \boldsymbol{\beta} - 2\boldsymbol{\gamma}}(\boldsymbol{\eta}).$$

Then let $\boldsymbol{\vartheta} = \boldsymbol{\alpha} - \boldsymbol{\gamma}$ and $\boldsymbol{\nu} = \boldsymbol{\beta} - \boldsymbol{\gamma}$, whereas the condition $\boldsymbol{\gamma} \leqslant \min\{\boldsymbol{\alpha}, \boldsymbol{\beta}\}$ is equivalent to $\boldsymbol{\vartheta} \geqslant \mathbf{0}$, $\boldsymbol{\nu} \geqslant \mathbf{0}$. Hence, we can rewrite the above summation as

$$X_t Y_t = \sum_{\boldsymbol{\vartheta} \in \mathcal{I}} \sum_{\boldsymbol{\nu} \in \mathcal{I}} \sum_{\boldsymbol{\gamma} \in \mathcal{I}} x_{\boldsymbol{\vartheta} + \boldsymbol{\gamma}}(t) y_{\boldsymbol{\nu} + \boldsymbol{\gamma}}(t) \bar{C}(\boldsymbol{\vartheta} + \boldsymbol{\gamma}, \boldsymbol{\nu} + \boldsymbol{\gamma}, \boldsymbol{\gamma}) \Psi^{\boldsymbol{\vartheta} + \boldsymbol{\nu}}(\boldsymbol{\eta}).$$

In the next step, denote $\boldsymbol{\kappa} = \boldsymbol{\vartheta} + \boldsymbol{\nu}$, then $\boldsymbol{\vartheta} = \boldsymbol{\kappa} - \boldsymbol{\nu} \geqslant \mathbf{0}$ and $\mathbf{0} \leqslant \boldsymbol{\nu} \leqslant \boldsymbol{\kappa}$, yielding

$$X_t Y_t = \sum_{\boldsymbol{\kappa} \in \mathcal{I}} \sum_{\boldsymbol{\vartheta} + \boldsymbol{\nu} = \boldsymbol{\kappa}} \sum_{\boldsymbol{\gamma} \in \mathcal{I}} x_{\boldsymbol{\vartheta} + \boldsymbol{\gamma}}(t) y_{\boldsymbol{\nu} + \boldsymbol{\gamma}}(t) \bar{C}(\boldsymbol{\vartheta} + \boldsymbol{\gamma}, \boldsymbol{\nu} + \boldsymbol{\gamma}, \boldsymbol{\gamma}) \Psi^{\boldsymbol{\kappa}}(\boldsymbol{\eta})$$

$$= \sum_{\boldsymbol{\kappa} \in \mathcal{I}} \sum_{0 \leqslant \boldsymbol{\nu} \leqslant \boldsymbol{\kappa}} \sum_{\boldsymbol{\gamma} \in \mathcal{I}} x_{\boldsymbol{\kappa} - \boldsymbol{\nu} + \boldsymbol{\gamma}}(t) y_{\boldsymbol{\nu} + \boldsymbol{\gamma}}(t) \bar{C}(\boldsymbol{\kappa} - \boldsymbol{\nu} + \boldsymbol{\gamma}, \boldsymbol{\nu} + \boldsymbol{\gamma}, \boldsymbol{\gamma}) \Psi^{\boldsymbol{\kappa}}(\boldsymbol{\eta}).$$

Defining $C(\boldsymbol{\kappa}, \boldsymbol{\nu}, \boldsymbol{\gamma}) \stackrel{\text{def}}{=} \bar{C}(\boldsymbol{\kappa} - \boldsymbol{\nu} + \boldsymbol{\gamma}, \boldsymbol{\nu} + \boldsymbol{\gamma}, \boldsymbol{\gamma})$ finishes the proof. $\qquad \square$

Remark 5.4

In [184] the convergence behavior of products of one-dimensional chaos expansions is analyzed in detail. In particular, it is shown that given two random variables $u(\xi), v(\xi) \in L^2(\Omega, \mathcal{F}, \mathbb{P})$ depending on $\xi \in L^2(\Omega, \mathcal{F}, \mathbb{P})$ and their corresponding chaos expansions, the chaos coefficients of the product can not always be described by the product formula (5.33). To guarantee its

applicability, certain additional conditions are necessary, i.e., one needs for all $n \in \mathbb{N}$

$$\|u(\xi)\Psi^n(\xi)\|_{L^2(\Omega)} < \infty, \qquad \|v(\xi)\Psi^n(\xi)\|_{L^2(\Omega)} < \infty,$$

and, in particular,

$$\sum_{p=0}^{\infty}\sum_{j=0}^{n}\left|C(n,j,p)u_{j+p}v_{n-j+p}\right| < \infty, \tag{5.35}$$

which is a more precise condition than $\mathbb{E}\left[|uv|^2\right] < \infty$ from Theorem 5.6.

In other words, one has to ensure that the rearrangement of coefficients—which is an essential step in the proof of Theorem 5.6—is allowed, i.e., one has to require absolute convergence. In [184] it is furthermore shown that this condition is satisfied if the series $u^{(p_u)}v^{(p_v)}$, that is the series of the product of the chaos expansions of u and v truncated at the orders p_u and p_v, respectively, converges in the mean-square sense to uv for $p_u, p_v \to \infty$.

A vivid interpretation of this condition is that one has to ensure a sufficient decaying rate of the chaos expansion coefficients. However, throughout our numerical computations in the subsequent Chapters 6 and 8 we did not encounter any problems related to that issue in our context of multi-variate GAUSSIAN random variables and the chaos expansions of stochastic processes depending on them. In all instances, the chaos coefficients decreased very fast in magnitude, which is why we always assume the additional condition on absolute convergence to be fulfilled in the sequel.

An alternative formula to derive the product of the chaos expansions of random variables X_t and Y_t, which does not necessitate condition (5.35), can be derived by using Lemmata 5.3 and 5.5.

5.3 MALLIAVIN Calculus

The field of MALLIAVIN calculus is a very broad infinite dimensional differential calculus, acting on GAUSSIAN processes. Thus, it provides an analogue to common differential calculus in a stochastic environment. Originating from the work of PAUL MALLIAVIN [177], exhaustive presentations of this topic can be found in [125, 153, 178, 192, 194]. Here, we restrict ourselves only to those parts of MALLIAVIN calculus necessary throughout the rest of this work. In that regard we focus again on the specific setting where we consider the underlying HILBERT space $\mathfrak{H} = L^2(\mathcal{T})$ for a given time set $\mathcal{T} = [0, t_{\mathrm{f}}]$. Again, the filtration $\mathcal{F}$ we assume to be generated by W. For notational ease by $L^2(\Omega)$ we always mean $L^2(\Omega, \mathcal{F}, \mathbb{P})$.

The Derivative Operator

The most important element of MALLIAVIN calculus we need is the derivative of a random variable $X \in L^2(\Omega)$. However, we cannot apply the classical ideas to differentiating X with respect to $\omega \in \Omega$ as usually the probability space does not hold the structure to define that derivative. Moreover, random variables are in general defined only almost everywhere. The remedy to that problem is considering a derivative with respect to the element $h \in L^2(\mathcal{T})$, i.e., taking an isonormal GAUSSIAN process W over an HILBERT space as the basis.

Definition 5.5 (Smooth Random Variable)

Let F be a random variable given through

$$F = f(W(h_1), \ldots, W(h_n)) \tag{5.36}$$

with $n \in \mathbb{N}$, $f : \mathbb{R}^n \to \mathbb{R}$ being infinitely often continuously differentiable, such that f and its partial derivatives $\frac{\partial f}{\partial x_i}$ have at most polynomial growth, and $h_i \in L^2(\mathcal{T})$ for all $i = 1, \ldots, n$. Then such a random variable F is said to be smooth. △

Lemma 5.6 ([194])

The space $\mathcal{S}$ of smooth random variables is dense in $L^2(\Omega)$. △

Definition 5.6 (MALLIAVIN Derivative)

Let F be a smooth random variable defined by (5.36). The MALLIAVIN derivative of F (with respect to W) is the $L^2(\mathcal{T})$-valued random variable given through

$$DF = \sum_{i=1}^{n} \frac{\partial}{\partial x_i} f(W(h_1), \ldots, W(h_n)) \cdot h_i. \tag{5.37}$$

△

Example 5.3

From the definition of the MALLIAVIN derivative we directly obtain $DW(h) = h$ and $DB_t = DW(\mathbb{1}_{[0,t]}) = \mathbb{1}_{[0,t]}$.

Furthermore, DF can be interpreted as a directional derivative in the following sense. For any $h \in L^2(\mathcal{T})$ we have

$$\langle DF, h \rangle_{L^2(\mathcal{T})} = \lim_{\varepsilon \to 0} \frac{1}{\varepsilon} \Big(f\left(W(h_1) + \varepsilon \langle h_1, h \rangle_{L^2(\mathcal{T})}, \ldots, W(h_n) + \varepsilon \langle h_n, h \rangle_{L^2(\mathcal{T})}\right)$$
$$- f(W(h_1), \ldots, W(h_n))\Big).$$

The iteration of the derivative operator D is defined via:

Definition 5.7 (k-th MALLIAVIN Derivative)

Let F be a smooth random variable and $k \in \mathbb{N}$. Then the k-th MALLIAVIN derivative of F is a random variable taking values from the space $L^2(\mathcal{T})^{\otimes k} = \underbrace{L^2(\mathcal{T}) \otimes \cdots \otimes L^2(\mathcal{T})}_{k \text{ times}}$, i.e.,

$$D^k F = \sum_{i_1, \ldots, i_k = 1}^{n} \frac{\partial^k}{\partial x_{i_1} \cdots \partial x_{i_k}} f(W(h_1), \ldots, W(h_n)) \cdot h_{i_1} \otimes \cdots \otimes h_{i_k}. \tag{5.38}$$

△

Of great importance for the remainder of this work is the next result, which provides the basic form of the *integration by parts formula* of MALLIAVIN calculus.

Lemma 5.7 ([194])

Suppose F is a smooth random variable and $h \in L^2(\mathcal{T})$. Then the integration by parts formula

$$\mathbb{E}\left[\langle DF, h \rangle_{L^2(\mathcal{T})}\right] = \mathbb{E}[FW(h)] \tag{5.39}$$

holds. △

From Equation (5.39) we obtain the rule for calculating the derivative of a product of random variables.

Lemma 5.8 ([194])
Let $F, G \in \mathcal{S}$ and $h \in L^2(\mathcal{T})$. Then it holds

$$\mathbb{E}\left[G\langle DF, h\rangle_{L^2(\mathcal{T})}\right] = \mathbb{E}\left[FGW(h) - F\langle DG, h\rangle_{L^2(\mathcal{T})}\right]. \tag{5.40}$$

△

Proof ([194]) From the definition of MALLIAVIN's derivative and the product rule of classical differential calculus we deduce $D(FG) = F \cdot DG + DF \cdot G$. Inserting this relation into (5.39) yields the assertion. □

Theorem 5.7 ([194])
The operator D is closable from $L^2(\Omega)$ to $L^2(\mathcal{T} \times \Omega)$.

△

We will denote the *domain of the derivative operator D* by $\mathbb{D}^{1,2}$. That is, $\mathbb{D}^{1,2}$ is the closure of the class $\mathcal{S}$ of smooth random variables with respect to the norm $\|\cdot\|_{1,2}$ defined through the scalar product

$$\langle F, G\rangle_{1,2} = \mathbb{E}[FG] + \mathbb{E}\left[\langle DF, DG\rangle_{L^2(\mathcal{T})}\right] \qquad \forall F, G \in \mathbb{D}^{1,2}.$$

Certainly, closability follows for the k-th MALLIAVIN derivative D^k as well, provided the norm $\|\cdot\|_{k,2}$ defined by an analogous scalar product including all derivatives up to order k.

Remark 5.5
In the context of a general real-valued, separable HILBERT space $\mathfrak{H}$ the derivative operator is closable from $L^2(\Omega)$ to $L^2(\Omega; \mathfrak{H})$, where $L^2(\Omega; \mathfrak{H})$ is the class of $\mathfrak{H}$-valued random elements Z that are $\mathcal{F}$-measurable and such that $\mathbb{E}\left[\|Z\|_{\mathfrak{H}}^2\right] < \infty$. In the case $\mathfrak{H} = L^2(\mathcal{T})$ this class can be identified with $L^2(\mathcal{T} \times \Omega)$, cf. [194].

As we consider the underlying HILBERT space $L^2(\mathcal{T})$, the derivative of a random variable $F \in \mathbb{D}^{1,2}$ is again a stochastic process $\{D_t F\}_{t \in \mathcal{T}}$. $D_t F$ is defined almost everywhere with respect to the measure $\mu \otimes \mathbb{P}$. Similarly, the k-th MALLIAVIN derivative of a random variable $F \in \mathbb{D}^{k,2}$ is a measurable function in the space $L^2(\mathcal{T}^k \times \Omega)$. Hence, it is a k-parameter stochastic process

$$D^k F = \left\{D^k_{t_1, \ldots, t_k} F\right\}_{t_i \in \mathcal{T}, i=1, \ldots, n}$$

To complete the suite of instruments to use the MALLIAVIN derivative later on, we state the *chain rule*.

Theorem 5.8 ([153, 194])
Let $\boldsymbol{f} = (F_1, \ldots, F_{n_F})$ be a vector of random variables with $F_i \in \mathbb{D}^{1,2}$, $i = 1, \ldots, n_F$, and $g : \mathbb{R}^{n_F} \to \mathbb{R}$ be continuously differentiable with bounded partial derivatives. Then $g(\boldsymbol{f}) \in \mathbb{D}^{1,2}$ and the chain rule

$$Dg(\boldsymbol{f}) = \sum_{i=1}^{n_F} \frac{\partial}{\partial x_i} g(\boldsymbol{f}) DF_i \tag{5.41}$$

for the MALLIAVIN derivative holds.

△

Example 5.4

Consider the basis polynomials Ψ^{α} introduced in (5.22) for fixed $\alpha \in \mathcal{I}$. Exploiting the rule (5.2) for differentiating HERMITE polynomials and the definition (5.23) of the standard GAUSSIAN random variables η_i, $i \in \mathbb{N}$, we deduce

$$
\begin{aligned}
D_s \Psi^{\alpha}(\eta) &= D_s \left(\sqrt{\alpha!} \prod_{i=1}^{\infty} H_{\alpha_i}(W(m_i)) \right) \\
&= \sum_{j=1}^{\infty} \sqrt{\alpha!} \prod_{\substack{i=1 \\ i \neq j}}^{\infty} H_{\alpha_i}(W(m_i)) \cdot H_{\alpha_j - 1}(W(m_j)) \cdot m_j(s) \\
&= \sum_{j=1}^{\infty} \sqrt{\alpha_j} m_j(s) \Psi^{\alpha^-(j)}(\eta)
\end{aligned}
\tag{5.42}
$$

with the diminished multi-index $\alpha^-(j)$ defined through

$$
\alpha_i^-(j) = \begin{cases} \alpha_i, & i \neq j, \\ \alpha_i - 1, & i = j. \end{cases}
\tag{5.43}
$$

Remark 5.6

Note that whenever the diminished multi-index $\alpha^-(j)$ has a negative component, it is not a valid element of the index set $\mathcal{I}$ anymore.

The Divergence Operator

While in classical calculus we have the well-known connection between differentiation and integration, in the context of MALLIAVIN calculus the pendant to an integral is defined in the following way, cf. [194]. Note, that we identify the underlying HILBERT space $\mathfrak{H} = L^2(\mathcal{T})$.

Definition 5.8 (Divergence Operator)
By δ we denote the adjoint of the operator D. That is, δ is an unbounded operator on $L^2(\mathcal{T} \times \Omega)$ with values in $L^2(\Omega)$ such that
  (i) the domain of δ, $\mathrm{Dom}\, \delta$, is the set of $L^2(\mathcal{T})$-valued, square-integrable random variables $v \in L^2(\mathcal{T} \times \Omega)$ with $\left| \mathbb{E} \left[\langle DF, v \rangle_{L^2(\mathcal{T})} \right] \right| \leqslant c \|F\|_2$ for all $F \in \mathbb{D}^{1,2}$ and a constant c depending only on v,
  (ii) if $v \in \mathrm{Dom}\, \delta$ then $\delta(v)$ is the element of $L^2(\Omega)$ with

$$
\mathbb{E}[F \delta(v)] = \mathbb{E} \left[\langle DF, v \rangle_{L^2(\mathcal{T})} \right] \qquad \forall F \in \mathbb{D}^{1,2}.
\tag{5.44}
$$

δ is also called divergence operator. *As the adjoint of an unbounded and densely defined operator it is closed as well.* △

Example 5.5

From taking $F = 1$ in (5.44) we see that $\mathbb{E}[\delta(v)] = 0$ for all $v \in \mathrm{Dom}\, \delta$.
Consider $v \in \mathcal{S}(L^2(\mathcal{T}))$ given by $v = Xh$ with $h \in L^2(\mathcal{T})$. Then $X \in \mathrm{Dom}\, \delta$ and for all $Y \in \mathbb{D}^{1,2}$ we get

$$
\mathbb{E}[Y \delta(v)] = \mathbb{E} \left[\langle DY, v \rangle_{L^2(\mathcal{T})} \right] = \mathbb{E} \left[X \langle DY, h \rangle_{L^2(\mathcal{T})} \right] = \mathbb{E} \left[Y \left(XW(h) - \langle DX, h \rangle_{L^2(\mathcal{T})} \right) \right]
$$

by Equation (5.40).

Moreover, the divergence operator is linear and we can derive a commutativity relation between the derivative D and the divergence δ:

Theorem 5.9 ([153, 194])
Let $v \in \mathbb{D}^{1,2}(L^2(\mathcal{T})) \subset \mathrm{Dom}\,\delta$, $\langle Dv, h \rangle_{L^2(\mathcal{T})} \in \mathrm{Dom}\,\delta$, and $h \in L^2(\mathcal{T})$. Then the HEISENBERG *commutativity relationship*

$$\langle D(\delta(v)), h \rangle_{L^2(\mathcal{T})} = \langle v, h \rangle_{L^2(\mathcal{T})} + \delta\left(\langle Dv, h \rangle_{L^2(\mathcal{T})} \right) \tag{5.45}$$

holds. △

Another important property is given by the next result. It allows to factor out scalar random variables from a divergence.

Theorem 5.10 ([192])
Let $F \in \mathbb{D}^{1,2}$ and $v \in \mathrm{Dom}\,\delta$ such that $Fv \in L^2(\mathcal{T} \times \Omega)$. Then $Fv \in \mathrm{Dom}\,\delta$ and the equality

$$\delta(Fv) = F\delta(v) - \langle DF, v \rangle_{L^2(\mathcal{T})} \tag{5.46}$$

is true if the right-hand side of (5.46) *is square-integrable.* △

Proof ([192]) For any smooth random variable G with compact support we derive, using Lemma 5.8,

$$
\begin{aligned}
\mathbb{E}[F\delta(Fv)] &= \mathbb{E}\left[\langle DG, Fv \rangle_{L^2(\mathcal{T})} \right] \\
&= \mathbb{E}\left[\langle D(FG), v \rangle_{L^2(\mathcal{T})} - G \langle DF, v \rangle_{L^2(\mathcal{T})} \right] \\
&= \mathbb{E}\left[FG\delta(v) - G \langle DF, v \rangle_{L^2(\mathcal{T})} \right] \\
&= \mathbb{E}\left[G \left(F\delta(v) - \langle DF, v \rangle_{L^2(\mathcal{T})} \right) \right].
\end{aligned}
$$ □

Due to our choice of underlying HILBERT space, we have $\mathrm{Dom}\,\delta \subset L^2(\mathcal{T} \times \Omega)$ and its elements are, thus, square-integrable processes. With this setting the divergence is often called SKORO-HOD *integral* of v. In the case of $v \in L^2_A(\mathcal{T} \times \Omega)$, i.e., v being an adapted process, the SKOROHOD integral and the ITŌ integral coincide [194], we have

$$\delta(v) = \int_{\mathcal{T}} v_t \, \mathrm{d}B_t.$$

Hence, we obtain another version of the integration by parts formulae (5.39) and (5.44), holding for restrictions to the time interval $[t_0, t] \subseteq \mathcal{T}$.

Lemma 5.9
Let $\{X_t\}_{t \in \mathcal{T}}$ be a square-integrable and $\mathcal{F}_t$-measurable random variable. Then for all $F \in \mathbb{D}^{1,2}$ we obtain the relation

$$\mathbb{E}\left[F \int_{t_0}^{t} X_s \, \mathrm{d}B_s \right] = \mathbb{E}\left[\int_{t_0}^{t} D_s F X_s \, \mathrm{d}s \right]. \tag{5.47}$$

△

Proof With $\{\tilde{X}_t\}_{t\in\mathcal{T}}$ denoting the restriction of the original process X on the time interval $[t_0, t]$ we calculate

$$\mathbb{E}\left[F\int_{t_0}^t X_s \, \mathrm{d}B_s\right] = \mathbb{E}\left[F\int_{\mathcal{T}} X_s \cdot \mathbb{1}_{s\in[t_0,t]} \, \mathrm{d}B_s\right] = \mathbb{E}\left[F\delta(\tilde{X})\right]$$

$$= \mathbb{E}\left[\langle DF, \tilde{X}\rangle_{L^2(\mathcal{T})}\right] = \mathbb{E}\left[\int_{\mathcal{T}} D_s F \cdot X_s \cdot \mathbb{1}_{s\in[t_0,t]} \, \mathrm{d}s\right]$$

$$= \mathbb{E}\left[\int_{t_0}^t D_s F X_s \, \mathrm{d}s\right].$$

$\square$

Multiple WIENER Integrals

The original chaos expansion of a random variable $F \in L^2(\Omega)$ introduced by NORBERT WIENER [246] does not consist of HERMITE polynomials. Instead it is based on multiple stochastic integrals:

Theorem 5.11 (WIENER Chaos Expansion; [246])
Any square-integrable random variable $F \in L^2(\Omega, \mathcal{F}, \mathbb{P})$, where the filtration $\mathcal{F}$ is generated by the BROWNian motion B, admits the expansion

$$F = \sum_{n=0}^\infty I_n(f_n), \tag{5.48}$$

where $I_n(\cdot)$ denotes the multiple stochastic integral

$$I_n(f_n) = \underbrace{\int_{\mathcal{T}} \cdots \int_{\mathcal{T}}}_{n \text{ times}} f_n(t_1, \ldots, t_n) \, \mathrm{d}B_{t_1} \ldots \mathrm{d}B_{t_n} \tag{5.49}$$

for $f_n \in L^2(\mathcal{T}^n)$. Then it holds $f_0 = \mathbb{E}[F]$ with the identity mapping $I_0(\cdot)$. Additionally, we can assume that the kernel functions $f_n \in L^2(\mathcal{T}^n)$ are symmetric and uniquely determined by F. $\triangle$

Similar to the HERMITE polynomials, appropriate rules for multiplying multiple stochastic integrals can be deduced [125, 192, 194].

If F now is a square-integrable random variable with chaos expansion (5.48), its MALLIAVIN derivative can be computed using the next results.

Theorem 5.12 ([192, 194])
Let $F \in \mathbb{D}^{1,2}$ be given through (5.48). Then we have

$$D_t F = \sum_{n=1}^\infty n I_{n-1}(f_n(\cdot, t)). \tag{}$$

$\triangle$

Proof ([192]) We start by showing by induction that for all $n \in \mathbb{N}$, $h \in L^2(\mathcal{T})^{\otimes n}$, we have $\delta^n(h) \in \mathbb{D}^{1,2}$ and

$$D\delta^n(h) = n\delta^{n-1}(h), \tag{5.50}$$

where δ^n is the adjoint of the operator D^n, i.e., the n-th divergence or SKOROHOD integral. For $n = 1$ this is a direct consequence of the HEISENBERG commutativity relation (5.45). Now let (5.50) be true. For any $g \in L^2(\mathcal{T})^{\otimes(n+1)}$ we deduce

$$D\delta^{n+1}(g) = D\delta(\delta^n(g)) = \delta^n(g) + \delta(D\delta^n(g))$$
$$= \delta(n\delta^{n-1}(g)) + \delta^n(g) = (n+1)\delta^n(g).$$

With this result at hand, we obtain for any $F = I_n(f_n)$ that

$$DF = DI_n(f_n) = D\delta^n(f_n) = n\delta^{n-1}(f_n) = nI_{n-1}(f_n),$$

yielding the assertion. $\qquad\square$

With the help of these preliminary statements, we find that the necessary connection between the HERMITE polynomials $H_n(\cdot)$ and the multiple stochastic integrals $I_n(\cdot)$ is given through the next important result.

Theorem 5.13 ([124, 192, 194])
Let $h \in L^2(\mathcal{T})$ with $\|h\|_{L^2(\mathcal{T})} = 1$ be given. Then for any $n \in \mathbb{N}$ the connection

$$\sqrt{n!}H_n(W(h)) = I_n(h^{\otimes n}) \tag{5.51}$$

holds. Furthermore, the multiple integral $I_n(\cdot)$ maps $L^2(\mathcal{T}^n)$ onto the WIENER chaos $\mathcal{H}_n$. $\qquad\triangle$

Proof ([192]) We show Equation (5.51) by induction on n. For $n = 1$

$$H_1(W(h)) = W(h) = \int_{\mathcal{T}} h\, dB_t = I_1(h).$$

Now assume the assertion holds for all orders $1, \ldots, n$. Then with the correspondence to the divergence operator and using the integration by parts formula we calculate

$$\begin{aligned}
I_{n+1}(h^{\otimes(n+1)}) &= \delta(I_n(h^{\otimes n})h) \\
&= I_n(h^{\otimes n})\delta(h) - \langle DI_n(h^{\otimes n}), h\rangle_{L^2(\mathcal{T})} \\
&= I_n(h^{\otimes n})W(h) - nI_{n-1}(h^{\otimes(n-1)}) \cdot \|h\|^2_{L^2(\mathcal{T})} \\
&= \sqrt{n!}H_n(W(h)) \cdot W(h) - n\sqrt{(n-1)!}H_{n-1}(W(h)) \\
&= \sqrt{n!}\left(H_n(W(h)) \cdot W(h) - \sqrt{n}H_{n-1}(W(h))\right) \\
&= \sqrt{(n+1)!}H_{n+1}(W(h)).
\end{aligned}$$

Then let $L^2_S(\mathcal{T}^n)$ be the closed subspace of $L^2(\mathcal{T})$ consisting of symmetric functions. On $L^2_S(\mathcal{T}^n)$ it holds $\mathbb{E}\left[I_n(f)^2\right] = n!\|f\|^2_{L^2(\mathcal{T}^n)}$. Thus, the image $I_n(L^2_S(\mathcal{T}^n))$ is closed and it contains the random variables $H_n(W(h))$, $h \in L^2(\mathcal{T})$, $\|h\|_{L^2(\mathcal{T})} = 1$. Therefore, the chaos $\mathcal{H}_n$ is a subset of $L^2_S(\mathcal{T}^n)$. As multiple integrals of different order are (as the corresponding HERMITE polynomials) orthogonal, it holds that $I_n(L^2_S(\mathcal{T}^n))$ is orthogonal to $\mathcal{H}_m$ for $n \neq m$. Hence, $\mathcal{H}_n = I_n(L^2_S(\mathcal{T}^n))$. $\qquad\square$

To finish this chapter we provide a useful connection between multiple integrals, MALLIAVIN calculus, and the WIENER chaos expansion (5.30) of a stochastic process $\{X_t\}_{t \in \mathcal{T}}$. From (5.51)

we find that given a basis $\{m_i(\cdot)\}_{i\in\mathbb{N}}$ of $L^2(\mathcal{T})$, for any $\boldsymbol{\alpha} \in \mathcal{I}$ with $|\boldsymbol{\alpha}| = p$ it holds [194]

$$\Psi^{\boldsymbol{\alpha}}(\boldsymbol{\eta}) = \prod_{i=1}^{\infty} H_{\alpha_i}(W(m_i)) = \prod_{i=1}^{\infty} \frac{1}{\sqrt{\alpha_i!}} I_{\alpha_i}\left(m_i^{\otimes\alpha_i}\right) = \frac{1}{\sqrt{\boldsymbol{\alpha}!}} I_p\left(\bigotimes_{i=1}^{\infty} m_i^{\otimes\alpha_i}\right). \tag{5.52}$$

By applying the integration-by-parts formula we then derive

$$x_{\boldsymbol{\alpha}}(t) = \mathbb{E}\left[X_t \Psi^{\boldsymbol{\alpha}}(\boldsymbol{\eta})\right] = \frac{1}{\sqrt{\boldsymbol{\alpha}!}} \mathbb{E}\left[\left\langle D^p X_t, \bigotimes_{i=1}^{\infty} m_i^{\otimes\alpha_i} \right\rangle_{L^2(\mathcal{T})^{\otimes p}}\right]. \tag{5.53}$$

Example 5.6

If $\{X_t\}_{t\in\mathcal{T}} = \{B_t\}_{t\in\mathcal{T}}$ we have $D_s B_t = \mathbb{1}_{\{s\leqslant t\}}$. Thus, the coefficients of the chaos expansion for $p = |\boldsymbol{\alpha}|$ are

$$p = 0: \quad x_{\boldsymbol{0}}(t) = \mathbb{E}\left[B_t\right] = 0,$$

$$p = 1: \quad x_{\boldsymbol{e}_i}(t) = \mathbb{E}\left[\langle DB_t, m_i\rangle_{L^2(\mathcal{T})}\right] = \int_0^t m_i(s)\,\mathrm{d}s \overset{\text{def}}{=} M_i(t), i \in \mathbb{N},$$

$$p \geqslant 2: \quad x_{\boldsymbol{\alpha}}(t) = \mathbb{E}\left[\langle 0, \otimes m_i^{\otimes\alpha_i}\rangle_{L^2(\mathcal{T})^{\otimes p}}\right] = 0.$$

Example 5.7

Consider the *geometric* BROWN*ian motion process* $\{X_t\}_{t\in\mathcal{T}}$ on $\mathcal{T} = [0, t_f]$ determined by the Stochastic Differential Equation (SDE)

$$dX_t = \mu X_t\,\mathrm{d}t + \sigma X_t\,\mathrm{d}B_t, \quad X_0 = x_0.$$

This process has the analytical solution

$$X_t = x_0 \exp\left(\left(\mu - \frac{\sigma^2}{2}\right)t + \sigma B_t\right),$$

giving its MALLIAVIN derivative $D_s X_t = \sigma X_t \mathbb{1}_{[0,t]}(s)$. Hence, we derive the coefficients of the chaos expansion for $p = |\boldsymbol{\alpha}|$ as

$$p = 0: \quad x_{\boldsymbol{0}}(t) = \mathbb{E}\left[X_t\right] = x_0\,\mathrm{e}^{\mu t},$$

$$p = 1: \quad x_{\boldsymbol{e}_i}(t) = \mathbb{E}\left[\langle \sigma X_t \mathbb{1}_{[0,t]}(\cdot), m_i(\cdot)\rangle_{L^2(\mathcal{T})}\right]$$

$$= \mathbb{E}\left[\sigma X_t \int_0^t m_i(s)\,\mathrm{d}s\right] = x_0\sigma\,\mathrm{e}^{\mu t}\,M_i(t), \quad i \in \mathbb{N},$$

$$p = 2: \quad x_{\boldsymbol{\alpha}}(t) = \frac{1}{\sqrt{\boldsymbol{\alpha}!}}\mathbb{E}\left[\langle \sigma^2 X_t \cdot \mathbb{1}_{[0,t]}(\cdot)\mathbb{1}_{[0,t]}(\cdot), \otimes m_i^{\otimes\alpha_i}(\cdot)\rangle_{L^2(\mathcal{T})^{\otimes 2}}\right]$$

$$= \begin{cases} \frac{1}{\sqrt{2}}\mathbb{E}\left[\langle \sigma^2 X_t \mathbb{1}_{[0,t]}(\cdot), m_i^{\otimes 2}(\cdot)\rangle_{L^2(\mathcal{T})^{\otimes 2}}\right], & \boldsymbol{\alpha} = 2\boldsymbol{e}_i, i \in \mathbb{N}, \\ \mathbb{E}\left[\langle \sigma^2 X_t \mathbb{1}_{[0,t]}(\cdot), m_i(\cdot) \otimes m_j(\cdot)\rangle_{L^2(\mathcal{T})^{\otimes 2}}\right], & \boldsymbol{\alpha} = \boldsymbol{e}_i + \boldsymbol{e}_j, i \neq j \in \mathbb{N}, \end{cases}$$

$$= \begin{cases} \frac{1}{\sqrt{2}}x_0\sigma^2\,\mathrm{e}^{\mu t}\,(M_i(t))^2, & \boldsymbol{\alpha} = 2\boldsymbol{e}_i, i \in \mathbb{N}, \\ x_0\sigma^2\,\mathrm{e}^{\mu t}\,M_i(t)M_j(t), & \boldsymbol{\alpha} = \boldsymbol{e}_i + \boldsymbol{e}_j, i \neq j \in \mathbb{N}, \end{cases}$$

$$p \geqslant 3: \quad x_{\boldsymbol{\alpha}}(t) = \frac{1}{\sqrt{\boldsymbol{\alpha}!}} \mathbb{E}\left[\left\langle \sigma^p X_t \cdot \mathbb{1}_{[0,t]}(\cdot), \otimes m_i^{\otimes \alpha_i}(\cdot) \right\rangle_{L^2(\mathcal{T})^{\otimes p}} \right]$$

$$= \frac{1}{\sqrt{\boldsymbol{\alpha}!}} x_0 \sigma^p \, \mathrm{e}^{\mu t} \prod_{i=1}^{\infty} (M_i(t))^{\alpha_i} \, .$$

Finally, if $X_t \in L^2(\mathcal{T} \times \Omega)$ is a random variable belonging to the domain space $\mathbb{D}^{\infty,2} = \bigcap_{k \geqslant 1} \mathbb{D}^{k,2}$ admitting a chaos expansion

$$X_t = \sum_{n=0}^{\infty} I_n\left(\xi_n(t_1, \ldots, t_n; t)\right)$$

with symmetric kernel functions $\xi_n(\cdot)$, then for every $n \geqslant 0$ we have [194, 232]

$$\xi_n(\cdot; t) = \frac{1}{n!} \mathbb{E}\left[D_\cdot^n X_t \right]. \tag{5.54}$$

5.4 Summary

In this chapter we discussed the two different notions of WIENER chaos expansion—the first constructed in a FOURIER-like manner and based upon multi-dimensional HERMITE polynomials of random basis functions, the second consisting of multiple stochastic integrals.

Moreover, we gave an introduction to MALLIAVIN calculus, a stochastic counterpart of differential calculus, providing the essential MALLIAVIN derivative. With the help of this methodology we explored the connection of the two expansion types, constituting the fundaments of finding chaos decompositions of stochastic processes that are determined by SDEs. This will be considered in the following chapter.

6 Numerical Solution to Stochastic Differential Equations Using the WIENER Chaos Approach

In this chapter we present methods to solve Stochastic Differential Equations (SDEs) numerically. As finding an analytical solution to those equations is in fact even more complicated than in the deterministic context, the need for such numerical approximations is immense. We start by exemplary discussing techniques that are related to deterministic numerical integration schemes like the EULER method.

Afterwards we develop a connection between SDEs and systems of Ordinary Differential Equations (ODEs) by applying the ideas of the previous chapter. This leads us to the so-called *propagator method* for solving SDEs. We present the truncations that are necessary to use the propagator numerically and develop an error analysis of the truncated chaos expansion.

6.1 Numerical Integration of Stochastic Differential Equations

As we have noticed in Chapter 4 when defining the ITŌ stochastic integral, its integrand function has to be evaluated at the left-hand endpoint of the discretization interval. Hence, deriving a numerical scheme to integrate a SDE needs much more care then in the deterministic case, where the integrand of a RIEMANN integral can be evaluated at any point of the interval. To remain consistent with ITŌ stochastic calculus, the numerical schemes for deducing approximative solutions to SDEs are based on *stochastic* TAYLOR *expansions*. The underlying theory can be found in, e.g., [126, 141, 142], here we only give a very brief overview to explain the general approach. To begin, let us take a closer look at the easiest stochastic integration method, analogous to the deterministic EULER scheme.

6.1.1 The EULER-MARUYAMA Scheme

We consider the one-dimensional ITŌ SDE

$$X_t = X_{t_0} + \int_{t_0}^t b(s, X_s)\,\mathrm{d}s + \int_{t_0}^t \sigma(s, X_s)\,\mathrm{d}B_s \tag{6.1}$$

in its integral from over the time horizon $\mathcal{T} = [t_0, t_f]$ for a given initial value X_{t_0}. Then the stochastic counterpart of the famous EULER method, the EULER-MARUYAMA *scheme* for the SDE (6.1) is obtained as we discretize the time interval $\mathcal{T}$ by $t_0 < t_1 < \ldots < t_N = t_f$ and get a time-discrete stochastic process $\{Y_t\}_{t \in \mathcal{T}}$ following the recursion

$$Y_{n+1} = Y_n + b(t_n, Y_n)\Delta_n + \sigma(t_n, Y_n)\Delta B_n \tag{6.2}$$

for $n = 0, \ldots, N-1$ and with initial value $Y_0 = X_{t_0}$, where Y_n always denotes $Y(t_n)$, $\Delta_n = t_{n+1} - t_n$, and $\Delta B_n = B_{t_{n+1}} - B_{t_n}$.

In numerical applications often equidistant time step sizes $\Delta_n = h$ are used. Furthermore, the scheme (6.2) and the subsequently presented ones are usually referred to as continuous, although they virtually only define values at the discretization points. If necessary, the intermediate instants are interpolated either piecewise constantly or linearly.

In comparison to the deterministic EULER scheme we would obtain for a vanishing diffusion coefficient $\sigma(\cdot)$, the recursion (6.2) is depending on the random increments ΔB_n of the standard BROWNian motion process $\{B_t\}_{t \in \mathcal{T}}$ included through the ITŌ integral. However, from Definition 4.3 and Corollary 4.1 we know that ΔB_n are independent GAUSSian random variables with

$$\mathbb{E}[\Delta B_n] = 0, \qquad \mathbb{E}[(\Delta B_n)^2] = \Delta_n.$$

Thus, within the numerical integration scheme (6.2) one is dependent on using independent GAUSSian random variables which are obtained, e.g., by pseudo-random number generators, cf. [103, 142, 189]. The generalization to multi-dimensional stochastic process $\{X_t\}_{t \in \mathcal{T}}$ is straightforward.

To classify the integration schemes for solving SDEs we distinguish usually between *strong* and *weak convergence*. Consequently, we also differentiate strong and weak approximation schemes, depending on whether the obtained realizations of the stochastic process or only their probability distributions are required to be of desired quality.

Definition 6.1 (Strong/Weak Convergence of Order p/q)

Let $\mathcal{T} = [t_0, t_f]$ be a given fixed time interval and X_t the exact n_X-dimensional solution to a SDE at time instant $t \in \mathcal{T}$. Y_t^Δ be the approximate solution obtained through a numerical integration scheme with maximum step size $\Delta = \max_n \Delta_n$ for a given partition $t_0 < t_1 < \ldots < t_N = t_f$ of $\mathcal{T}$. Then the numerical scheme is said to converge with strong order p *if, for sufficiently small Δ,*

$$\mathbb{E}\left[\left|Y_{t_f}^\Delta - X_{t_f}\right|\right] \leqslant C\Delta^p \xrightarrow{\Delta \to \infty} 0 \tag{6.3}$$

with constant C independent of Δ, and to converge with weak order q *if*

$$\left|\mathbb{E}\left[\varphi(Y_{t_f}^\Delta)\right] - \mathbb{E}\left[\varphi(X_{t_f})\right]\right| \leqslant D\Delta^q \xrightarrow{\Delta \to \infty} 0 \tag{6.4}$$

for all test functions $\varphi : \mathbb{R}^{n_X} \to \mathbb{R}$ being sufficiently often continuously differentiable, having, together with their partial derivatives, polynomial growth, and with constant D depending only on the function φ and t_f. △

The EULER-MARUYAMA scheme (6.2) has strong order $p = \frac{1}{2}$. Under specific assumptions on the diffusion term, e.g., for σ depending only on time, strong convergence of order $\tilde{p} = 1$ is achieved [141]. If drift and diffusion coefficients are four times continuously differentiable the scheme converges with weak order $q = 1$ [141, 183].

However, for weak convergence to hold it is only necessary to approximate the measure induced by the stochastic process $\{X_t\}_{t \in \mathcal{T}}$, meaning that the increments ΔB_n can be replaced by random variables ΔW_n with merely similar moments. Therefore, in the weak sense the

EULER-MARUYAMA recursion (6.2) can be simplified to

$$Y_{n+1} = Y_n + b(t_n, Y_n)\Delta_n + \sigma(t_n, Y_n)\Delta W_n$$

with ΔW_n being independent, $\mathcal{F}_{t_{n+1}}$-measurable random variables satisfying the moment condition

$$\left| \mathbb{E}\left[\Delta W_n\right] \right| + \left| \mathbb{E}\left[(\Delta W_n)^3\right] \right| + \left| \mathbb{E}\left[(\Delta W_n)^2 - \Delta_n\right] \right| \leqslant C\Delta_n{}^2.$$

E.g., one may choose ΔW_n to take only the values $\pm\sqrt{\Delta_n}$ with probability $\frac{1}{2}$ each.

To obtain higher order schemes more information about the behavior of the BROWNian motion is necessary than the simple approximation by ΔB_n can provide. Hence, stochastic TAYLOR expansions including multiple stochastic integrals need to be applied in order to remain consistent with ITŌ calculus. The sole adaptation of sophisticated deterministic schemes in most cases does not meet this stipulation.

6.1.2 Stochastic TAYLOR Expansions

Again, we consider the SDE (6.1) in integral form over $t \in \mathcal{T} = [t_0, t_f]$ with the drift and diffusion coefficient function b and σ being sufficiently smooth. Applying ITŌ's formula (4.22) to the scalar function $f(t, X_t)$ yields

$$f(t, X_t) = f(t_0, X_{t_0}) + \int_{t_0}^{t} \mathcal{L}^0 f(s, X_s)\,\mathrm{d}s + \int_{t_0}^{t} \mathcal{L}^1 f(s, X_s)\,\mathrm{d}B_s,$$

where we have introduced differential operators $\mathcal{L}^0$ and $\mathcal{L}^1$ defined through

$$\mathcal{L}^0 = \frac{\partial}{\partial t} + b(\cdot)\frac{\partial}{\partial x} + \frac{1}{2}\sigma(\cdot)^2\frac{\partial^2}{\partial x^2}, \qquad \mathcal{L}^1 = \sigma(\cdot)\frac{\partial}{\partial x}. \tag{6.5}$$

Now the idea of a stochastic TAYLOR expansion is to apply ITŌ's formula to the integrand functions, i.e., $f(t, x) = b(t, x)$ and $f(t, x) = \sigma(t, x)$, and inserting the results in the original SDE, giving

$$\begin{aligned}
X_t &= X_{t_0} + \int_{t_0}^{t}\left(b(t_0, X_{t_0}) + \int_{t_0}^{s}\mathcal{L}^0 b(u, X_u)\,\mathrm{d}u + \int_{t_0}^{s}\mathcal{L}^1 b(u, X_u)\,\mathrm{d}B_u\right)\mathrm{d}s \\
&\quad + \int_{t_0}^{t}\left(\sigma(t_0, X_{t_0}) + \int_{t_0}^{s}\mathcal{L}^0 \sigma(u, X_u)\,\mathrm{d}u + \int_{t_0}^{s}\mathcal{L}^1 \sigma(u, X_u)\,\mathrm{d}B_u\right)\mathrm{d}B_s \\
&= X_{t_0} + b(t_0, X_{t_0})(t - t_0) + \sigma(t_0, X_{t_0})(B_t - B_{t_0}) + R_1(t_0, t)
\end{aligned} \tag{6.6}$$

with the remainder term

$$\begin{aligned}
R_1(t_0, t) &= \int_{t_0}^{t}\int_{t_0}^{s}\mathcal{L}^0 b(u, X_u)\,\mathrm{d}u\,\mathrm{d}s + \int_{t_0}^{t}\int_{t_0}^{s}\mathcal{L}^1 b(u, X_u)\,\mathrm{d}B_u\,\mathrm{d}s \\
&\quad + \int_{t_0}^{t}\int_{t_0}^{s}\mathcal{L}^0 \sigma(u, X_u)\,\mathrm{d}u\,\mathrm{d}B_s + \int_{t_0}^{t}\int_{t_0}^{s}\mathcal{L}^1 \sigma(u, X_u)\,\mathrm{d}B_u\,\mathrm{d}B_s.
\end{aligned}$$

If we neglect the remainder $R_1(t_0, t)$ in (6.6) we obtain the previously introduced EULER-MARUYAMA integration scheme. Higher order recursions are deduced by applying ITō's formula successively to the integrand function of the remainder term. As $R_1(t_0, t)$ admits already four possible starting points, the number of integration schemes obtainable by that approach is enormous. A very prominent choice is using the integrand $\mathcal{L}^1\sigma(\cdot)$ of the double ITō integral, resulting in the expansion

$$X_t = X_{t_0} + b(t_0, X_{t_0})(t - t_0) + \sigma(t_0, X_{t_0})(B_t - B_{t_0})$$
$$+ \mathcal{L}^1\sigma(t_0, X_{t_0})\int_{t_0}^t \int_{t_0}^s dB_u\, dB_s + R_2(t_0, t) \tag{6.7}$$

with

$$R_2(t_0, t) = \int_{t_0}^t \int_{t_0}^s \mathcal{L}^0 b(u, X_u)\, du\, ds + \int_{t_0}^t \int_{t_0}^s \mathcal{L}^1 b(u, X_u)\, dB_u\, ds$$
$$+ \int_{t_0}^t \int_{t_0}^s \mathcal{L}^0\sigma(u, X_u)\, du\, dB_s + \int_{t_0}^t \int_{t_0}^s \int_{t_0}^u \mathcal{L}^0\mathcal{L}^1\sigma(v, X_v)\, dv\, dB_u\, dB_s$$
$$+ \int_{t_0}^t \int_{t_0}^s \int_{t_0}^u \mathcal{L}^1\mathcal{L}^1\sigma(v, X_v)\, dB_v\, dB_u\, dB_s.$$

This results in the MILSTEIN *scheme*, having both strong and weak convergence orders $p = q = 1$. I.e., with the discretization $t_0 < t_1 < \ldots t_N = t_\mathrm{f}$ of $\mathcal{T}$ we get the approximating process $\{Y_t\}_{t \in \mathcal{T}}$ following the MILSTEIN recursion

$$Y_{n+1} = Y_n + b(t_n, Y_n)\Delta_n + \sigma(t_n, X_n)\Delta B_n + \frac{1}{2}\sigma(t_n, Y_n)\frac{\partial\sigma}{\partial x}(t_n, Y_n)\big((\Delta B_n)^2 - \Delta_n\big) \tag{6.8}$$

for all $n = 0, \ldots, N - 1$ and $Y_0 = X_{t_0}$, cf. [126].

Remark 6.1

When using strong or weak numerical integration schemes for SDEs in applications, it is often disadvantageous to have to evaluate the derivatives of the drift and diffusion coefficients, especially as their orders grow depending on the order of the scheme. Therefore, *explicit approximation recursions* exist, related to deterministic RUNGE-KUTTA schemes but particularly regarding the specific properties of ITō stochastic calculus.

Moreover, to ensure numerical stability there are *implicit* stochastic integration schemes as well, tackling stiff SDEs.

An extensive description of explicit and implicit strong and weak methods together with detailed examples can be found in, e.g., [141, 142, 183].

Remark 6.2

The proofs of convergence orders for the different stochastic integration schemes assume the coefficients within the TAYLOR approximations to be uniformly bounded on the appropriate domains, cf. [141, 183], which is in fact needed for the partial derivatives of the coefficient functions $b(\cdot)$ and $\sigma(\cdot)$. However, in many applications those assumptions cannot be satisfied. E.g., the SDE

$$dX_t = -X_t{}^3\, dt + dB_t$$

has a globally pathwise asymptotically stable stochastic stationary solution [126]. On $\mathcal{T} = [0,1]$ the solution for initial value $X_0 = 0$ has finite first moment $\mathbb{E}[|X_1|] < \infty$. Nevertheless, the EULER-MARUYAMA approximation does neither converge strongly nor weakly as

$$\lim_{N \to \infty} \mathbb{E}[|Y_N - X_1|] = \infty,$$

cf. [119].

6.2 The WIENER Chaos Approach for Solving Stochastic Differential Equations

As we have seen in the previous section, there is a large variety of integration schemes available to solve SDEs numerically. Still, all of these ideas depend on random numbers in each time step, which in return have to be provided by pseudo-random number generators.

In the following Chapter 7 we want to consider SDEs in the context of optimal control problems. In particular, we want to make use of the direct multiple shooting approach introduced in Section 1.3, but if the considered dynamic process is given by a SDE. Within that framework the ideas presented above to integrate SDEs are not applicable as they always derive pathwise solutions to the equations.

6.2.1 The Propagator System

To that end we present an entirely different methodology to solve SDEs that is founded on the WIENER chaos expansion. Let us start again with a one-dimensional stochastic process $\{X_t\}_{t \in \mathcal{T}}$ defined over the time horizon $\mathcal{T} = [t_0, t_f]$ by the SDE

$$\mathrm{d}X_t = b(t, X_t)\,\mathrm{d}t + \sigma(t, X_t)\,\mathrm{d}B_t, \qquad X_{t_0} = x_0, \tag{6.9}$$

or, conveniently, written in its integral form

$$X_t = x_0 + \int_{t_0}^t b(s, X_s)\,\mathrm{d}s + \int_{t_0}^t \sigma(s, X_s)\,\mathrm{d}B_s. \tag{6.10}$$

The idea behind the following theorem is motivated by the *intrusive* Polynomial Chaos (PC) approach [16, 110], adapted to the field of SDEs [115, 116]. While, e.g., [121, 241] analyze the original WIENER chaos expansion (5.48) based on multiple stochastic integrals in the context of SDEs, we make use of the equivalent expansion (5.30) from Theorem 5.5 determined by HERMITE polynomials. This expansion is valid if the considered SDE (6.10) has a square integrable solution over $\mathcal{T}$.

Remark 6.3
We focus on the one-dimensional case, the generalization to multi-dimensional processes $\{\boldsymbol{X}_t\}_{t \in \mathcal{T}}$ and $\{\boldsymbol{B}_t\}_{t \in \mathcal{T}}$ follows straightforwardly, only the notation getting more cumbersome.

Theorem 6.1
Let $\{X_t\}_{t \in \mathcal{T}}$ be given through the SDE (6.10) and assume that $X \in L^2(\mathcal{T} \times \Omega)$. Then X_t can be

written in its WIENER *chaos expansion*

$$X_t = \sum_{\boldsymbol{\alpha} \in \mathcal{I}} x_{\boldsymbol{\alpha}}(t) \Psi^{\boldsymbol{\alpha}}(\boldsymbol{\eta})$$

with basis polynomials $\Psi^{\boldsymbol{\alpha}}(\boldsymbol{\eta})$ *as defined in (5.22), including the basis functions* $\{m_i(\cdot)\}_{i \in \mathbb{N}}$ *of the underlying* HILBERT *space* $L^2(\mathcal{T})$. *The deterministic coefficients functions* $x_{\boldsymbol{\alpha}}(t)$ *are determined by the following* propagator *on* $\mathcal{T}$:

$$\dot{x}_{\boldsymbol{\alpha}}(t) = b_{\boldsymbol{\alpha}}(t, X_t) + \sum_{j=1}^{\infty} \sqrt{\alpha_j}\, m_j(t)\, \sigma_{\boldsymbol{\alpha}^-(j)}(t, X_t), \tag{6.11a}$$

$$x_{\boldsymbol{\alpha}}(0) = \mathbb{1}_{\{\boldsymbol{\alpha}=\boldsymbol{0}\}} \cdot x_0. \tag{6.11b}$$

Within this system of ODEs, $b_{\boldsymbol{\alpha}}(\cdot)$ *and* $\sigma_{\boldsymbol{\alpha}}(\cdot)$ *denote again the* $\boldsymbol{\alpha}$-*coefficients of the chaos expansions of the functions* $b(\cdot)$ *and* $\sigma(\cdot)$ *(depending on* t *and* X_t*) and* $\boldsymbol{\alpha}^-(\boldsymbol{j})$ *the diminished multi-index as defined in (5.43).* △

Proof Inserting the chaos expansion of the process $\{X_t\}_{t \in \mathcal{T}}$ into (6.10), multiplying with the basis polynomial $\Psi^{\boldsymbol{\beta}}(\boldsymbol{\eta})$, $\boldsymbol{\beta} \in \mathcal{I}$, and calculating expectations yields for all $\boldsymbol{\beta} \in \mathcal{I}$ and $t \in \mathcal{T}$

$$x_{\boldsymbol{\beta}}(t) = x_0 \cdot \mathbb{1}_{\{\boldsymbol{\beta}=\boldsymbol{0}\}} + \int_0^t \mathbb{E}\left[b(s, X_s)\Psi^{\boldsymbol{\beta}}(\boldsymbol{\eta})\right] ds + \mathbb{E}\left[\Psi^{\boldsymbol{\beta}}(\boldsymbol{\eta}) \cdot \int_0^t \sigma(s, X_s)\, dB_s\right].$$

While the first appearing integral is a standard deterministic one and the expectation forming the integrand can be represented by the corresponding coefficient function of the expansion of $b(t, X_t)$, the second integral has to be treated with the integration by parts formula (5.47). This yields

$$
\begin{aligned}
x_{\boldsymbol{\beta}}(t) &= x_0 \cdot \mathbb{1}_{\{\boldsymbol{\beta}=\boldsymbol{0}\}} + \int_0^t b_{\boldsymbol{\beta}}(s, X_s)\, ds + \mathbb{E}\left[\int_0^t D_s \Psi^{\boldsymbol{\beta}}(\boldsymbol{\eta})\, \sigma(s, X_s)\, ds\right] \\
&= x_0 \cdot \mathbb{1}_{\{\boldsymbol{\beta}=\boldsymbol{0}\}} + \int_0^t b_{\boldsymbol{\beta}}(s, X_s)\, ds \\
&\quad + \sum_{j=1}^{\infty} \int_0^t \sqrt{\beta_j}\, m_j(s) \mathbb{E}\left[\sigma(s, X_s)\Psi^{\boldsymbol{\beta}^-(j)}(\boldsymbol{\eta})\right] ds \\
&= x_0 \cdot \mathbb{1}_{\{\boldsymbol{\beta}=\boldsymbol{0}\}} + \int_0^t b_{\boldsymbol{\beta}}(s, X_s)\, ds + \sum_{j=1}^{\infty} \int_0^t \sqrt{\beta_j}\, m_j(s)\, \sigma_{\boldsymbol{\beta}^-(j)}(s, X_s)\, ds. \tag{6.12}
\end{aligned}
$$

As for all $\boldsymbol{\beta} \in \mathcal{I}$ there are only a finite number of non-zero components β_i, $i \in \mathbb{N}$, compare (5.21), the formally infinite sum on the right-hand side of (6.12) is in fact finite. Hence, the assertion follows after differentiating with respect to t. □

Remark 6.4

Keeping in mind the definition of the random variables η_i (5.23) depending on the basis $\{m_i(\cdot)\}_{i \in \mathbb{N}}$ of $L^2(\mathcal{T})$ and their significance in constructing the BROWNian motion (5.24), we see that all information about the behavior of the stochastic process $\{X_t\}_{t \in \mathcal{T}}$ is implicitly captured within the *deterministic* ODE system (6.11a).

In the context of generalized solutions of *Stochastic Partial Differential Equations (SPDEs)* driven by GAUSSian white noise, a similar propagator has been derived and initially used as a numerical tool in nonlinear filtering problems, later on as a general modeling and simulation methodology for elliptic SPDEs, cf. [169, 170, 172, 182, 245]. Furthermore, in [113, 164, 165, 166] a systematic approach to generalized processes and certain classes of SDEs based on white noise in combination with MALLIAVIN calculus is presented.

One major advantage of this approach of solving SDEs is that the expectation of the desired solution process, $\mathbb{E}[X_t]$, is directly given by the zero-order coefficient $x_{\{\boldsymbol{\alpha}=0\}}(t)$. Hence, it need not be calculated by, e.g., *Monte Carlo* methods, where a huge amount of sample paths (computed by a standard stochastic integration recursion as presented in the previous section) is necessary. Here, if one is interested in the behavior of sample paths, these can be determined by using realizations of the random vector $\boldsymbol{\eta}$ *after* the system has been solved. Similar to the expectation, the variance of the process and all higher moments are completely specified by the deterministic coefficient functions of the chaos expansion, compare (5.31).

6.2.2 Truncation of the Propagator

In order to use the propagator numerically, we certainly have to truncate the chaos expansion of $\{X_t\}_{t \in \mathcal{T}}$ and, therefore, the system (6.11a) of ODEs. There are basically two major aspects that compose this truncation.

Truncating the Order of the Chaos Expansion

The first form of truncation arises as we limit the maximum order p of the chaos expansion. When considering the original WIENER expansion (5.48) consisting of multiple ITŌ stochastic integrals, this is equivalent to letting the final summand be $I_p(\cdot)$, i.e., using only the first $p+1$ chaos spaces $\mathcal{H}_0, \ldots, \mathcal{H}_p$ to make the expansion.

In terms of HERMITE polynomials this form of truncation restricts the maximum order of the basis polynomials $\Psi^{\boldsymbol{\alpha}}(\cdot)$ due to Theorem 5.13. We obtain the truncated index set $\mathcal{I}_p$ defined as

$$\mathcal{I}_p \stackrel{\text{def}}{=} \left\{ \boldsymbol{\alpha} \in \mathcal{I} \, \middle| \, |\boldsymbol{\alpha}| = \sum_{i=1}^{\infty} \alpha_i \leqslant p \right\}. \tag{6.13}$$

Truncating the Length of the Multi-Index

The second type of truncation focusses on the maximum length k of the multi-indices $\boldsymbol{\alpha} \in \mathcal{I}$. It originates from the number k of basis functions of the underlying HILBERT space $L^2(\mathcal{T})$ that we use to construct the random variables η_i, $i = 1, \ldots, k$, incorporated in the basis polynomials $\Psi^{\boldsymbol{\alpha}}(\boldsymbol{\eta})$. Hence, in the formalism of the HERMITE polynomial chaos expansion this results in the truncated index set $\mathcal{I}_{p,k}$ (if we start directly from the index set $\mathcal{I}_p$ with truncated order):

$$\mathcal{I}_{p,k} \stackrel{\text{def}}{=} \left\{ \boldsymbol{\alpha} = (\alpha_i)_{i=1,\ldots,k} \, \middle| \, |\boldsymbol{\alpha}| \leqslant p \right\}. \tag{6.14}$$

Remark 6.5

If we think again of the KARHUNEN-LOÈVE Expansion (KLE) of the BROWNian motion (4.8) or, equivalently, the FOURIER-HERMITE expansion (5.24), only the truncation due to the number
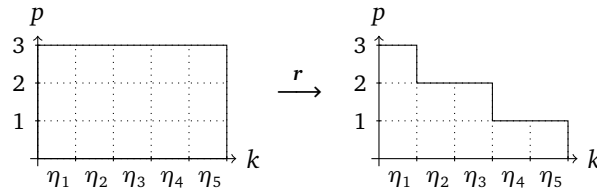
Figure 6.1: Schematic example of a sparse index $r = (3, 2, 2, 1, 1)$ in comparison with the full index set $\mathcal{I}_{p,k}$ for $k = 5$ random variables and maximum order $p = 3$ of the chaos basis polynomials $\Psi^{\alpha}(\eta)$.

k of entering random variables is important. Truncating the order of the expansion becomes unnecessary as the coefficients corresponding to all basis polynomials $\Psi^{\beta}(\cdot)$ with $|\beta| \geqslant 2$ vanish.

Sparse Truncation

The importance of the coefficient functions $x_{\alpha}(\cdot)$ decays depending on the order p of the basis polynomials $\Psi^{\alpha}(\cdot)$ and the decaying rate of the GAUSSian expansion, i.e., the index of the random variables η_i, $i \in \{1, \ldots, k\}$, used for the construction of $\Psi^{\alpha}(\eta)$, compare, e.g., (4.9). Especially if we consider coefficients with index $\bar{\alpha}$, where $|\bar{\alpha}|$ is large and $\bar{\alpha}$ consists of a combination of random variables η_j with large indices j, the information gained is very low, cf. [172].

Hence, we define a *sparse index* for truncating the index set $\mathcal{I}$ (compare [97, 172]).

Definition 6.2 (Sparse Truncation)

Let p be the maximum order of the index $\alpha \in \mathcal{I}_{p,k}$. Then the sparse index $r = (r_1, \ldots, r_k)$ satisfies $p = r_1 \geqslant r_2 \geqslant \cdots \geqslant r_k$ and we define the sparse index set

$$\mathcal{I}_{p,k}^r = \left\{ \alpha \in \mathcal{I}_{p,k} \,\middle|\, \alpha_i \leqslant r_i \,\forall i \leqslant k \right\}. \tag{6.15}$$

$\triangle$

Example 6.1

Let $k = 5$ and $p = 3$. Then a possible choice of the sparse index is $r = (3, 2, 2, 1, 1)$. Figure 6.1 visualizes the sparse index set $\mathcal{I}_{k,p}^r$. For constructing the first order polynomials all five random variables (and the corresponding first order HERMITE polynomials) can be used. The second order polynomials are comprised by all possible combinations of first order HERMITE polynomials depending on $\eta_1, \ldots, \eta_5$ and the second order HERMITE polynomials of η_1, η_2, η_3. Analogously, the third order polynomials are constructed.

Remark 6.6

By using this sparse index set $\mathcal{I}_{k,p}^r$ the number of coefficient functions $x_{\alpha}(\cdot)$ appearing within the propagator system (6.11a) can be reduced drastically without impairing the solution much. In the above Example 6.1 the full index set $\mathcal{I}_{k,p}$ consists of $\frac{(k+p)!}{k!p!} = 56$ terms [16, 172], whereas the sparse truncated index set includes 42 terms.

Adaptive Truncation

An even better reduction in the number of coefficients included in the propagator system of ODEs can be achieved if we use an *adaptive* index, i.e., a series of sparse indices $\left(r^j \right)_{j=0,\ldots,p}$ that

depend on the actual order of the polynomials $\Psi^{\boldsymbol{\alpha}}(\cdot)$ with $j = |\boldsymbol{\alpha}|$, cf. [172]. By that approach one is able to exclude crossing products of random variables η_i from the construction of higher order basis polynomials $\Psi^{\boldsymbol{\alpha}}(\boldsymbol{\eta})$ that add only negligible information to the system.

Definition 6.3 (Adaptive Truncation)
Let p be the maximum order of the index $\boldsymbol{\alpha} \in \mathcal{I}_{p,k}$. Then the adaptive index $(\boldsymbol{r}) = \left(\boldsymbol{r}^j\right)_{j \leqslant p}$ *is a series of sparse indices $\boldsymbol{r}^j = \left(r_1^j, \ldots, r_k^j\right)$ satisfying $j = r_1^j \geqslant r_2^j \geqslant \cdots \geqslant r_k^j$ for all $j = |\boldsymbol{\alpha}| \leqslant p$ and we define the* adaptive index set

$$\mathcal{I}_{p,k}^{(r)} = \left\{ \boldsymbol{\alpha} \in \mathcal{I}_{p,k} \,\middle|\, \alpha_i \leqslant r_i^j \; \forall i \leqslant k, \; \forall j \leqslant p \right\}. \tag{6.16}$$

$\triangle$

Example 6.2
If we consider again the setting of Example 6.1 with $k = 5$ and $p = 3$, then one possible choice of an adaptive index is given by $\boldsymbol{r}^1 = (1, 1, 1, 1, 1)$, $\boldsymbol{r}^2 = (2, 2, 2, 1, 0)$, $\boldsymbol{r}^3 = (3, 2, 0, 0, 0)$. That means, in constructing basis polynomials of order $|\boldsymbol{\alpha}| = 3$ we can use all combinations of HERMITE polynomials depending on the first two random variables η_1 and η_2 up to orders 3 and 2, respectively. Thus, these are $\sqrt{6}H_3(\eta_1)$, $\sqrt{2}H_2(\eta_1)H_1(\eta_2)$, and $\sqrt{2}H_1(\eta_1)H_2(\eta_2)$, compare (5.22) and [172].

Table 6.1 lists the sparse and adaptive indices that are used for the numerical examples in Section 6.2.3 and Chapter 8 together with their number of coefficient functions.

However, the usual idea of adaptive truncation ideas comes from non-intrusive polynomial chaos approaches, often used for differential equations with a (generally low) number of random parameters included. In that framework, sparse-grid ideas based on the SMOLYAK scheme [99, 135, 229] have proven to be very effective. Additionally, methods built on the decomposition of the underlying random space are applied [243]. In the intrusive-type environment that the propagator represents, they cannot be deployed directly. Alternative schemes can be developed from the *sparsity-of-effects* principle and the *least angle regression* or *compressed sensing* [44, 179], which provides a more general truncation than the heuristic approach introduced above.

6.2.3 Error Analysis of the Propagator

In general, the derivation of an adequate error estimate for the propagator system (6.11a) is intricate. For analyzing polynomial chaos based solutions to differential equations that include random parameters, e.g., [54] gives an a posteriori error analysis. In [52] explicit bounds are given for simulating Backward Stochastic Differential Equations (BSDEs) through a combination of the WIENER chaos expansion and PICARD iterations. The error analysis provided there mainly builds upon the special choice of the HAAR wavelets (5.28) as basis of the underlying HILBERT space $L^2(\mathcal{T})$, leading to an error estimator that has the order $\mathcal{O}\left(k^{-1}\right)$ for the truncation of the number k of basis elements of $L^2(\mathcal{T})$.

In [172] there is an analysis of the errors made through truncating the propagator provided for several examples of solving SPDEs via a WIENER chaos approach based on HERMITE polynomials. Therein, it is made use of semi-analytic solutions to the considered equations in order to derive error estimates for the full truncated index set as well as the consequences for the sparse and adaptive ones.

Table 6.1: List of (sp)arse and (ad)aptive indices used for the numerical examples together with their number of resulting coefficient functions. The reference numbers coincide with those in Tables 6.2, 8.1, 8.3, and 8.4.

symbol	p	k	index $\boldsymbol{r}/(\boldsymbol{r})$	# coefficients
sp^1	2	10	$\boldsymbol{r} = (2,2,2,2,2,1,1,1,1,1)$	61
sp^2	2	20	$\boldsymbol{r} = (2,2,2,2,2,1,\ldots,1)$	216
sp^3	3	5	$\boldsymbol{r} = (3,3,2,1,1)$	42
ad^1	2	20	$\boldsymbol{r}^1 = (1,\ldots,1)$	71
			$\boldsymbol{r}^2 = (2,2,2,2,2,1,1,1,1,1,0,\ldots,0)$	
ad^2	2	40	$\boldsymbol{r}^1 = (1,\ldots,1)$	91
			$\boldsymbol{r}^2 = (2,2,2,2,2,1,1,1,1,1,0,\ldots,0)$	
ad^3	2	100	$\boldsymbol{r}^1 = (1,\ldots,1)$	151
			$\boldsymbol{r}^2 = (2,2,2,2,2,1,1,1,1,1,0,\ldots,0)$	
ad^4	3	10	$\boldsymbol{r}^1 = (1,\ldots,1)$	42
			$\boldsymbol{r}^2 = (2,2,2,2,2,2,0,0,0,0)$	
			$\boldsymbol{r}^3 = (3,3,3,0,\ldots,0)$	
ad^5	3	20	$\boldsymbol{r}^1 = (1,\ldots,1)$	125
			$\boldsymbol{r}^2 = (2,2,2,2,2,2,1,1,1,1,0,\ldots,0)$	
			$\boldsymbol{r}^3 = (3,3,3,2,2,2,0,\ldots,0)$	
ad^6	3	40	$\boldsymbol{r}^1 = (1,\ldots,1)$	145
			$\boldsymbol{r}^2 = (2,2,2,2,2,2,1,1,1,1,0,\ldots,0)$	
			$\boldsymbol{r}^3 = (3,3,3,2,2,2,0,\ldots,0)$	
ad^7	4	10	$\boldsymbol{r}^1 = (1,\ldots,1)$	57
			$\boldsymbol{r}^2 = (2,2,2,2,2,2,0,\ldots,0)$	
			$\boldsymbol{r}^3 = (3,3,3,3,0,\ldots,0)$	
			$\boldsymbol{r}^4 = (4,4,0,\ldots,0)$	
ad^8	4	20	$\boldsymbol{r}^1 = (1,\ldots,1)$	131
			$\boldsymbol{r}^2 = (2,2,2,2,2,2,1,1,1,1,0,\ldots,0)$	
			$\boldsymbol{r}^3 = (3,3,3,3,2,2,0,\ldots,0)$	
			$\boldsymbol{r}^4 = (4,4,0,\ldots,0)$	

[31, 32, 58] develop a priori error estimates for truncated WIENER chaos expansion for elliptic WICK SPDEs. In [18, 98, 245] this is done without employing the specific WICK framework. [170] present error estimates in the context of nonlinear filtering, where both the signal and the observation processes are diffusions and the optimal filter is obtained by applying the WIENER chaos approach to the unnormalized filtering density which is the solution to the (partial differential) ZAKAI equation [253]. The corresponding estimates are deduced by exploiting the semigroup generated by the differential operator of the ZAKAI equation and the choice (5.27) of basis functions of $L^2(\mathcal{T})$, giving an error of order $\mathcal{O}\big(((p+1)!)^{-1}\big) + \mathcal{O}\big(k^{-1}\big)$ depending on the order p of the chaos expansion and the number k of used basis functions. Before deriving a generic error estimator for the truncated WIENER chaos solution of a SDE 6.9 obtained through the propagator system (6.11a), let us consider a special example—the linear SDE generating the geometric BROWNian motion—and calculating the error made by solving this equation via the propagator approach.

Error Estimator for the Geometric BROWNian Motion

Let the stochastic process $\{X_t\}_{t\in\mathcal{T}}$ be determined through the SDE

$$dX_t = \mu X_t\, dt + \sigma X_t\, dB_t, \qquad X_0 = x_0 \tag{6.17}$$

on the time horizon $\mathcal{T} = [0,1]$, where μ and σ are real, positive constants and $x_0 \in \mathbb{R}$. The solution process is analytically given by

$$X_t = x_0 \exp\left(\left(\mu - \frac{\sigma^2}{2}\right)t + \sigma B_t\right). \tag{6.18}$$

Now let X_t be expressed in its WIENER chaos decomposition

$$X_t = \sum_{\boldsymbol{\alpha}\in\mathcal{I}} x_{\boldsymbol{\alpha}}(t)\Psi^{\boldsymbol{\alpha}}(\boldsymbol{\eta}),$$

with $\mathcal{I}$ being the complete multi-index set as in (5.21) and $\Psi^{\boldsymbol{\alpha}}(\boldsymbol{\eta})$ the multi-variate orthonormal HERMITE polynomial (5.22). In the following we choose the basis functions of the underlying HILBERT space $L^2([0,1])$ again as

$$m_i(t) = \sqrt{2}\cos\left(\left(i - \frac{1}{2}\right)\pi t\right), \quad t \in [0,1]. \tag{6.19}$$

Then by Theorem 6.1 the deterministic coefficient functions $x_{\boldsymbol{\alpha}}(\cdot)$ of the WIENER chaos expansion of the geometric BROWNian motion that are defined in the FOURIER-like fashion as $x_{\boldsymbol{\alpha}}(t) = \mathbb{E}\left[X_t \Psi^{\boldsymbol{\alpha}}(\boldsymbol{\eta})\right]$ satisfy the following propagator equations:

$$\dot{x}_{\boldsymbol{\alpha}}(t) = \mu x_{\boldsymbol{\alpha}}(t) + \sigma \sum_{j=1}^{\infty} \sqrt{\alpha_j}\, m_j(t) x_{\boldsymbol{\alpha}^-(j)}(t) \tag{6.20a}$$

$$x_{\boldsymbol{\alpha}}(0) = x_0 \cdot \mathbb{1}_{\{\boldsymbol{\alpha}=\mathbf{0}\}}, \tag{6.20b}$$

where $\boldsymbol{\alpha}^-(j)$ denotes again the diminished multi-index defined in (5.43).

To give an impression of the structure of the ODE system (6.20), let us consider the resulting

equations when $|\alpha| = 0, 1, 2$:

$|\alpha| = 0$: This condition is only satisfied if $\alpha \equiv 0$. Hence, the differential equation determining the zero-order coefficient reduces to

$$\dot{x}_0(t) = \mu x_0(t),$$
$$x_0(0) = x_0.$$

$|\alpha| = 1$: In this case α takes the form $\alpha = e_i$ for $i \geqslant 1$, where e_i denotes the i-th (infinite dimensional) canonical unit vector. Thus, we obtain for all $i \geqslant 1$

$$\dot{x}_{e_i}(t) = \mu x_{e_i}(t) + \sigma m_i(t) x_0(t),$$
$$x_{e_i}(0) = 0.$$

$|\alpha| = 2$: Here, α can be either of the form $\alpha = 2e_i$ for $i \geqslant 1$ or $\alpha = e_i + e_j$ for $i \neq j$. In the first case we deduce for $i \geqslant 1$

$$\dot{x}_{2e_i}(t) = \mu x_{2e_i}(t) + \sqrt{2}\sigma m_i(t) x_{e_i}(t),$$
$$x_{2e_i}(0) = 0,$$

and in the second case for $i \neq j$

$$\dot{x}_{e_i+e_j}(t) = \mu x_{e_i+e_j}(t) + \sigma m_i(t) x_{e_j}(t) + \sigma m_j(t) x_{e_i}(t),$$
$$x_{e_i+e_j}(0) = 0.$$

Remark 6.7

From equation (6.20) we see that for a linear SDE the propagator equations of order $|\alpha| = p$ depend only on the coefficient $x_\alpha(t)$ itself and on coefficients of order $p-1$. Hence, this system can be solved recursively.

Remembering Example 5.7 we reason the following result.

Theorem 6.2

For a general $\alpha \in \mathcal{I}$ of order $|\alpha| = p$ the solution of the corresponding propagator equation (6.20) is given by

$$x_\alpha(t) = \frac{\sigma^p}{\sqrt{\alpha!}} x_0 \, e^{\mu t} \prod_{i=1}^{\infty} (M_i(t))^{\alpha_i}, \tag{6.21}$$

where $M_i(t) = \int_0^t m_i(s)\,ds$. △

Proof We show the assertion by differentiating the chaos coefficients (6.21) with respect to t,

i.e.,

$$
\begin{aligned}
\dot{x}_{\boldsymbol{\alpha}}(t) &= \mu x_{\boldsymbol{\alpha}}(t) + \frac{\sigma^p}{\sqrt{\boldsymbol{\alpha}!}} x_0 \, \mathrm{e}^{\mu t} \frac{\mathrm{d}}{\mathrm{d}t}\left(\prod_{i=1}^{\infty}(M_i(t))^{\alpha_i}\right) \\
&= \mu x_{\boldsymbol{\alpha}}(t) + \frac{\sigma^p}{\sqrt{\boldsymbol{\alpha}!}} x_0 \, \mathrm{e}^{\mu t} \sum_{j=1}^{\infty} \prod_{\substack{i=1 \\ i \neq j}}^{\infty}(M_i(t))^{\alpha_i} \cdot \alpha_j \left(M_j(t)\right)^{\alpha_j - 1} m_j(t) \\
&= \mu x_{\boldsymbol{\alpha}}(t) + \sigma \sum_{j=1}^{\infty} \sqrt{\alpha_j}\, m_j(t) \frac{\sigma^{p-1}}{\sqrt{\boldsymbol{\alpha}^-(j)!}} x_0 \, \mathrm{e}^{\mu t} \prod_{i=1}^{\infty}(M_i(t))^{\alpha_i} \cdot \left(M_j(t)\right)^{\alpha_j - 1} \\
&= \mu x_{\boldsymbol{\alpha}}(t) + \sigma \sum_{j=1}^{\infty} \sqrt{\alpha_j}\, m_j(t)\, x_{\boldsymbol{\alpha}^-(j)}(t).
\end{aligned}
$$

Additionally, for the initial values of the propagator ODEs we obtain

$$
x_{\boldsymbol{\alpha}}(0) = \frac{\sigma^p}{\sqrt{\boldsymbol{\alpha}!}} x_0 \, \mathrm{e}^{\mu \cdot 0} \prod_{i=1}^{\infty}(M_i(0))^{\alpha_i} = \frac{\sigma^p}{\sqrt{\boldsymbol{\alpha}!}} x_0 \cdot \mathbb{1}_{\{\boldsymbol{\alpha}=\mathbf{0}\}} = \begin{cases} x_0, & \boldsymbol{\alpha} = \mathbf{0}, \\ 0, & \text{otherwise,} \end{cases}
$$

where we used the convention $0^0 = 1$ again. $\qquad\square$

With this theorem at hand, we consider now the truncated version of the propagator (6.20). Therefore, let the truncated index set $\mathcal{I}_{p,k}$ be given as in (6.14). Furthermore, let the *actual length* of the multi-index $\boldsymbol{\alpha}$, denoted as $d(\boldsymbol{\alpha})$, identify the largest index i at which $\boldsymbol{\alpha}$ has a non-zero entry. Hence, for all $\boldsymbol{\alpha} \in \mathcal{I}_{p,k}$ we have $d(\boldsymbol{\alpha}) \leqslant k$.

Then we are interested in estimating the error one makes when truncating the propagator, depending on the choices of p and k. Consequently, $X_t^{p,k}$ denotes the WIENER chaos decomposition

$$
X_t^{p,k} = \sum_{\boldsymbol{\alpha} \in \mathcal{I}_{p,k}} x_{\boldsymbol{\alpha}}(t) \Psi^{\boldsymbol{\alpha}}(\boldsymbol{\eta}) \tag{6.22}
$$

for the truncated index set.

To obtain an impression on the behavior of the error, Figure 6.2 depicts the development of the variance's absolute error $\left|\mathbb{V}[X_t] - \mathbb{V}\left[X_t^{p,k}\right]\right|$ depending on the choices of p, k, and, as appropriate, the type of sparse or adaptive index set used for the truncation. Table 6.2 lists the absolute errors $\left|\mathbb{V}[X_1] - \mathbb{V}\left[X_1^{p,k}\right]\right|$ at the final time of consideration $t_\mathrm{f} = 1$ and the computation times which were necessary to solve the resulting ODE system. Note here, that for the geometric BROWNian motion the propagator method always yield the exact expectation $\mathbb{E}[X_t] = x_0 \, \mathrm{e}^{\mu t}$.

Nevertheless, in Figure 6.2 we notice that the absolute error of the variance erratically increases at the end of the time interval $\mathcal{T}$, particularly for the chaos expansion orders $p = 3$ and $p = 4$. One reason for this behavior is the use of an adaptive index $\mathcal{I}_{p,k}^{(r)}$. The principal cause, however, is the combination of using a truncated number k of $L^2(\mathcal{T})$ basis functions and the same integration and interpolation interval $\mathcal{T}$. Both coincide as those cosine basis functions of the underlying HILBERT space are defined on $\mathcal{T}$. As the resulting coefficients $x_{\boldsymbol{\alpha}}(\cdot)$ of higher orders
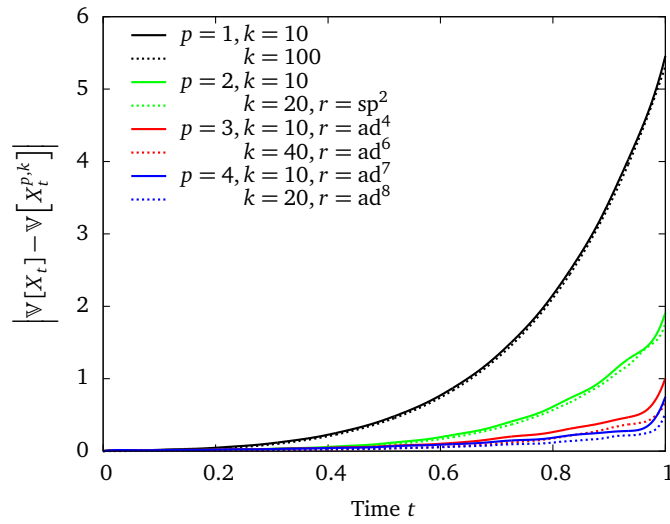
Figure 6.2: Development of the absolute errors between the variance of the exact solution to the SDE (6.17) determining the geometric BROWNian motion and the solution calculated by solving the ODE system (6.20) of the propagator method. The figure depicts the errors over the time horizon $\mathcal{T} = [0,1]$ for different magnitudes and/or types of truncation. The sparse and adaptive indices used correspond to those of Table 6.1.

We detect that the error decreases both with increasing the number k of basis functions $m_i(\cdot)$, $i = 1, \ldots, k$, of the underlying HILBERT space $L^2(\mathcal{T})$ and the maximum order p of the chaos expansion used to generate the truncated propagator system. Therein, the influence of the order p is more relevant.

Note that the error increases erratically at the end of the time interval $\mathcal{T}$, particularly for chaos expansion orders $p = 3$ and $p = 4$. To a minor extent this is caused by the missing coefficients omitted by using an adaptive index set. The major reason for this phenomenon is the combination of truncating the number of $L^2(\mathcal{T})$ basis functions and using the same integration and interpolation horizon $\mathcal{T}$. Due to the definition of $m_i(\cdot)$ the absence of p-th order coefficients depending on basis functions with index $i > k$ is most obvious at the end of the interval.

Table 6.2: Absolute errors between the variance of the exact geometric BROWNian motion process and the solution of the propagator method evaluated at the final time $t_f = 1$ of the considered time horizon for different magnitudes and/or types of truncation. The abbreviations of the sparse and adaptive indices correspond to those of Table 6.1.
We notice that the error decreases with increasing number k of included basis functions of the underlying HILBERT space $L^2(\mathcal{T})$, but more intensely with increased maximum order p of the chaos expansion.

p	k	r	# coefficients	$\left\lvert \mathbb{V}[X_1] - \mathbb{V}[X_1^{p,k}] \right\rvert$	time in s
1	10	-	11	5.4570	0.105
1	20	-	11	5.3823	0.167
1	40	-	11	5.3449	0.918
1	100	-	11	5.3224	11.963
2	10	-	66	1.9106	0.760
2	20	sp^2	216	1.7626	15.070
2	40	ad^2	91	1.7988	3.707
3	10	ad^4	42	1.0069	0.252
3	20	ad^5	125	0.7249	2.829
3	40	ad^6	145	0.6875	7.350
4	10	ad^7	57	0.7502	0.324
4	20	ad^8	131	0.5223	2.918

oscillate to a greater extent, the absence of p-th order coefficients depending on basis functions $m_i(\cdot)$ with index $i > k$ is most obvious at the end of the integration interval, even if the overall error decreases in p.

Theorem 6.3

Suppose we are given the truncated WIENER *chaos expansion* (6.22) *of the geometric* BROWN*ian motion. Then we deduce the mean-square error estimate of the truncation depending on the order p and the number k of basis functions* (6.19) *of $L^2([0,1])$ as*

$$\mathbb{E}\left[\left\lvert X_1 - X_1^{p,k} \right\rvert^2\right] \leqslant 2\,{x_0}^2\,\mathrm{e}^{2\mu}\left(\frac{(\sigma^2)^{p+1}}{(p+1)!}\,\mathrm{e}^{\sigma^2} + \frac{C(p)}{\pi k}\frac{(\sigma^2)^{p+1}-1}{\sigma^2-1}\right) \tag{6.23}$$

with a constant C depending on p. △

Remark 6.8

From Equation (6.23) we directly see that for fixed chaos order p we always obtain a specific error bound, even for $k \to \infty$. This emphasizes the independence of the twofold truncation: While p regulates the quality of the actual chaos expansion, the number k of used basis functions characterizes the approximation within each chaos $\mathcal{H}_\cdot$.

Proof Inserting the infinite and truncated WIENER chaos expansions and using the orthonor-

mality of the basis polynomials $\Psi^{\boldsymbol{\alpha}}(\boldsymbol{\eta})$ yields

$$\mathbb{E}\left[\left|X_1 - X_1^{p,k}\right|^2\right]$$

$$\leqslant 2\,\mathbb{E}\left[\left|X_1 - X_1^p\right|^2\right] + 2\,\mathbb{E}\left[\left|X_1^p - X_1^{p,k}\right|^2\right]$$

$$= 2\,\mathbb{E}\left[\left|\sum_{i=p+1}^{\infty}\sum_{|\boldsymbol{\alpha}|=i} x_{\boldsymbol{\alpha}}(1)\Psi^{\boldsymbol{\alpha}}(\boldsymbol{\eta})\right|^2\right] + 2\,\mathbb{E}\left[\left|\sum_{l=k+1}^{\infty}\sum_{i=0}^{p}\sum_{\substack{|\boldsymbol{\alpha}|=i \\ d(\boldsymbol{\alpha})=l}} x_{\boldsymbol{\alpha}}(1)\Psi^{\boldsymbol{\alpha}}(\boldsymbol{\eta})\right|^2\right]$$

$$= 2\underbrace{\sum_{i=p+1}^{\infty}\sum_{|\boldsymbol{\alpha}|=i} x_{\boldsymbol{\alpha}}{}^2(1)}_{A_1} + 2\underbrace{\sum_{l=k+1}^{\infty}\sum_{i=0}^{p}\sum_{\substack{|\boldsymbol{\alpha}|=i \\ d(\boldsymbol{\alpha})=l}} x_{\boldsymbol{\alpha}}{}^2(1)}_{A_2}. \tag{6.24}$$

To calculate A_1 let us consider the variance of the stochastic process defined by (6.17), i.e.,

$$\mathbb{V}[X_t] = x_0{}^2\,\mathrm{e}^{2\mu t}\left(\mathrm{e}^{\sigma^2 t} - 1\right).$$

Replacing the last factor by its infinite TAYLOR expansion gives

$$\mathbb{V}[X_t] = x_0{}^2\,\mathrm{e}^{2\mu t}\sum_{i=1}^{\infty}\sigma^{2i}\frac{t^i}{i!}.$$

On the other hand, from the WIENER chaos expansion, in particular Equation (5.31), and Theorem 6.2 we know that

$$\mathbb{V}[X_t] = \sum_{|\boldsymbol{\alpha}|\geqslant 1} x_{\boldsymbol{\alpha}}{}^2(t) = \sum_{|\boldsymbol{\alpha}|\geqslant 1} x_0{}^2\,\mathrm{e}^{2\mu t}\frac{\sigma^{2p}}{\boldsymbol{\alpha}!}\prod_{j=1}^{\infty}\left(M_j(t)\right)^{2\alpha_j}$$

$$= \sum_{i=1}^{\infty} x_0{}^2\,\mathrm{e}^{2\mu t}\,\sigma^{2i}\sum_{|\boldsymbol{\alpha}|=i}\prod_{j=1}^{\infty}\frac{\left(M_j(t)\right)^{2\alpha_j}}{\alpha_j!}.$$

By the definition of $M_i(t)$ and Lemma 4.1 we infer that for every $t \in \mathcal{T} = [0,1]$ and $|\boldsymbol{\alpha}| = q$ it holds that

$$\sum_{|\boldsymbol{\alpha}|=q}\prod_{j=1}^{\infty}\frac{\left(M_j{}^2(t)\right)^{\alpha_j}}{\alpha_j!} = \psi(q)t^q$$

with some function $\psi\colon \mathbb{R} \to \mathbb{R}$ depending on the order q of the multi-index $\boldsymbol{\alpha}$. This allows us to compare the coefficients of the two expansions of $\mathbb{V}[X_t]$, resulting in

$$\sum_{|\boldsymbol{\alpha}|=q}\prod_{j=1}^{\infty}\frac{\left(M_j{}^2(t)\right)^{\alpha_j}}{\alpha_j!} = \frac{t^q}{q!}. \tag{6.25}$$

Thus, the error estimate for truncating the order of the multi-index becomes

$$A_1 = 2 \sum_{i=p+1}^{\infty} \sum_{|\boldsymbol{\alpha}|=i} x_0{}^2 \, e^{2\mu} \, \sigma^{2i} \prod_{j=1}^{\infty} \frac{\left(M_j{}^2(1)\right)^{\alpha_j}}{\alpha_j!} = 2 \, x_0{}^2 \, e^{2\mu} \sum_{i=p+1}^{\infty} \sigma^{2i} \frac{1}{i!}$$

$$\leqslant 2 \, x_0{}^2 \, e^{2\mu} \frac{\left(\sigma^2\right)^{p+1}}{(p+1)!} \, e^{\sigma^2}. \tag{6.26}$$

To determine A_2 we first show by induction over p that

$$\sum_{l=k+1}^{\infty} \sum_{\substack{|\boldsymbol{\alpha}|=p \\ d(\boldsymbol{\alpha})=l}} \prod_{j=1}^{l} \frac{\left(M_j{}^2(t)\right)^{\alpha_j}}{\alpha_j!} \leqslant \frac{C(p)}{\pi k} \tag{6.27}$$

with a constant C depending on the order p of the multi-index $\boldsymbol{\alpha}$. For $p = 1$ we get

$$\sum_{l=k+1}^{\infty} \sum_{\substack{|\boldsymbol{\alpha}|=1 \\ d(\boldsymbol{\alpha})=l}} \prod_{j=1}^{l} \frac{\left(M_j{}^2(t)\right)^{\alpha_j}}{\alpha_j!} = \sum_{l=k+1}^{\infty} M_l{}^2(t) = \sum_{l=k+1}^{\infty} \frac{2\sin\left(\left(l-\frac{1}{2}\right)\pi t\right)^2}{\left(l-\frac{1}{2}\right)^2 \pi^2}$$

$$\leqslant \sum_{l=k+1}^{\infty} \frac{2}{\left(l-\frac{1}{2}\right)^2 \pi^2} \leqslant \sum_{l=k}^{\infty} \frac{2}{l^2 \pi^2}$$

$$\leqslant \frac{1}{\pi k},$$

corresponding to the error of truncating the BROWNian motion expansion (4.9). Now let us assume (6.27) is valid for a given p. Then with $\boldsymbol{\alpha} = \tilde{\boldsymbol{\alpha}} + e_l$ we can write

$$\sum_{l=k+1}^{\infty} \sum_{\substack{|\boldsymbol{\alpha}|=p+1 \\ d(\boldsymbol{\alpha})=l}} \prod_{j=1}^{l} \frac{\left(M_j{}^2(t)\right)^{\alpha_j}}{\alpha_j!} = \sum_{l=k+1}^{\infty} \sum_{\substack{|\tilde{\boldsymbol{\alpha}}|=p \\ d(\tilde{\boldsymbol{\alpha}})\leqslant l}} \frac{M_l{}^2(t)}{\tilde{\alpha}_l + 1} \cdot \prod_{j=1}^{l} \frac{\left(M_j{}^2(t)\right)^{\tilde{\alpha}_j}}{\tilde{\alpha}_j!}.$$

As $|\boldsymbol{\alpha}| = p + 1$ it follows that $|\tilde{\boldsymbol{\alpha}}| = p$. However, because $1 \leqslant \alpha_l \leqslant p$ we have to distinguish between $d(\tilde{\boldsymbol{\alpha}}) = l$ and $d(\tilde{\boldsymbol{\alpha}}) < l$. Therefore,

$$\sum_{l=k+1}^{\infty} \sum_{\substack{|\boldsymbol{\alpha}|=p+1 \\ d(\boldsymbol{\alpha})=l}} \prod_{j=1}^{l} \frac{\left(M_j{}^2(t)\right)^{\alpha_j}}{\alpha_j!}$$

$$= \sum_{l=k+1}^{\infty} \sum_{\substack{|\tilde{\boldsymbol{\alpha}}|=p \\ d(\tilde{\boldsymbol{\alpha}})=l}} \frac{M_l{}^2(t)}{\tilde{\alpha}_l + 1} \cdot \prod_{j=1}^{l} \frac{\left(M_j{}^2(t)\right)^{\tilde{\alpha}_j}}{\tilde{\alpha}_j!} + \sum_{l=k+1}^{\infty} \sum_{\substack{|\tilde{\boldsymbol{\alpha}}|=p \\ d(\tilde{\boldsymbol{\alpha}})<l}} M_l{}^2(t) \cdot \prod_{j=1}^{d(\tilde{\boldsymbol{\alpha}})} \frac{\left(M_j{}^2(t)\right)^{\tilde{\alpha}_j}}{\tilde{\alpha}_j!}.$$

Within the first summand we estimate (as then $\tilde{\alpha}_l \geqslant 1$)

$$\frac{M_l{}^2(t)}{\tilde{\alpha}_l + 1} = \frac{2\sin\left(\left(l-\frac{1}{2}\right)\pi t\right)^2}{\left(l-\frac{1}{2}\right)^2 \pi^2 \left(\tilde{\alpha}_l + 1\right)} \leqslant \frac{1}{\left(l-\frac{1}{2}\right)^2 \pi^2} \leqslant \frac{1}{\pi^2 k^2} \quad \forall l \geqslant k+1$$

and within the second summand

$$\sum_{\substack{|\tilde{\boldsymbol{\alpha}}|=p \\ d(\tilde{\boldsymbol{\alpha}})<l}} \prod_{j=1}^{d(\tilde{\boldsymbol{\alpha}})} \frac{\left(M_j{}^2(t)\right)^{\tilde{\alpha}_j}}{\tilde{\alpha}_j!} = \sum_{i=1}^{l-1} \sum_{\substack{|\tilde{\boldsymbol{\alpha}}|=p \\ d(\tilde{\boldsymbol{\alpha}})=i}} \prod_{j=1}^{i} \frac{\left(M_j{}^2(t)\right)^{\tilde{\alpha}_j}}{\tilde{\alpha}_j!} \leqslant \sum_{|\tilde{\boldsymbol{\alpha}}|=p} \prod_{j=1}^{\infty} \frac{\left(M_j{}^2(t)\right)^{\tilde{\alpha}_j}}{\tilde{\alpha}_j!} \leqslant \frac{t^p}{p!}.$$

Thus, we further deduce (using the induction basis and hypothesis)

$$\sum_{l=k+1}^{\infty} \sum_{\substack{|\boldsymbol{\alpha}|=p+1 \\ d(\boldsymbol{\alpha})=l}} \prod_{j=1}^{l} \frac{\left(M_j{}^2(t)\right)^{\alpha_j}}{\alpha_j!}$$

$$\leqslant \sum_{l=k+1}^{\infty} \frac{1}{\pi^2 k^2} \sum_{\substack{|\tilde{\boldsymbol{\alpha}}|=p \\ d(\tilde{\boldsymbol{\alpha}})=l}} \prod_{j=1}^{l} \frac{\left(M_j{}^2(t)\right)^{\tilde{\alpha}_j}}{\tilde{\alpha}_j!} + \sum_{l=k+1}^{\infty} M_l{}^2(t) \frac{t^p}{p!}$$

$$\leqslant \frac{1}{\pi^2 k^2} \cdot \frac{C(p)}{\pi k} + \frac{1}{\pi k} \cdot \frac{t^p}{p!}$$

$$\leqslant \frac{C(p+1)}{\pi k}.$$

Finally, with

$$A_2 = 2 \sum_{l=k+1}^{\infty} \sum_{i=0}^{p} \sum_{\substack{|\boldsymbol{\alpha}|=i \\ d(\boldsymbol{\alpha})=l}} x_0{}^2 \, \mathrm{e}^{2\mu} \, \sigma^{2i} \prod_{j=1}^{\infty} \frac{\left(M_j{}^2(1)\right)^{\alpha_j}}{\alpha_j!}$$

$$\leqslant 2 \, x_0{}^2 \, \mathrm{e}^{2\mu} \sum_{i=0}^{p} \sigma^{2i} \frac{C(i)}{\pi k}$$

$$\leqslant 2 \, x_0{}^2 \, \mathrm{e}^{2\mu} \frac{\left(\sigma^2\right)^{p+1} - 1}{\sigma^2 - 1} \cdot \frac{\tilde{C}(p)}{\pi k}, \tag{6.28}$$

where $\tilde{C}(p) = \max\{C(i) \mid 0 \leqslant i \leqslant p\}$, the proof is finished. □

General Error Estimator

With this exemplary error result at hand, we finally come to one of the main results of the thesis. We derive a general error estimator for a truncated WIENER chaos solution of a SDE on the time interval $\mathcal{T} = [0, t_{\mathrm{f}}]$.

Theorem 6.4

Let the random process $X_t \in L^2(\mathcal{T} \times \Omega)$ be driven on the time interval $\mathcal{T} = [0, t_{\mathrm{f}}]$ by the SDE

$$\mathrm{d}X_t = b(t, X_t) \, \mathrm{d}t + \sigma(t, X_t) \, \mathrm{d}B_t, \qquad X_0 = x_0. \tag{6.29}$$

Suppose that the coefficient functions $b(\cdot)$, $\sigma(\cdot)$ satisfy the LIPSCHITZ and linear growth conditions

$$|b(t, x) - b(t, y)| + |\sigma(t, x) - \sigma(t, y)| \leqslant K |x - y|, \qquad t \in \mathcal{T}, \tag{6.30}$$

$$|b(t, x)|^2 + |\sigma(t, x)|^2 \leqslant K^2 \left(1 + |x|^2\right), \qquad t \in \mathcal{T}. \tag{6.31}$$

Moreover, suppose they are infinitely often differentiable in their second argument and at least once

in their first argument and that the partial derivatives of all orders are LIPSCHITZ *continuous and bounded by K.*

Let the basis $\{m_i\}_{i \in \mathbb{N}_0}$ *of the underlying* HILBERT *space* $L^2(\mathcal{T})$ *be given as in (5.26) and denote*

$$X_t^{p,k} = \sum_{\boldsymbol{\alpha} \in \mathcal{I}_{p,k}} x_{\boldsymbol{\alpha}}(t) \Psi^{\boldsymbol{\alpha}}(\boldsymbol{\eta})$$

with coefficient functions $x_{\boldsymbol{\alpha}}(\cdot)$ *determined through the propagator system (6.11).*

Then the mean-square error of the truncated WIENER *chaos expansion at the terminal time* $X_{t_f}^{p,k}$ *depending on the order p and the maximum length k of the expansion, i.e., the number k of included basis functions* $m_i(\cdot)$ *can be estimated by*

$$\mathbb{E}\left[\left|X_{t_f} - X_{t_f}^{p,k}\right|^2\right] \leqslant C_1(1 + x_0{}^2) e^{(C_1 + \Xi^2)t_f} \frac{\left(\Xi^2 t_f\right)^{p+1}}{(p+1)!} + C_2(1 + x_0{}^2) e^{C_2 t_f} \frac{t_f^4}{k}, \qquad (6.32)$$

with constants C_1, C_2 *depending on K and t_f, and Ξ depending only on K.* $\triangle$

Remark 6.9

The terms e^{Ct_f} in Equation (6.32) can be compared with what we could expect from GRON-WALL's lemma [24, 102]. Moreover, we observe the same independence of the truncation of p and k as in the error estimation of the geometric BROWNian motion, cf. Equation (6.23) and Remark 6.8. Truncating the order p affects the quality of the chaos expansion, truncating the number k of basis functions the approximation within each chaos $\mathcal{H}_\cdot$.

As GRONWALL's inequality generally overestimates the error and for practical purposes one cannot draw on the used LIPSCHITZ constants, an adaptive approach might be beneficial. One possibility would be to work with different magnitudes of truncation (for both p and k) and to refine if necessary. However, due to the coupling of the propagator equations (6.11), each refinement might require a new solution of the system.

Remark 6.10

The chain of proof of Theorem 6.4 follows basically [170, Proof of Theorem 2.2]. However, the arguments therein are premised on the semigroup generated by the differential operator of the ZAKAI equation. Here, we will make use of multiple MALLIAVIN derivatives of the process X_t. Besides, we use a different (and slightly more general) basis of the underlying HILBERT space $L^2(\mathcal{T})$.

Proof (of Theorem 6.4) From (6.24) we already know that

$$\mathbb{E}\left[\left|X_{t_f} - X_{t_f}^{p,k}\right|^2\right] \leqslant 2 \underbrace{\sum_{n=p+1}^{\infty} \sum_{|\boldsymbol{\alpha}|=n} x_{\boldsymbol{\alpha}}{}^2(t_f)}_{A_1} + 2 \underbrace{\sum_{l=k+1}^{\infty} \sum_{n=0}^{p} \sum_{\substack{|\boldsymbol{\alpha}|=n \\ d(\boldsymbol{\alpha})=l}} x_{\boldsymbol{\alpha}}{}^2(t_f)}_{A_2}.$$

To determine A_1, we use the chaos expansions (5.30) and (5.48) of X_t, i.e.,

$$X_t = \sum_{n=0}^{\infty} \sum_{|\boldsymbol{\alpha}|=n} x_{\boldsymbol{\alpha}}(t) \Psi^{\boldsymbol{\alpha}}(\boldsymbol{\eta}) = \sum_{n=0}^{\infty} I_n(\xi_n(\boldsymbol{t}^n; t)),$$

with $t^n = (t_1, \dots, t_n)$ and symmetric kernel functions $\xi_n(t^n; t)$ for all $n \in \mathbb{N}_0$, to reason that

$$
\begin{aligned}
\sum_{|\alpha|=n} x_\alpha{}^2(t) = \mathbb{E}\left[\left(\sum_{|\alpha|=n} x_\alpha(t)\Psi^\alpha(\eta)\right)^2\right] &= \mathbb{E}\left[(I_n(\xi_n(t^n; t)))^2\right] \\
&= n!\,\langle\xi_n(t^n; t), \xi_n(t^n; t)\rangle_{L^2(\mathcal{T}^n)} \\
&= (n!)^2 \overset{(n)}{\int}_{}^{t}(\xi_n(t^n; t))^2\,\mathrm{d}t^n,
\end{aligned}
\tag{6.33}
$$

where we abbreviate

$$
\overset{(k)}{\int}_{}^{t} f(\cdot)\,\mathrm{d}t^k \overset{\text{def}}{=} \int_0^t \dots \int_0^{t_2} f(\cdot)\,\mathrm{d}t_1 \dots \mathrm{d}t_k.
$$

Therefore, we deduce with the help of (5.54)

$$
A_1 = \sum_{n=p+1}^\infty (n!)^2 \overset{(n)}{\int}_{}^{t_\mathrm{f}}(\xi_n(t^n; t_\mathrm{f}))^2\,\mathrm{d}t^n \leqslant \sum_{n=p+1}^\infty \overset{(n)}{\int}_{}^{t_\mathrm{f}} \mathbb{E}\left[\left(D_{t_1,\dots,t_n}^n X_{t_\mathrm{f}}\right)^2\right]\mathrm{d}t^n.
\tag{6.34}
$$

To proceed further we need

Lemma 6.1

Under the assumptions of Theorem 6.4, i.e., especially under the LIPSCHITZ*, linear growth, and differentiability conditions on the coefficients functions $b(\cdot)$ and $\sigma(\cdot)$ of the SDE (6.29), we estimate*

$$
\mathbb{E}\left[\left|D_{s_1,\dots,s_n}^n X_t\right|^2\right] \leqslant C\Xi^{2n}(1 + x_0{}^2)\,\mathrm{e}^{Ct},
\tag{6.35}
$$

with the constant Ξ depending only on K, and C depending on K and t_f. △

Proof (of Lemma 6.1) We show the assertion by induction over n. For $n = 0$ it is true by Theorem 4.6, in particular Equation (4.30), so let us consider the case $n = 1$ to start. As X_t is a solution of the SDE (6.29) with the coefficients being LIPSCHITZ continuous on $\mathcal{T}$ with linear growth, we know from [194, Theorem 2.2.1] that $X_t \in \mathbb{D}^{1,\infty}$ for all $t \in \mathcal{T}$. Moreover, the MALLIAVIN derivative of X_t is bounded. From its properties and by using the integration by parts-formula, we calculate that for all $s \leqslant t$ it satisfies

$$
\begin{aligned}
D_s X_t &= D_s x_0 + D_s\left(\int_0^t b(u, X_u)\,\mathrm{d}u\right) + D_s\left(\int_0^t \sigma(u, X_u)\,\mathrm{d}B_u\right) \\
&= \int_0^t D_s b(u, X_u)\,\mathrm{d}u + \sigma(s, X_s) + \int_0^t D_s \sigma(u, X_u)\,\mathrm{d}B_u, \\
&= \int_0^t \frac{\partial}{\partial x} b(u, X_u) \cdot D_s X_u \cdot \mathbb{1}_{\{s \leqslant u\}}\,\mathrm{d}u + \sigma(s, X_s) + \int_0^t \frac{\partial}{\partial x}\sigma(u, X_u) \cdot D_s X_u \cdot \mathbb{1}_{\{s \leqslant u\}}\,\mathrm{d}B_u, \\
&= \sigma(s, X_s) + \int_s^t \frac{\partial}{\partial x} b(u, X_u) D_s X_u\,\mathrm{d}u + \int_s^t \frac{\partial}{\partial x}\sigma(u, X_u) D_s X_u\,\mathrm{d}B_u.
\end{aligned}
\tag{6.36}
$$

For $s > t$ we directly obtain $D_s X_t = 0$.

Then under our assumptions, the SDE system

$$X_t = X_s + \int_s^t b(u, X_u) \, du + \int_s^t \sigma(u, X_u) \, dB_u,$$

$$D_s X_t = \sigma(s, X_s) + \int_s^t \frac{\partial}{\partial x} b(u, X_u) D_s X_u \, du + \int_s^t \frac{\partial}{\partial x} \sigma(u, X_u) D_s X_u \, dB_u,$$

for all $s \leqslant t \in \mathcal{T}$ is again a diffusion process satisfying the conditions of Theorem 4.6 as $b(\cdot)$, $\sigma(\cdot)$, and their partial derivatives (with respect to the second component) are LIPSCHITZ continuous and bounded or of at most linear growth, respectively. Thus, with denoting $Y_{s;t}^{(1)} = (X_t, D_s X_t)^T$, we apply Equation (4.30) to obtain

$$\begin{aligned}
\mathbb{E}\left[|D_s X_t|^2\right] &\leqslant \mathbb{E}\left[|X_t|^2\right] + \mathbb{E}\left[|D_s X_t|^2\right] = \mathbb{E}\left[\left\|Y_{s;t}^{(1)}\right\|^2\right] \\
&\leqslant C\left(1 + \mathbb{E}\left[\left\|Y_{s;s}^{(1)}\right\|^2\right]\right) e^{Ct} \\
&\leqslant C\left(1 + \mathbb{E}\left[|X_s|^2\right] + \mathbb{E}\left[|\sigma(s, X_s)|^2\right]\right) e^{Ct} \\
&\leqslant C\left(1 + \mathbb{E}\left[|X_s|^2\right] + K^2\left(1 + \mathbb{E}\left[|X_s|^2\right]\right)\right) e^{Ct} \\
&\leqslant C \Xi^2\left(1 + \mathbb{E}\left[|X_s|^2\right]\right) e^{Ct} \\
&\leqslant C \Xi^2\left(1 + \hat{C}\left(1 + x_0^2\right) e^{\hat{C}s}\right) e^{Ct} \\
&\leqslant \tilde{C}\left(1 + x_0^2\right) \Xi^2 e^{\tilde{C}t}.
\end{aligned} \tag{6.37}$$

Note that the SDE describing the MALLIAVIN derivative DX_t is in fact linear with the coefficients being LIPSCHITZ continuous and of at most linear growth by the assumptions on $b(\cdot)$ and $\sigma(\cdot)$. By [194, Lemma 2.2.2] the derivative process $\{D_s X_t\}$ belongs to the space $\mathbb{D}^{1,\infty}$ again and its derivative in return satisfies a linear equation of a similar form. Hence (cf. [194, Theorem 2.2.2]), we can recursively apply the previous idea to determine a SDE describing the n-th order MALLIAVIN derivative $D^n X_t$, which depends on the original process X_t and all derivatives up to order n, but only linearly on $D^n X_t$. By that means, we find that for each n the process $Y_{s_1,\ldots,s_n;t}^{(n)} = \left(X_t, \ldots, D_{s_1,\ldots,s_n}^n X_t\right)^T$ is an ITÔ diffusion satisfying the conditions of Theorem 4.6.

To reason the induction step, assume that the assertion holds for all $k = 1, \ldots, n-1$. In order to calculate the estimation, we have to apply the initial values of the SDE system that $Y_{s_1,\ldots,s_n;t}^{(n)}$ satisfies. The formula to derive them is proven in [194, Theorem 2.2.2]; before we state it, we need some additional notation. The stochastic process $D^m X_t = \left\{D_{s_1,\ldots,s_m}^m X_t \mid (s_1,\ldots,s_m) \in \mathcal{T}\right\}$ depends on the m time instants $s_1, \ldots, s_m$. For any subset $J = \{j_1 < \ldots < j_\eta\}$ of $\{1,\ldots,m\}$ with $|J| = \eta \leqslant m$ elements, denote $s(J) = s_{j_1}, \ldots, s_{j_\eta}$. Further on, we define

$$\mathfrak{z}(t, s_1, \ldots, s_m) = \sum_{\mathfrak{P}^m} \frac{\partial^m}{\partial x^m} \sigma(t, X_t) \cdot D_{s(J_1)}^{|s(J_1)|} X_t \cdots D_{s(J_\nu)}^{|s(J_\nu)|} X_t, \tag{6.38}$$

and

$$\mathfrak{y}(t, s_1, \ldots, s_m) = \sum_{\mathfrak{P}^m} \frac{\partial^m}{\partial x^m} b(t, X_t) \cdot D_{s(J_1)}^{|s(J_1)|} X_t \cdots D_{s(J_\nu)}^{|s(J_\nu)|} X_t, \tag{6.39}$$

where the sums run over the set $\mathfrak{P}^m$ of all partitions $J_1 \cup \cdots \cup J_\nu$ of $\{1, \ldots, m\}$. We determine

$\mathfrak{z}(t) = \sigma(t, X_t)$ as well. With these notations at hand, we find that the n-th order MALLIAVIN derivative $D^n_{s_1,\dots,s_n} X_t$ satisfies the linear SDE

$$D^n_{s_1,\dots,s_n} X_t = \sum_{i=1}^n \mathfrak{z}(s_i, s_1, \dots, s_{i-1}, s_{i+1}, \dots, s_n)$$

$$+ \int_{\hat{s}}^t \mathfrak{y}(u, s_1, \dots, s_n)\,\mathrm{d}u + \int_{\hat{s}}^t \mathfrak{z}(u, s_1, \dots, s_n)\,\mathrm{d}B_u \tag{6.40}$$

for $\hat{s} \overset{\text{def}}{=} \max\{s_1, \dots, s_n\} \leqslant t$ and $D^n_{s_1,\dots,s_n} X_t = 0$ else. Hence, its initial value is given by

$$\sum_{i=1}^n \mathfrak{z}(s_i, s_1, \dots, s_{i-1}, s_{i+1}, \dots, s_n),$$

where

$$\mathfrak{z}(s_1, \dots, s_n) = \frac{\partial^n}{\partial x^n} \sigma(s_1, X_{s_1}) \times$$

$$\times \left(D_{s_2} X_{s_1} \cdots D_{s_n} X_{s_1} + D^2_{s_2,s_3} X_{s_1} \cdot D_{s_4} X_{s_1} \cdots D_{s_n} X_{s_1} + \dots + D^{n-1}_{s_2,\dots,s_n} X_{s_1} \right).$$

To give an illustrative example, if $n = 2$ we obtain the initial value of $D^2_{s_1,s_2} X_t$ with $t \geqslant \max\{s_1, s_2\}$ as

$$\mathfrak{z}(s_1, s_2) + \mathfrak{z}(s_2, s_1) = \frac{\partial}{\partial x} \sigma(s_1, X_{s_1}) \cdot D_{s_2} X_{s_1} + \frac{\partial}{\partial x} \sigma(s_2, X_{s_2}) \cdot D_{s_1} X_{s_2},$$

resulting in the following estimation of the initial value, depending on the relation of the time instants s_1 and s_2:

$$s_1 < s_2: \quad \mathbb{E}\left[|\mathfrak{z}(s_1, s_2) + \mathfrak{z}(s_2, s_1)|^2\right] = \mathbb{E}\left[\left|\frac{\partial}{\partial x} \sigma(s_2, X_{s_2}) \cdot D_{s_1} X_{s_2}\right|^2\right]$$

$$\leqslant K^2 \mathbb{E}\left[\left|D_{s_1} X_{s_2}\right|^2\right] \leqslant K^2 \mathbb{E}\left[\left\|Y^{(1)}_{s_1;s_2}\right\|^2\right]$$

$$\leqslant C \Xi^4 \left(1 + x_0^2\right) \mathrm{e}^{Cs_2},$$

$$s_2 < s_1: \quad \mathbb{E}\left[|\mathfrak{z}(s_1, s_2) + \mathfrak{z}(s_2, s_1)|^2\right] = \mathbb{E}\left[\left|\frac{\partial}{\partial x} \sigma(s_1, X_{s_1}) \cdot D_{s_2} X_{s_1}\right|^2\right]$$

$$\leqslant C \Xi^4 \left(1 + x_0^2\right) \mathrm{e}^{Cs_1},$$

$$s_1 = s_2: \quad \mathbb{E}\left[|\mathfrak{z}(s_1, s_2) + \mathfrak{z}(s_2, s_1)|^2\right] = \mathbb{E}\left[\left|2\frac{\partial}{\partial x} \sigma(s_1, X_{s_1}) \cdot D_{s_1} X_{s_1}\right|^2\right]$$

$$\leqslant 2K^2 \mathbb{E}\left[\left|D_{s_1} X_{s_1}\right|^2\right] \leqslant 2K^2 \mathbb{E}\left[\left|\sigma(s_1, X_{s_1})\right|^2\right]$$

$$\leqslant C \Xi^4 \left(1 + x_0^2\right) \mathrm{e}^{Cs_1}.$$

For $n = 3$ the initial value of $D^3_{s_1,s_2,s_3} X_t$ with $t \geqslant \max\{s_1, s_2, s_3\}$ is

$$
\begin{aligned}
\mathfrak{z}(s_1&, s_2, s_3) + \mathfrak{z}(s_2, s_1, s_3) + \mathfrak{z}(s_3, s_1, s_2) \\
&= \frac{\partial^2}{\partial x^2} \sigma(s_1, X_{s_1}) \cdot \left(D_{s_2} X_{s_1} \cdot D_{s_3} X_{s_1} + D^2_{s_2, s_3} X_{s_1} \right) \\
&\quad + \frac{\partial^2}{\partial x^2} \sigma(s_2, X_{s_2}) \cdot \left(D_{s_1} X_{s_2} \cdot D_{s_3} X_{s_2} + D^2_{s_1, s_3} X_{s_2} \right) \\
&\quad + \frac{\partial^2}{\partial x^2} \sigma(s_3, X_{s_3}) \cdot \left(D_{s_1} X_{s_3} \cdot D_{s_2} X_{s_3} + D^2_{s_1, s_2} X_{s_3} \right).
\end{aligned}
$$

Now let us return to the induction step, i.e., the case $k = n$. We estimate the appropriate initial value in the mean-square sense in exactly the same way as for the exemplary case $n = 2$ and derive for constants c_i, $0 \leqslant i \leqslant n$, and by denoting $\hat{s} = \max\{s_1, \ldots, s_n\}$ again, the estimate

$$
\begin{aligned}
\mathbb{E}\left[\left| D^n_{s_1, \ldots, s_n} X_t \right|^2 \right] &\leqslant \mathbb{E}\left[\left\| Y^{(n)}_{s_1, \ldots, s_n; t} \right\|^2 \right] \\
&\leqslant C\left(1 + \mathbb{E}\left[|X_{\hat{s}}|^2 \right] + \ldots + \mathbb{E}\left[\left| \sum_{i=1}^{k} \mathfrak{z}(s_i, s_1, \ldots s_{i-1}, s_{i+1}, \ldots, s_n) \right|^2 \right] \right) e^{Ct} \\
&\leqslant C\left(c_0 \left(1 + x_0{}^2\right) e^{c_0 \hat{s}} + c_1 \Xi^2 \left(1 + x_0{}^2\right) e^{c_1 \hat{s}} + \ldots + c_n \Xi^{2n} \left(1 + x_0{}^2\right) e^{c_n \hat{s}} \right) e^{Ct} \\
&\leqslant \tilde{C} \left(1 + x_0{}^2\right) \Xi^{2n} e^{\tilde{C} t}. \qquad \qquad \square
\end{aligned}
$$

With this result at hand, we obtain the estimate for A_1 as

$$
\begin{aligned}
A_1 &\leqslant \sum_{n=p+1}^{\infty} \overset{(n)}{\int} \int^{t_\mathrm{f}} \mathbb{E}\left[\left(D^n_{t_1, \ldots, t_n} X_{t_\mathrm{f}} \right)^2 \right] \mathrm{d}\boldsymbol{t}^n \\
&\leqslant \sum_{n=p+1}^{\infty} \overset{(n)}{\int} \int^{t_\mathrm{f}} C \left(1 + x_0{}^2\right) \Xi^{2n} e^{C t_\mathrm{f}} \mathrm{d}\boldsymbol{t}^n \\
&\leqslant C \left(1 + x_0{}^2\right) e^{C t_\mathrm{f}} \sum_{n=p+1}^{\infty} \Xi^{2n} \frac{t_\mathrm{f}{}^n}{n!} \\
&\leqslant C \left(1 + x_0{}^2\right) \frac{\left(\Xi^2 t_\mathrm{f}\right)^{p+1}}{(p+1)!} e^{(C + \Xi^2) t_\mathrm{f}}.
\end{aligned}
\tag{6.41}
$$

For the second part of the proof, i.e., the estimation of A_2, we introduce further notation. Let $\boldsymbol{\alpha}$ be a multi-index of order $|\boldsymbol{\alpha}| = n$ and length $d(\boldsymbol{\alpha}) = \max_i \{\alpha_i > 0\} = l$. Then the *characteristic set* (cf. [170]) of $\boldsymbol{\alpha}$ is the vector $(i_1, \ldots, i_n)$ with $i_1 \leqslant i_2 \leqslant \ldots \leqslant i_n$, where i_1 is the index number of the first non-zero component of $\boldsymbol{\alpha}$. i_2 is equal to i_1 if $\alpha_{i_1} > 1$, otherwise it is the index of the second non-zero component of $\boldsymbol{\alpha}$. In that fashion, the characteristic set is constructed further, resulting in the observation that $d(\boldsymbol{\alpha}) = l = i_n$.

Additionally, for any $\boldsymbol{\alpha}$ of order n and a basis $\{m_i(\cdot)\}_{i \in \mathbb{N}}$ of $L^2(\mathcal{T})$, by $\tilde{m}_{\boldsymbol{\alpha}}(\boldsymbol{t}^n)$ we denote a *symmetrized* form of $\bigotimes m_i^{\otimes \alpha_i}$ defined via

$$
\tilde{m}_{\boldsymbol{\alpha}}(\boldsymbol{t}^n) \overset{\text{def}}{=} \sum_{\pi \in \mathfrak{P}^n} m_{i_1}\left(t_{\pi(1)}\right) \cdots m_{i_n}\left(t_{\pi(n)}\right),
\tag{6.42}
$$

where the sum runs over all permutations π within the permutation group $\mathfrak{P}^n$ of $\{1, \ldots, n\}$.

Then from the FOURIER connection $x_{\alpha}(t) = \mathbb{E}[X_t \Psi^{\alpha}(\eta)]$, the chaos expansion (5.48), and the definition of the basis polynomials $\Psi^{\alpha}(\cdot)$, i.e.,

$$\Psi^{\alpha}(\eta) = \frac{1}{\sqrt{\alpha!}} I_{|\alpha|} \left(\bigotimes_{i=1}^{\infty} m_i^{\otimes \alpha_i} \right) = \frac{1}{\sqrt{\alpha!}} I_{|\alpha|} \left(\frac{1}{|\alpha|!} \tilde{m}_{\alpha} \right)$$

(cf. Equation (5.52) and [194]), we derive for any $\alpha \in \mathcal{I}$ with $|\alpha| = n$

$$x_{\alpha}(t_{\mathrm{f}}) = \frac{n!}{\sqrt{\alpha!}} \overset{(n)}{\int}^{t_{\mathrm{f}}} \xi_n(t^n; t_{\mathrm{f}}) \tilde{m}_{\alpha}(t^n) \, dt^n. \tag{6.43}$$

Note again, that each basis function $m_i(\cdot) \in L^2(\mathcal{T})$ is defined through (5.26). As

$$\tilde{m}_{\alpha}(t^n) = \sum_{j=1}^{n} m_{i_n}(t_j) \cdot \tilde{m}_{\alpha-(i_n)}(t_j^n),$$

where t_j^n is obtained from t^n by omitting t_j and $\alpha^-(\cdot)$ denotes the diminished multi-index as in (5.43), we deduce

$$x_{\alpha}(t_{\mathrm{f}}) = \frac{n!}{\sqrt{\alpha!}} \sum_{j=1}^{n} \overset{(n-1)}{\int}^{t_{\mathrm{f}}} \left(\int_{t_{j-1}}^{t_{j+1}} \xi_n(t^n; t_{\mathrm{f}}) m_{i_n}(t_j) \, dt_j \right) \tilde{m}_{\alpha-(i_n)}(t_j^n), \tag{6.44}$$

with $t_0 \overset{\mathrm{def}}{=} 0$ and $t_{n+1} \overset{\mathrm{def}}{=} t_{\mathrm{f}}$, by changing the order of integration. Then for any $i_n = l \geqslant 1$ we integrate by parts to deduce

$$\int_{t_{j-1}}^{t_{j+1}} \xi_n(t^n; t_{\mathrm{f}}) m_l(t_j) \, dt_j = \left[\xi_n(t^n; t_{\mathrm{f}}) M_l(t_j) \right]_{t_{j-1}}^{t_{j+1}} - \int_{t_{j-1}}^{t_{j+1}} \frac{\partial}{\partial t_j} \xi_n(t^n; t_{\mathrm{f}}) M_l(t_j) \, dt_j. \tag{6.45}$$

Notice that

$$M_i(s) = \int_0^s m_i(u) \, du = \frac{\sqrt{2t_{\mathrm{f}}}}{(i - \frac{1}{2})\pi} \sin\left(\left(i - \frac{1}{2} \right) \frac{\pi s}{t_{\mathrm{f}}} \right).$$

Now we rename t_j^n in the following way for each j: With $s_i = t_i$ for all $i \leqslant j - 1$ and $s_i = t_{i+1}$ for all $i > j - 1$, we have $s^{n-1} \overset{\mathrm{def}}{=} t_j^n$ by setting $s_0 = 0$ and $s_n = t_{\mathrm{f}}$. Moreover, we denote with $s^{n-1,r}$, $r = 1, \ldots, n-1$, the set that is generated from s^{n-1} by taking s_r twice. To finalize this notation, we set $s^{n-1,0} = (s_0, s_1, \ldots, s_{n-1})$ and $s^{n-1,n} = (s_1, \ldots, s_{n-1}, s_n)$. Then

$$\left[\xi_n(t^n; t_{\mathrm{f}}) M_l(t_j) \right]_{t_{j-1}}^{t_{j+1}} = \xi_n(s^{n-1,j}) M_l(s_j) - \xi_n(s^{n-1,j-1}) M_l(s_{j-1}), \qquad j = 1, \ldots, n.$$

Because $M_l(s_0) = M_l(0) = 0$ and $M_l(t_n) = M_l(t_{\mathrm{f}})$, from (6.45) we see that by summing over j

all terms except one cancel out. What remains can be collected to

$$
\begin{aligned}
\psi_l(\boldsymbol{s}^{n-1}; t_{\mathrm{f}}) \stackrel{\text{def}}{=} & (-1)^{l-1} \frac{\sqrt{2t_{\mathrm{f}}}}{\left(l-\frac{1}{2}\right)\pi} \cdot \xi_n(\boldsymbol{s}^{n-1,n}; t_{\mathrm{f}}) \\
& - \int_0^{s_1} \frac{\partial}{\partial s_1} \xi_n(\tau, \boldsymbol{s}^{n-1}; t_{\mathrm{f}}) M_l(\tau)\,\mathrm{d}\tau \\
& - \sum_{j=2}^{n-1} \int_{s_{j-1}}^{s_j} \frac{\partial}{\partial s_j} \xi_n(\ldots, s_{j-1}, \tau, s_{j+1}, \ldots; t_{\mathrm{f}}) M_l(\tau)\,\mathrm{d}\tau \\
& - \int_{s_{n-1}}^{s_n} \frac{\partial}{\partial s_n} \xi_n(\boldsymbol{s}^{n-1}, \tau; t_{\mathrm{f}}) M_l(\tau)\,\mathrm{d}\tau,
\end{aligned}
$$

so from (6.44) we obtain

$$
\begin{aligned}
\sum_{\substack{|\boldsymbol{\alpha}|=n \\ i_n=d(\boldsymbol{\alpha})=l}} {x_{\boldsymbol{\alpha}}}^2(t_{\mathrm{f}}) = & \sum_{\substack{|\boldsymbol{\alpha}|=n \\ i_n=d(\boldsymbol{\alpha})=l}} \left(\frac{n!}{\sqrt{\boldsymbol{\alpha}!}} \overset{(n-1)}{\int}{}^{t_{\mathrm{f}}} \psi_l(\boldsymbol{s}^{n-1}; t_{\mathrm{f}}) \tilde{m}_{\boldsymbol{\alpha}^-(l)}(\boldsymbol{s}^{n-1})\,\mathrm{d}\boldsymbol{s}^{n-1} \right)^2 \\
& \leqslant n^2 \sum_{|\boldsymbol{\beta}|=n-1} \left(\frac{(n-1)!}{\sqrt{\boldsymbol{\beta}!}} \overset{(n-1)}{\int}{}^{t_{\mathrm{f}}} \psi_l(\boldsymbol{s}^{n-1}; t_{\mathrm{f}}) \tilde{m}_{\boldsymbol{\beta}}(\boldsymbol{s}^{n-1})\,\mathrm{d}\boldsymbol{s}^{n-1} \right)^2,
\end{aligned}
$$

since $\left|\boldsymbol{\alpha}^-(i_{|\boldsymbol{\alpha}|})\right| = |\boldsymbol{\alpha}|-1$ and $\boldsymbol{\alpha}! \geqslant \boldsymbol{\alpha}^-(i_{|\boldsymbol{\alpha}|})!$. The last sum can be interpreted as the sum over all squared chaos coefficients $\tilde{x}_{\boldsymbol{\beta}}$ of a random variable $\tilde{X}_{t_{\mathrm{f}}}$, whereas we can reason

$$
\sum_{\substack{|\boldsymbol{\alpha}|=n \\ i_n=l}} {x_{\boldsymbol{\alpha}}}^2(t_{\mathrm{f}}) \leqslant (n!)^2 \overset{(n-1)}{\int}{}^{t_{\mathrm{f}}} \left(\psi_l(\boldsymbol{s}^{n-1}; t_{\mathrm{f}}) \right)^2 \,\mathrm{d}\boldsymbol{s}^{n-1}
$$

similar to (6.33).

In the next step we estimate the new integrand function. By multiple usage of the CAUCHY-SCHWARZ inequality we find

$$
\begin{aligned}
\left| \psi_l(\boldsymbol{s}^{n-1}; t_{\mathrm{f}}) \right|^2 \leqslant (n+1) \Bigg(& \frac{2t_{\mathrm{f}}}{\left(l-\frac{1}{2}\right)^2 \pi^2} \cdot \left| \xi_n(\boldsymbol{s}^{k-1,k}; t_{\mathrm{f}}) \right|^2 \\
& + \left| \int_0^{s_1} \frac{\partial}{\partial s_1} \xi_n(\tau, \boldsymbol{s}^{k-1}; t_{\mathrm{f}}) M_l(\tau)\,\mathrm{d}\tau \right|^2 \\
& + \ldots + \left| \int_{s_{n-1}}^{s_n} \frac{\partial}{\partial s_n} \xi_n(\boldsymbol{s}^{k-1}, \tau; t_{\mathrm{f}}) M_l(\tau)\,\mathrm{d}\tau \right|^2 \Bigg)
\end{aligned}
$$

$$\leqslant (n+1)\left(\frac{2t_f}{\left(l-\frac{1}{2}\right)^2 \pi^2} \cdot \left|\xi_n(\mathbf{s}^{k-1,k}; t_f)\right|^2\right.$$

$$+ \int_0^{s_1} \left|\frac{\partial}{\partial s_1}\xi_n(\tau, \mathbf{s}^{k-1}; t_f)\right|^2 \mathrm{d}\tau \cdot \int_0^{t_f} |M_l(\tau)|^2 \, \mathrm{d}\tau$$

$$\left.+ \ldots + \int_{s_{n-1}}^{s_n} \left|\frac{\partial}{\partial s_n}\xi_n(\mathbf{s}^{k-1}, \tau; t_f)\right|^2 \mathrm{d}\tau \cdot \int_0^{t_f} |M_l(\tau)|^2 \, \mathrm{d}\tau\right).$$

As we have already seen, the kernel functions $\xi_n(\cdot; t)$ can be estimated with the help of Lemma 6.1. However, from their connection to multiple MALLIAVIN derivatives via (5.54), the representation of these derivatives as solutions of SDEs, and our assumptions on the boundedness of the partial derivatives of the coefficient functions $b(\cdot)$ and $\sigma(\cdot)$ with respect to their first argument, it follows that

$$\left|\frac{\partial}{\partial t_i}\xi_n(t_1, \ldots, t_n; t)\right|^2 \leqslant \frac{1}{n!}C^n(1+x_0{}^2)\mathrm{e}^{Ct}, \quad i = 1, \ldots, n,$$

with a constant C depending on t_f and K again. Therefore, we calculate

$$\left|\psi_l(\mathbf{s}^{n-1}; t_f)\right|^2 \leqslant (n+1)\left(\frac{2t_f}{\left(l-\frac{1}{2}\right)^2 \pi^2} \cdot C_1\left(1+x_0{}^2\right)\frac{\Xi^{2n}}{(n!)^2}\mathrm{e}^{C_1 t_f}\right.$$

$$+ \left(1+x_0{}^2\right)\frac{C_2{}^n}{(n!)^2}\mathrm{e}^{C_2 t_f} \cdot s_1 \cdot \frac{2t_f{}^2}{\left(l-\frac{1}{2}\right)^2 \pi^2}$$

$$\left.+ \ldots + \left(1+x_0{}^2\right)\frac{C_2{}^n}{(n!)^2}\mathrm{e}^{C_2 t_f} \cdot (s_n - s_{n-1}) \cdot \frac{2t_f{}^2}{\left(l-\frac{1}{2}\right)^2 \pi^2}\right)$$

$$\leqslant \frac{n+1}{(n!)^2} \cdot \frac{\left(1+x_0{}^2\right)}{\left(l-\frac{1}{2}\right)^2 \pi^2}\left(C_1 t_f \Xi^{2n}\mathrm{e}^{C_1 t_f} + C_2{}^n t_f{}^3 \mathrm{e}^{C_2 t_f}\right)$$

$$\leqslant \frac{n+1}{(n!)^2} \cdot \frac{\left(1+x_0{}^2\right)}{\left(l-\frac{1}{2}\right)^2 \pi^2}C_\Xi{}^n t_f{}^3 \mathrm{e}^{Ct_f},$$

where C_Ξ is a constant depending on Ξ, K, and t_f, i.e., on K and t_f. Hence, we finally obtain

$$\sum_{\substack{|\boldsymbol{\alpha}|=n \\ i_n=l}} x_{\boldsymbol{\alpha}}{}^2(t_f) \leqslant (n!)^2 \overset{(n-1)}{\int} \int_0^{t_f} \left|\psi_l(\mathbf{s}^{n-1}; t_f)\right|^2 \mathrm{d}\mathbf{s}^{n-1}$$

$$\leqslant (n+1)\frac{\left(1+x_0{}^2\right)}{\left(l-\frac{1}{2}\right)^2 \pi^2}C_\Xi{}^n t_f{}^3 \mathrm{e}^{Ct_f}\frac{t_f{}^{n-1}}{(n-1)!}$$

and, therefore, the error estimate A_2 as

$$
\begin{aligned}
A_2 &= \sum_{l=k+1}^{\infty} \sum_{n=1}^{p} \sum_{\substack{|\boldsymbol{\alpha}|=n \\ i_n=l}} x_{\boldsymbol{\alpha}}{}^2(t_{\mathrm{f}}) \\
&\leqslant \tilde{C}_{\Xi}\left(1+x_0{}^2\right) t_{\mathrm{f}}{}^3\, \mathrm{e}^{Ct_{\mathrm{f}}} \sum_{n=1}^{\infty} \frac{(n+1)\left(C_{\Xi}t_{\mathrm{f}}\right)^{n-1}}{(n-1)!} \cdot \sum_{l=k}^{\infty} \frac{1}{l^2} \\
&\leqslant \bar{C}_{\Xi}\left(1+x_0{}^2\right) t_{\mathrm{f}}{}^3\, \mathrm{e}^{Ct_{\mathrm{f}}} \cdot \left(C_{\Xi}t_{\mathrm{f}}+2\right) \mathrm{e}^{C_{\Xi}t_{\mathrm{f}}} \cdot \frac{1}{k} \\
&\leqslant \hat{C}_{\Xi}\left(1+x_0{}^2\right) \frac{t_{\mathrm{f}}{}^4}{k}\, \mathrm{e}^{\hat{C}_{\Xi}t_{\mathrm{f}}}.
\end{aligned}
\tag{6.46}
$$

Then the proof is completed by combining A_1 and A_2. $\qquad\square$

6.3 Summary

In this chapter we first presented the standard idea to solve SDEs numerically. With the help of a time discretization specific integration schemes are established to find solutions in a recursive manner. These approaches are similar to well-known deterministic ones, but suffer from the need of random variables that have to be included within the schemes to handle the stochastic integral part.

As an alternative method we developed an adaptation of the WIENER chaos expansion method to SDEs. To that end, we particularly used the MALLIAVIN derivative and integration by parts formula in order to transform a SDE into a system of ODEs. The resulting system—i.e., the coupling of the components' equations and the dependency on the underlying HILBERT space basis functions—completely describes the stochasticity of the original equation, without being dependent on the external generation of random numbers.

For the efficient numerical use of this idea, we showed different types of sparse and adaptive truncation schemes of the infinite-dimensional ODE system that are beneficial to reduce the overall computational effort without impairing the obtained solutions.

Additionally, we established an error analysis of the introduced propagator method depending on the approximation order of the used chaos expansion and the number of basis functions of the underlying HILBERT space. We started by considering the geometric BROWNian motion process and afterwards proved a general error estimate of the WIENER chaos expansion for SDEs. While related estimates exist for certain classes of SPDEs, where the exploitation of specific structures is possible, here we built or investigations on multiple MALLIAVIN derivatives of the stochastic process described by the considered SDE.

This eventually gives us the opportunity to use the WIENER chaos expansion in the context of random processes describing the dynamics of a system to be controlled. We will describe this approach in detail in the following chapter.

7 Optimal Control Problems Driven by Stochastic Differential Equations

In this chapter we analyze continuous Optimal Control Problems (OCPs) that are driven by Stochastic Differential Equations (SDEs). We present how these problems differ from deterministic OCPs, effecting the methodologies to solve them. To that end we introduce standard approaches to tackle continuous Stochastic Optimal Control Problems (SOCPs), including the HAMILTON-JACOBI-BELLMAN *(HJB) equation* and the MARKOV *Chain Approximation (MCA) method*.

Afterwards we adapt the propagator method for solving SDEs to the special case of SOCPs, leading to a reformulation of the original stochastic problem as a purely deterministic OCP.

7.1 Problem Formulation

Definition 7.1 (Stochastic Optimal Control Problem)
A continuous stochastic optimal control problem *over a probability space* $(\Omega, \mathcal{F}, \mathbb{P})$ *is an infinite-dimensional optimization problem of the form*

$$\min_{\boldsymbol{u} \in \mathcal{A}} \quad J(t_0, \boldsymbol{x}_0, \boldsymbol{u}(\cdot)) \tag{7.1a}$$

$$s.t. \quad \mathrm{d}\boldsymbol{X}_t = \boldsymbol{b}(t, \boldsymbol{X}_t, \boldsymbol{u}_t)\,\mathrm{d}t + \boldsymbol{\sigma}(t, \boldsymbol{X}_t, \boldsymbol{u}_t)\,\mathrm{d}\boldsymbol{B}_t \quad \forall t \in \mathcal{T}, \tag{7.1b}$$

$$\boldsymbol{X}_{t_0} = \boldsymbol{x}_0. \tag{7.1c}$$

Therein the dynamic process is a n_X-dimensional stochastic process $\{\boldsymbol{X}_t\}_{t \in \mathcal{T}}$ on $(\Omega, \mathcal{F}, \mathbb{P})$ with $\boldsymbol{X} \colon \mathcal{T} \times \Omega \to \mathbb{R}^{n_X}$, driven by a SDE (7.1b) with respect to the initial condition (7.1c). It is determined by the drift coefficient function $\boldsymbol{b} \colon \mathcal{T} \times \mathbb{R}^{n_X} \times \mathbb{R}^{n_u} \to \mathbb{R}^{n_X}$ and the diffusion coefficient function $\boldsymbol{\sigma} \colon \mathcal{T} \times \mathbb{R}^{n_X} \times \mathbb{R}^{n_u} \to \mathbb{R}^{n_X \times n_B}$, where $\{\boldsymbol{B}_t\}_{t \in \mathcal{T}}$ denotes a n_B-dimensional BROWNian motion. The state process is affected by a control process $\boldsymbol{u} = \{\boldsymbol{u}_t\}_{t \in \mathcal{T}}$ to minimize a performance index $J \colon \mathcal{U} \to \mathbb{R}$. △

For the state process $\{\boldsymbol{X}_t\}_{t \in \mathcal{T}}$ we have $\boldsymbol{X}_t \in \mathcal{X} \subset \mathbb{R}^{n_X}$ for all $t \in \mathcal{T}$. It can be influenced by a *control input* $\boldsymbol{U}_t \in \mathcal{U} \subset \mathbb{R}^{n_u}$ at any time instant $t \in \mathcal{T}$. Further on, it is chosen over a set $\mathcal{A}$ of *admissible controls* to minimize the cost functional $J(\cdot)$. Then the control has to be a stochastic process $\{\boldsymbol{u}_t\}_{t \in \mathcal{T}} = \{\boldsymbol{u}(t, \omega)\}_{t \in \mathcal{T}}$ as well. Moreover, it has to be at least $\mathcal{F}_t$-adapted for all $t \in \mathcal{T}$, since the decisions taken at time instant t can only be depending on the history up to t.

The most common choices of admissible controls are [195]
- *deterministic* controls $\boldsymbol{U}(t, \omega) = \boldsymbol{U}(t)$,
- *open-loop* controls, which are non-anticipative with respect to the BROWNian motion $\{\boldsymbol{B}_t\}_{t \in \mathcal{T}}$, and

- MARKOV controls $U(t, \omega) = U_M(t, X_t(\omega))$ with a non-random and LEBESGUE-measurable function $U_M : \mathcal{T} \times \mathbb{R}^{n_X} \to \mathbb{R}^{n_u}$. With such a control the state process $\{X_t\}_{t \in \mathcal{T}}$ becomes an ITŌ diffusion.

For the existence of $\{X_t\}_{t \in \mathcal{T}}$ as a L^2-process, certain conditions on the drift and diffusion coefficients $b(\cdot)$ and $\sigma(\cdot)$ need to be satisfied, compare Chapter 4.4. In the following we always assume existence of $\{X_t\}_{t \in \mathcal{T}}$. Furthermore, we restrict ourselves to MARKOV controls $U_M(\cdot)$, writing $U_t = U(t, X_t)$ for convenience. Additionally, we assume the MARKOV control $U(\cdot)$ to be sufficiently smooth whenever necessary.

Objective Functions

The performance index $J(\cdot)$ of the SOCP (7.1) is usually very similar to the one for deterministic OCPs, for one crucial difference: As we deal with stochastic processes, pathwise optimization over single trajectories of the processes is in general not possible. Hence, the cost criterion has to be given in a probabilistic fashion which is often accomplished by using the expectation value, i.e.,

$$J(t, x, u(\cdot)) = \mathbb{E}\left[\int_t^\tau L(s, X_s, u_s) \, \mathrm{d}s + M(\tau, X_\tau) \cdot \mathbb{1}_{\tau < \infty} \,\middle|\, X_t = x\right]. \tag{7.2}$$

The time instant τ within (7.2) facilitates many possibilities for SOCPs. E.g.,

- if $\mathcal{G} \subseteq \mathcal{T} \times \mathbb{R}^{n_X}$ is a fixed domain, then τ can denote the *first exit time* after t_0 from the domain $\mathcal{G}$ for the state process $\{X_t\}_{t \in \mathcal{T}}$, i.e.,

$$\tau = \inf_{\vartheta > t_0} \{(\vartheta, X_\vartheta(\omega)) \notin \mathcal{G}\} \leqslant \infty.$$

- As in the deterministic case, τ can characterize a *variable end time* that is free for optimization. In particular in the context of discounted performance criteria or *optimal stopping problems* this is a common choice.
- Thirdly, we can assume to stop the process $\{X_t\}_{t \in \mathcal{T}}$ at a *terminal time* $\tau = t_f$ rather than letting it evolve until it leaves the predefined region $\mathcal{G}$.

This lastly mentioned possibility will be the choice of τ throughout the rest of this work.

7.2 Solution Methodologies for Optimal Control Problems Driven by Stochastic Differential Equations

In the case of *discrete time* stochastic optimal control there are manifold methodologies to solve the arising problems numerically. Most of them are based on *stochastic programming* techniques [205, 215, 224] including *scenario tree* ideas. Recent approaches [60] mix approaches from stochastic and dynamic programming creating *particle methods*.

However, in continuous time methods for solving problems of type (7.1) can roughly be classified as we have seen in the deterministic setting of Chapter 1. Applying BELLMAN's *Principle of Optimality* leads to the stochastic HJB equation which is related to the dynamic programming idea. *Indirect* methods for stochastic optimal control build upon the *Stochastic Maximum Principle (SMP)*, whereas *direct* approaches approximate the original problem first and solve the resulting optimization problem thereafter.

For numerical applications there are basically two major standard methods for solving OCPs driven by SDEs: Ideas that focus on solving the HJB equation and approaches that approximate the original problem by one relying on MARKOV chains.

7.2.1 The HAMILTON-JACOBI-BELLMAN Equation

Let the stochastic process $\{X_t\}_{t \in \mathcal{T}}$ be given through the controlled SDE (7.1b) with the MARKOV control $U(t, X_t)$ chosen so as to optimize the objective function given by (7.2). Then the minimum value of the cost functional

$$V(t, x) = \min_{u(\cdot)} J(t, x, u(\cdot))$$

can be characterized by the principle of optimality, cf. Theorem 1.1, as in the deterministic setting.

Theorem 7.1 (HAMILTON-JACOBI-BELLMAN Equation; [141])
Let the optimal cost-to-go function $V(\cdot)$ of the SOCP (7.1) be sufficiently smooth and the terminal time t_f fixed. Then in a viscosity sense it satisfies the HAMILTON-JACOBI-BELLMAN (HJB) Partial Differential Equation (PDE)

$$0 = \min_{u \in \mathcal{U}} \left\{ L(t, x, u) + \frac{\partial V}{\partial t}(t, x) + \frac{\partial V}{\partial x}(t, x) b(t, x, u) + \frac{1}{2} \frac{\partial^2 V}{\partial x^2}(t, x)(\sigma \sigma^T)(t, x, u) \right\} \quad \text{(7.3a)}$$

with the terminal condition

$$V(t_\mathrm{f}, x) = M(t_\mathrm{f}, x) \tag{7.3b}$$

for all $t \in \mathcal{T}$ and all feasible $x \in \mathcal{X}$. △

If the minimum exists, it has to satisfy this necessary optimality condition. By adding certain regularity assumptions, cf. [141] and, in particular, [195], both existence and sufficiency can be proven. Hence, the problem of finding an optimal MARKOV control $u(\cdot)$ for the SOCP (7.1) shifts to finding a solution to the PDE (7.3).

The main difference to the HJB equation (1.13) for deterministic OCPs lies in the additional term

$$\frac{\partial^2 V}{\partial x^2}(t, x)(\sigma \sigma^T)(t, x, u)$$

including second order partial derivatives of the cost functional. These summand is implied by the diffusion part of the SDE (7.1b) determining the dynamics of the state process, as by the ITŌ isometry (4.18) we reason that in expectation it holds $(dB_t)^2 = dt$, slightly abusing notation.

Remark 7.1
If we assume the process $\{X_t\}_{t \in \mathcal{T}}$ to evolve within a specified domain $\mathcal{G}$ until it exits from it, the HJB equation (7.3a) is valid for all points $(t, x) \in \mathcal{G}$ and the terminal condition (7.3b) changes to a boundary condition that has to be satisfied for all $(t, x) \in \partial \mathcal{G}$, cf. [195]. In SOCPs with terminal conditions an approach including LAGRANGE multipliers for the constraints has proven to be applicable [195].

Remark 7.2

The HJB equation is closely related with the KOLMOGOROV *backward equation* [144]. If the process $\{X_t\}_{t \in \mathcal{T}}$ is given by a SDE with drift coefficient $\boldsymbol{b}(\cdot)$ and diffusion coefficient $\boldsymbol{\sigma}(\cdot)$, where these are moderately regular functions, than the transition probability of the process evolving from point $(t, \boldsymbol{x})$ to point $(s, \boldsymbol{y})$ at time $s > t$ has the density $p(t, \boldsymbol{x}; s, \boldsymbol{y})$ satisfying the KOLMOGOROV backward equation

$$\frac{\partial}{\partial t}\bar{p}(t,\boldsymbol{x}) + \frac{\partial}{\partial \boldsymbol{x}}\bar{p}(t,\boldsymbol{x})\boldsymbol{b}(t,\boldsymbol{x}) + \frac{1}{2}\frac{\partial^2}{\partial \boldsymbol{x}^2}\bar{p}(t,\boldsymbol{x})(\boldsymbol{\sigma}\boldsymbol{\sigma}^T)(t,\boldsymbol{x}) = 0,$$

where $\bar{p}(t,\boldsymbol{x}) = p(t,\boldsymbol{x}; s,\boldsymbol{y})$ for fixed s and $\boldsymbol{y}$, cf. [141].

In general, a solution to the HJB equation need not exist. Another impediment is that it often has an only formal meaning, and for a number of problems one cannot even write it down [157]. If there is a solution, it might be only piecewise continuous or measurable. For a detailed study of SOCPs and their corresponding HJB PDEs we refer to, e.g., [78, 92, 93, 149].

If we can assure that there exists a solution to the HJB equation, in most practical cases it will not be deducible analytically. Therefore, computational methods from numerical analysis for PDEs have to be applied. E.g., [3, 91, 238] and [95] give an overview of different ideas set up for problems and illustrations motivated by financial applications.

7.2.2 Indirect Methods Based on the SMP

In analogy to PONTRYAGIN*'s Maximum Principle (PMP)* for deterministic OCPs and starting with the work of HAROLD KUSHNER [154], the Stochastic Maximum Principle (SMP) has been developed in [30, 43, 107] and generalized by [47, 199]. In a similar fashion as for the PMP, it relies on introducing adjoint variables and then states necessary conditions of optimality depending on the states, controls, adjoint states, and possibly appearing constraints. Thereby a coupled system of *forward-backward SDEs* is obtained that—in combination with the appropriate conditions of optimality and adaptivity—can be used to solve the SOCP numerically.

The main difficulty therein is to preserve that the adjoint states, which are determined by backward SDEs with given terminal conditions, are adapted to the natural filtration of the BROWNian motion process. Recently, the development of special algorithms to solve these systems of forward-backward SDEs has been advanced, cf. [29, 72, 171]. However, often these approaches depend on the repeated calculation of expectations which has to be performed using, e.g., *Monte Carlo* approximations. Additionally, up to now the applicability of these algorithms is ensured only for forward-backward systems of SDEs that are weakly coupled.

7.2.3 Direct Methods: The MARKOV Chain Approximation Method

While numerically solving the system obtained by applying the SMP is an *indirect method* for SOCPs as seen for deterministic OCPs in Section 1.2.2 and tackling the HJB equation is related to the idea of dynamic programming, the following second standard approach can be seen as an analogue of a *direct method*.

Let the state process $\{X_t\}_{t \in \mathcal{T}}$ again be given by the controlled ITŌ diffusion (7.1b) with initial condition (7.1c). For the general method to be described now, it can as well be a *jump diffusion* including a POISSON jump process, but we restrict ourselves on the case stated in (7.1). Then

the basic idea of the MARKOV *Chain Approximation (MCA)* [155, 156, 157] method is to replace the original SOCP by a simpler stochastic process model and an appropriate cost functional. The first step is to approximate the original (controlled) state process by a (controlled) discrete parameter MARKOV *chain* $\xi^h = \{\xi_n^h \mid n \in \mathbb{N}_0\}$ on the discretized state space $\mathcal{R}^h \in \mathbb{R}^{n_X}$, where $h > 0$ is an approximation parameter. The stochastic evolution of the MARKOV chain process ξ^h is determined by the transition probability function $p^h(x, y \mid u)$ with $x, y \in \mathcal{R}^h$ and $u \in \mathcal{U}$, denoting the probability of the state switching from point x to y in one time step when the control action u is applied.

The necessary requirement for the MARKOV chain to be a good approximation of the original process $\{X_t\}_{t \in \mathcal{T}}$ is the *local consistency criterion* [157], which states from a local point of view that the conditional mean and covariance of changes in the state of the MARKOV chain are proportional to those of the original process. I.e., let an interpolation interval $\Delta t^h(x, u) > 0$ be given. We define $\Delta t_n^h = \Delta t^h(\xi_n^h, u_n^h)$, where u_n^h denotes the random variable that is the actual control action at step n. Furthermore, we assume that $\sup_{x,u} \Delta t^h(x, u) \to 0$ for $h \to 0$ and $\inf_{x,u} \Delta t^h(x, u) > 0$ for each $h > 0$. Finally, let $\Delta \xi_n^h = \xi_{n+1}^h - \xi_n^h$.

Definition 7.2 (Local Consistency Criterion)

The MARKOV *chain satisfies the* local consistency conditions *if*

$$
\begin{aligned}
&b^h(t, x, u) \cdot \Delta t^h(x, u) \\
&\quad \stackrel{\text{def}}{=} \mathbb{E}_{x,u}^{h,n}\left[\Delta \xi_n^h\right] = b(t, x, u) \cdot \Delta t^h(x, u) + o(\Delta t^h(x, u)), \quad\quad (7.4\text{a}) \\
&\hat{\sigma}^h(t, x, u) \cdot \Delta t^h(x, u) \\
&\quad \stackrel{\text{def}}{=} \mathbb{E}_{x,u}^{h,n}\left[\left(\Delta \xi_n^h - b^h(t, x, u) \cdot \Delta t^h(x, u)\right) \cdot \left(\Delta \xi_n^h - b^h(t, x, u) \cdot \Delta t^h(x, u)\right)^T\right] \\
&\quad = \left(\sigma \sigma^T\right)(t, x, u) \cdot \Delta t^h(x, u) + o(\Delta t^h(x, u)) \quad\quad (7.4\text{b})
\end{aligned}
$$

with $\mathbb{E}_{x,u}^{h,n}[\cdot] = \mathbb{E}\left[\cdot \mid \xi_i^h, u_i^h, i \leqslant n; \xi_n^h = x, u_n^h = u\right]$ *and* $\sup_{h,\omega}\left|\xi_{n+1}^h - \xi_n^h\right| \xrightarrow{h \to 0} 0$. $\triangle$

By that condition, the approximating MARKOV chain has the local properties of mean and variance of the process $\{X_t\}_{t \in \mathcal{T}}$. A continuous parameter interpolation of the chain is most often obtained by setting $\xi^h(t) = \xi_n^h$ and $u^h(t) = u_n^h$ for all $t \in [t_{n+1}^h, t_n^h)$.

The second step of the MCA method is to replace the original cost functional $J(\cdot)$ by one that is appropriate for the considered MARKOV chain. Therefor, let N^h denote the number of discretization steps of the time horizon $[t, t_f]$, i.e., $t_{N^h}^h = t_f$. Then we approximate $J(\cdot)$ by

$$
J^h(t, x, u^h(\cdot)) = \mathbb{E}\left[\sum_{i=0}^{N^h-1} L(t_i^h, \xi_i^h, u_i^h)\Delta t_i^h + M(t_{N^h}^h, \xi_{N^h}^h) \,\middle|\, t_0^h = t, \xi_0^h = x\right], \quad\quad (7.5)
$$

where the control policy $u^h = \{u_n^h \mid n \in \mathbb{N}_0\}$ for the chain is admissible, i.e., it satisfies the MARKOV property

$$
\mathbb{P}\left[\xi_{n+1}^h = y \,\middle|\, \xi_i^h, u_i^h, i \leqslant n\right] = p^h(\xi_n^h, y \mid u_n^h).
$$

If

$$
V^h(t, x) = \inf_{u^h} J^h(t, x, u^h(\cdot)),
$$

then the *dynamic programming* equation for the cost functional (7.5) becomes

$$V^h(t_n^h, \boldsymbol{x}) = \min_{\boldsymbol{u} \in \mathcal{U}} \left\{ \sum_{\boldsymbol{y} \in \mathcal{R}^h} p^h(\boldsymbol{x}, \boldsymbol{y} \mid \boldsymbol{u}) \cdot V(t_{n+1}^h, \boldsymbol{y}) + L(t_n^h, \boldsymbol{x}, \boldsymbol{u}) \cdot \Delta t^h(\boldsymbol{x}, \boldsymbol{u}) \right\}, \qquad (7.6a)$$

for all $n = 0, \ldots, N^h - 1$, all $\boldsymbol{x}, \boldsymbol{y} \in \mathcal{R}^h$, and with terminal condition

$$V^h(t_{N^h}^h, \boldsymbol{x}) = M(t_{N^h}^h, \boldsymbol{x}). \qquad (7.6b)$$

Eventually, this can be solved by, e.g., descent methods in the space of control policies, by JACOBI or GAUSS-SEIDEL iterations, cf. [157] or [106].

Typical examples for a numerical scheme to build the approximating MARKOV chain are finite difference methods with *nearest neighbor transitions* [157]. An alternative idea introduced by JACEK KRAWCZYK in [148] is based on the application of *weak approximations* of SDEs to derive the MARKOV chain. By that, the transitions probabilities $p^h(\cdot \mid \cdot)$ are only necessary for certain transitions which reduces the overall computational effort to solve the dynamic programming recursion (7.6). Figure 7.1 depicts the difference between the original MCA idea and the one based on a weak EULER-MARUYAMA approximation, where the noise increments $\Delta \boldsymbol{B}_t$ take only two values.

Remark 7.3

The MCA method is applicable to more kinds of problems that fit into the wide class of *stochastic control,* including *stopped* and *absorbed* controlled processes, ones that are *reflected at boundaries* of the state space; *discounted* cost functionals, *optimal stopping* and *infinite horizon* problems, etc. [157] gives a very extensive overview of those topics.

From a computational point of view both the discretization of the HJB equations and the MCA method depend on a fixed lattice regardless of the structure of the approximating MARKOV chain. Further on, the size of the grid is growing exponentially with the dimension of the state space, which certainly limits the size of the problems to be considered.

7.2.4 Alternative Approaches

Despite the previously mentioned methods are the most important and influential tools for solving SOCPs, there are more, partially relatively restrictive, ideas.

A first idea presented in [151] addresses the optimal control of nonlinear stochastic systems by considering the corresponding FOKKER-PLANCK-KOLMOGOROV *equation*. It provides a computational method based on policy iterations in the original infinite dimensional function space and on finite dimensional approximations of the controlled diffusion operator. Hence, low order approximations of this operator allow for significant reductions of the dimensionality.

Related to the MCA method the approach of [68, 69] approximates the diffusion process by a finite-dimensional MARKOV chain through the application of generalized *cell to cell mappings*. Unfortunately, the idea suffers from the curse of dimensionality as well.

As both the HJB and MCA methods do not work well for problems that are linear in the control and include stopping the process optimally, [64] provides an approximation of the solution by *polynomial interpolation* and solves for the optimal strategy switching between a maximum and a minimum mode by a collocation method with quadratic spline functions.
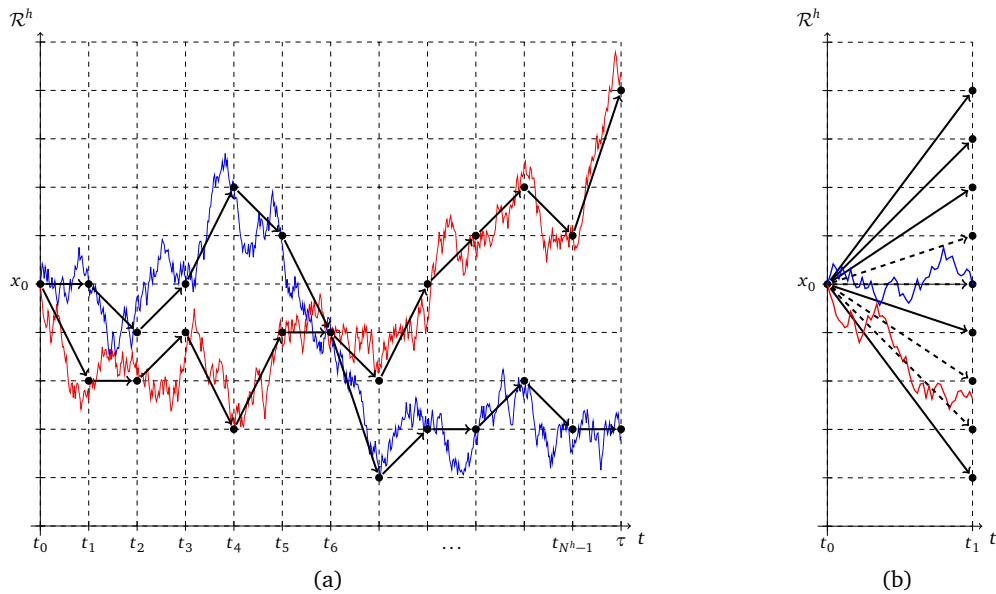
Figure 7.1: Visualization of the MARKOV chain approximation method. The *left* Figure (a) depicts two sample trajectories of a (controlled) stochastic process together with a chain approximating them. The *right* Figure (b) shows the difference between the original MARKOV chain approximation of HAROLD KUSHNER [156, 157] and the weak approximation idea of JACEK KRAWCZYK [148]: While in the original method in one time step transitions to each state $y \in \mathcal{R}^h$ of the lattice are possible with a positive probability $p^h(x, y \mid u) \geqslant 0$—visualized by the *solid* and *dashed* arrows—, with the weak approximation approach—depicted by only the *dashed* arrows—only a specific small number of grid points are reachable from x, depending on the chosen weak scheme. Hence, the transition probabilities are only positive for those grid points that are neighbored to the state points, where the weakly approximated process moves to under decision u.

Note that in this illustration these grid points of the weak approximation are chosen as to match with the sample trajectories of the process. In general this will not be the case: The appropriate grid points are determined by the weak scheme and the decision u depending on the actual time t and state point x.

Especially for high-dimensional biological systems [225] presents an idea of approximating the solution to the continuous problem by using continuous *function approximators* including a state augmentation. However, this method is very sensitive to the choice of parameters adjusting the function approximation.

[131] considers a special class of nonlinear, non-quadratic control problems where the nonlinear HJB equation can be transformed into a linear equation. Then, the usual backward integration of the dynamic programming recursion can be replaced by computing expectations and a forward diffusion process. This requires stochastic integration over trajectories that can be described by a *path integral*.

Another alternative is based on the *optimal quantization* of stochastic processes, cf. [173, 174, 197], which analyzes the optimal approximation of random vectors by *quantized* vectors taking only a finite number of values. In financial applications of stochastic control where the underlying state process can be split into a (multi-dimensional) uncontrolled process $\{Y_t\}_{t \in \mathcal{T}}$ and a—usually one-dimensional—controlled process $\{Z_t\}_{t \in \mathcal{T}}$, [198] describes a method in which the original process is firstly approximated by the EULER-MARUYAMA scheme. Afterwards, the discretized parts $\{\tilde{Y}_t\}_{t \in \mathcal{T}}$ and $\{\tilde{Z}_t\}_{t \in \mathcal{T}}$ are quantized by an optimal grid making use of the

quantization of the BROWNian motion (for $\{\tilde{Y}_t\}_{t\in\mathcal{T}}$), and using an orthogonal lattice and a simple closest neighbor projection onto it (for $\{\tilde{Z}_t\}_{t\in\mathcal{T}}$), respectively. This procedure allows to preserve the MARKOV structure of the considered original process to be able to apply general control theory, in particular dynamic programming, but with largely reduced dimensions.

7.3 Finite Horizon Stochastic Optimal Control and the WIENER Chaos Approach

In this section we apply the WIENER chaos approach that we have introduced in Chapter 5 and applied to numerically solve SDEs in the previous one to finite horizon OCPs (7.1) that are driven by controlled stochastic processes. To keep notations clear, we restrict ourselves again to the one-dimensional case $n_X = n_B = 1$. Generalizations to multi-dimensionality can be done straightforwardly.

We consider the SDE (7.1b), where we proceed in a similar way as before to obtain the propagator of the system. Besides the expansion of the state process $\{X_t\}_{t\in\mathcal{T}}$ we have to include a second chaos expansion determining the control process $\{u_t\}_{t\in\mathcal{T}}$, i.e., (with the basis polynomials $\Psi^{\boldsymbol{\alpha}}(\boldsymbol{\eta})$ defined as before), i.e.,

$$u_t = \sum_{\boldsymbol{\alpha}\in\mathcal{I}} u_{\boldsymbol{\alpha}}(t)\Psi^{\boldsymbol{\alpha}}(\boldsymbol{\eta}). \tag{7.7}$$

Remark 7.4
By incorporating expansion (7.7) directly in the propagator obtained for a controlled SDE, we cannot guarantee the assumed feedback character of the MARKOV control $u_t = u(t, X_t)$ anymore.

From a computational point of view, there is another disadvantage of directly implementing the expansion (7.7) of the control process: The final *deterministic* optimal control problem we want to deduce would contain the same number of state and control functions $x_{\boldsymbol{\alpha}}(t)$ and $u_{\boldsymbol{\alpha}}(t)$ in that case. Hence, the resulting problem would be very hard to solve numerically.

The remedy to both problems lies in the following theorem, cf. [116].

Theorem 7.2
Assume that the MARKOV control $u_t = u(t, X_t)$ can be TAYLOR-expanded in terms of X_t. Then by considering the q-th order polynomial

$$u^q(t, X_t) = \sum_{i=0}^{q} \hat{u}_i(t) X_t{}^i, \tag{7.8}$$

the original control coefficients $u_{\boldsymbol{\alpha}}(t)$ of (7.7) are characterized completely by the q+1 new control functions $\hat{u}_i(t)$, $i = 0,\ldots,q$, and the state coefficients $x_{\boldsymbol{\alpha}}(t)$. Furthermore, the resulting control u_t^q is automatically non-anticipative and tends to u_t for $q \to \infty$. △

Proof In contrast to expanding $u(t, X_t)$ in t, for calculating the expansion in terms of X_t we do not need a stochastic TAYLOR expansion as introduced in Section 6.1.2 to derive high

order numerical integration schemes for SDEs. It suffices to apply a standard (infinite) TAYLOR expansion in $X_t = \xi$, yielding

$$u_t = \sum_{n=0}^{\infty} \frac{1}{n!} \frac{\partial^n u}{\partial x^n}(t, X_t)\big|_{X_t = \xi} (X_t - \xi)^n$$

which can always be rewritten in powers of X_t. Hence, with defining new control functions $\hat{u}_i(t)$, $i \in \mathbb{N}$, as the coefficient terms of these powers, one arrives at the infinite version of (7.8). Similarly, a finite version up to order q can be defined with the q-th term corresponding to the remaining error. The convergence to u_t follows directly and so does the non-anticipativity as we express u_t through the state process which fulfills the property by definition.

Now if we compare (7.7) and (7.8)

$$\sum_{\boldsymbol{\alpha} \in \mathcal{I}} u_{\boldsymbol{\alpha}}(t) \Psi^{\boldsymbol{\alpha}}(\boldsymbol{\eta}) = \sum_{i=0}^{q} \hat{u}_i(t) X_t^{\,i} \tag{7.9}$$

by inserting the chaos expansion (5.30) of X_t and projecting the resulting expression onto the chaos bases, we obtain a system describing the original control coefficients $u_{\boldsymbol{\alpha}}(t)$ by the new control functions $\hat{u}_i(t)$ and the state coefficients $x_{\boldsymbol{\alpha}}(t)$, while having the feedback character of the MARKOV control included implicitly. □

Example 7.1

Assume $q = 2$. Then the quadratic and non-anticipative expansion of the control process $\{u_t\}_{t \in \mathcal{T}}$ is given by (7.7), where the coefficients $u_{\boldsymbol{\alpha}}(t)$ are defined by the system

$$u_{\boldsymbol{\alpha}}(t) = \hat{u}_0(t) \cdot \mathbb{1}_{\{\boldsymbol{\alpha}=0\}} + \hat{u}_1(t) \cdot x_{\boldsymbol{\alpha}}(t)$$
$$+ \hat{u}_2(t) \cdot \sum_{\boldsymbol{\beta} \in \mathcal{I}} \sum_{0 \leqslant \boldsymbol{\gamma} \leqslant \boldsymbol{\alpha}} C(\boldsymbol{\alpha}, \boldsymbol{\gamma}, \boldsymbol{\beta}) x_{\boldsymbol{\alpha}-\boldsymbol{\gamma}+\boldsymbol{\beta}}(t) x_{\boldsymbol{\gamma}+\boldsymbol{\beta}}(t) \tag{7.10}$$

for all $\boldsymbol{\alpha} \in \mathcal{I}$ and $C(\boldsymbol{\alpha}, \boldsymbol{\gamma}, \boldsymbol{\beta})$ given by (compare Theorem 5.6, in particular Equation (5.34), [172])

$$C(\boldsymbol{\alpha}, \boldsymbol{\gamma}, \boldsymbol{\beta}) = \sqrt{\binom{\boldsymbol{\alpha}}{\boldsymbol{\gamma}} \binom{\boldsymbol{\gamma}+\boldsymbol{\beta}}{\boldsymbol{\beta}} \binom{\boldsymbol{\alpha}-\boldsymbol{\gamma}+\boldsymbol{\beta}}{\boldsymbol{\beta}}}.$$

All multi-index operations are defined component-wise again, including the binomial coefficient that is calculated as the product of the component's binomial coefficients. Note as well that by $0 \leqslant \boldsymbol{\gamma} \leqslant \boldsymbol{\alpha}$ it holds $\boldsymbol{\alpha} + \boldsymbol{\gamma} - \boldsymbol{\beta} \in \mathcal{I}$ and $\boldsymbol{\gamma} + \boldsymbol{\beta} \in \mathcal{I}$.

Combining Theorems 6.1 and 7.2 we obtain a deterministic reformulation of the controlled SDE (7.1b). Hence, the only missing part of our transformation method is the objective function (7.1a) of the original SOCP. But as this is already formulated as an expectation value, it can be rewritten directly in terms of the deterministic coefficients $x_{\boldsymbol{\alpha}}(t)$ of the state process $\{X_t\}_{t \in \mathcal{T}}$ and the (new) control functions $\hat{u}_i(t)$. Hence, confining again to the one-dimensional case for notational reasons, we obtain a deterministic OCP that fully captures the original stochastic problem if we do not apply any form of truncation, i.e., if we do not restrict p, k, or q.

Corollary 7.1

The deterministic OCP

$$\min_{\{\hat{u}_i(\cdot)\}_{i\in\mathbb{N}}} J\left(t_0, x_0, \{\hat{u}_i(\cdot)\}_{i\in\mathbb{N}}\right) \tag{7.11a}$$

$$s.t. \quad \dot{x}_{\boldsymbol{\alpha}}(t) = b_{\boldsymbol{\alpha}}\left(t, X_t, \sum_{i=1}^{\infty} \hat{u}_i(t) X_t^{\ i}\right) + \sum_{j=1}^{\infty} \sqrt{\alpha_j} m_j(t) \sigma_{\boldsymbol{\alpha}^-(j)}\left(t, X_t, \sum_{i=1}^{\infty} \hat{u}_i(t) X_t^{\ i}\right)$$

$$\forall t \in \mathcal{T}, \ \forall \boldsymbol{\alpha} \in \mathcal{I}, \tag{7.11b}$$

$$x_{\boldsymbol{\alpha}}(t_0) = \mathbb{1}_{\{\boldsymbol{\alpha}=0\}} x_0. \tag{7.11c}$$

is equivalent to the original SOCP (7.1). Having deduced the set of optimal control coefficient functions $\{\hat{u}_i(t)\}_{t\in\mathcal{T}, i\in\mathbb{N}}$, the optimal MARKOV *control policy $u(t, X_t)$ is obtainable immediately through Theorem 7.2.* △

In applications, the controlled SDE (7.1b) generally includes nonlinear drift or diffusion terms—e.g., square roots or fractions of stochastic processes—that cannot be treated by the multiplication formula (5.33) of chaos expansions and a basic comparison of coefficients. In the field of general Polynomial Chaos (PC), [70] describes an idea to reformulate those nonlinearities as complex equation systems. This requires the introduction of auxiliary algebraic states and results in a propagator Differential-Algebraic Equation (DAE) system instead of the Ordinary Differential Equation (ODE) system (7.11b). However, this DAE system can be efficiently solved in the context of direct optimal control. Additionally, this allows the consideration of algebraic equations in the original SOCP (7.1) as well. We will illustrate this procedure in the following Chapter 8.3.

The following Algorithm 7.1 summarizes the steps to solve a SOCP by the introduced WIENER chaos method.

Algorithm 7.1: Necessary steps for solving a finite-horizon SOCP (7.1) by the proposed WIENER chaos method.

---

input : Order p of the chaos expansions and number k of included random variables, adaptivity vector $(\boldsymbol{r})$, order q of the control expansion.

output: Optimal control coefficients $\hat{u}_i(t)$, $i = 0, \ldots, q$, and optimal chaos coefficients $x_{\boldsymbol{\alpha}}(t)$, $\boldsymbol{\alpha} \in I_{k,p}^{(r)}$ for all $t \in \mathcal{T}$, optimal objective function value.

1 Prepare the index set $I_{k,p}^{(r)}$ of multi-indices $\boldsymbol{\alpha}$.

2 Calculate the control expansion (7.8), i.e., the control chaos coefficients $u_{\boldsymbol{\alpha}}(\cdot)$ depending on the new control functions $\hat{u}_i(\cdot)$ and the state chaos coefficients $x_{\boldsymbol{\alpha}}(\cdot)$.

3 Derive the propagator system of the controlled SDE (7.1b). This might require the introduction of (auxiliary) algebraic state coefficients for nonlinear dynamics or general algebraic terms.

4 Transform the objective function (7.1a) depending on the chaos expansions of state and control.

5 Solve the resulting deterministic OCP.

Remark 7.5

Choosing p and k adaptively to satisfy given error bounds (cf. Theorems 6.3 and 6.4) might be profitable. However, refining the used truncation orders would generally require calculating

new control chaos coefficients and deriving and solving a new propagator system of state chaos coefficients. This is caused by the associated extension of the multi-index set and the coupling of the propagator equations.

If, for numerical applicability, we use any form of truncation, the resulting deterministic OCP is an approximation of the original one. Its solution tends to the solution of (7.1) for $p, k, q \to \infty$. We give detailed examples for solving SOCPs by applying Corollary 7.1 and different magnitudes of truncation in Chapter 8.

Remark 7.6

To reflect that optimal controls can be discontinuous, our preference for solving the resulting deterministic OCP after applying expansion (7.8) is BOCK's direct multiple shooting approach, compare Section 1.3. Within this method controls are identified on a discrete multiple shooting grid, see (1.15), allowing discontinuous control profiles for each $\hat{u}_i(t)$, $i = 0, \ldots, q$.

Moreover, through the introduced methodology we can as well consider SOCPs with *integer control functions* $v(t) \in \mathcal{V} = \{v^1, \ldots, v^{n_v}\}$, $t \in \mathcal{T}$. Efficient approaches to treat these controls can be found in, e.g., [217, 218].

7.4 Summary

In this chapter we defined a class of OCPs that are modeled by making use of SDEs. We surveyed standard numerical approaches for solving problems of this class and showed connections to related methods of deterministic optimal control.

Thereafter, we applied the ideas of the previous chapter, i.e., the propagator method based on the WIENER chaos expansion, to SOCPs. This idea results in a generic approach to solve finite horizon SOCPs.

To ensure the feedback character of the appearing control process, we utilized a suited expansion of the MARKOV control. Together with the numerically necessary truncations we have already presented, we obtained a tractable deterministic counterpart of the original SOCP that can be efficiently solved by the direct multiple shooting method of deterministic optimal control. Consequently, this new methodology facilitates the application of state-of-the-art methods of deterministic optimization and control to the broad context of random processes and SDEs.

8 Numerical Application: Stochastic Optimal Control and the WIENER Chaos Approach

In this chapter we finally apply all the results of Part II to numerically solve Stochastic Optimal Control Problems (SOCPs) by using their deterministic WIENER chaos reformulations and appropriate methods of deterministic optimal control. First we consider a standard problem of stochastic optimal control—*the linear-quadratic stochastic regulator problem*—where we have the opportunity to compare the computational results of the propagator method to the analytical solution of the problem. Afterwards we analyze a more advanced regulator problem where a nonlinear Stochastic Differential Equation (SDE) determines the dynamics of the system and which does not exhibit such an analytical solution. These results appeared mostly in [115, 116].

We finish the chapter by returning to the conspicuous consumption problem of Chapter 3 and considering the recession strength as a random process.

8.1 A Linear-Quadratic Stochastic Regulator Problem

Our first example for solving optimal control problems driven by SDEs with the help of the novel chaos approach developed in Chapters 6 and 7 is the standard linear-quadratic stochastic regulator problem [141, 195]. The advantage of this academic example is that we can solve the corresponding HAMILTON-JACOBI-BELLMAN (HJB) partial differential equation analytically, i.e., we have an exact solution to compare our numerical results with.

On the time horizon $\mathcal{T} = [0, 1]$ we consider the one-dimensional stochastic regulator problem

$$\min_{u. \in \mathcal{A}} \quad \mathbb{E}\left[\frac{1}{2}\int_0^1 \left(X_t{}^2 + u_t{}^2\right) \mathrm{d}t + \frac{1}{2}X_1^2\right] \tag{8.1a}$$

$$\text{s.t.} \quad \mathrm{d}X_t = (X_t + u_t)\,\mathrm{d}t + \sigma\,\mathrm{d}B_t, \tag{8.1b}$$

$$X_0 = x_0, \tag{8.1c}$$

where the coefficient $\sigma \in \mathbb{R}$ determining the diffusion term of the controlled stochastic process $\{X_t\}_{t\in[0,1]}$ is merely a scalar. Then the optimal MARKOV feedback rule solving the SOCP (8.1) can be calculated as

$$u_t(\omega) = u^*(t, X_t(\omega)) = \left(\sqrt{2}\tanh\left(\sqrt{2}(t-1)\right) - 1\right) \cdot X_t(\omega) \quad \forall t \in [0, 1]. \tag{8.2}$$

We have to keep in mind that the feedback rule (8.2) at each instant of time $t \in [0, 1]$ depends linearly on the actual state X_t of the system, as each such pair of time and state can be inter-

preted as the initial point of a separate problem. Further on, the MARKOV control u_t depends explicitly on the time t. The optimal cost of the problem is

$$J^*(t_0 = 0, x_0) = \frac{1}{2}\left(1 + \sqrt{2}\tanh\left(\sqrt{2}\right)\right)x_0{}^2 + \frac{1}{2}\sigma^2\left(1 + \ln\left(\cosh\left(\sqrt{2}\right)\right)\right)$$

and the expectation and variance of the solution process can be calculated analytically as well, using the properties of the stochastic integral and ITŌ's formula, giving

$$\mathbb{E}[X_t] = x_0 \frac{\cosh\left(\sqrt{2}(t-1)\right)}{\cosh\left(\sqrt{2}\right)},$$

$$\mathbb{V}[X_t] = \frac{\sigma^2}{2\sqrt{2}}\left(2\tanh\left(\sqrt{2}\right)\cosh^2\left(\sqrt{2}(t-1)\right) + \sinh\left(2\sqrt{2}(t-1)\right)\right).$$

Applying the propagator method of Sections 6.2 and 7.3 to the SDE (8.1b) in its integral form, we deduce

$$x_{\boldsymbol{\alpha}}(t) = x_0 \cdot \mathbb{1}_{\{\boldsymbol{\alpha}=0\}} + \int_0^t (x_{\boldsymbol{\alpha}}(s) + u_{\boldsymbol{\alpha}}(s))\, ds + \sum_{j=1}^\infty \int_0^t \sqrt{\alpha_j}\, m_j(s)\, \mathbb{E}\left[\sigma\, \Psi^{\boldsymbol{\alpha}^-(j)}(\boldsymbol{\eta})\right] ds,$$

with the basis functions $m_i(\cdot)$ of $L^2(\mathcal{T})$, $i \in \mathbb{N}$, defined as in (5.25) and the control coefficients $u_{\boldsymbol{\alpha}}(t)$ given by (7.8) and (7.9)—for preparing a system to be used numerically this will be up to some order q. The expectation value within the last summand is not equal to zero only if $\boldsymbol{\alpha}^-(j) = \boldsymbol{0}$ or, equivalently, $\boldsymbol{\alpha} = \boldsymbol{e}_j$, $j \in \mathbb{N}$. Therefore, the resulting system of Ordinary Differential Equations (ODEs) reads for all $\boldsymbol{\alpha} \in \mathcal{I}$ and $u_{\boldsymbol{\alpha}}(t)$ expanded as explained

$$\dot{x}_{\boldsymbol{\alpha}}(t) = x_{\boldsymbol{\alpha}}(t) + u_{\boldsymbol{\alpha}}(t) + \sigma\, m_j(t) \cdot \mathbb{1}_{\{\boldsymbol{\alpha}=\boldsymbol{e}_j,\, j\in\mathbb{N}\}},$$

$$x_{\boldsymbol{\alpha}}(0) = x_0 \cdot \mathbb{1}_{\{\boldsymbol{\alpha}=0\}}.$$

As stated before, we can transform the objective function (8.1a) by directly inserting the chaos expansions (5.22) and (7.8) of X_t and the MARKOV control u_t. However, our numerical experiences showed that it is beneficial to convert MAYER-type objectives into their corresponding LAGRANGE form. Despite a slightly better convergence behavior, the computational costs are reduced notably.

Hence, applying ITŌ's formula (4.22) to the function $f(X_t) = \frac{1}{2}X_t{}^2$ yields

$$\mathbb{E}\left[\frac{1}{2}X_1{}^2\right] = \frac{1}{2}x_0{}^2 + \mathbb{E}\left[\int_0^1\left(X_t(X_t + u_t) + \frac{1}{2}\sigma^2\right)dt\right] + \underbrace{\mathbb{E}\left[\int_0^1 \sigma X_t\, dB_t\right]}_{=0}$$

$$= \frac{1}{2}x_0{}^2 + \frac{1}{2}\sigma^2 + \mathbb{E}\left[\int_0^1 X_t(X_t + u_t)\, dt\right].$$

This changes the objective function (8.1a) to

$$\mathbb{E}\left[\frac{1}{2}\int_0^1 (X_t{}^2 + u_t{}^2)\, dt + \frac{1}{2}X_1{}^2\right]$$

$$= \frac{1}{2}(x_0{}^2 + \sigma^2) + \mathbb{E}\left[\frac{1}{2}\int_0^1 \left(X_t{}^2 + u_t{}^2 + 2X_t(X_t + u_t)\right)\mathrm{d}t\right]$$

$$= \frac{1}{2}(x_0{}^2 + \sigma^2) + \mathbb{E}\left[\frac{1}{2}\int_0^1 \left((X_t + u_t)^2 + 2X_t{}^2\right)\mathrm{d}t\right]$$

$$= \frac{1}{2}(x_0{}^2 + \sigma^2) + \frac{1}{2}\int_0^1 \sum_{\boldsymbol{\alpha}\in\mathcal{I}} \left((x_{\boldsymbol{\alpha}}(t) + u_{\boldsymbol{\alpha}}(t))^2 + 2x_{\boldsymbol{\alpha}}{}^2(t)\right)\mathrm{d}t.$$

Finally, for numerical investigations we have to truncate the index set $\mathcal{I}$ and the control expansion (7.8) appropriately. In the sequel we assume a quadratic approximation of the control rule, i.e., $q = 2$. Remember that the exact control (8.2) is only linear in X_t. Additionally, we use different choices of (simply and adaptively) truncated index sets $\mathcal{I}_{k,p}^{(r)}$, compare Section 6.2.2 and, in particular, Table 6.1. We deduce the deterministic optimal control problem

$$\min_{\hat{u}_0(\cdot),\hat{u}_1(\cdot),\hat{u}_2(\cdot)} \left\{\frac{1}{2}(x_0{}^2 + \sigma^2) + \frac{1}{2}\int_0^1 \sum_{\boldsymbol{\alpha}\in\mathcal{I}_{k,p}^{(r)}} \left((x_{\boldsymbol{\alpha}}(t) + u_{\boldsymbol{\alpha}}(t))^2 + 2x_{\boldsymbol{\alpha}}{}^2(t)\right)\mathrm{d}t\right\} \tag{8.3a}$$

$$\text{s.t.} \quad \dot{x}_{\boldsymbol{\alpha}}(t) = x_{\boldsymbol{\alpha}}(t) + u_{\boldsymbol{\alpha}}(t) + \sigma\, m_j(t)\cdot \mathbb{1}_{\{\boldsymbol{\alpha}=e_j\}} \tag{8.3b}$$

$$x_{\boldsymbol{\alpha}}(0) = x_0 \cdot \mathbb{1}_{\{\boldsymbol{\alpha}=0\}} \tag{8.3c}$$

with

$$u_{\boldsymbol{\alpha}}(t) = \hat{u}_0(t)\cdot \mathbb{1}_{\{\boldsymbol{\alpha}=0\}} + \hat{u}_1(t)\,x_{\boldsymbol{\alpha}}(t)$$
$$+ \hat{u}_2(t)\cdot \sum_{\boldsymbol{\beta}\in\mathcal{I}_{k,p}^{(r)}} \sum_{0\leqslant\gamma\leqslant\boldsymbol{\alpha}} C(\boldsymbol{\alpha},\boldsymbol{\gamma},\boldsymbol{\beta})\,x_{\boldsymbol{\alpha}-\gamma+\beta}(t)\,x_{\gamma+\beta}(t) \tag{8.3d}$$

as given in Example 7.1.

The resulting problem (8.3) can now be solved by sophisticated methods of deterministic optimal control as it does not explicitly involve random components anymore. All stochastic information is included within the ODE system (8.3b). The problem includes $|\mathcal{I}_{k,p}^{(r)}|$ state functions corresponding to the coefficients $x_{\boldsymbol{\alpha}}(t)$ of the chaos expansion and three control functions as we use a quadratic approximation of the feedback rule.

Our method of choice for obtaining the numerical results presented now is the software package MUSCOD-II [160] built upon BOCK's direct multiple shooting approach. The corresponding numerical experiments have been performed using the initial values $x_0 = \frac{1}{2}$ and $x_0 = 1$, the diffusion parameter $\sigma = 0.15$, and different truncation numbers k and approximation orders p of the chaos expansion. Furthermore, we computed the solutions of all problems using $N_{\text{shoot}} = 40$ multiple shooting nodes, a constant control discretization (1.15), and the RUNGE-KUTTA-FEHLBERG scheme *RKF45* [87] to integrate the ODE system on each multiple shooting interval. The derivatives and sensitivities have been calculated by a Internal Numerical Differentiation (IND) procedure. By the use of the relatively large number of 40 shooting nodes (on the comparatively small time horizon $\mathcal{T} = [0, 1]$) we still achieve a very good variability of the obtained control functions $\hat{u}_i(\cdot)$, $i = 0,\ldots,q$.

Remark 8.1

The deterministic Optimal Control Problem (OCP) (8.3) cannot be implemented straightfor-
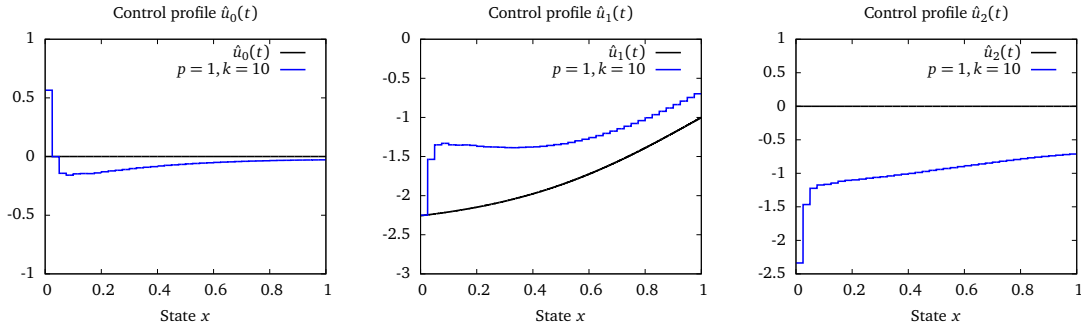
Figure 8.1: Optimal controls of the linear-quadratic stochastic regulator problem (8.1). The plots depict solutions of the deterministic optimal control problem (8.3) resulting from applying the WIENER chaos methodology of Chapters 6 and 7, i.e., the new control functions $\hat{u}_i(t)$, $i = 0, \ldots, q$ introduced in the expansion (7.8) with $q = 2$ to preserve the non-anticipativity of the MARKOV control in its chaos expansion. In comparison the exact functions (compare (8.2)) are shown.

Here the new control functions are obtained from truncating the index set $\mathcal{I}$ of the chaos expansion with $k = 10$ basis functions $m_i(\cdot)$ of the underlying HILBERT space $L^2([0, 1])$ (which corresponds to $k = 10$ random variables) and approximation order $p = 1$, resulting in eleven basis polynomials that describe the stochastic system. Because of that simple GAUSSIAN approximation the quadratic expansion of the MARKOV control collapses to a linear one, whereas these apparently wrong solutions yield good results, compare Figure 8.3.
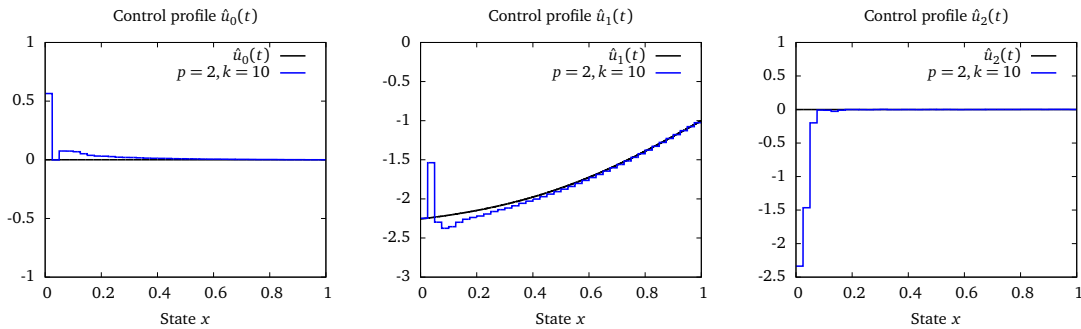
Figure 8.2: Optimal controls of the linear-quadratic stochastic regulator problem (8.1) as in Figure 8.1. Now the controls are computed for $k = 10$ random variables and approximation order $p = 2$. Thus, we come very close to the desired results, including $\hat{u}_2(t) \approx 0$ as supposed.

wardly in `MUSCOD-II` as the software does not support multi-indexing of the appearing variables, i.e., the state and control coefficients $x_{\alpha}(\cdot)$ and $u_{\alpha}(\cdot)$ depending on the multi-indices $\alpha \in \mathcal{I}_{k,p}^{(r)}$. To overcome this issue, we use `MATLAB`'s functionality to generate the set $\mathcal{I}_{k,p}^{(r)}$, perform the problem-specific calculations of multi-indices, deduce the objective function and the propagator system depending on the multi-indices, and export the resulting OCP to a `MUSCOD-II` problem source file by a tailored script. Within this script the multi-index α is transformed into a one-dimensional index with the help of a search algorithm.

Figures 8.1 and 8.2 illustrate the behavior of the new control functions $\hat{u}_i(t)$, $i = 0, \ldots, q = 2$, that we introduce to preserve the feedback character of the MARKOV control $u_t = u(t, X_t)$ of the original stochastic problem (8.1). Note that we use a quadratic expansion (7.8) although the exact feedback rule is only linear in X_t (compare (8.2)). The solutions shown in Figure 8.1 are computed by a purely GAUSSIAN approximation of the chaos space, i.e., by truncating the index set $\mathcal{I}$ with an approximation order $p = 1$. This leaves only first order chaos basis polynomials $\Psi^{\alpha = e_i}(\eta) = \eta_i$ for $i \in \mathbb{N}$ within the construction (apart from the zero-order one),
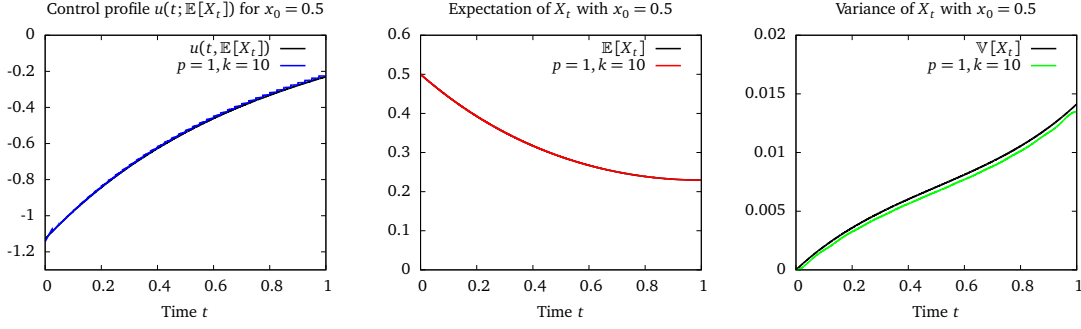
Figure 8.3: Solution paths of the linear-quadratic stochastic regulator problem (8.1) with initial value $x_0 = 0.5$. All plots show again a comparison of exact solutions and the corresponding path obtained by the introduced WIENER chaos approach, i.e., a solution to the transformed deterministic optimal control problem (8.3) with $k = 10$ included basis functions/random variables and an approximation order $p = 1$.
The *first* plot depicts the control profile $u(t; \mathbb{E}[X_t])$, the *second* one the expectation of the state process $\mathbb{E}[X_t]$, and the *third* figure its variance $\mathbb{V}[X_t]$.

which are standard GAUSSian random variables. Hence, the system of control coefficients $u_{\boldsymbol{\alpha}}(t)$ induced by (7.8) as in Example 7.1 is not quadratic in the state coefficients $x_{\boldsymbol{\alpha}}(t)$ anymore. To justify this, we calculate

$$u_{\mathbf{0}}(t) = \hat{u}_0(t) + \hat{u}_1(t) x_{\mathbf{0}}(t) + \hat{u}_2(t) \cdot \sum_{\boldsymbol{\beta} \in \mathcal{I}_{1,k}} \underbrace{C(\mathbf{0}, \mathbf{0}, \boldsymbol{\beta})}_{=1} x_{\boldsymbol{\beta}}{}^2(t),$$

where the last term can merely be seen as a multiple of the process's variance plus the quadratic expectation, and for $\boldsymbol{\alpha} \neq \mathbf{0}$

$$
\begin{aligned}
u_{\boldsymbol{\alpha}}(t) = {} & \hat{u}_1(t) x_{\boldsymbol{\alpha}}(t) + \\
& + \hat{u}_2(t) \cdot \sum_{\boldsymbol{\beta} \in \mathcal{I}_{1,k}} \left(C(\boldsymbol{\alpha}, \mathbf{0}, \boldsymbol{\beta}) x_{\boldsymbol{\alpha}+\boldsymbol{\beta}}(t) x_{\boldsymbol{\beta}}(t) + C(\boldsymbol{\alpha}, \boldsymbol{\alpha}, \boldsymbol{\beta}) x_{\boldsymbol{\beta}}(t) x_{\boldsymbol{\alpha}+\boldsymbol{\beta}}(t) \right) \\
= {} & \hat{u}_1(t) x_{\boldsymbol{\alpha}}(t) + 2\, \hat{u}_2(t) x_{\mathbf{0}}(t) x_{\boldsymbol{\alpha}}(t),
\end{aligned}
$$

as all appearing coefficients $\boldsymbol{\alpha}$, $\boldsymbol{\beta}$, and $\boldsymbol{\alpha}+\boldsymbol{\beta}$ have to be within the index set $\mathcal{I}_{k,1}$. This explains the differences of the exact solutions and the ones shown in Figure 8.1. Moreover, only $k = 10$ random variables, i.e., basis functions, $\eta_i = W(m_i)$, $i = 1, \ldots, k$, are included in the construction of the basis polynomials $\Psi^{\boldsymbol{\alpha}}(\boldsymbol{\eta})$ used to obtain the plotted solutions. By increasing the order p, the system of control coefficients becomes quadratic in the state coefficients, which is why the solutions shown in Figure 8.2 (computed with $k = 10$ and $p = 2$) come closer to the exact ones, including $\hat{u}_2(t) \approx 0$ as anticipated.

Figure 8.3 shows different solution paths of the transformed deterministic OCP (8.3) in comparison with the appropriate exact solutions of the original stochastic problem (8.1) for given initial values x_0. Again the results of the chaos approach are obtained with the simple truncation (6.14) using $k = 10$ basis functions $m_i(\cdot)$ of the space $L^2(\mathcal{T})$ giving $k = 10$ random variables and an approximation order $p = 1$ for constructing the basis polynomials $\Psi^{\boldsymbol{\alpha}}(\boldsymbol{\eta})$ with $\boldsymbol{\alpha} \in \mathcal{I}_{p,k}$.

Within the figure the first plot depicts the optimal control profile depending on the time $t \in \mathcal{T} = [0,1]$ and the expectation of the process at that time, i.e., the control function
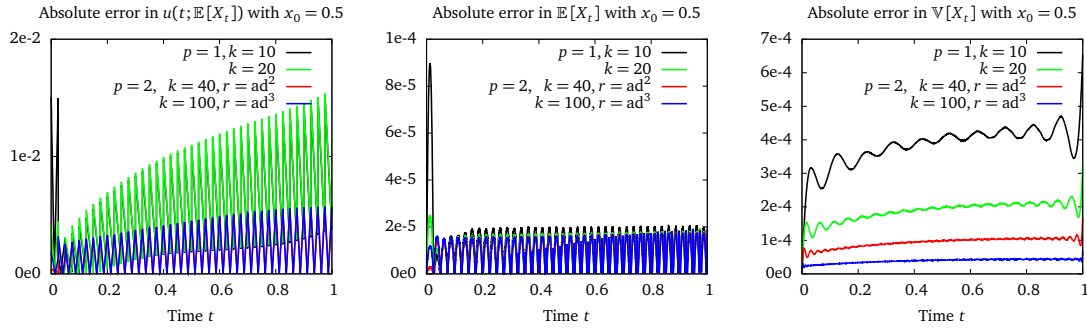
Figure 8.4: Absolute errors of the solutions of the linear-quadratic stochastic regulator problem (8.1) computed by the novel chaos approach for different numbers k of involved random variables and orders p to construct the basis polynomials $\Psi^\alpha(\eta)$. The sequence of plots is as in Figure 8.3, i.e., the *first* one showing the errors within the control profile $u(t; \mathbb{E}[X_t])$, the *second* one errors in the expectation $\mathbb{E}[X_t]$, and the *third* plot errors in the variance $\mathbb{V}[X_t]$.

$u(t; \mathbb{E}[X_t | X_0 = x_0])$. By viewing this uncommon profile we get an impression of the accuracy of the numerically obtained control at states where the process will be most likely or better to say, in expectation, at time t. The remaining two plots of Figure 8.3 show the corresponding expectation and variance of the process.

From purely visual comparison we see how well the introduced chaos method works, even for very low approximations of the WIENER chaos space and even as the new control functions $\hat{u}_i(t), i = 0, \ldots, q = 2$, deviate from their exact counterparts as we saw in Figure 8.1. This holds especially if we are interested in calculating the objective, expectations and possibly higher moments of the solution process for a given initial value to the original problem because they are a direct byproduct of the new methodology.

Figure 8.4 illustrates the absolute errors of $u(t; \mathbb{E}[X_t])$, $\mathbb{E}[X_t]$, and $\mathbb{V}[X_t]$ over time for $x_0 = 0.5$ and different choices of truncation. We notice that the error decreases if the number of random variables k and the approximation order p are increased. E.g., the absolute error of the expectation process $\mathbb{E}[X_t]$ in the time interval $[0, 1]$ is at most $1 \cdot 10^{-4}$ for the low approximation $(p, k) = (1, 10)$ and decays to $2 \cdot 10^{-5}$ for $(p, k) = (2, 40)$, which is very astonishing. Particularly the enhancement of the approximation order has a great influence on the error performance as we have already experienced while simulating SDEs by the propagator method in Section 6.2.3 and in view of the error estimates given in Theorems 6.3 and 6.4. Here it can be seen most clearly in the error plots of the control profile $u(t; \mathbb{E}[X_t])$ and the variance $\mathbb{V}[X_t]$. The jagged behavior of the graphs is due to our choice of constant control base functions (1.15) for $\hat{u}_i(t), i = 0, \ldots, q$, on each multiple shooting interval, which is carried over to all solution processes.

In general, we should note that the absolute errors in the variance appear much smaller in the control context than the errors we have observed when simulating the geometric BROWNian motion process by the chaos methodology in Chapter 6.2, cf. 6.2. This is mainly caused by the type of objective function of our considered SOCP (8.1). This objective function can be interpreted as being of energy-minimizing type which is related to a variance-reduction term. Furthermore, Table 8.1 presents additional information about the performance of the chaos approach for solving this SOCP, depending on the type and accuracy of the truncation of the index set. Therein, we see that at least in this first example the order p of the used basis polynomials $\Psi^\alpha(\eta)$ and their corresponding state coefficient functions x_α is less important

Table 8.1: Comparison of optimal values and numerical expenses for solving the deterministic OCP (8.3) for initial values $x_0 = 0.5$ (*columns 5–7*) and $x_0 = 1$ (*columns 8–10*) depending on the type and accuracy of truncating the index set $\mathcal{I}$. We notice that the accuracy of the objective function value mainly depends on the number k of incorporated basis functions $m_i(\cdot)$ of $L^2([0,1])$, i.e., random variables $\eta_i = W(m_i)$. Runtime increases with the dimension of the resulting deterministic problems and the associated coupling of the state variables within the system. The major part of the computational effort is required by calculating the derivatives of the state variables.

The symbol "—" in the r-column indicates that the simple truncation (6.14) was used, "sp" marks the use of a sparse (6.15) and "ad" of an adaptive index set (6.16). Compare Table 6.1 for a detailed description of the appropriate index denoted by the reference symbol and number.

k	p	r	# coeff. x_α	objective value	time in s	# SQP	objective value	time in s	# SQP
				$x_0 = 0.5$			$x_0 = 1.0$		
10	1	—	11	0.301731	2.0	44	1.147880	2.7	52
10	2	—	66	0.301731	186.8	135	1.147879	360.5	300
10	2	sp[1]	61	0.301731	117.7	101	1.147880	103.1	111
20	1	—	21	0.301898	8.8	46	1.148046	14.4	70
20	2	—	231	0.301898	3341.1	103	1.148046	4948.7	150
20	2	ad[1]	71	0.301898	168.5	90	1.148046	240.1	124
20	3	ad[5]	125	0.301898	1053.3	119	1.148046	1020.7	103
40	1	—	41	0.301979	57.8	54	1.148127	85.3	76
40	2[†]	ad[2]	91	0.301979	694.6	100	1.148127	1211.0	233
100	1	—	101	0.302027	585.6	48	1.148174	888.7	71
100	2[†]	ad[3]	151	0.302026	3669.9	132	1.148175	3233.5	119
exact				0.302054			1.148191		
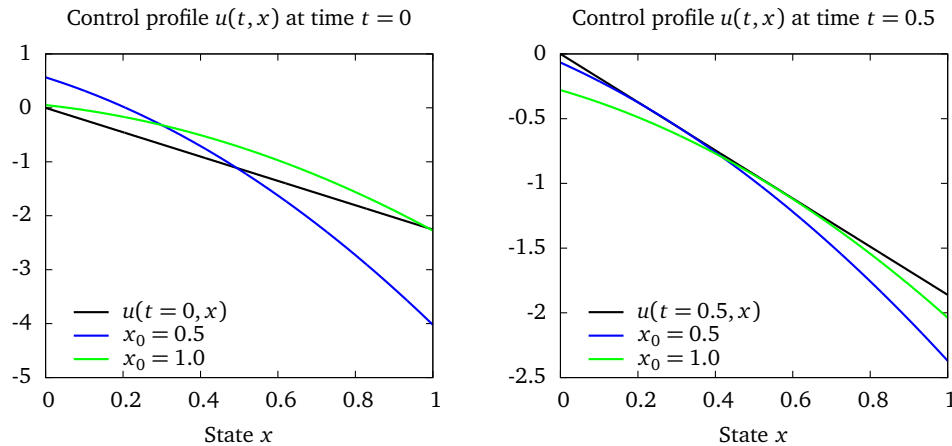
Figure 8.5: Control profiles of the linear-quadratic stochastic regulator problem (8.1) computed by the novel chaos approach in comparison with the exact solutions. Both plots show control profiles $u(t, x)$ for fixed time instants t depending on the state x of the solution process $\{X_t\}_{t \in [0,1]}$. They are calculated with a quadratic approximation of the MARKOV control and a low (full) truncation of the index set $\mathcal{I}$, i.e., $k = 10$ and $p = 1$.

One notices that using this truncation the controls at time $t = 0$ are only adequate for the initial value x_0 of the solved deterministic problem. In the course of time they become more accurate for varying states, which is caused by the implicit capture of the process's variance within the deterministic system.

than the number of incorporated basis functions and, thus, random variables k if we desire a good result of the objective function. This is mainly due to the fact that the BROWNian motion enters the SDE (8.1b) in a purely additive way.

Moreover, Table 8.1 gives the dimensions of the resulting deterministic OCPs (8.3) and the computational effort to solve them numerically. Note that by using sparse or adaptive index sets $\mathcal{I}_{k,p}^r$ and $\mathcal{I}_{k,p}^{(r)}$ the number of coefficient functions within the deterministic system (and, therefore, computation time) can partly be reduced drastically without impairing the solution. The most astonishing result is that if we are interested in the objective value, the expectation of the resulting state process, and its variance for a given initial value x_0, we can obtain these items with very little effort, the appearing relevant systems can be solved in a few seconds. In general, the largest part of the computation time, i.e., about 90%, is necessary to calculate derivatives and sensitivities by IND. Thus, there is a great potential to reduce the computational expenses through parallelization.

However, if one is not only interested in the solution to the SOCP for one certain initial value x_0, but possibly for an environment of x_0, the low approximation of Figure 8.3 is too inaccurate, as Figure 8.5 illustrates.

From the left plot we see that using a low chaos approximation, e.g., a GAUSSian one ($p = 1$) with $k = 10$ random variables $\eta_i = W(m_i)$, the control obtained via solving the resulting deterministic optimal control problem (8.3) is only accurate for the initial value x_0 employed. When we move further in time the control is very precise for states that the process will attain in expectation (see again the left plots in Figure 8.3 for comparison), but additionally there is a certain robustness against deviations from that states. This is natural due to the randomness that is implicitly captured within the deterministic system of ODEs (8.3b). Nevertheless, if we are interested in applying one (optimal) control—that is obtained through one specified initial value x_0—for several control problems depending on a whole environment of initial
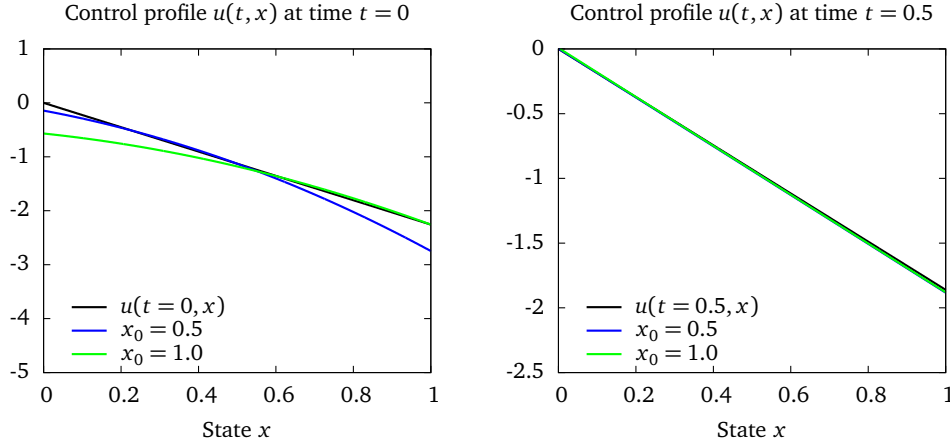
Figure 8.6: Control profiles as in Figure 8.5 but for an advanced chaos approximation (8.4) with $p = 2$, $k = 40$, and an adaptively truncated index set $\mathcal{I}_{p,k}^{(r)}$ (compare Tables 6.1 and 8.1, in particular Item ad[2]).

values around x_0, a low chaos approximation is useless. In that case more information of the stochastic behavior of the system is needed within the deterministic transformation. In particular, the crucial factor of a better approximation here is the order p rather than the number of incorporated basis function $m_i(\cdot)$, i.e., random variables η_i, $i = 1, \ldots, k$. In this first example it is sufficient to apply the following truncation with $p = 2$, $k = 40$, and an adaptive index $\left(r^j\right)_{j=1,2}$ (compare (6.16)) to obtain the desired *robustness property* of the optimal control profile:

$$\mathcal{I}_{2,40}^{(r)} = \left\{ \boldsymbol{\alpha} = (\alpha_1, \ldots, \alpha_{40}) \; \middle| \; 0 \leqslant \alpha_i \leqslant r_i^j \; \forall i \in \{1, \ldots, k\}, \; \forall j = 1, 2, \; |\boldsymbol{\alpha}| \leqslant 2; \right.$$
$$\left. \boldsymbol{r}^1 = (1, \ldots, 1), \; \boldsymbol{r}^2 = (\underbrace{2, \ldots, 2}_{5}, \underbrace{1, \ldots, 1}_{5}, \underbrace{0, \ldots, 0}_{30}) \right\}. \qquad (8.4)$$

Figure 8.6 validates this. In general, we notice a connection of the behavior of the control profiles $u(t, x)$, t fixed, shown in Figures 8.5 and 8.6 and the new control functions $\hat{u}_i(t)$, $i = 0, \ldots, q$, in Figures 8.1 and 8.2. The better those new control functions coincide with their exact counterparts, the better the state dependent profiles at fixed time instants fit and the more robust the solutions become.

Altogether, this simple example shows that up to this point the results of our novel chaos reformulation of a continuous finite-horizon SOCP as a deterministic OCP are very promising. In the next section we consider a problem that cannot be solved analytically anymore. In fact, the state process $\{X_t\}_{t \in \mathcal{T}}$ is determined by a SDE with state dependent diffusion term and a drift that is a nonlinear combination of the state and the control processes.

8.2 A Nonlinear Stochastic Regulator Problem

Let us consider a stochastic optimal control problem with the same objective function as for the linear-quadratic stochastic regulator of the previous section, but with a nonlinear diffusion

driving the state process $\{X_t\}_{t \in \mathcal{T}}$ within the time interval $\mathcal{T} = [0, 1]$.

$$\min_{u. \in \mathcal{A}} \ \mathbb{E}\left[\frac{1}{2} \int_0^1 \left(X_t{}^2 + u_t{}^2 \right) dt + \frac{1}{2} X_1{}^2 \right] \tag{8.5a}$$

$$\text{s.t.} \quad dX_t = X_t u_t \, dt + \sigma X_t \, dB_t, \tag{8.5b}$$

$$X_0 = x_0. \tag{8.5c}$$

Because of this enhancement, problem (8.5) cannot be solved analytically. Nevertheless, in [106] it is shown that a solution to (8.5) exists, even in a more general formulation. Therefore, we can apply our WIENER chaos methodology of Chapters 6 and 7 again to transform this stochastic control problem into a deterministic one. The propagator of the SDE (8.5b) can be derived straightforwardly as it includes only a product of two chaos expansions. It reads as follows (with the constant $C(\boldsymbol{\alpha}, \boldsymbol{\gamma}, \boldsymbol{\beta})$ and the diminished multi-index $\boldsymbol{\alpha}^-(j)$ defined as before in (5.34) and (5.43), and $\{m_i(\cdot)\}_{i \in \mathbb{N}}$ denoting the basis functions (5.25) of $L^2([0, 1])$):

$$x_{\boldsymbol{\alpha}}(t) = x_0 \cdot \mathbb{1}_{\{\boldsymbol{\alpha}=0\}} + \int_0^t \sum_{\boldsymbol{\beta} \in \mathcal{I}} \sum_{0 \leqslant \boldsymbol{\gamma} \leqslant \boldsymbol{\alpha}} C(\boldsymbol{\alpha}, \boldsymbol{\gamma}, \boldsymbol{\beta}) \, x_{\boldsymbol{\alpha}-\boldsymbol{\gamma}+\boldsymbol{\beta}}(s) \, u_{\boldsymbol{\gamma}+\boldsymbol{\beta}}(s) \, ds$$

$$+ \sigma \int_0^t \sum_{j=1}^\infty \sqrt{\alpha_j} \, m_j(s) \, x_{\boldsymbol{\alpha}^-(j)}(s) \, ds. \tag{8.6}$$

Therein, the control coefficients $u_{\boldsymbol{\alpha}}(\cdot)$ are again defined via comparing the formal chaos expansion (7.7) of u_t and the TAYLOR expansion (7.8), i.e., depending on the new control functions $\hat{u}_i(\cdot)$, $i = 0, \ldots, q$. The first integral in (8.6) follows from the chaos expansion of the product $X_t \cdot u_t$.

To reformulate the objective function (8.5a) in terms of the deterministic coefficient functions, we start again by converting the MAYER-type part using ITŌ's formula (4.22). Then inserting the chaos expansions of X_t and u_t yields the desired form. With $\mathcal{I}_{k,p}^{(r)}$ denoting the (simply, sparsely, or adaptively) truncated index set as before and approximating the MARKOV control by (7.9), e.g., with a quadratic expansion as in (8.3), we obtain the deterministic OCP corresponding to (8.1),

$$\min_{\hat{u}_i(\cdot), i=0,\ldots,q} \left\{ \frac{1}{2} x_0{}^2 + \frac{1}{2} \int_0^1 \sum_{\boldsymbol{\alpha} \in \mathcal{I}_{k,p}^{(r)}} \left[(1 + \sigma^2) x_{\boldsymbol{\alpha}}{}^2(t) + u_{\boldsymbol{\alpha}}{}^2(t) \right. \right.$$

$$\left. \left. + 2 \sum_{\boldsymbol{\beta} \in \mathcal{I}_{k,p}^{(r)}} \sum_{0 \leqslant \boldsymbol{\gamma} \leqslant \boldsymbol{\alpha}} C(\boldsymbol{\alpha}, \boldsymbol{\gamma}, \boldsymbol{\beta}) \, x_{\boldsymbol{\alpha}-\boldsymbol{\gamma}+\boldsymbol{\beta}}(t) \, x_{\boldsymbol{\gamma}+\boldsymbol{\beta}}(t) \, u_{\boldsymbol{\alpha}}(t) \right] dt \right\} \tag{8.7a}$$

$$\text{s.t.} \quad \dot{x}_{\boldsymbol{\alpha}}(t) = \sum_{\boldsymbol{\beta} \in \mathcal{I}_{k,p}^{(r)}} \sum_{0 \leqslant \boldsymbol{\gamma} \leqslant \boldsymbol{\alpha}} C(\boldsymbol{\alpha}, \boldsymbol{\gamma}, \boldsymbol{\beta}) \, x_{\boldsymbol{\alpha}-\boldsymbol{\gamma}+\boldsymbol{\beta}}(t) \, u_{\boldsymbol{\gamma}+\boldsymbol{\beta}}(t)$$

$$+ \sigma \sum_{j=1}^\infty \sqrt{\alpha_j} \, m_j(t) \, x_{\boldsymbol{\alpha}^-(j)}(t) \tag{8.7b}$$

$$x_{\boldsymbol{\alpha}}(0) = x_0 \cdot \mathbb{1}_{\{\boldsymbol{\alpha}=0\}}. \tag{8.7c}$$

Table 8.2: Optimal values of problem (8.5) calculated with the software package SOCSol4L. The problem was solved in the predefined state space $\mathcal{G} = [-0.7, 1.2]$ for different space and time discretizations Δ_x and Δ_t. After calculating optimal control policies, the optimal cost function values have been approximated by a Monte Carlo simulation with 100 000 and 1 million sample paths and different simulation step sizes Δ_{Sim} for the weak approximation scheme of the SDE. Each simulation therefore gives a different result. The runtimes (in *min*) include both solving the MARKOV decision process by a dynamic programming technique and performing the Monte Carlo simulation to eventually obtain the desired result.

discretization	# simulations	Δ_{Sim}	optimal value	runtime in *min*
$\Delta_x = 0.005$ $\Delta_t = 0.001$	100 000	0.01	0.2113440 0.2117336	100
	1 000 000		0.2115376 0.2115948	925
$\Delta_x = 0.002$ $\Delta_t = 0.001$	100 000	0.001	0.2112635	1 000
	1 000 000		0.2114620	9 200

As the solution of problem (8.5) cannot be deduced analytically, we have to compare the results of our chaos approach with other numerical methods. It is intricate to solve the HJB Partial Differential Equation (PDE) induced by (8.5) numerically because we have no information about appropriate boundary conditions for the region of interest. In financial problems this can often be overcome by economic argumentation, however, in this case it is not possible. Therefore, we use the software package SOCSol4L [17, 148] for obtaining reference solutions. It transforms the original continuous stochastic control problem into a MARKOV decision chain by utilizing the MARKOV Chain Approximation (MCA) method combined with a *weak* EULER-MARUYAMA *integration* procedure of the SDE on a chosen time and space grid for a predefined region $\mathcal{G}$ of interest, compare Section 7.2.3. Afterwards, this MARKOV decision chain problem is solved by a dynamic programming technique. Table 8.2 gives an overview of optimal values obtained with that software and the computational effort needed therefor. Note that while our new chaos methodology provides the expectation of the process $\{X_t\}_{t \in \mathcal{T}}$ and the optimal cost automatically, within SOCSol4L these quantities have to be approximated by using a *Monte Carlo simulation*.

The reference solution that is used within the following figures is obtained with a state discretization step size $\Delta_x = 0.002$ and a time discretization step $\Delta_t = 0.001$. All expectations and variances are simulated with 300 000 sample paths.

Figure 8.7 shows solution paths of the deterministic OCP (8.7) with a quadratic TAYLOR expansion (7.8) of the control function in comparison with the SOCSol4L-reference solution for the initial value $x_0 = 0.5$ and a diffusion parameter $\sigma = 0.3$. The settings of the software package MUSCOD-II have been the same as for the computations in the previous section. These solutions are again obtained with a simple truncation (6.14) and $k = 10$ basis functions $m_i(\cdot)$ of $L^2([0,1])$, i.e., $k = 10$ random variables $\eta_i = W(m_i)$ and order $p = 1$ for constructing the chaos basis polynomials $\Psi^\alpha(\eta)$. The order of the plots within is as in Figures 8.3 and 8.4, i.e., the left plot depicting the control function $u(t; \mathbb{E}[X_t])$, the middle one the expectation $\mathbb{E}[X_t]$, and the right one the variance $\mathbb{V}[X_t]$ of the solution process. And again these paths show that

Table 8.3: Optimal values and numerical expenses for solving the SOCP (8.5) with the chaos method-
ology, i.e., solving the deterministic problem (8.7) with MUSCOD-II. We use the initial values
$x_0 = 0.5$ (*columns 5–7*) and $x_0 = 1$ (*columns 8–10*), the diffusion parameter $\sigma = 0.3$, a qua-
dratic expansion of the control function ($q = 2$) and different types and accuracies of trun-
cating the index set $\mathcal{I}$. The accuracy of the objective function values does not only depend
on the number k of incorporated basis function of the underlying HILBERT space $L^2([0, 1])$,
i.e., random variables, but as well on the approximation order p. Runtime increases again
with the dimension of the resulting deterministic problems and the associated coupling of
the state variables within the system.
The symbol "—" in the r-column indicates that the simple truncation (6.14) was used, "sp"
marks the use of a sparse (6.15) and "ad" of an adaptive index set (6.16). Compare Table
6.1 for a detailed description of the appropriate index denoted by the reference symbol and
number.

k	p	r	# coeff. x_α	objective value	time in s	# SQP	objective value	time in s	# SQP
					$x_0 = 0.5$			$x_0 = 1.0$	
5	2	—	21	0.211509	42.2	234	0.620330	46.7	224
5	3	—	56	0.211502	476.0	215	0.620325	330.6	143
5	3	sp[3]	42	0.211503	170.2	156	0.620326	190.8	163
10	1	—	11	0.211733	3.8	46	0.620489	3.6	46
10	2	—	66	0.211458	713.6	178	0.619768	740.1	192
10	2	sp[1]	61	0.211458	631.2	202	0.619769	544.8	161
10	3	—	286	0.211451	27311.5	144	0.619761	25650.7	123
10	3	ad[4]	42	0.211462	233.3	165	0.619799	189.2	120
10	4	ad[7]	57	0.211462	510.6	198	0.619798	558.7	195
20	1	—	21	0.211714	14.0	42	0.620214	19.0	53
20	2	—	231	0.211432	18293.5	179	0.619469	11484.4	79
20	2	sp[2]	216	0.211432	13557.4	121	0.619470	22281.2	179
20	2	ad[1]	71	0.211439	1557.2	241	0.619498	1337.0	187
20	3	ad[5]	125	0.211433	7041.0	254	0.619493	5933.2	196
20	4	ad[8]	131	0.211433	6679.2	213	0.619492	3744.5	110
40	2	ad[2]	91	0.211430	2256.8	139	0.619359	2813.2	156
40	3	ad[6]	145	0.211423	9300.2	118	0.619353	13341.8	153
100	1	—	101	0.211698	1962.9	79	0.619986	3389.7	125
100	2	ad[3]	151	0.211424	12985.6	145	0.619273	14423.5	149
SOCSol4L (300 000 sim.)				0.211707	169159.0		0.619434	168315.7	
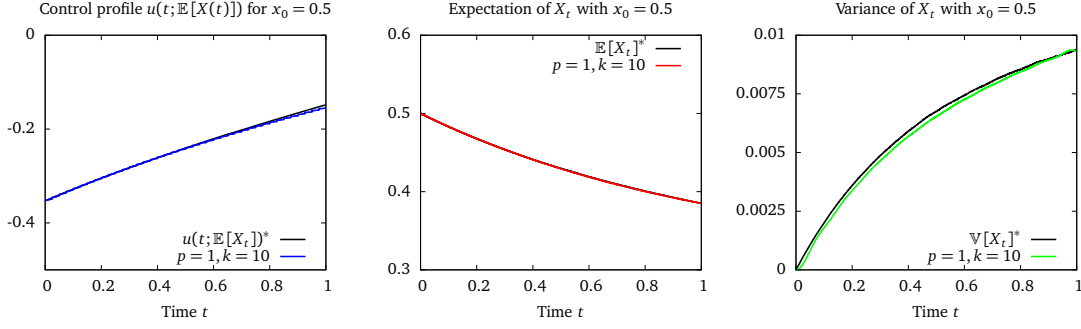
Figure 8.7: Solution paths of the SOCP (8.5) with initial value $x_0 = 0.5$. All plots show a comparison of paths obtained by the introduced chaos approach, i.e., a solution to the transformed deterministic OCP (8.7) with $k = 10$ included basis function/random variables, approximation order $p = 1$, a quadratic expansion of the control ($q = 2$), and a reference solution obtained with SOCSol4L ($\mathcal{G} = [-0.7, 1.2]$, $\Delta_x = 0.002$, $\Delta_t = 0.001$ and a Monte Carlo simulation with 300 000 sample paths).

The *first* plot depicts the control profile $u(t; \mathbb{E}[X_t])$, the *second* one the expectation of the state process $\mathbb{E}[X_t]$, and the *third* figure its variance $\mathbb{V}[X_t]$. The star symbol * in the key of each plot denotes that the reference solution has been calculated by SOCSol4L.
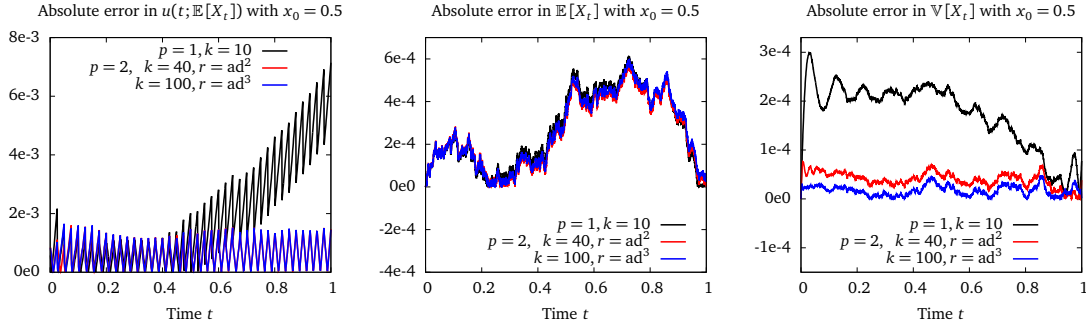
Figure 8.8: Absolute errors of the solutions of the stochastic control problem (8.5) computed by the novel chaos approach for different chaos approximation orders p and numbers k of involved basis function/random variables to construct the basis polynomials $\Psi^\alpha(\eta)$ (in comparison to the reference solutions calculated with SOCSol4L). For all shown results a quadratic expansion (7.8) has been used.

The sequence of plots is as in Figure 8.7, i.e., the *first* showing the errors within the control profile $u(t; \mathbb{E}[X_t])$, the *second* one errors in the expectation $\mathbb{E}[X_t]$, and the *third* plot errors in the variance $\mathbb{V}[X_t]$.

by this low approximation we obtain very good results if we are interested in the optimal value, expectation, and related quantities, even as the state SDE (8.5b) is much more complex than in the linear-quadratic stochastic regulator problem (8.1) and, hence, the deterministic system (8.7) much more coupled. This quality of the solution is confirmed by the corresponding error plots in Figure 8.8 and the optimal values stated in Table 8.3. The very noisy shape of the absolute errors is caused by the Monte Carlo approximation—even with the large amount of 300 000 sample simulations the values deviate notably (compare Table 8.2).

Like for the linear-quadratic regulator problem we notice from Figure 8.8 that especially increasing the approximation order p leads to a decrease of the absolute errors in the control profile $u(t; \mathbb{E}[X_t])$ and the variance $\mathbb{V}[X_t]$, while the expectation is already very accurately approximated with order $p = 1$. If we compare the optimal objective values in Table 8.3 we see that for this nonlinear example it is not sufficient to increase the number of incorporated
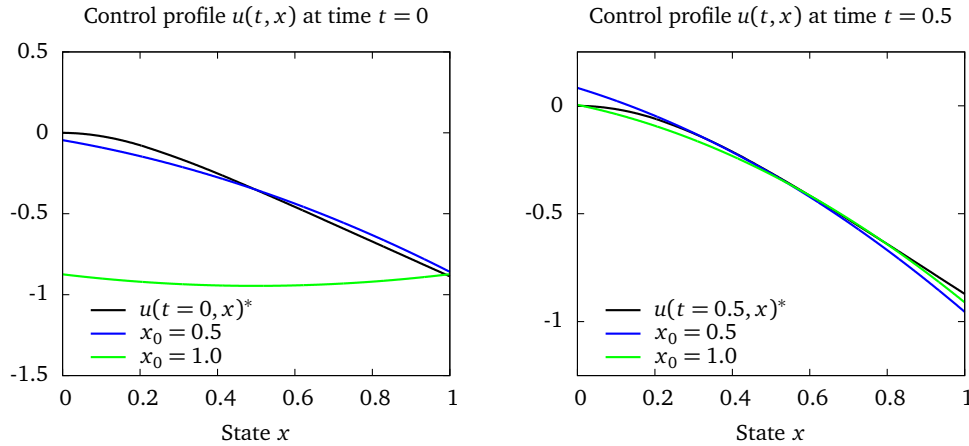
Figure 8.9: Control profiles of the nonlinear control problem (8.5) computed by the novel chaos approach in comparison with the reference solutions obtained by SOCSol4L. Both plots show control functions $u(t, x)$ for fixed time instants t depending on the state x of the process. They are calculated with a quadratic approximation of the MARKOV control and a low truncation of the index set $\mathcal{I}$, i.e., with $p = 1$ and $k = 10$.
One notices again that using this truncation the controls at time $t = 0$ are only accurate for the initial value x_0 of the solved deterministic problem.

random variables $\eta_i = W(m_i)$, $i = 1, \ldots, k$, to obtain better results; here increasing the order p is important as well.

From a computational point of view Table 8.3 shows that the deterministic OCP (8.7) is much more challenging than (8.3). While the number of Sequential Quadratic Programming (SQP) iterations needed to solve the problems remains at a comparable level, the runtimes for solving (8.7) are notably higher. This results from a distinctive coupling of the deterministic state functions x_α within the ODE system (8.7b) and, therefore, a higher expense for calculating their derivatives by IND, which requires about 95% of the overall computational effort.

Now let us take a look on the control profiles $u(t, x)$ for fixed times $t \in [0, 1]$ depending on the state x of the process $\{X_t\}_{t \in [0,1]}$. As in the previous section, the control obtained via the low truncation ($p = 1$, $k = 10$) does not encourage its application to initial values deviating from x_0, see Figure 8.9. If we want to guarantee a certain robustness of the validity of a control $u(\cdot)$ (calculated with initial value x_0) for applying it to initial values in an environment of x_0, we have to enhance the accuracy of the WIENER chaos approximation. Figure 8.10 shows the control profiles $u(t, x)$ calculated for the adaptive truncation (8.4), i.e., $p = 2$, $k = 40$, and (r) given by Item ad[2], cf. Table 6.1. However, in comparison to the linear-quadratic regulator problem the impact of this enhancement turns out lower. This might originate from the fact that the variance of the process $\{X_t\}_{t \in [0,1]}$ in the actual example is generally smaller than the variance of the regulator process, hence the process will not deviate that heavily from its expectation. Nevertheless, qualitatively better approximations can be obtained by increasing the truncation characteristics p and k or the order q of the MARKOV control expansion further— at the cost of higher computation times.

We complete the examination of this nonlinear example by giving an impression on the consequences of applying a cubic control expansion (7.8). In combination with formula (5.33), we
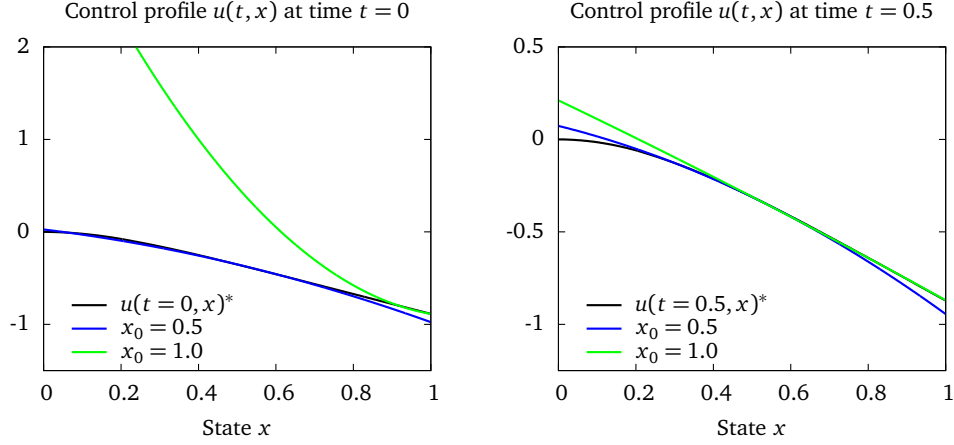
Figure 8.10: Control profiles as in Figure 8.9 but for the advanced chaos approximation (8.4) with an approximation order $p = 2$ and $k = 40$ included random variables, using an adaptive index (r).

calculate for all $\boldsymbol{\alpha} \in \mathcal{I}$, new control coefficient functions $\hat{u}_i(\cdot)$, $i = 0, \ldots, 3$, and $t \in \mathcal{T}$

$$u_{\boldsymbol{\alpha}}(t) = \hat{u}_0(t) \cdot \mathbb{1}_{\{\boldsymbol{\alpha}=\boldsymbol{0}\}} + \hat{u}_1(t) \cdot x_{\boldsymbol{\alpha}}(t) + \hat{u}_2(t) \cdot \sum_{\gamma \in \mathcal{I}} \sum_{0 \leqslant \beta \leqslant \alpha} C(\boldsymbol{\alpha}, \boldsymbol{\beta}, \boldsymbol{\gamma}) x_{\boldsymbol{\alpha}-\boldsymbol{\beta}+\boldsymbol{\gamma}}(t) x_{\boldsymbol{\beta}+\boldsymbol{\gamma}}(t)$$

$$+ \hat{u}_3(t) \cdot \sum_{\nu \in \mathcal{I}} \sum_{0 \leqslant \mu \leqslant \alpha} C(\boldsymbol{\alpha}, \boldsymbol{\mu}, \boldsymbol{\nu}) \times$$

$$\times \sum_{\gamma \in \mathcal{I}} \sum_{0 \leqslant \beta \leqslant \alpha-\mu+\nu} C(\boldsymbol{\alpha}-\boldsymbol{\mu}+\boldsymbol{\nu}, \boldsymbol{\beta}, \boldsymbol{\gamma}) x_{\boldsymbol{\alpha}-\boldsymbol{\mu}+\boldsymbol{\nu}-\boldsymbol{\beta}+\boldsymbol{\gamma}}(t) x_{\boldsymbol{\beta}+\boldsymbol{\gamma}}(t) x_{\boldsymbol{\mu}+\boldsymbol{\nu}}(t), \quad (8.8)$$

with the constant $C(\cdot)$ defined as in (5.34). Truncation of the index set $\mathcal{I}$ to $\mathcal{I}_{k,p}^{(r)}$ then gives the control coefficients to be used within the deterministic OCP (8.7).

Table 8.4 states the differences in the objective function value and the computation times of solving the deterministic OCP with control approximations of orders $q = 1, 2, 3$ and varying truncations of the index set $\mathcal{I}$. One notices that increasing the order of the control expansion (7.8) from linear to quadratic improves the result clearly, whereas the step from a quadratic to a cubic expansion leads to only marginal improvements of the objective function values. Nevertheless, the cost of increasing the control expansion order q are (considerably) higher computation times. This is particularly caused by the increasingly coupled structure of the ODE system (8.7b), wherefore the computation of sensitivities by IND becomes much more challenging and time consuming. Nevertheless, by using parallelized numerical methods this drawback can be qualified.

From Figure 8.11 we see that in general increasing the order of the control expansion has a positive effect on the robustness of applying control profiles $u(\cdot)$ computed for a certain initial value x_0 to initial values deviating from it. This influence is most apparent when comparing a quadratic expansion against a linear one; the step to a cubic expansion is less prominent here as well; additionally it is more apparent in the case of solving the problem for the initial value $x_0 = 1.0$. Certainly, to see this behavior we need to consider a problem with an index set truncated with a chaos expansion order $p \geqslant q$; in Figure 8.11 the exemplary case with $k = 10$, $p = 4$, and (r) given by Item ad[7] is depicted. That means, at least in this nonlinear example, the application of a cubic control expansion (7.8) is not beneficial, comparing the impact of the

Table 8.4: Optimal values and numerical expenses for solving the SOCP (8.5) with the chaos method-
ology as in Table 8.3, but with the focus on the order q of the control expansion (7.8). Again
we use the initial values $x_0 = 0.5$ (*columns 4–12*) and $x_0 = 1$ (*columns 13–21*), the diffusion
parameter $\sigma = 0.3$, and different types and accuracies of truncating the index set $\mathcal{I}$.

Wee observe that increasing the order of the expansion from a linear to a quadratic one
improves the objective function value much, whereas the improvement of passing from a
quadratic to a cubic expansion is only marginal. However, higher control expansions are ac-
companied by notably higher computation times, caused by a significantly stronger coupling
of the ODE system (8.7b) and, therefore, the increased effort to calculate derivatives and
sensitivities.

Note that by the dash "—" we mean that the corresponding problem has not been solved due
to an unreasonable computation time.

k	p	r	objective value	time in s	# SQP	objective value	time in s	# SQP	objective value	time in s	# SQP
						$x_0 = 0.5$					
10	1	—	0.211733	2.7	54	0.211733	3.8	46	0.211732	7.3	71
10	2	—	0.211479	135.5	59	0.211458	713.6	178	0.211458	5743.3	155
10	3	ad^4	0.211483	49.5	59	0.211462	233.3	165	0.211462	1807.1	137
10	4	ad^7	0.211482	11.7	61	0.211462	510.6	198	0.211462	14490.1	199
20	2	ad^1	0.211460	199.2	46	0.211439	1557.2	241	0.211439	7408.7	110
20	3	ad^5	0.211454	1121.6	57	0.211433	7041.0	254	0.211433	315875.2	133
20	4	ad^8	0.211454	1184.3	54	0.211433	6679.2	213		—	
40	2	ad^2	0.211451	633.3	57	0.211430	2256.8	139	0.211430	24635.3	137
40	3	ad^6	0.211445	1876.9	45	0.211423	9300.2	118		—	
						$x_0 = 1.0$					
10	1	—	0.620489	3.1	57	0.620489	3.6	46	0.620450	11.0	89
10	2	—	0.619799	144.6	58	0.619768	740.1	192	0.619759	5323.0	133
10	3	ad^4	0.619830	63.9	70	0.619799	189.2	120	0.619798	2382.6	166
10	4	ad^7	0.619829	114.4	58	0.619798	558.7	195	0.619797	13601.0	176
20	2	ad^1	0.619528	241.5	53	0.619498	1337.0	187	0.619498	9476.9	128
20	3	ad^5	0.619522	835.9	39	0.619493	5933.2	196	0.619491	659281.3	239
20	4	ad^8	0.619522	1388.1	58	0.619492	3744.5	110		—	
40	2	ad^2	0.619388	639.4	54	0.619359	2813.2	156	0.619359	25397.9	131
40	3	ad^6	0.619382	2574.2	56	0.619353	13341.8	153		—	
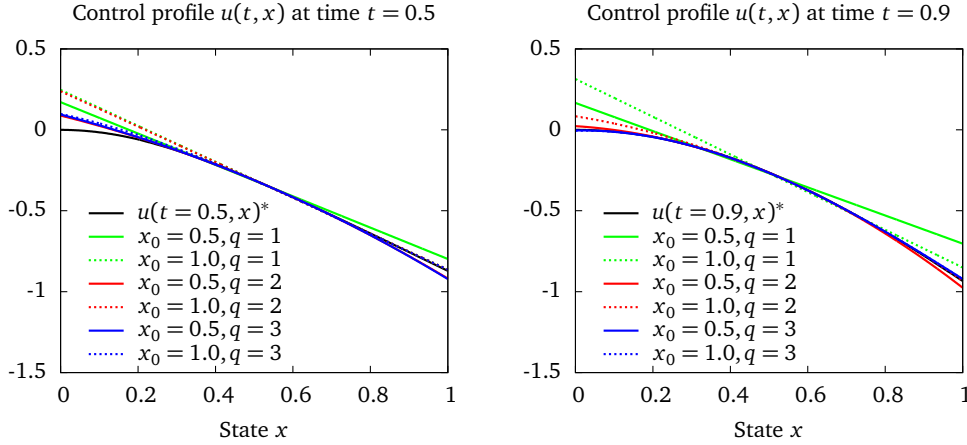
Figure 8.11: Control profiles of the nonlinear control problem (8.5) computed by the chaos approach for different orders q of the control expansion as in Figure 8.9 but for the time instants $t = 0.5$ and $t = 0.9$ and a truncation with $k = 10$ $L^2([0, 1])$-basis functions and order $p = 4$.

One notices that the step from a linear to a quadratic expansion improves the solution, whereas the difference between the quadratic and the cubic expansion is only marginal, at least in this example.

extension on objective function values, robustness of the solution control profiles with respect to deviations of the initial value, and the increased computational effort caused by the higher expansion.

8.3 The Stochastic Conspicuous Consumption Problem

In our final example we return to the conspicuous consumption problem of Chapter 3 and enhance it by a time-dependent recession strength process. Thus, the duration of the crisis does not have to be considered as a separate random variable, but can be connected with the strength. One does not assume the crisis to be finished at some specific time instant τ. Instead, the evolution of the strength process over time determines when the recession is mild, severe, or merely not existent at all. However, this implies that the additional cash state variable $B(\cdot)$ that we needed in Chapter 3 can be neglected completely now.

Let the recession strength be given as the (one-dimensional) stochastic process ς_t. It may be defined as, e.g., a geometric BROWNian motion (6.17) or through $\varsigma_t = c_0 + c_1 B_t$, where B_t denotes again a standard BROWNian motion and c_0, c_1 are positive adjustment parameters. The demand function $D(\cdot)$ (cf. Equation (3.3)) depending on the brand image A and the price P of the product becomes

$$D_t(A_t, P_t) = m - \frac{P_t}{A_t{}^\beta} - \varsigma_t, \tag{8.9}$$

where m denotes again the potential market size and $0 < \beta < 1$. Hence, the demand is a stochastic process. In the most general case this means, that the brand image $A_.$ and the price $P_.$ are stochastic processes as well, where the price is assumed to be a MARKOV control (cf. Section 7.1) again.

On the time horizon $\mathcal{T} = [0, t_\mathrm{f}]$ we obtain the conspicuous consumption SOCP

$$\max_{P_{\cdot} \in \mathcal{A}} \ \mathbb{E}\left[\int_0^{t_\mathrm{f}} \mathrm{e}^{-rt}\, (P_t \cdot D_t(A_t, P_t) - C)\, \mathrm{d}t \right] \tag{8.10a}$$

$$\text{s.t.} \qquad \mathrm{d}A_t = \kappa(\gamma P_t - A_t)\,\mathrm{d}t, \quad t \in \mathcal{T}, \tag{8.10b}$$

$$A_0 = a_0, \tag{8.10c}$$

$$D_t(A_t, P_t) = m - \frac{P_t}{A_t^{\beta}} - \varsigma_t, \quad t \in \mathcal{T}, \tag{8.10d}$$

$$\mathbb{E}\left[D_t(A_t, P_t) \right] \geqslant 0, \qquad\qquad t \in \mathcal{T}. \tag{8.10e}$$

The only remaining constraint of Problem (8.10) is to require a positive demand on $\mathcal{T}$.

The construction of the propagator system describing the stochastic brand image and demand in terms of their chaos coefficients is more difficult than in the problem instances of Sections 8.1 and 8.2. The reason for this is the presence of the fraction and the non-integer power in (8.9). As briefly described in Section 7.3, we reformulate those nonlinearities as a Differential-Algebraic Equation (DAE) system, which we can efficiently deal with in the context of BOCK's direct multiple shooting approach.

We fix $\beta = 0.5$ as in Chapter 3. Let the chaos expansions of the brand image process $\{A_t\}_{t\in\mathcal{T}}$ and the demand $\{D_t\}_{t\in\mathcal{T}}$ be given through

$$A_t = \sum_{\boldsymbol{\alpha}\in\mathcal{I}} a_{\boldsymbol{\alpha}}(t)\Psi^{\boldsymbol{\alpha}}(\boldsymbol{\eta}), \qquad D_t = \sum_{\boldsymbol{\alpha}\in\mathcal{I}} d_{\boldsymbol{\alpha}}(t)\Psi^{\boldsymbol{\alpha}}(\boldsymbol{\eta}).$$

Reasoned by the observations in Chapter 3, we assume a linear expansion of the MARKOV control process $\{P_t\}_{t\in\mathcal{T}}$ depending on the reputation process, i.e., for all $t \in \mathcal{T}$ we have

$$P_t = \hat{P}_0(t) + \hat{P}_1(t)A_t.$$

The propagator equation of the brand image is for all $\boldsymbol{\alpha} \in \mathcal{I}$ and all $t \in \mathcal{T}$ given through

$$\dot{a}_{\boldsymbol{\alpha}}(t) = \kappa\gamma\hat{P}_0(t) + \kappa\left(\gamma\hat{P}_1(t) - 1\right)a_{\boldsymbol{\alpha}}(t),$$

$$a_{\boldsymbol{\alpha}}(0) = \mathbb{1}_{\{\boldsymbol{\alpha}\equiv 0\}} \cdot A_0.$$

To calculate the algebraic equations for the demand process, we first need a representation of $\sqrt{A_t}$ in terms of the chaos coefficients $a_{\boldsymbol{\alpha}}(t)$, $\boldsymbol{\alpha} \in \mathcal{I}$. Let the auxiliary process $Z_t = \sqrt{A_t}$ have the WIENER chaos expansion

$$Z_t = \sum_{\boldsymbol{\alpha}\in\mathcal{I}} z_{\boldsymbol{\alpha}}(t)\Psi^{\boldsymbol{\alpha}}(\boldsymbol{\eta}).$$

As $A_t = Z_t^{\,2}$, with the product formula (5.33) we obtain the algebraic equation system

$$0 = a_{\boldsymbol{\alpha}}(t) - \sum_{\boldsymbol{\beta}\in\mathcal{I}} \sum_{0\leqslant\boldsymbol{\gamma}\leqslant\boldsymbol{\alpha}} C(\boldsymbol{\alpha}, \boldsymbol{\gamma}, \boldsymbol{\beta}) z_{\boldsymbol{\alpha}-\boldsymbol{\gamma}+\boldsymbol{\beta}}(t) z_{\boldsymbol{\gamma}+\boldsymbol{\beta}}(t)$$

for all $\boldsymbol{\alpha} \in \mathcal{I}$. Finally, to derive the chaos coefficients $d_{\boldsymbol{\alpha}}(\cdot)$, $\boldsymbol{\alpha} \in \mathcal{I}$, of the demand process, let

the strength process $\{\varsigma_t\}_{t\in\mathcal{T}}$ be given as a translated BROWNian motion

$$\varsigma_t = c_0 + c_1 B_t$$

with constants c_0, $c_1 > 0$ and the standard BROWNian motion process $\{B_t\}_{t\in\mathcal{T}}$, which has the FOURIER-HERMITE expansion

$$B_t = \sum_{i=1}^{\infty} \eta_i \int_0^t m_i(s)\,\mathrm{d}s.$$

The coefficients $\{m_i(\cdot)\}_{i\in\mathbb{N}}$ are a basis of the underlying HILBERT space $L^2(\mathcal{T})$ as before, cf. Theorem 5.4. For notational convenience, we introduce for all $t \in \mathcal{T}$ the integrated basis functions

$$M_{\boldsymbol{\alpha}}(t) \overset{\text{def}}{=} \begin{cases} \int_0^t m_i(s)\,\mathrm{d}s, & \boldsymbol{\alpha} = \boldsymbol{e}_i,\ i \in \mathbb{N}, \\ 0, & \text{else.} \end{cases} \tag{8.11}$$

This gives

$$B_t = \sum_{\boldsymbol{\alpha}\in\mathcal{I}} M_{\boldsymbol{\alpha}}(t)\Psi^{\boldsymbol{\alpha}}(\boldsymbol{\eta}). \tag{8.12}$$

Equation (8.9) yields

$$(m - c_0 - c_1 B_t - D_t) \cdot Z_t = \hat{P}_0(t) + \hat{P}_1(t)A_t.$$

Then by inserting the chaos expansions of the demand, the auxiliary process, the brand image, and the BROWNian motion (8.12), and projecting the resulting equation onto each basis component, we obtain

$$0 = \hat{P}_0(t) + \hat{P}_1(t)a_{\boldsymbol{\alpha}}(t) - (m - c_0)z_{\boldsymbol{\alpha}}(t) + c_1 \sum_{\boldsymbol{\beta}\in\mathcal{I}} \sum_{0\leqslant\boldsymbol{\gamma}\leqslant\boldsymbol{\alpha}} C(\boldsymbol{\alpha},\boldsymbol{\gamma},\boldsymbol{\beta})M_{\boldsymbol{\alpha}-\boldsymbol{\gamma}+\boldsymbol{\beta}}(t)z_{\boldsymbol{\gamma}+\boldsymbol{\beta}}(t)$$
$$+ \sum_{\boldsymbol{\beta}\in\mathcal{I}} \sum_{0\leqslant\boldsymbol{\gamma}\leqslant\boldsymbol{\alpha}} C(\boldsymbol{\alpha},\boldsymbol{\gamma},\boldsymbol{\beta})d_{\boldsymbol{\alpha}-\boldsymbol{\gamma}+\boldsymbol{\beta}}(t)z_{\boldsymbol{\gamma}+\boldsymbol{\beta}}(t)$$

for all $\boldsymbol{\alpha} \in \mathcal{I}$ and $t \in \mathcal{T}$.

Because the objective function (8.10a) is again an expectation value, it turns into a deterministic integral depending on the chaos coefficients of the demand and the brand image.

$$\mathbb{E}\left[\int_0^{t_f} \mathrm{e}^{-rt}\left(P_t D_t(A_t, P_t) - C\right)\mathrm{d}t\right]$$
$$= \mathbb{E}\left[\int_0^{t_f} \mathrm{e}^{-rt}\left(\left(\hat{P}_0(t) + \hat{P}_1(t)\sum_{\boldsymbol{\alpha}\in\mathcal{I}} a_{\boldsymbol{\alpha}}(t)\Psi^{\boldsymbol{\alpha}}(\boldsymbol{\eta})\right)\cdot\sum_{\boldsymbol{\alpha}\in\mathcal{I}} d_{\boldsymbol{\alpha}}(t)\Psi^{\boldsymbol{\alpha}}(\boldsymbol{\eta}) - C\right)\mathrm{d}t\right]$$
$$= \int_0^{t_f} \mathrm{e}^{-rt}\left(\hat{P}_0(t)d_{\mathbf{0}}(t) + \hat{P}_1(t)\sum_{\boldsymbol{\alpha}\in\mathcal{I}} a_{\boldsymbol{\alpha}}(t)d_{\boldsymbol{\alpha}}(t) - C\right)\mathrm{d}t.$$

Hence, with $\mathcal{I}_{k,p}^{(r)}$ denoting again a truncated index set, the resulting deterministic OCP is

$$\max_{\hat{P}_0(\cdot),\hat{P}_1(\cdot)} \int_0^{t_f} \mathrm{e}^{-rt} \left(\hat{P}_0(t)d_{\mathbf{0}}(t) + \hat{P}_1(t) \sum_{\boldsymbol{\alpha} \in \mathcal{I}_{k,p}^{(r)}} a_{\boldsymbol{\alpha}}(t)d_{\boldsymbol{\alpha}}(t) - C \right) \mathrm{d}t \tag{8.13a}$$

$$\text{s.t.} \quad \dot{a}_{\boldsymbol{\alpha}}(t) = \kappa\gamma\hat{P}_0(t) + \kappa\left(\gamma\hat{P}_1(t) - 1\right)a_{\boldsymbol{\alpha}}(t), \qquad \boldsymbol{\alpha} \in \mathcal{I}_{k,p}^{(r)}, t \in \mathcal{T}, \tag{8.13b}$$

$$0 = a_{\boldsymbol{\alpha}}(t) - \sum_{\boldsymbol{\beta} \in \mathcal{I}_{k,p}^{(r)}} \sum_{0 \leqslant \boldsymbol{\gamma} \leqslant \boldsymbol{\alpha}} C(\boldsymbol{\alpha},\boldsymbol{\gamma},\boldsymbol{\beta})z_{\boldsymbol{\alpha}-\boldsymbol{\gamma}+\boldsymbol{\beta}}(t)z_{\boldsymbol{\gamma}+\boldsymbol{\beta}}(t),$$

$$\boldsymbol{\alpha} \in \mathcal{I}_{k,p}^{(r)}, t \in \mathcal{T}, \tag{8.13c}$$

$$0 = \hat{P}_0(t) + \hat{P}_1(t)a_{\boldsymbol{\alpha}}(t) - (m - c_0)z_{\boldsymbol{\alpha}}(t)$$

$$+ c_1 \sum_{\boldsymbol{\beta} \in \mathcal{I}_{k,p}^{(r)}} \sum_{0 \leqslant \boldsymbol{\gamma} \leqslant \boldsymbol{\alpha}} C(\boldsymbol{\alpha},\boldsymbol{\gamma},\boldsymbol{\beta})M_{\boldsymbol{\alpha}-\boldsymbol{\gamma}+\boldsymbol{\beta}}(t)z_{\boldsymbol{\gamma}+\boldsymbol{\beta}}(t)$$

$$+ \sum_{\boldsymbol{\beta} \in \mathcal{I}_{k,p}^{(r)}} \sum_{0 \leqslant \boldsymbol{\gamma} \leqslant \boldsymbol{\alpha}} C(\boldsymbol{\alpha},\boldsymbol{\gamma},\boldsymbol{\beta})d_{\boldsymbol{\alpha}-\boldsymbol{\gamma}+\boldsymbol{\beta}}(t)z_{\boldsymbol{\gamma}+\boldsymbol{\beta}}(t),$$

$$\boldsymbol{\alpha} \in \mathcal{I}_{k,p}^{(r)}, t \in \mathcal{T}, \tag{8.13d}$$

$$a_{\boldsymbol{\alpha}}(0) = \mathbb{1}_{\{\boldsymbol{\alpha} \equiv \mathbf{0}\}} \cdot A_0, \qquad \boldsymbol{\alpha} \in \mathcal{I}_{k,p}^{(r)}, \tag{8.13e}$$

$$d_{\mathbf{0}}(t) \geqslant 0, \qquad t \in \mathcal{T}. \tag{8.13f}$$

We solve this deterministic problem with the direct multiple shooting software MUSCOD-II again. For integrating the DAE system (8.13b)–(8.13e), however, the RUNGE-KUTTA-FEHLBERG scheme *RKF45* is not applicable anymore. Instead, we use the variable order and variable step-size Backward Differentiation Formula (BDF) method *DAESOL-II* [4, 6, 7].

For the numerical evaluation of the problem, we used the following parameters, mostly coinciding with (3.14):

$$\kappa = 2.0, \qquad \gamma = 5.0, \qquad C = 7.5, \qquad m = 3.0,$$
$$\beta = 0.5, \qquad r = 0.1, \qquad t_f = 20.$$

Figures 8.12–8.14 depict optimal solutions of the OCP (8.13), i.e., the price coefficients $\hat{P}_0(t)$, $\hat{P}_1(t)$ and a selection of brand image coefficients $a_{\boldsymbol{\alpha}}(t)$ and demand coefficients $d_{\boldsymbol{\alpha}}(t)$, calculated by using the truncated index set $\mathcal{I}_{10,1}$ of multi-indices $\boldsymbol{\alpha}$ with $k = 10$ random variables and a first order ($p = 1$) approximation of the chaos space. Additionally, the initial brand image $A_0 = 50$ and the recession strength constants $c_0 = 0.5$ and $c_1 = 0.1$ are used.

From Figure 8.12 we see that the price coefficient $\hat{P}_0(\cdot)$ is equal to zero over the entire time horizon $\mathcal{T}$, whereas the first order coefficient $\hat{P}_1(\cdot)$ is approximately $0.2 = \frac{1}{\gamma}$. Comparing this to the steady state prices (3.15) and (3.16) of the deterministic conspicuous consumption problem, we see a direct connection between the stochastic price process and those steady state prices. Only in the initial and terminal phase of the considered time horizon there are small deviations from $\hat{P}_1(\cdot)$ being constant. They are due to building up the largest possible reputation depending on the strength process ς_t in the beginning and the usual finite horizon artefacts in the end, respectively.

Figure 8.13 shows some chaos coefficients of the optimal solution of Problem (8.13). We clearly
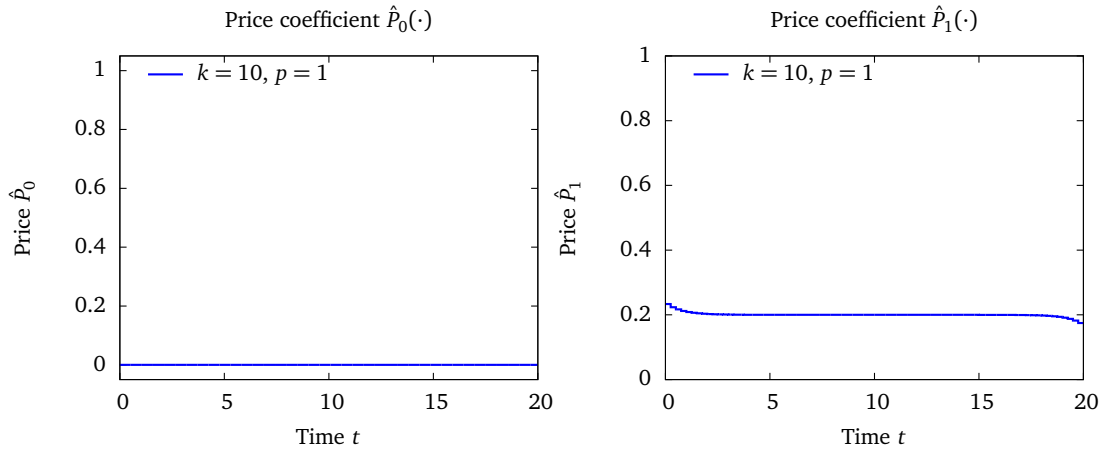
Figure 8.12: Optimal solution of the stochastic conspicuous consumption problem (8.10). The plots show the optimal price coefficients $\hat{P}_0(\cdot)$ and $\hat{P}_1(\cdot)$ resulting from the first order expansion of the original MARKOV control P_t. They are calculated by solving the deterministic OCP (8.13) with the truncated index set $\mathcal{I}_{10,1}$ of multi-indices $\boldsymbol{\alpha}$, initial brand image A_0, and the recession strength parameters $c_0 = 0.5$ and $c_1 = 0.1$.

We see that the zero-order coefficients vanishes and the first order coefficient nearly coincides with the constant $\frac{1}{\gamma}$. Therefore, the connection between the optimal MARKOV control $P_t = \hat{P}_0(t) + \hat{P}_1(t) \cdot A_t$ and the steady state price of the deterministic consumption problem (cf. (3.15) and (3.16)) becomes obvious.

see that only the zero-order coefficient $a_{\boldsymbol{0}}(\cdot)$ does not vanish. Hence, the reputation process $\{A_t\}_{t \in \mathcal{T}}$ is in fact deterministic again. The demand process, however, is truly stochastic, as we see from the non-vanishing coefficients in Figure 8.14. This behavior is caused by the structure of the SOCP (8.10). The stochastic demand process enters only the objective function in a direct fashion, which in turn is an expectation over all trajectories.

Solving the deterministic OCP (8.13) with more advanced approximations of the chaos space, i.e., higher orders $p > 1$ and more random variables $k > 10$, does not affect the solution depicted in Figures 8.12–8.14. The brand image chaos coefficients $a_{\boldsymbol{\alpha}}(t) \equiv 0$ for all $\boldsymbol{\alpha} \neq \boldsymbol{0}$, which yields that even the optimal objective values do not change, cf. Table 8.5.

For varying recession strength parameters c_0 and c_1 the optimal objective function values change, cf. Table 8.6 and Figure 8.15. The higher the principal market reduction parameter c_0, the lower the objective function value. Additionally, the steady state reputation and the expected demand $d_{\boldsymbol{0}}(\cdot)$ decrease. Note that—especially in the case of a principally severe recession, i.e., $c_0 = 1.0$—the initial brand image A_0 needs to be larger. For our numerical tests we use $A_0 = 90$. In the cases of $c_0 = 0.836$ and $c_0 = 1.0$, i.e., for principally intermediate and severe recessions, the LAGRANGE type objective function (8.13a) is not positive over the entire time horizon $\mathcal{T} = [0, t_f]$. For $c_0 = 0.836$ it is only marginally negative in the beginning phase of the horizon and at the terminal time t_f we obtain a positive value. For $c_0 = 1.0$ instead, the cost function is negative most of the time, including t_f. Hence, it would not be possible for the firm to survive this specific recession if there where no possibility to borrow money from the market or to issue new shares.

When comparing the results of the stochastic conspicuous consumption problem with those of Chapter 3, we notice that due to the missing constraint of requiring the cash being positive throughout the complete recession phase there is no obvious adaptivity in the optimal pricing strategy over time. Hence, it is difficult to qualitatively compare the solutions of the stochastic
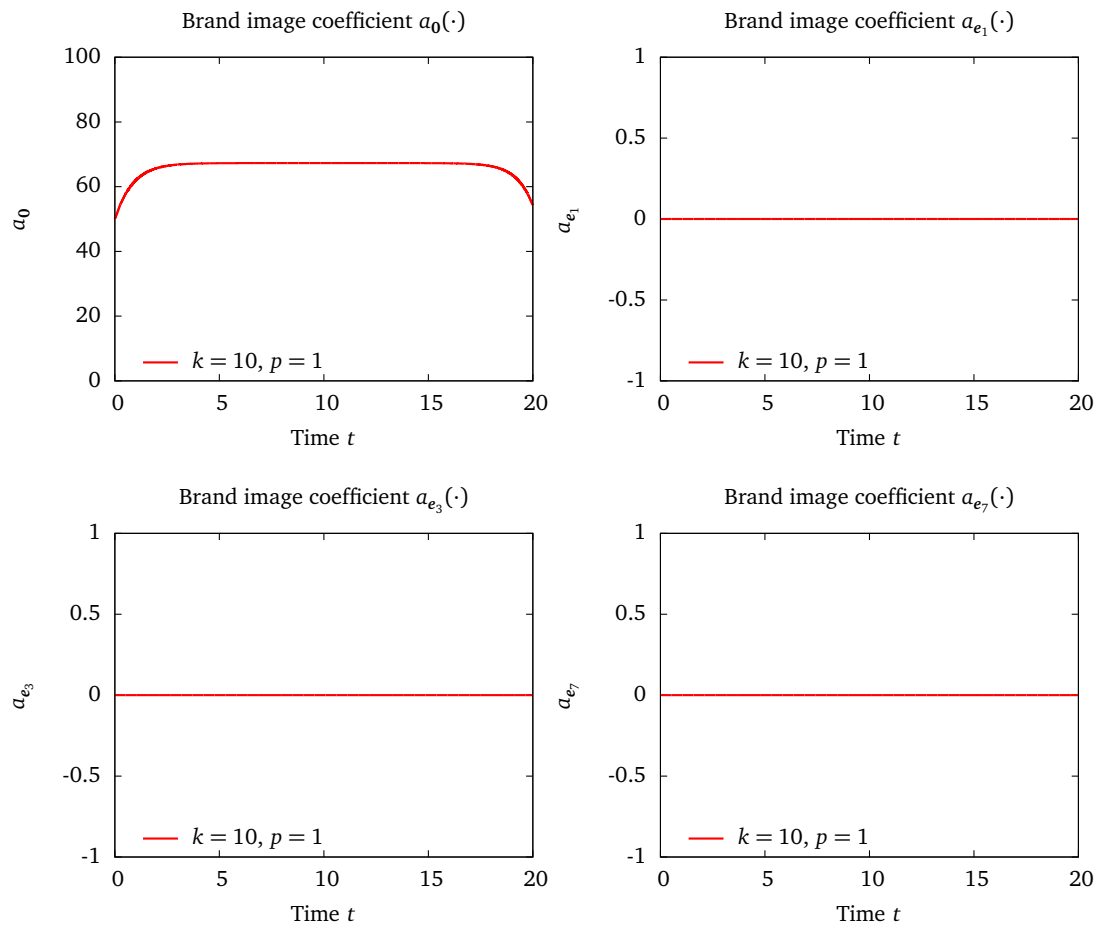
Figure 8.13: Selection of optimal chaos coefficients $a_\alpha(\cdot)$ of the brand image process. They have been derived by solving (8.13) with the a first order ($p = 1$) chaos expansion with $k = 10$ random variables.
We notice that—apart from the zero-order coefficient $a_0(\cdot)$ representing the expectation of the brand image process—all coefficients are identically zero. Hence, the reputation is in fact deterministic.
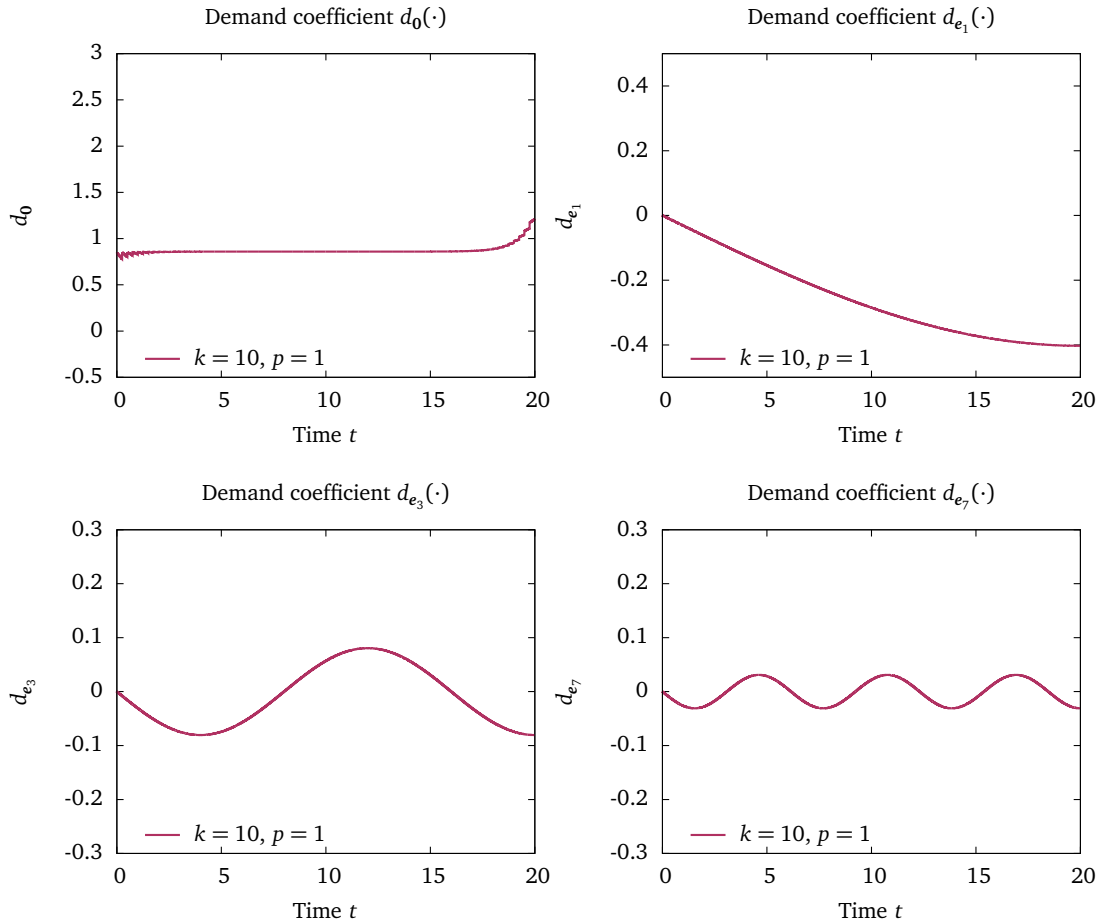
Figure 8.14: Selection of optimal chaos coefficients $d_\alpha(\cdot)$ of the algebraic demand process.

Table 8.5: Optimal values and numerical expenses for solving the SOCP (8.10) with the chaos method-
ology, i.e., solving the deterministic OCP (8.13) with MUSCOD-II. Based on the observations
in Chapter 3, we use a linear expansion of the control process ($q = 1$) and different types
and accuracies of truncating the index set $\mathcal{I}$.

The optimal objective function values do not depend on the number k of incorporated basis
functions of the underlying HILBERT space $L^2(\mathcal{T})$ or on the approximation order p. Never-
theless, runtime increases for higher p and k, because the dimension of the resulting deter-
ministic problems and the associated coupling of the state variables of the system increases.
The symbol "—" in the r-column indicates that the simple truncation (6.14) was used, "ad"
denotes the use of an adaptive index set (6.16). Compare Table 6.1 for a detailed description
of the appropriate index denoted by the reference symbol and number.

k	p	r	# differential coeff. a_α	# algebraic coeff. z_α & d_α	objective value	time in s	# SQP
10	1	—	11	22	33.78136	31.1	18
10	2	—	66	132	33.78136	136.6	22
20	1	—	21	42	33.78136	1734.4	23
20	2	ad[1]	71	142	33.78136	1930.3	16
40	2	ad[2]	91	182	33.78136	1725.1	19

Table 8.6: Comparison of the optimal objective values of the stochastic conspicuous consumption problem (8.10) depending on the strength parameters c_0 and c_1.
We observe that the higher c_0, i.e., the principal market reduction, the lower is the objective function value. In the last example, the objective function values is negative. Hence, the firm would not survive the recession without the possibility to borrow money from the market!

k	p	r	A_0	c_0	c_1	objective value	time in s	# SQP
10	1	—	50	0.5	0.1	33.78136	31.1	18
10	1	—	50	0.836	0.2	0.02621	19.2	15
10	1	—	90	1.0	0.2	-11.17930	24.7	15
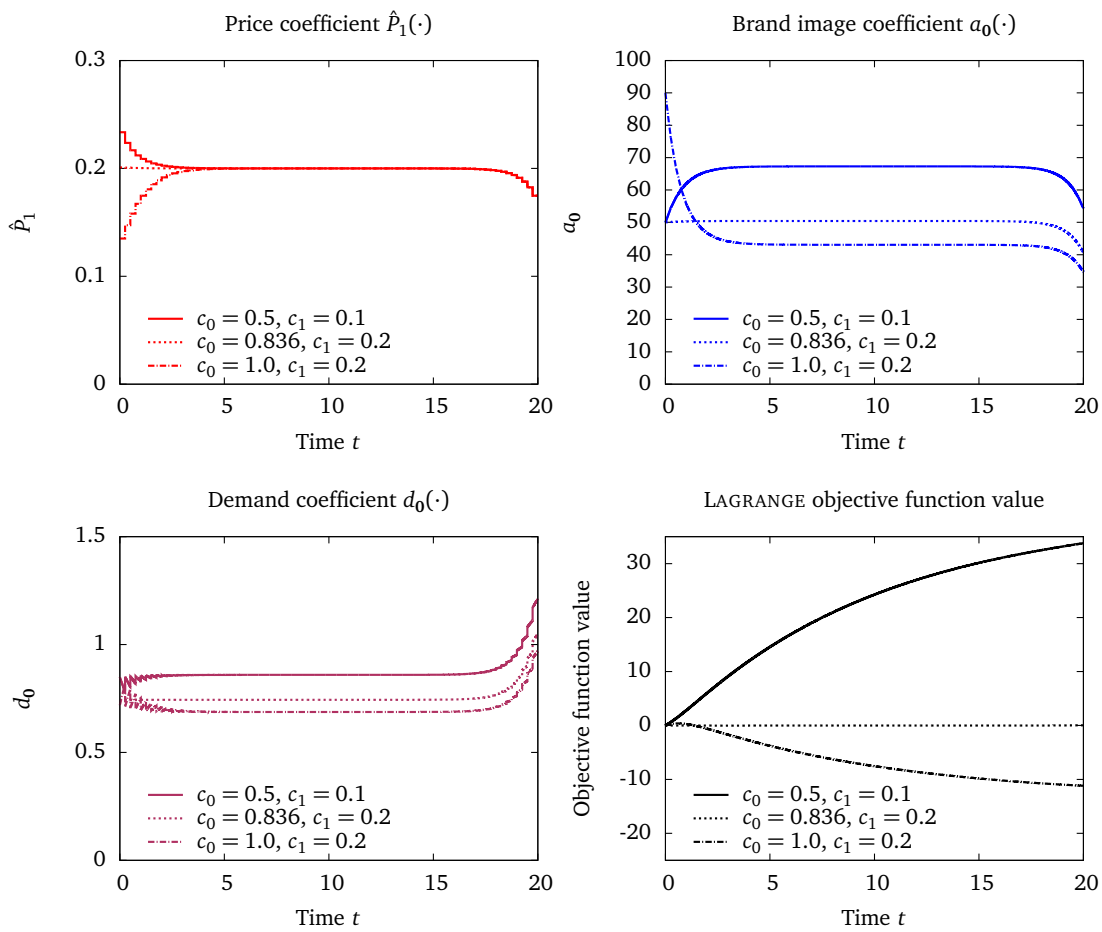
Figure 8.15: Comparison of selected solution trajectories of the stochastic conspicuous consumption problem (8.10) depending on the recession strength parameters c_0 and c_1.
We notice that the price coefficient $\hat{P}_1(\cdot)$ remains (mainly) unchanged, showing only mild adjustments in the beginning phase of the horizon. The brand image coefficient $a_0(\cdot)$ and the expected demand $d_0(\cdot)$ decrease with increasing c_0.
The optimal objective function value decreases as well if c_0 increases. Additionally, in the cases of $c_0 = 0.836$ and $c_0 = 1.0$ we notice, that the LAGRANGE type objective function (8.13a) is not positive over the entire time horizon $\mathcal{T}$. In the latter case the terminal value, i.e., the optimal objective function value, is negative, too. Hence, the firm would not survive the recession without the possibility to borrow money from the market.

and the robust OCP. However, in the stochastic problem the steady state brand image of the recession phase is lower than in the original problem with fixed recession strength ς. This can be seen best if we consider the intermediate recession case ($\varsigma = c_0 = 0.836$) and compare the corresponding phase diagram in Figure 3.6 and the plot of the brand image coefficient $a_0(t)$ in Figure 8.13.

8.4 Summary

In this final chapter we applied the propagator method based on the WIENER chaos approach to SOCPs of type (7.1). We considered the prominent linear-quadratic stochastic regulator problem, a nonlinear extension of this example, and a stochastic adaptation of the conspicuous consumption problem that we introduced in Chapter 3. We regarded the structural properties of the completely deterministic reformulations of the original problems and solved them via the direct multiple shooting approach. Therein, the reformulated problems contained ODE systems describing the dynamic state processes as well as DAE for appearing algebraic states. We analyzed the quality of the solutions depending on both the orders of the different chaos decomposition truncation types and the order of the control expansion. Additionally, we highlighted the strengths and weaknesses of the developed method for its practical purposes and from a computational point of view.

Our analysis yielded very promising results. In particular, if one is interested mainly in the optimal objective value of the problem, the expectations of the optimally controlled states process(es), and variances for only one or a small number of initial values, then the methodology gives fast and reliable results for very basic approximations of the chaos space, i.e., truncations of the propagator. Transferred from it, the expectation of the considered state process and the objective value of the problem are obtained as a side product, which is a huge computational advantage compared to the standard approaches of SOCP that are dependent on simulations of the process.

If the emphasis is more on the control profiles to be robust against deviations in the initial value, more advanced approximations created by using more basis functions of the underlying HILBERT space and a higher order chaos expansion are necessary in general. The stochastic conspicuous consumption problem constitutes an exception to that rule as the considered dynamic state process is in fact deterministic and only the demand function—represented as an algebraic state process—is truly stochastic, but merely enters the objective function.

For more general problems including higher nonlinearities or long-time integration intervals $\mathcal{T}$ higher numerical effort is required [15, 134]. Alternatively, approaches to overcome this issue need to applied, e.g., partitioning of the random space or combinations of the WIENER chaos idea and targeted Monte Carlo corrections [172].

In general, the introduced propagator method constitutes an efficient alternative for solving the challenging class of finite horizon SOCPs apart from the HJB theory and dynamic programming techniques based on MARKOV chain approximations. Due to the use of BOCK's direct multiple shooting approach the method is even applicable for problems including algebraic stochastic states.

A Stochastic Basics

In this supplementary chapter we introduce the necessary stochastic and measure-theoretical terms and definitions that we need throughout this thesis. For a detailed overview see [21, 195].

Definition A.1 (σ-Algebra)
Let a sample space $\Omega \neq \emptyset$ be given. A σ-algebra $\mathcal{F}$ on Ω is a family of subsets of Ω with the following properties:

  (i) $\Omega \in \mathcal{F}$,

  (ii) $A \in \mathcal{F} \Rightarrow \bar{A} \in \mathcal{F}$, where $\bar{A} \stackrel{\text{def}}{=} \Omega \setminus A$ is the complement of A in Ω,

  (iii) $A_i \in \mathcal{F}, \in \mathbb{N} \Rightarrow A \stackrel{\text{def}}{=} \bigcup_{i=1}^{\infty} A_i \in \mathcal{F}$.

The elements of $\mathcal{F}$ are called measurable sets, *$(\Omega, \mathcal{F})$ is referred to as a* measurable space.   △

Definition A.2 (Generated σ-Algebra)
Let $\mathcal{G}$ be any family of subsets of a sample space Ω. The smallest σ-algebra $\sigma(\mathcal{G})$ containing $\mathcal{G}$, i.e.,

$$\sigma(\mathcal{G}) \stackrel{\text{def}}{=} \bigcap \{\mathcal{F} \mid \mathcal{F} \text{ is } \sigma\text{-algebra of } \Omega, \mathcal{G} \subset \mathcal{F}\}, \tag{A.1}$$

is called the σ-algebra generated by $\mathcal{G}$.   △

Definition A.3 (Probability Measure)
A probability measure $\mathbb{P}$ on a measurable space $(\Omega, \mathcal{F})$ is a function $\mathbb{P}\colon \mathcal{F} \to [0,1]$ such that

  (i) $\mathbb{P}[\emptyset] = 0$, $\mathbb{P}[\Omega] = 1$,

  (ii) *if $A_i \in \mathcal{F}$, $i \in \mathbb{N}$, and $A_i \cup A_j = \emptyset$ for $i \neq j$, then*

$$\mathbb{P}\left[\bigcup_{i=1}^{\infty} A_i\right] = \sum_{i=1}^{\infty} \mathbb{P}[A_i].$$

The triple $(\Omega, \mathcal{F}, \mathbb{P})$ is called a probability space. *It is named a* complete probability space *if $\mathcal{F}$ contains all subsets $G \in \Omega$ with $\mathbb{P}$-outer measure zero, i.e., with*

$$\mathbb{P}^*[G] \stackrel{\text{def}}{=} \inf\{\mathbb{P}[F] \mid F \in \mathcal{F}, G \subset F\} = 0. \qquad △$$

Any probability space $(\Omega, \mathcal{F}, \mathbb{P})$ can be completed by extending the σ-algebra $\mathcal{F}$ by the sets of outer measure zero and appropriately extending the probability measure $\mathbb{P}$, cf. [195]. In this work we assume all appearing probability spaces to be complete.

Definition A.4 (Measurable Function)
Let $(\Omega, \mathcal{F}, \mathbb{P})$ be a given probability space. A function $X\colon \Omega \to \mathbb{R}^{n_X}$ is called $\mathcal{F}$-measurable if

$$X^{-1}(Q) \stackrel{\text{def}}{=} \{\omega \in \Omega \mid X(\omega) \in Q\} \in \mathcal{F} \tag{A.2}$$

for all open sets $Q \in \mathbb{R}^{n_X}$ or, equivalently, for all BOREL sets $Q \subset \mathbb{R}^{n_X}$. △

If the function $X\colon \Omega \to \mathbb{R}^{n_X}$ is given, the σ-algebra $\sigma(X)$ generated by X is the smallest σ-algebra on Ω containing all sets $X^{-1}(Q)$ with open $Q \subset \mathbb{R}^{n_X}$.

Definition A.5 (Random Variable)
Let $(\Omega, \mathcal{F}, \mathbb{P})$ be given again. A random variable X *is a $\mathcal{F}$-measurable function $X\colon \Omega \to \mathbb{R}^{n_X}$. Every random variable X induces a probability measure μ_X on $\mathbb{R}^{n_X}$ through*

$$\mu_X(Q) \stackrel{\text{def}}{=} \mathbb{P}\big[X^{-1}(Q)\big]. \tag{A.3}$$

Then μ_X is called the distribution *of X.* △

Definition A.6 (Cumulative Distribution Function)
On the probability space $(\Omega, \mathcal{F}, \mathbb{P})$, let $X\colon \Omega \to \mathbb{R}^{n_X}$ be a random variable. The induced probability distribution on $\mathbb{R}^{n_X}$ has the cumulative distribution function $F_X\colon \mathbb{R}^{n_X} \to [0,1]$ *defined via*

$$F_X(x) \stackrel{\text{def}}{=} \mathbb{P}\big[\omega \in \Omega \,|\, X(\omega) \leqslant x\big], \tag{A.4}$$

where $X(\omega) \leqslant x$ is only true if the relation holds for every component X_i, $1 \leqslant i \leqslant n_X$, of X. △

Definition A.7 (Expectation)
If $\int_\Omega |X(\omega)|\, \mathrm{d}\mathbb{P}[\omega] < \infty$, the expectation *of X with respect to $\mathbb{P}$ is defined as*

$$\mathbb{E}[X] \stackrel{\text{def}}{=} \int_\Omega X(\omega)\, \mathrm{d}\mathbb{P}[\omega] = \int_{\mathbb{R}^{n_X}} x\, \mathrm{d}\mu_X(x). \tag{A.5}$$

If $f\colon \mathbb{R}^{n_X} \to \mathbb{R}$ is BOREL measurable and $\int_\Omega |f(X(\omega))|\, \mathrm{d}\mathbb{P}[\omega] < \infty$, we have

$$\mathbb{E}[f(X)] \stackrel{\text{def}}{=} \int_\Omega f(X(\omega))\, \mathrm{d}\mathbb{P}[\omega] = \int_{\mathbb{R}^{n_X}} f(x)\, \mathrm{d}\mu_X(x). \tag{A.6}$$

△

Definition A.8 (Variance)
If $\int_\Omega |X(\omega)|^2\, \mathrm{d}\mathbb{P}[\omega] < \infty$, the variance *of X with respect to $\mathbb{P}$ is defined as*

$$\mathbb{V}[X] \stackrel{\text{def}}{=} \int_\Omega (X(\omega) - \mathbb{E}[X(\omega)])^2\, \mathrm{d}\mathbb{P}[\omega]. \tag{A.7}$$

△

Bibliography

[1] C. Acerbi. Spectral Measures of Risk: A Coherent Representation of Subjective Risk Aversion. *Journal of Banking and Finance*, 26:1505–1518, 2002.

[2] C. Acerbi and D. Tasche. On the Coherence of Expected Shortfall. *Journal of Banking and Finance*, 26:1487–1503, 2002.

[3] M. Akian. Analyse de l'Algorithme Multigrille FMGH de Résolution d'Équations d'Hamilton-Jacobi-Bellman. In *Analysis and Optimization of Systems*, volume 144 of *Lecture Notes in Control and Information Sciences*, pages 113–122. Springer, 1990.

[4] J. Albersmeyer. Effiziente Ableitungserzeugung in einem adaptiven BDF-Verfahren. Diploma thesis, Ruprecht-Karls-Universität Heidelberg, 2005.

[5] J. Albersmeyer. *Adjoint Based Algorithms and Numerical Methods for Sensitivity Generation and Optimization of Large Scale Dynamic Systems*. PhD thesis, Ruprecht-Karls-Universität Heidelberg, 2010.

[6] J. Albersmeyer and H. G. Bock. Sensitivity Generation in an Adaptive BDF-Method. In *Modeling, Simulation and Optimization of Complex Processes: Proceedings of the International Conference on High Performance Scientific Computing, March 6–10, 2006, Hanoi, Vietnam*, pages 15–24. Springer, 2008.

[7] J. Albersmeyer and H. G. Bock. Efficient Sensitivity Generation for Large Scale Dynamic Systems. Technical report, SPP 1253 Preprints, Universität Erlangen, 2009.

[8] J. Albersmeyer and M. Diehl. The Lifted Newton Method and its Application in Optimization. *SIAM Journal on Optimization*, 20:1655–1684, 2010.

[9] W. Amaldoss and S. Jain. Conspicuous Consumption and Sophisticated Thinking. *Management Science*, 51:1449–1466, 2005.

[10] W. Amaldoss and S. Jain. Pricing of Conspicuous Goods: A Competitive Analysis of Social Effects. *Journal of Marketing Research*, 42:30–42, 2005.

[11] E. Anderson, H. Xu, and D. Zhang. Confidence Levels for CVaR Risk Measures and Minimax Limits. Optimization Online, 2014. (2014/01/4212.pdf).

[12] P. Artzner, F. Delbaen, J.-M. Eber, and D. Heath. Coherent Measures of Risk. *Mathematical Finance*, 9:203–228, 1999.

[13] P. K. Asea and P. J. Zak. Time-to-Build and Cycles. *Journal of Economic Dynamics & Control*, 23:1155–1175, 1999.

[14] A. C. Atkinson. A Method for Discriminating Between Models. *Journal of the Royal Statistical Society, Series B (Methodological)*, 32:323–353, 1970.

[15] F. Augustin and P. Rentrop. Stochastic Galerkin Techniques for Random Ordinary Differential Equations. *Numerische Mathematik*, 122:399–419, 2012.

[16] F. Augustin, A. Gilg, M. Paffrath, P. Rentrop, and U. Wever. Polynomial Chaos for the Approximation of Uncertainties: Chances and Limits. *European Journal of Applied Mathematics*, 19:149–190, 2008.

[17] J. D. Azzato and J. B. Krawczyk. SOCSol4L: An Improved MATLAB Package for Approximating the Solution to a Continuous-Time Stochastic Optimal Control Problem. Technical report, School of Economics and Finance, Victoria University of Wellington, 2006. MPRA Paper No. 10015.

[18] I. Babuška, R. Tempone, and G. E. Zouraris. Galerkin Finite Element Approximations of Stochastic Elliptic Partial Differential Equations. *SIAM Journal on Numerical Analysis*, 42:800–825, 2004.

[19] M. Bambi. Endogenous Growth and Time to Build: The AK Case. *Journal of Economic Dynamics and Control*, 32:1015–1040, 2008.

[20] V. Bär. Ein Kollokationsverfahren zur numerischen Lösung allgemeiner Mehrpunkt-randwertaufgaben mit Schalt- und Sprungbedingungen mit Anwendungen in der optimalen Steuerung und der Parameteridentifizierung. Diploma thesis, Rheinische Friedrich-Wilhelms-Universität Bonn, 1983.

[21] H. Bauer. *Wahrscheinlichkeitstheorie und Grundzüge der Maßtheorie*. DeGruyter, 1991.

[22] I. Bauer. *Numerische Verfahren zur Lösung von Anfangswertaufgaben und zur Generierung von ersten und zweiten Ableitungen mit Anwendungen bei Optimierungsaufgaben in Chemie und Verfahrenstechnik*. PhD thesis, Ruprecht-Karls-Universität Heidelberg, 1999.

[23] D. Beigel. *Efficient Goal-Oriented Global Error Estimation for BDF-Type Methods Using Discrete Adjoints*. PhD thesis, Ruprecht-Karls-Universität Heidelberg, 2012.

[24] R. Bellman. The Stability of Solutions of Linear Differential Equations. *Duke M*, 10:643–647, 1943.

[25] R. E. Bellman. *Dynamic Programming*. University Press, 1957.

[26] A. Ben-Tal and A. Nemirovski. Robust Convex Optimization. *Mathematics of Operations Research*, 23:769–805, 1998.

[27] A. Ben-Tal and A. Nemirovski. Robust Solutions of Uncertain Linear Programs. *Operations Research Letters*, 25:1–13, 1999.

[28] A. Ben-Tal and A. Nemirovski. Robust Solutions of Linear Programming Problems Contaminated with Uncertain Data. *Mathematical Programming*, 88:411–424, 2000.

[29] C. Bender and J. Zhang. Time Discretization and Markovian Iteration for Coupled FB-SDEs. *The Annals of Applied Probability*, 18:143–177, 2008.

[30] A. Bensoussan. *Nonlinear Filtering and Stochastic Control*, volume 972 of *Lecture Notes in Mathematics*, chapter Lectures on Stochastic Control, pages 1–62. Springer, 1982.

[31] F. E. Benth and J. Gjerde. Convergence Rates for Finite Element Approximations of Stochastic Partial Differential Equations. *Stochastics and Stochastic Reports*, 63:313–326, 1998.

[32] F. E. Benth and T. G. Theting. Some Regularity Results for the Stochastic Pressure Equation of Wick-Type. *Stochastic Analysis and Applications*, 20:1191–1223, 2002.

[33] D. P. Bertsekas. *Dynamic Programming and Optimal Control, Volume 1*. Athena Scientific, 2005. ISBN 1-886529-26-4 ; 978-1-886529-26-7.

[34] D. P. Bertsekas. *Dynamic Programming and Optimal Control, Volume 2*. Athena Scientific, Belmont, Mass., 4. ed. edition, 2012.

[35] D. Bertsimas and D. B. Brown. Constrained Stochastic LQC: A Tractable Approach. *IEEE Transactions on Automatic Control*, 52:1826–1841, 2007.

[36] D. Bertsimas and M. Sim. The Price of Robustness. *Operations Research*, 52:35–53, 2004.

[37] D. Bertsimas, D. Pachamanova, and M. Sim. Robust Linear Optimization Under General Norms. *Operations Research Letters*, 32:510–516, 2004.

[38] D. Bertsimas, D. B. Brown, and C. Caramanis. Theory and Applications of Robust Optimization. *SIAM Review*, 53:464–501, 2011.

[39] J. T. Betts. *Practical Methods for Optimal Control Using Nonlinear Programming*. Advances in Design and Control. Society for Industrial and Applied Mathematics, 2001.

[40] L. Biegler. Solution of dynamic optimization problems by successive quadratic programming and orthogonal collocation. *Computers & Chemical Engineering*, 8:243–248, 1984.

[41] L. Biegler. An overview of simultaneous strategies for dynamic optimization. *Chemical Engineering and Processing*, 46:1043–1053, 2007.

[42] L. T. Biegler, O. Ghattas, M. Heinkenschloss, and B. van Bloemen Waanders. *Large-Scale PDE-Constrained Optimization*, volume 30 of *Lecture Notes in Computational Science and Engineering*. Springer, 2003.

[43] J.-M. Bismut. An Introductory Approach to Duality in Optimal Stochastic Control. *SIAM Review*, 20:62–78, 1978.

[44] G. Blatman and B. Sudret. Sparse Polynomial Chaos Expansions Based on an Adaptive Least Angle Regression Algorithm. In *19ème Congrès Français de Mécanique*, 2009.

[45] H. G. Bock. Numerische Optimierung zustandsbeschränkter parameterabhängiger Prozesse mit linear auftretender Steuerung unter Anwendung der Mehrzielmethode. Diploma thesis, Universität zu Köln, 1974.

[46] H. G. Bock and K. J. Plitt. A Multiple Shooting Algorithm for Direct Solution of Optimal Control Problems. In *Proceedings of the 9th IFAC World Congress*, pages 242–247. Pergamon Press, 1984.

[47] J. F. Bonnans and F. J. Silva. First and Second Order Necessary Conditions for Stochastic Optimal Control Problems. *Applied Mathematics & Optimization*, 65:403–439, 2012.

[48] E. Borel. Les Probabilités Dénombrables et Leurs Applications Arithmétiques. *Rendiconti del Circolo Matematico di Palermo*, 27:247–271, 1909.

[49] R. Boucekkine, O. Licandro, L. A. Puch, and F. del Rio. Vintage Capital and the Dynamics of the AK Model. *Journal of Economic Theory*, 120:39–72, 2005.

[50] J. P. Boyd. *Chebyshev and Fourier Spectral Methods*. Dover Publishing Inc., 2003.

[51] U. Brandt-Pollmann, R. Winkler, S. Sager, U. Moslener, and J. P. Schlöder. Numerical Solution of Optimal Control Problems with Constant Control Delays. *Computational Economics*, 31:181–206, 2008.

[52] P. Briand and C. Labart. Simulation of BSDEs by Wiener Chaos Expansion. *Annals of Applied Probability*, 24:1129–1171, 2014.

[53] R. Bulirsch. Die Mehrzielmethode zur numerischen Lösung von nichtlinearen Randwertproblemen und Aufgaben der optimalen Steuerung. Technical report, Carl-Cranz-Gesellschaft, 1971.

[54] T. D. Butler, C. N. Dawson, and T. Wildey. A Posteriori Error Analysis of Stochastic Differential Equations Using Polynomial Chaos Expansions. *SIAM Journal on Scientific Computing*, 33:1267–1291, 2011.

[55] G. Calafiore and M. C. Campi. Uncertain Convex Programs: Randomized Solutions and and Confidence Levels. *Mathematical Programming*, 102:25–46, 2005.

[56] R. H. Cameron and W. T. Martin. The Orthogonal Development of Non-Linear Functionals in Series of Fourier-Hermite Functionals. *Annals of Mathematics*, 48:385–392, 1947.

[57] F. P. Cantelli. Sulla Probabilità Come Limite Della Frequenza. *Accademia Nazionale dei Lincei*, 26:39–45, 1917.

[58] Y. Cao. On Convergence Rate of Wiener-Ito Expansion for Generalized Random Variables. *Stochastics*, 78:179–187, 2006.

[59] L. Carlitz. The Product of Several Hermite or Laguerre Polynomials. *Monatshefte für Mathematik*, 66:393–396, 1962.

[60] P. Carpentier, G. Cohen, and A. Dallagi. Particle Methods for Stochastic Optimal Control Problems. *Computational Optimization and Applications*, 56:635–674, 2013.

[61] J. P. Caulkins, G. Feichtinger, D. Grass, R. F. Hartl, P. M. Kort, and A. Seidl. Two-Stage Conspicuous Consumption Model. Working paper, 2010.

[62] J. P. Caulkins, R. F. Hartl, and P. M. Kort. Delay Equivalence in Capital Accumulation Models. *Journal of Mathematical Economics*, 46:1243–1246, 2010.

[63] J. P. Caulkins, G. Feichtinger, D. Grass, R. F. Hartl, P. M. Kort, and A. Seidl. Optimal Pricing of a Conspicuous Product During a Recession that Freezes Capital Markets. *Journal of Economic Dynamics and Control*, 35:163–174, 2011.

[64] W. Chavanasporn and C.-O. Ewald. A Numerical Method for Solving Stochastic Optimal Control Problems with Linear Control. *Computational Economics*, 39:429–446, 2012.

[65] A. S. Cherny and H.-J. Engelbert. *Singular Stochastic Differential Equations*. Springer, 2005.

[66] A. Cohen, R. DeVore, and C. Schwab. Convergence Rates of Best N-term Galerkin Approximations for a Class of Elliptic sPDEs. *Foundations of Computational Mathematics*, 10:615–646, 2010.

[67] F. Collard, O. Licandro, and L. A. Puch. The Short-Run Dynamics of Optimal Growth Models with Delays. *Annales d'Économie et de Statistique*, 90:127–143, 2008.

[68] L. G. Crespo and J.-Q. Sun. Stochastic Optimal Control of Nonlinear Systems via Short-Time Gaussian Approximation and Cell Mapping. *Nonlinear Dynamics*, 28:323–342, 2002.

[69] L. G. Crespo and J.-Q. Sun. Stochastic Optimal Control via Bellman's Principle. *Automatica*, 39:2109–2114, 2003.

[70] B. J. Debusschere, H. N. Najm, P. P. Pébay, O. M. Knio, R. G. Ghanem, and O. P. Le Maître. Numerical Challenges in the Use of Polynomial Chaos Representations for Stochastic Processes. *SIAM Journal on Scientific Computing*, 26(2):698–719, 2005.

[71] W. D. Dechert and K. Nishimura. A Complete Characterization of Optimal Growth Paths in an Aggregated Model with a Non-Concave Production Function. *Journal of Economic Theory*, 31:332–354, 1983.

[72] F. Delarue and S. Menozzi. A Forward-Backward Stochastic Algorithm for Quasi-Linear PDEs. *The Annals of Applied Probability*, 16:140–184, 2006.

[73] M. Diehl. *Real-Time Optimization for Large Scale Nonlinear Processes*. PhD thesis, Ruprecht-Karls-Universität Heidelberg, 2001.

[74] M. Diehl, H. G. Bock, and E. Kostina. An Approximation Technique for Robust Nonlinear Optimization. *Mathematical Programming*, 107:213–230, 2006.

[75] M. Diehl, J. Gerhard, W. Marquardt, and M. Moennigmann. Numerical Solution Approaches for Robust Optimal Control Problems. *Computers & Chemical Engineering*, 32: 1279–1292, 2008.

[76] S. E. Dreyfus. *Dynamic Programming and the Calculus of Variations*. Academic Press, 1965.

[77] G. E. Dullerud and F. Paganini. *A Course in Robust Control Theory: A Convex Approach*. Springer, 1999.

[78] E. B. Dynkin and A. A. Yushkevich. *Controlled Markov Processes*. Springer, 1979.

[79] T. Economist. Riding the Rollercoaster: Six Firms in Cyclical Industries and Battle Excess Debt. The Economist, December 11 2008.

[80] E. Eich. *Projizierende Mehrschrittverfahren zur numerischen Lösung von Bewegungsgleichungen technischer Mehrkörpersysteme mit Zwangsbedingungen und Unstetigkeiten*. PhD thesis, Universität Augsburg, 1991.

[81] L. El Ghaoui and H. Lebret. Robust Solutions to Least-Squares Problems with Uncertain Data. *SIAM Journal of Matrix Analysis and Applications*, 18:1035–1064, 1997.

[82] L. El Ghaoui, F. Oustry, and H. Lebret. Robust Solutions to Uncertain Semidefinite Programs. *SIAM Journal on Optimization*, 9:33–52, 1998.

[83] M. A. El-Hodiri, E. Loehman, and A. Whinston. An Optimal Growth Model with Time Lags. *Econometrica*, 40:1137–1146, 1972.

[84] S. K. Eldersveld and M. A. Saunders. A Block-LU Update for Large Scale Linear Programming. *SIAM Journal of Matrix Analysis and Applications*, 13:191–201, 1992.

[85] E. Erdoğan and G. Iyengar. Ambiguous Chance Constrained Problems and Robust Optimization. *Mathematical Programming*, 107:37–61, 2006.

[86] V. V. Fedorov. *Theory of Optimal Experiments*. Academic Press, New York and London, 1972.

[87] E. Fehlberg. Low-Order Classical Runge-Kutta Formulas with Stepsize Control and Their Application to Some Heat Transfer Problems. Technical Report R-315, NASA, 1969.

[88] A. A. Feldbaum. Dual Control Theory I. *Avtomatika i Telemekhanika*, 21:1240–1249, 1960.

[89] A. A. Feldbaum. Dual Control Theory II. *Avtomatika i Telemekhanika*, 2:1453–1464, 1960.

[90] E. Feldheim. Expansions and Integral Transforms for Products of Laguerre and Hermite Polynomials. *Quarterly Journal of Mathematics*, 11:18–29, 1940.

[91] B. G. Fitzpatrick and W. H. Fleming. Numerical Methods for an Optimal Investment-Consumption Model. *Mathematics of Operations Research*, 16:823–841, 1991.

[92] W. H. Fleming and R. W. Rishel. *Deterministic and Stochastic Optimal Control*. Springer, 1982.

[93] W. H. Fleming and H. M. Soner. *Controlled Markov Processes and Viscosity Solutions*. Springer, 1993.

[94] R. Fletcher. *Practical Methods of Optimization*. Wiley, 1987.

[95] P. A. Forsyth and G. Labahn. Numerical Methods for Controlled Hamilton-Jacobi-Bellman PDEs in Finance. *Journal of Computational Finance*, 11:1–44, 2007/2008.

[96] J. V. Frasch, S. Sager, and M. Diehl. A Parallel Quadratic Programming Method for Dynamic Optimization Problems. *Mathematical Programming Computation*, 2013. (submitted).

[97] P. Frauenfelder, C. Schwab, and R. A. Todor. Finite elements for elliptic problems with stochastic coefficients. *Computational Methods of Applied Mechanical Engineering*, 194: 205–228, 2005.

[98] J. Galvis. *Domain Decomposition Analysis for Heterogeneous Darcy's Flow*. PhD thesis, Instituto Nacional de Matemática Pura e Aplicada, 2008.

[99] B. Ganapathysubramanian and N. Zabaras. Sparse Grid Collocation Schemes for Stochastic Natural Convection Problems. *Journal of Computational Physics*, 225:652–685, 2007.

[100] R. G. Ghanem and P. D. Spanos. *Stochastic Finite Elements*. Springer, 1991.

[101] D. Grass, J. P. Caulkins, G. Feichtinger, G. Tragler, and D. A. Behrens. *Optimal Control of Nonlinear Processes: With Applications in Drugs, Corruption, and Terror*. Springer, 2008.

[102] T. H. Gronwall. Note on the Derivatives with Respect to a Parameter of the Solutions of a System of Differential Equations. *Annals of Mathematics*, 20:292–296, 1919.

[103] M. Günther and A. Jüngel. *Finanzderivate mit MATLAB*. Vieweg+Teubner, 2010.

[104] A. Haar. Zur Theorie der orthogonalen Funktionensysteme. *Mathematische Annalen*, 69:331–371, 1910.

[105] J. K. Hale. *Ordinary Differential Equations*. John Wiley & Sons, 1969.

[106] F. B. Hanson. *Stochastic Digital Control System Techniques*, volume 76 of *Control And Dynamic Systems: Advances in Theory and Applications*, chapter Techniques in Computational Stochastic Dynamic Programming, pages 103–162. Academic Press, 1996.

[107] U. G. Haussmann. General Necessary Conditions for Optimal Control of Stochastic Systems. *Mathematical Programming Studies*, 6:30–48, 1975.

[108] T. Heine, M. Kawohl, and R. King. Robust Model Predictive Control Using the Unscented Transformation. In *IEEE International Conference on Control Applications*, pages 224–230, 2006.

[109] T. Heine, M. Kawohl, and R. King. A New Approach for Robust Optimization Based Open- and Closed-Loop Control of Nonlinear Processes. *Automatisierungstechnik*, 54: 614–621, 2006.

[110] M. Herzog, A. Gilg, M. Paffrath, P. Rentrop, and U. Wever. Intrusive versus Non-Intrusive Methods for Stochastic Finite Elements. In *From Nano to Space*, Applied Mathematics inspired by R. Bulirsch. Springer, 2007.

[111] G. A. Hicks and W. H. Ray. Approximation Methods for Optimal Control Synthesis. *The Canadian Journal of Chemical Engineering*, 49:522–528, 1971.

[112] C. Hoffmann. Numerical Methods for the Discrimination of DAE Models with Applications in Enzyme Kinetics. Diploma thesis, Ruprecht-Karls-Universität Heidelberg, 2005.

[113] H. Holden, B. Øksendal, J. Ubøe, and T. Zhang. *Stochastic Partial Differential Equations*. Springer, 2010.

[114] B. Houska, H. J. Ferreau, and M. Diehl. An Auto-Generated Real-Time Iteration Algorithm for Nonlinear MPC in the Microsecond Range. *Automatica*, 47:2279–2285, 2011.

[115] T. Huschto and S. Sager. Stochastic Optimal Control in the Perspective of the Wiener Chaos. In *Proceedings of the 12th European Control Conference*, pages 3059–3064, 2013.

[116] T. Huschto and S. Sager. Solving Stochastic Optimal Control Problems by a Wiener Chaos Approach. *Vietnam Journal of Mathematics*, 42:83–113, 2014.

[117] T. Huschto and S. Sager. Pricing Conspicuous Consumption Products in Recession Periods with Uncertain Strength. *EURO Journal on Decision Processes*, 2:3–30, 2014.

[118] T. Huschto, G. Feichtinger, P. M. Kort, R. F. Hartl, S. Sager, and A. Seidl. Numerical Solution of a Conspicuous Consumption Model with Constant Control Delay. *Automatica*, 47:1868–1877, 2011.

[119] M. Hutzenthaler, A. Jentzen, and P. E. Kloeden. Strong and Weak Divergence in Finite Time of Euler's Method for Stochastic Differential Equations with Non-globally Lipschitz Continuous Coefficients. *Proceedings of the Royal Society of London Series A*, 467:1563–1576, 2011.

[120] A. D. Ioffe and V. M. Tichomirov. *Theorie der Extremalaufgaben*. VEB Deutscher Verlag der Wissenschaften, 1979. Translation from the Russian original by Bernd Luderer.

[121] E. Isobe and S. Sato. Wiener-Hermite Expansion of a Process Generated by an Itô Stochastic Differential Equation. *Journal of Applied Probability*, 20:754–765, 1983.

[122] K. Itō. Stochastic Integral. *Proceedings of the Imperial Academy*, 20:519–524, 1944.

[123] K. Itō. On a Stochastic Integral Equation. *Proceedings of the Japan Academy*, 22:32–35, 1946.

[124] K. Itō. Multiple Wiener Integral. *Journal of the Mathematical Society of Japan*, 3:157–169, 1951.

[125] S. Janson. *Gaussian Hilbert Spaces*. Cambridge University Press, 1997.

[126] A. Jentzen and P. E. Kloeden. *Taylor Approximations for Stochastic Partial Differential Equations*. CMBS-NSF Regional Conference Series in Applied Mathematics 83. Society for Industrial and Applied Mathematics, 2011.

[127] P. Jorion. *Value at Risk: The New Benchmark for Managing Financial Risk*. McGraw-Hill, 2006.

[128] S. J. Julier and J. K. Uhlmann. A General Method for Approximating Nonlinear Transformations of Probability Distributions. Technical report, University of Oxford, 1996.

[129] S. J. Julier and J. K. Uhlmann. A New Extension of the Kalman Filter to Nonlinear Systems. In *Proceedings of the International Symposium on Aerospace/Defense Sensing, Simulation, and Controls*, volume 3, 1997.

[130] M. Kalecki. A Macroeconomic Theory of Business Cycles. *Econometrica*, 3:327–344, 1935.

[131] H. J. Kappen. Path Integrals and Symmetry Breaking for Optimal Control Theory. *Journal of Statistical Mechanics: Theory and Experiment*, P11011, 2005.

[132] I. Karatzas and S. E. Shreve. *Brownian Motion and Stochastic Calculus*. Spinger, 2007.

[133] K. Karhunen. *Über lineare Methoden in der Wahrscheinlichkeitsrechnung*, volume 37. Annales Academiæ Scientiarum Fennicæ, Series A.I, 1947.

[134] G. E. Karniadikis, C.-H. Su, D. Xiu, D. Lucor, C. Schwab, and R. A. Todor. Generalized Polynomial Chaos Solution for Differential Equations with Random Inputs. Report Nr. 2005-01, ETH Zürich, 2005.

[135] A. Keese and H. G. Matthies. Numerical Methods and Smolyak Quadrature for Nonlinear Stochastic Partial Differential Equations. Informatikbericht Nr.: 2003-5, TU Braunschweig, 2003.

[136] C. Kirches. A Numerical Method for Nonlinear Robust Optimal Control with Implicit Discontinuities and an Application to Powertrain Oscillations. Diploma thesis, Ruprecht-Karls-Universität Heidelberg, 2006.

[137] C. Kirches. *Fast Numerical Methods for Mixed-Integer Nonlinear Model-Predictive Control*. Advances in Numerical Mathematics. Springer Vieweg, 2011.

[138] C. Kirches, S. Sager, H. G. Bock, and J. P. Schlöder. Time-Optimal Control of Automobile Test Drives with Gear Shifts. *Optimal Control Applications and Methods*, 31:137–153, 2010.

[139] C. Kirches, H. G. Bock, J. P. Schlöder, and S. Sager. Complementary Condensing for the Direct Multiple Shooting Method. In H. Bock, H. Phu, R. Rannacher, and J. Schlöder, editors, *Modeling, Simulation, and Optimization of Complex Processes. Proceedings of the Fourth International Conference on High Performance Scientific Computing, March 2–6, 2009, Hanoi, Vietnam*, pages 195–206. Springer, 2012.

[140] C. Kirches, L. Wirsching, H. G. Bock, and J. P. Schlöder. Efficient Direct Multiple Shooting for Nonlinear Model Predictive Control on Long Horizons. *Journal of Process Control*, 22:540–550, 2012.

[141] P. E. Kloeden and E. Platen. *Numerical Solution of Stochastic Differential Equations*. Springer, 1999.

[142] P. E. Kloeden, E. Platen, and H. Schurz. *Numerical Solution of SDE Through Computer Experiments*. Springer, 2007.

[143] V. B. Kolmanovskii and A. D. Myshkis. *Applied Theory of Functional Differential Equations*. Kluwer Academic Publishers, 1992.

[144] A. Kolmogorov. Über die analytischen Methoden in der Wahrscheinlichkeitsrechnung. *Mathematische Annalen*, 104:415–468, 1931.

[145] S. Körkel. *Numerische Methoden für Optimale Versuchsplanungsprobleme bei nichtlinearen DAE-Modellen*. PhD thesis, Ruprecht-Karls-Universität Heidelberg, 2002.

[146] R. Korn and E. Korn. *Option Pricing and Portfolio Optimization*. Graduate Studies in Mathematics. Oxford University Press, 2001.

[147] P. M. Kort, J. P. Caulkins, R. F. Hartl, and G. Feichtinger. Brand Image and Brand Dilution in the Fashion Industry. *Automatica*, 42:1363–1370, 2006.

[148] J. B. Krawczyk. A Markovian Approximated Solution to a Portfolio Management Problem. *Information Technology for Economics and Management (ITEM)*, 1:Paper 02, 2001.

[149] N. V. Krylov. *Controlled Diffusion Processes*. Springer, 1980.

[150] P. Kühl, M. Diehl, A. Milewska, E. Molga, and H. G. Bock. Robust NMPC for a Benchmark Fed-Batch Reactor with Runaway Conditions. In R. Findeisen, F. Allgoewer, and L. Biegler, editors, *Assessment and Future Directions of Nonlinear Model Predictive Control*, volume 358 of *Lecture Notes in Control and Information Sciences*, pages 455–464. Springer, 2007.

[151] M. Kumar, S. Chakravorty, and J. L. Junkins. Computational Nonlinear Stochastic Control Based on the Fokker-Planck Equation. In *AIAA Guidance, Navigation and Control Conference*, 2008. Paper 2008-6477.

[152] H. Kunita and S. Watanabe. On Square Integrable Martingales. *Nagoya Mathematical Journal*, 30:209–245, 1967.

[153] M. Kunze. An Introduction to Malliavin Calculus. Lecture Notes at the Universität Ulm, Summer Term 2013.

[154] H. J. Kushner. On the Stochastic Maximum Principle: Fixed Time of Control. *Journal of Mathematical Analysis and Applications*, 11:78–92, 1965.

[155] H. J. Kushner. *Probability Methods for Approximations in Stochastic Control and for Elliptic Equations*. Academic Press, 1977.

[156] H. J. Kushner. Numerical Methods for Stochastic Control Problems in Continuous Time. *SIAM Journal on Control and Optimization*, 28:999–1048, 1990.

[157] H. J. Kushner and P. Dupuis. *Numerical Methods for Stochastic Control Problems in Continuous Time*. Springer, 2001.

[158] P. Langevin. On the Theory of Brownian Motion. *Comptes Rendus de l'Académie des Sciences*, 146:530–533, 1908.

[159] O. P. Le Maître and O. M. Knio. *Spectral Methods for Uncertainty Quantification*. Scientific Computation. Springer, 2010.

[160] D. B. Leineweber. Analyse und Restrukturierung eines Verfahrens zur direkten Lösung von Optimal-Steuerungsproblemen. Diploma thesis, Ruprecht-Karls-Universität Heidelberg, 1995.

[161] D. B. Leineweber. *Efficient Reduced SQP Methods for the Optimization of Chemical Processes Described by Large Sparse DAE Models*, volume 613 of *Fortschritt-Berichte VDI Reihe 3, Verfahrenstechnik*. VDI Verlag, 1999.

[162] D. B. Leineweber, I. Bauer, H. G. Bock, and J. P. Schlöder. An Efficient Multiple Shooting Based Reduced SQP Strategy for Large-Scale Dynamic Process Optimization. Part I: Theoretical Aspects. *Computers & Chemical Engineering*, 27:157–166, 2003.

[163] S. M. Lenz, J. P. Schlöder, and H. G. Bock. Numerical Computation of Derivatives in Systems of Delay Differential Equations. *Mathematics and Computers in Simulation*, 96:124–156, 2014.

[164] T. Levajković. *Malliavin Calculus for Chaos Expansions of Generalized Stochastic Processes with Applications to Some Classes of Differential Equations*. PhD thesis, Univerzitet u Novom Sadu, 2011.

[165] T. Levajković and D. Seleši. Chaos Expansion Methods for Stochastic Differential Equations Involving the Malliavin Derivative–Part I. *Publications de l'Institute Mathématique*, 90:65–84, 2011.

[166] T. Levajković and D. Seleši. Chaos Expansion Methods for Stochastic Differential Equations Involving the Malliavin Derivative–Part II. *Publications de l'Institute Mathématique*, 90:85–98, 2011.

[167] P. Lévy. *Processus Stochastiques et Mouvement Brownien*. Gauthiers-Villars, 1948.

[168] M. Loève. *Probability Theory II*. Springer, 4th edition, 1978.

[169] S. V. Lototsky and B. L. Rozovskii. *From Stochastic Calculus to Mathematical Finance*, chapter Stochastic Differential Equations: A Wiener Chaos Approach, pages 433–506. Springer, Berlin, Heidelberg, 2006.

[170] S. V. Lototsky, R. Mikulevicius, and B. L. Rozovskii. Nonlinear Filtering Revisited: A Spectral Approach. *SIAM Journal on Control and Optimization*, 35:435–461, 1997.

[171] S. E. Ludwig. *Optimal Portfolio Allocation of Commodity Related Assets Using a Forward-Backward Algorithm*. PhD thesis, Ruprecht-Karls-Universität Heidelberg, 2013.

[172] W. Luo. *Wiener Chaos Expansion and Numerical Solutions of Stochastic Partial Differential Equations*. Caltech, 2006.

[173] H. Luschgy and G. Pàges. Functional Quantization of Gaussian Processes. *Journal of Functional Analysis*, 196:486–531, 2002.

[174] H. Luschgy and G. Pàges. Functional Quantization of a Class of Brownian Diffusions: A Constructive Approach. *Stochastic Processes and their Applications*, 116:310–336, 2006.

[175] D. L. Ma and R. D. Braatz. Worst-Case Analysis of Finite-Time Control Policies. *IEEE Transactions on Control Systems Technology*, 9:766–774, 2001.

[176] V. Mackevičius. On Polygonal Approximation of Brownian Motion in Stochastic Integral. *Stochastics*, 13:167–175, 1984.

[177] P. Malliavin. Stochastic Calculus of Variations and Hypoelliptic Operators. In *Proceedings of the International Symposium on Stochastic Differential Equations*, pages 195–263, 1978.

[178] P. Malliavin. *Stochastic Analysis*. Springer, 1997.

[179] L. Mathelin and K. A. Gallivan. A Compressed Sensing Approach for Partial Differential Equations with Random Data Input. *Communications in Computational Physics*, 12: 919–954, 2012.

[180] H. G. Matthies. *Extreme Man-Made and Natural Hazards in Dynamics of Structures*, chapter Quantifying Uncertainty: Modern Computational Representation of Probability and Applications, pages 105–135. NATO Security through Science Series. Springer, 2007.

[181] H. G. Matthies and A. Keese. Galerkin Methods for Linear and Nonlinear Elliptic Stochastic Partial Differential Equations. *Computational Methods of Applied Mechanical Engineering*, 194:1295–1331, 2005.

[182] R. Mikulevicius and B. L. Rozovskii. Linear Parabolic Stochastic PDEs and Wiener Chaos. *SIAM Journal on Mathematical Analysis*, 29:452–480, 1998.

[183] G. N. Milstein. *Numerical Integration of Stochastic Differential Equations*. Kluwer Academic Publishers, 1995.

[184] A. Mugler. *Verallgemeinertes polynomielles Chaos zur Lösung stationärer Diffusionsprobleme mit zufälligen Koeffizienten*. PhD thesis, Brandenburgische Technische Universität Cottbus, 2013.

[185] Z. K. Nagy and R. D. Braatz. Open-Loop and Closed-Loop Robust Optimal Control of Batch Processes Using Distributional and Worst-Case Analysis. *Journal of Process Control*, 14:411–422, 2004.

[186] K. Natarajan, D. Pachamanova, and M. Sim. Constructing Risk Measures From Uncertainty Sets. *Operations Research*, 57:1129–1141, 2009.

[187] R. M. A. Nelissen and M. H. C. Meijers. Social Benefits of Luxury Brands as Costly Signals of Wealth and Status. *Evolution and Human Behavior*, 32:343–355, 2011.

[188] A. Nemirovski and A. Shapiro. Convex Approximations of Chance Constrained Programs. *SIAM Journal on Optimization*, 17:969–996, 2006.

[189] H. Niederreiter. *Random Number Generation and Quasi-Monte Carlo Methods*. CMBS-NSF Regional Conference Series in Applied Mathematics 63. Society for Industrial and Applied Mathematics, 1992.

[190] N. Nielsen. *Recherches Sur Les Polynomes d'Hermite*. Kgl. Danske Videnskabernes Selskab, Matematisk-fysiske Meddelelser. Andr. Fred. Høst i komm, 1918.

[191] J. Nocedal and S. J. Wright. *Numerical Optimization*. Springer, 2006.

[192] I. Nourdin and G. Peccati. *Normal Approximations with Malliavin Calculus: From Stein's Method to Universality*. Cambridge University Press, 2012.

[193] A. Nouy. A Generalized Spectral Decomposition Technique to Solve a Class of Linear Stochastic Partial Differential Equations. *Computational Methods of Applied Mechanical Engineering*, 196:4521–4537, 2007.

[194] D. Nualart. *The Malliavin Calculus and Related Topics*. Springer, 2006.

[195] B. Øksendal. *Stochastic Differential Equations*. Springer, 2007.

[196] M. R. Osborne. On Shooting Methods for Boundary Value Problems. *Journal of Mathematical Analysis and Applications*, 27:417–433, 1969.

[197] G. Pàges and J. Printems. Optimal Quadratic Quantization for Numerics: The Gaussian Case. *Monte Carlo Methods and Applications*, 9:135–166, 2003.

[198] G. Pàges, H. Pham, and J. Printems. An Optimal Markovian Quantization Algorithm for Multidimensional Stochastic Control Problems. *Stochastics and Dynamics*, 4:501–545, 2004.

[199] S. Peng. A General Stochastic Maximum Principle for Optimal Control Problems. *SIAM Journal on Control and Optimization*, 28:966–979, 1990.

[200] L. Petzold, S. Li, Y. Cao, and R. Serban. Sensitivity Analysis of Differential-Algebraic Equations and Partial Differential Equations. *Computers & Chemical Engineering*, 30: 1553–1559, 2006.

[201] K. J. Plitt. Ein superlinear konvergentes Mehrzielverfahren zur direkten Berechnung beschränkter optimaler Steuerungen. Diploma thesis, Rheinische Friedrich-Wilhelms-Universität Bonn, 1981.

[202] L. S. Pontryagin, V. G. Boltyanski, R. V. Gamkrelidze, and E. F. Miscenko. *The Mathematical Theory of Optimal Processes*. Wiley, 1962.

[203] A. Potschka. Handling Path Constraints in a Direct Multiple Shooting Method for Optimal Control Problems. Diploma thesis, Ruprecht-Karls-Universität Heidelberg, 2006.

[204] A. Potschka, H. G. Bock, and J. P. Schlöder. A Minima Tracking Variant of Semi-Infinite Programming for the Treatment of Path Constraints within Direct Solution of Optimal Control Problems. *Optimization Methods and Software*, 24:237–252, 2009.

[205] A. Prékopa. *Stochastic Programming*. Kluwer Academic Publishers, 1995.

[206] M. L. Puterman. *Markov Decision Processes: Discrete Stochastic Dynamic Pogramming*. Wiley, 1994.

[207] S. Recker, P. Kühl, M. Diehl, H. G. Bock, and W. Marquardt. Sigmapoint Approach for Robust Optimization of Nonlinear Dynamic Systems. In *Proceedings of SIMULTECH 2012 - International Conference on Simulation and Modeling Methodologies, Technologies and Applications*, pages 199–207, 2012.

[208] D. Revuz and M. Yor. *Continuous Martingales and Brownian Motion*. Springer, 1999.

[209] P. Riede. *Optimierung von Dynamischen Multiple-Setpoint-Problemen mit Anwendung bei Fahrzeugmodellen*. PhD thesis, Ruprecht-Karls-Universität Heidelberg, 2006.

[210] F. Riesz and B. S. Nagy. *Functional Analysis*. Dover Publishing Inc., 1990.

[211] R. T. Rockafellar. *Tutorials in Operations Research: OR Tools and Applications: Glimpses of Future Technologies*, chapter Coherent Approaches to Risk in Optimization Under Uncertainty, pages 38–61. INFORMS, 2007.

[212] R. T. Rockafellar and S. P. Uryasev. Optimization of Conditional Value-at-Risk. *Journal of Risk*, 2:21–42, 2000.

[213] R. T. Rockafellar and S. P. Uryasev. Conditional Value-at-Risk for General Loss Distributions. *Journal of Banking and Finance*, 26:1443–1471, 2002.

[214] R. D. Russell and L. F. Shampine. A Collocation Method for Boundary Value Problems. *Numerische Mathematik*, 19:1–28, 1972.

[215] A. P. Ruszczyński and A. Shapiro, editors. *Stochastic Programming*. Elsevier, 2003.

[216] A. P. Ruszczyński and A. Shapiro. Conditional Risk Mappings. *Mathematics of Operations Research*, 31:544–561, 2006.

[217] S. Sager. Reformulations and Algorithms for the Optimization of Switching Decisions in Nonlinear Optimal Control. *Journal of Process Control*, 19:1238–1247, 2009.

[218] S. Sager. On the Integration of Optimization Approaches for Mixed-Integer Nonlinear Optimal Control. Ruprecht-Karls Universität Heidelberg, August 2011. Habilitation.

[219] R. W. H. Sargent and G. R. Sullivan. The Development of an Efficient Optimal Control Package. In *Proceedings of the 8th IFIP Conference on Optimization Techniques (1977), Part 2*. Springer, 1978.

[220] C. Schillings and V. Schulz. On the Influence of Robustness Measures on Shape Optimization with Stochastic Uncertainties. Technical report, Universität Trier, 2012.

[221] W. Schoutens. *Stochastic Processes and Orthogonal Polynomials*. Springer, 2000.

[222] S. P. Sethi. Nearest Feasible Paths in Optimal Control Problems: Theory, Examples, and Counterexamples. *Journal of Optimization Theory and Applications*, 23:563–579, 1977.

[223] S. P. Sethi. Optimal Advertising Policy with the Contagion Model. *Journal of Optimization Theory and Applications*, 29:615–627, 1979.

[224] A. Shapiro, D. Dentcheva, and A. P. Ruszczyński. *Lectures on Stochastic Programming: Modeling and Theory*. Society for Industrial and Applied Mathematics, 2009.

[225] A. Simpkins and E. Todorov. Practical Numerical Methods for Stochastic Optimal Control of Biological Systems in Continuous Time and Space. In *IEEE Symposium on Adaptive Dynamic Programming and Reinforcement Learning*, pages 212–218, 2009.

[226] T. Singh, P. Singla, and U. Konda. Polynomial Chaos Based Design Of Robust Input Shapers. *Journal of Dynamic Systems, Measurement, and Control*, 132:051010/1–051010/13, 2010.

[227] D. Skanda and D. Lebiedz. An Optimal Experimental Design Approach to Model Discrimination in Dynamic Biochemical Systems. *Bioinformatics*, 26:939–945, 2010.

[228] A. K. Skiba. Optimal Growth with a Convex-Concave Production Function. *Econometrica*, 46:527–539, 1978.

[229] S. A. Smolyak. Quadrature and Interpolation Formulas for Tensor Products of Certain Classes of Functions. *Soviet Mathematics Doklady*, 4:240–243, 1963.

[230] M. C. Steinbach. *Fast Recursive SQP Methods for Large-Scale Optimal Control Problems*. PhD thesis, Ruprecht-Karls-Universität Heidelberg, 1995.

[231] R. L. Stratonovich. A New Representation for Stochastic Integrals and Equations. *SIAM Journal on Control*, 4:362–371, 1966.

[232] D. W. Stroock. *Séminaire de Probabilités XXI*, volume 1247 of *Lecture Notes in Mathematics*, chapter Homogeneous Chaos Revisited, pages 1–7. Springer, 1987.

[233] H. J. Sussman. On the Gap Between Deterministic and Stochastic Ordinary Differential Equations. *Annals of Probability*, 6:19–41, 1978.

[234] G. Szegő. *Orthogonal Polynomials*. American Mathematical Society, 1939.

[235] S. J. Taylor. Exact Asymptotic Estimates of Brownian Path Variation. *Duke Mathematical Journal*, 39:219–241, 1972.

[236] T. N. Y. Times. Dim Days for Luxury Hotels. The New York Times, October 28 2008. By J. Sharkey.

[237] R. A. Todor and C. Schwab. Convergence Rates for Sparse Chaos Approximations of Elliptic Problems with Stochastic Coefficients. *IMA Journal of Numerical Analysis*, 27: 232–261, 2007.

[238] A. Tourin and T. Zariphopoulou. Numerical Schemes for Investment Models with Singular Transactions. *Computational Economics*, 7:287–307, 1994.

[239] T. H. Tsang, D. M. Himmelblau, and T. F. Edgar. Optimal Control via Collocation and Non-Linear Programming. *International Journal on Control*, 21:763–768, 1975.

[240] G. M. Vainikko. On the Stability and Convergence of the Collocation Method. *Differentsial'nye Uravneniya*, 1:244–254, 1965. (In Russian. Translated in Differential Equations, 1 (1965), pp. 186–194).

[241] A. Y. Veretennikov and N. V. Krylov. On Explicit Formulas for Solutions of Stochastic Equations. *Mathematics of the USSR: Sbornik*, 29:239–256, 1976.

[242] A. Wächter and L. T. Biegler. On the Implementation of an Interior-Point Filter Line-Search Algorithm for Large-Scale Nonlinear Programming. *Mathematical Programming*, 106:25–57, 2006.

[243] X. Wan and G. E. Karniadakis. *Computer Mathematics and its Applications: Advances and Developments (1994–2005)*, chapter Adaptive Numerical Solutions of Stochastic Differential Equations, pages 561–573. LEA Publishers, 2006.

[244] X. Wan and G. E. Karniadakis. Beyond Wiener Askey Expansions: Handling Arbitrary PDFs. *Journal of Scientific Computing*, 27:455–464, 2006.

[245] X. Wan, B. L. Rozovskii, and G. E. Karniadakis. A Stochastic Modeling Methodology Based on Weighted Wiener Chaos and Malliavin Calculus. In *Proceedings of the National Academy of Sciences of the United States of America*, volume 106, pages 14189–14194, 2009.

[246] N. Wiener. The Homogeneous Chaos. *American Journal of Mathematics*, 60:897–936, 1938.

[247] R. B. Wilson. *A Simplicial Algorithm for Concave Programming*. PhD thesis, Harvard University, 1963.

[248] R. Winkler, U. Brandt-Pollmann, U. Moslener, and J. P. Schlöder. Time-Lags in Capital Accumulation. In *Operations Research Proceedings 2003*, pages 451–458, 2003.

[249] E. Wong and M. Zakai. On the Convergence of Ordinary Integrals to Stochastic Integrals. *The Annals of Mathematical Statistics*, 36:1560–1564, 1965.

[250] D. Xiu and G. E. Karniadakis. The Wiener-Askey Polynomial Chaos for Stochastic Differential Equations. *SIAM Journal on Scientific Computing*, 24:619–644, 2002.

[251] T. Yamada and S. Watanabe. On the Uniqueness of Solutions of Stochastic Differential Equations. *Journal of Mathematics of Kyoto University*, 11:155–167, 1971.

[252] M. Yor. Introduction Au Calcul Stochastique. *Séminaire Bourbaki*, 24:275–292, 1981/1982.

[253] M. Zakai. On the Optimal Filtering of Diffusion Processes. *Zeitschrift für Wahrscheinlichkeitstheorie und Verwandte Gebiete,* 11:230–243, 1969.

[254] K. Zhou, J. C. Doyle, and K. Glover. *Robust and Optimal Control.* Prentice Hall, 1996.

BIBLIOGRAPHY

Nomenclature

Throughout this thesis, we use roman and greek letters in boldface ($\boldsymbol{x}$, $\boldsymbol{X}$, $\boldsymbol{p}$, $\boldsymbol{\Sigma}$, $\boldsymbol{\alpha}$) to denote multidimensionality. This includes, e.g., deterministic processes ($\boldsymbol{x}$, $\boldsymbol{u}$), multidimensional parameters ($\boldsymbol{p}$), stochastic processes ($\boldsymbol{X}$, $\boldsymbol{B}$), matrices ($\boldsymbol{\Sigma}$), and multi-indices ($\boldsymbol{\alpha}$). Scalars are denoted by roman and greek letters in normal print (f, g, λ, μ), while sets use uppercase calligraphic style ($\mathcal{I}$, $\mathcal{G}$, $\mathcal{T}$). Finally, number spaces are denoted in uppercase blackboard style ($\mathbb{N}$, $\mathbb{R}$).

The following list states frequently used symbols and notations. They are grouped thematically to avoid confusion as they can be used differently depending on the context.

List of Symbols

General Symbols

$\triangle$	End of a definition, lemma, theorem, or corollary
$\square$	End of a proof
$\stackrel{\text{def}}{=}$	Defined to be equal
$\mathbb{N}$, $\mathbb{N}_0$	Set of natural numbers (including zero)
$\mathbb{R}$	Set of real numbers
$(\cdot)$	Wildcard notation for the omitted list of function arguments
$|\cdot|$	Component-wise mapping of a real number to its absolute value
$\langle \cdot, \cdot \rangle_{\mathcal{C}}$	Inner product of the space $\mathcal{C}$
$\|\cdot\|_{\mathcal{C}}$	Norm of the space $\mathcal{C}$
$\|\cdot\|_2$	The (Euclidean) norm of a matrix or vector
$\mathbb{1}_{\mathcal{A}}(\cdot)$, $\mathbb{1}_{[a,b]}(\cdot)$	Characteristic function of a set $\mathcal{A}$ (an interval $[a, b]$)
$\delta_{n,m}$	Kronecker delta of n and m
$\{\ \}$	Set delimiters
$(\ )$	Sequence delimiters
$\subseteq, \subset$	Subset of a set ("is a (proper) subset of")
$\in, \notin$	Set membership ("is (not) an element of")
$\times$	Cartesian product of sets, multiplication in literal numbers
$\oplus$	Direct sum
$\forall$	Universal quantifier ("for all")
$\exists$	Existential quantifier ("there exists")

$\boldsymbol{v}^T, \boldsymbol{A}^T$	Transpose of a vector or matrix
$\boldsymbol{A}^{-1}$	Inverse of regular matrix $\boldsymbol{A}$
$f_{\boldsymbol{x}}$	Gradient of the scalar function $f(\cdot)$ with respect to the unknown $\boldsymbol{x}$

Specific Symbols in Optimal Control Context

t	Time instant
t_0	Initial time
t_{f}	Terminal time
$\mathcal{T}$	Time interval, usually $\mathcal{T} = [t_0, t_{\mathrm{f}}]$
$\boldsymbol{x}(\cdot)$	Trajectory of system states
$\boldsymbol{z}(\cdot)$	Trajectory of algebraic states
$\boldsymbol{u}(\cdot)$	Trajectory of controls
$\boldsymbol{f}$	ODE system right hand side function
$\boldsymbol{g}$	DAE system right hand side function
$\boldsymbol{f}^{\mathrm{tr}}$	Transition function between model stages
$\boldsymbol{c}$	Path constraint function
$\boldsymbol{r}$	Point constraint function
$\boldsymbol{p}$	Model parameters
$J(\cdot)$	Objective function
$V(\cdot)$	Cost-to-go function

Specific Symbols in Stochastic Context

Ω	Sample space, set of all possibles outcomes
$\mathcal{F}$	σ-algebra, collection of subsets of Ω which can be assigned probabilities
$\mathbb{P}$	Probability measure
$\mu, \varrho(\cdot)$	Gaussian probability measure; density of the Gaussian measure
$\mathcal{N}(0, 1)$	Standard normal/Gaussian distribution with zero mean and variance one
ξ, ξ_i	Standard Gaussian random variable
$\mathbb{E}[X]$	Expectation of a random variable X
$\mathbb{V}[X]$	Variance of a random variable X
$\mathrm{Cov}[X, Y]$	Covariance of two random variables X and Y
$\mathbb{P}[A]$	Probability of an event A
$q_\zeta(X)$	Quantile of the random variable X corresponding to the probability level ζ
ϖ	Confidence level
$\boldsymbol{X}, \boldsymbol{X}_t$	Stochastic process (at time instant t)
$\boldsymbol{B}, \boldsymbol{B}_t$	Brownian motion (at time instant t)
S, S_t	Simple stochastic process (at time instant t)

F	Smooth random variable
$\{\mathcal{F}_t\}_{t\in\mathcal{T}}$, $\{\mathcal{F}_t^B\}_{t\in\mathcal{T}}$	Filtration of $\mathcal{F}$; filtration generated by the BROWNian motion
$I(X)$, $I_t(X)$	ITŌ integral of a stochastic process X, X (up to time t)
$\boldsymbol{\alpha}$	Multi-index with a finite number of positive, non-zero entries
$\boldsymbol{\alpha}^-(\boldsymbol{j})$	Diminished multi-index with decremented j-th entry
$|\boldsymbol{\alpha}|$	Order of the multi-index $\boldsymbol{\alpha}$; $|\boldsymbol{\alpha}| = \sum_i \alpha_i$
$d(\boldsymbol{\alpha})$	Length of the multi-index $\boldsymbol{\alpha}$; $d(\boldsymbol{\alpha}) = \max\{i \in \mathbb{N} \mid \alpha_i > 0\}$
r	Sparse index for truncation of a multi-index $\boldsymbol{\alpha}$
(r)	Adaptive index for truncation of a multi-index $\boldsymbol{\alpha}$
$\mathcal{I}$, $\mathcal{I}_p$, $\mathcal{I}_{p,k}$	Index set of multi-indices $\boldsymbol{\alpha}$ (with $|\boldsymbol{\alpha}| \leqslant p$ [and $d(\boldsymbol{\alpha}) \leqslant k$])
$\mathcal{I}_{p,k}^r$, $\mathcal{I}_{p,k}^{(r)}$	Sparsely (adaptively) truncated index set of multi-indices $\boldsymbol{\alpha}$
$H_i(\cdot)$	i-th normalized HERMITE polynomial
$\mathfrak{H}$	HILBERT space
h	Element of the HILBERT space $\mathfrak{H}$
$W(h)$	Isonormal GAUSSian process over $h \in \mathfrak{H}$
$\Psi^{\boldsymbol{\alpha}}$	Orthonormal basis function of the chaos space $L^2(\Omega, \mathcal{F}, \mathbb{P})$
$\mathcal{H}_i$	i-th WIENER chaos space
$m_i(\cdot)$	Basis element of the HILBERT space $L^2([0,1])/L^2([0,t_{\mathrm{f}}])$
$M_i(\cdot)$	Integrated basis element
$L^2(\Omega)$	Space of square-integrable random variables
$L^2(\mathbb{R}, \mu)$	Space of square-integrable functions with GAUSSian measure μ
$L^2(\mathcal{T} \times \Omega)$	Space of square-integrable random processes
$L_{\mathrm{A}}^2(\mathcal{T} \times \Omega)$	Space of adapted square-integrable random processes
$D^k X$	k-th MALLIAVIN derivative of the random variable X
$\mathbb{D}^{k,2}$	Domain of the k-th MALLIAVIN derivative
$\|\cdot\|_{k,2}$	The corresponding norm
$\delta^k(X)$	k-th divergence/SKOROHOD integral of X
$\mathrm{Dom}\,\delta^k$	Domain of the k-th divergence

Symbols with Special Meaning in the Recession Problem

τ	Endpoint of the recession period
$A(\cdot)$	Trajectory of the brand image state function
$B(\cdot)$	Trajectory of the cash state function
$P(\cdot)$	Trajectory of the price function
$D(\cdot)$, $D_{\mathrm{R}}(\cdot)$, $D_{\mathrm{N}}(\cdot)$	Demand function (of the recession/normal stage)
σ	Constant control delay
$\eta(\cdot)$	Initialization of the control function $p(\cdot)$ due to the delay
κ	Scaling parameter of the brand image's response to price changes
γ	Scaling parameter

C	Fixed costs
δ	Short-time interest rate
β	Adjustment parameter for demand
m	Potential market size
r	Discount rate
ς	Recession strength
$\bar{\zeta}$	Mean value of recession strength
Σ	Variance of recession strength
λ	Rate parameter for exponential distribution of τ

List of Figures

List of Tables

List of Acronyms

BDF   Backward Differentiation Formula
BFGS   Broyden-Fletcher-Goldfarb-Shanno
BSDE   Backward Stochastic Differential Equation
BVP   Boundary Value Problem
cdf   cumulative distribution function
CPU   Central Processing Unit
CVaR   Conditional Value at Risk
DAE   Differential-Algebraic Equation
HJB   Hamilton-Jacobi-Bellman
IND   Internal Numerical Differentiation
IVP   Initial Value Problem
KKT   Karush-Kuhn-Tucker
KLE   Karhunen-Loève Expansion
MCA   Markov Chain Approximation
NLP   Nonlinear Program
NPV   Net Present Value
OCP   Optimal Control Problem
ODE   Ordinary Differential Equation
PC   Polynomial Chaos
PDE   Partial Differential Equation
QP   Quadratic Program
PMP   Pontryagin's Maximum Principle
RDE   Random Differential Equation
SDE   Stochastic Differential Equation
SMP   Stochastic Maximum Principle
SOCP   Stochastic Optimal Control Problem
SPDE   Stochastic Partial Differential Equation
SQP   Sequential Quadratic Programming
VaR   Value at Risk